

Axes determination in the frog *Xenopus laevis*: the function of *goosecoid*, *myo1d* and *dmrt2*

Dissertation for Obtaining the Doctoral Degree
of Natural Science (Dr. rer. nat.)

Faculty of Natural Science
University of Hohenheim

Institute of Biology, Dept. of Zoology (190z)

submitted by

Melanie Bianca Tingler

from Rottweil
2020

Dean: Prof. Dr. Uwe Beifuß

1st reviewer: apl. Prof. Dr. Axel Schweickert

2st reviewer: Prof. Dr. Heinz Breer

Submitted on: 08/27/2020

Oral examination on: 12/08/2020

The present work was accepted by the faculty of Natural Science as “Dissertation for obtaining the Doctoral Degree of Natural Science (Dr.rer.nat.)” on 09/07/2020.

Affidavit according to Sec. 7(7) of the University of Hohenheim doctoral degree regulations for Dr. rer. nat.

1. For the dissertation submitted on the topic

Axes determination in the frog *Xenopus laevis*: the function of *goosecoid*, *myo1d* and *dmrt2*

I hereby declare that I independently completed the work.

2. I only used the sources and aids documented and only made use of permissible assistance by third parties. In particular, I properly documented any contents which I used - either by directly quoting or paraphrasing - from other works.

3. I did not accept any assistance from a commercial doctoral agency or consulting firm.

4. I am aware of the meaning of this affidavit and the criminal penalties of an incorrect or incomplete affidavit.

I hereby confirm the correctness of the above declaration: I hereby affirm in lieu of oath that I have, to the best of my knowledge, declared nothing but the truth and have not omitted any information.

Place and Date

Signature

Abstract

During early embryogenesis, pattern formation processes along the head-trunk (anteroposterior, AP), belly-back (dorsoventral, DV) and left-right (LR) body axis generate the fundamental body plan of the bilateria. The formation of the LR axis is exceptional because externally our body is bilateral symmetric whereas most inner organs are shaped and positioned asymmetrically. The three body axes are basically specified during gastrulation and neurulation by a set of developmental control genes. The aim of this work was to analyze the function of the highly conserved genes, *gooseoid* (*gsc*), *myosin1d* (*myo1d*) und *dmrt2* during body axis determination in *Xenopus*.

The first chapter of this work describes the activity of the homeobox transcription factor Gooseoid during AP- and DV-axis formation. Gsc acts as an autoregulatory transcriptional repressor and importantly is expressed in the Spemann Organizer (SO) of all vertebrate embryos. The SO represents the main dorsal signaling center for primary axis induction, regulates embryonic patterning and cell movements. It is further required for AP i.e. head and trunk development. Transferring of SO or *gsc* misexpression to ventral half of embryos results in secondary axis formation i.e. siamese twins.

However, SO function of Gsc was enigmatic, as *gsc* mutants showed no defects on early developmental processes what challenged Gsc function in the SO. In this chapter, *gsc* was characterized by conducting gain of function experiments in the embryonic midline of *Xenopus* embryos. Gsc was able to repress planar cell polarity (PCP) in a cell- and non-cell autonomous fashion leading to neural tube closure defects. In the early gastrulae, Gsc separates the head from the trunk mesoderm by repressing the mesodermal t-box gene transcription factor T (Tbxt). This inhibition allows the migration of the head mesodermal cells whereas the trunk notochord elongates by mediolateral intercalation. Gsc activity on PCP signaling seems to be specific for vertebrates only and correlates with the presence of two novel domains.

The determination of the LR body axis is discussed in the second chapter of this work. At the so called left-right organizer (LRO) a cilia-mediated leftward-fluid flow initiates the symmetry breaking event in neurulae embryos. Lateral sensory cells (sLRO) of the LRO perceive flow on the left side and translate it into the left asymmetric induction of

the highly conserved Nodal cascade. If and how the unconventional, actin-associated motor protein Myosin1d (Myo1d) as well as the transcription factor Doublesex and mab-3 related 2 (Dmrt2) intervene in LR specification was analyzed in this chapter.

In evolutionary terms the study of *myo1d* was of high interest because in *Drosophila*, which lacks a ciliary flow mechanism, the homologous gene, *myo31df*, controls LR axis determination. Manipulations of *myo1d* in *Xenopus* demonstrated that in vertebrates Myo1d is involved in the cilia-based symmetry breakage event. By interacting with the PCP signaling pathway, Myo1d ensures leftward-fluid flow by regulating ciliary outgrowth and polarization. In *Drosophila* and *Xenopus* Myo1d interacts with PCP signaling and seems to link an ancestral symmetry breaking mechanism of the fly to the newly evolved leftward-fluid flow in vertebrates.

Based on studies in zebrafish, which identified Dmrt2 as another factor involved in LR development and somitogenesis, we started the analysis of *dmrt2* in *Xenopus*. Somitogenesis and laterality determination which on first sight are functionally distinct processes were analyzed in the context of *dmrt2* function. In *Xenopus*, flow-sensing cells are affiliated to the somitic cell lineage and therefore paraxial mesoderm specification is crucial for setting up a functional LRO. Dmrt2 specifies the paraxial mesoderm and especially the sLRO by inducing the myogenic transcription factor *myf5* in early gastrulae. This demonstrated for the first time experimentally how somitogenesis and laterality determination are intertwined and describes the genesis of the *Xenopus* sLRO cells in more detail.

Zusammenfassung

Während der frühen Embryogenese generieren embryonale Musterbildungsprozesse entlang der Kopf-Rumpf- (anteroposterior, AP), Rücken-Bauch- (dorsoventral, DV) und links-rechts (LR) Körperachse den grundlegenden Bauplan der Bilateria. Hierbei ist vor allem die Ausbildung der LR-Achse auffallend: sie besticht durch eine äußerlich sichtbare Symmetrie entlang der AP-Achse, wohingegen die asymmetrische Formgebung und Position der inneren Organe in der sekundären Leibeshöhle äußerlich nicht zu erkennen ist. Die Ausbildung der drei Körperachsen wird durch die Aktivität zahlreicher Gene während der Gastrulation und Neurulation reguliert. Ziel dieser Arbeit war es, die Rolle der hoch konservierten Gene *gooseoid* (*gsc*), *myosin1d* (*myo1d*) und *doublesex-and mab3 related transcription factor 2* (*dmrt2*) während der Ausbildung der Körperachsen in *Xenopus laevis* näher zu untersuchen.

Das erste Kapitel dieser Arbeit befasst sich mit der frühen Funktion des Homöobox-Transkriptionsfaktors Gooseoid während der Ausbildung der AP- und DV-Achse. Gsc wirkt als autoregulatorischer transkriptioneller Repressor, wird im Spemann-Organisator, dem Signalzentrum der primären Achseninduktion exprimiert und steuert die embryonale Musterbildung. Es reprimiert ventrale Signalwege im dorsalen Gewebe, separiert das Kopf- vom Chordamesoderm und reguliert Zellbewegungen im Zuge der Gastrulation und Neurulation.

Die frühe Funktion von *gsc* im Spemann-Organisator war bislang enigmatisch, da der Funktionsverlust von *gsc* die frühe embryonale Entwicklung nicht beeinträchtigte. Durch gezielte Überexpression von *gsc* in der dorsalen Mittellinie von *Xenopus* Embryonen wurde hier die frühe Funktion von *gsc* näher charakterisiert. Gsc agierte sowohl zell- als auch nicht-zell-autonom als Repressor planarer Zellpolarität (planar cell polarity, PCP). In der frühen Gastrula separierte Gsc durch die Repression des mesodermalen T-box Gen Transkriptionsfaktors T (*Tbxt*) das Kopf- vom Chordamesoderm. Dies ermöglichte das migrieren des Kopfmesoderms und beschränkte die durch *Tbxt*-induzierte PCP-vermittelte mediolaterale Interkalation auf das elongierende Notochord des Embryos. Diese Funktion von Gsc scheint sich im Zuge der Evolution durch die Etablierung zweier neuer, für Vertebraten spezifische Domänen etabliert zu haben.

Das zweite Kapitel befasst sich mit der Determinierung der LR-Körperachse in *Xenopus*, die als letzte der drei Körperachsen festgelegt wird. Diese wird durch einen Cilien-basierten nach links-gerichteten Flüssigkeitsstrom innerhalb des sog. links-rechts Organisators (LRO) in der Neurula initiiert. Die lateralen, linken sensorischen Zellen des LROs (sLRO) perzipieren den Flüssigkeitsstrom und translatieren dieses Signal in die Induktion der hoch konservierten Nodal Kaskade auf der linken Seite. Welche Funktion das unkonventionelle, Aktin-assoziierte Motorprotein Myo1d und der Transkriptionsfaktor Dmrt2 bei diesem Prozess einnimmt, wurde im Rahmen dieser Arbeit untersucht.

Die Analyse von *myo1d* war hierbei evolutionär von großer Bedeutung, da das homologe Gene *myo31df* in *Drosophila* die Entstehung der LR-Achse, unabhängig eines links-gerichteten Flüssigkeitsstrom und einer asymmetrischen Gen-Kaskade reguliert. Die Manipulation von *myo1d* in *Xenopus* demonstrierte, dass die Funktion von Myo1d konserviert ist und auch in Vertebraten für den Symmetriebruch benötigt wird. Durch Interaktion mit dem PCP Signalweg trägt Myo1d über die Polarisierung und Ausbildung der Cilien zum links-gerichteten Flüssigkeitsstrom und somit zur Lateralitätsdeterminierung in *Xenopus* bei. Durch den Einfluss von Myo1d auf die PCP in *Drosophila* und *Xenopus* stellt Myo1d eine direkte Verbindung zwischen dem ancestralen Mechanismus und des in Vertebraten neu-evolvierten Flüssigkeitsstrom zum Bruch der bilateralen Symmetrie dar.

Studien aus dem Zebrafisch identifizierten Dmrt2 als einen weiteren Faktor, der sowohl für die Somitogenese als auch für die Ausbildung der LR-Körperachse benötigt wird. Ein Zusammenhang zwischen diesen Prozessen ist ein lang bekanntes Phänomen, dessen Ursache bisher nicht geklärt wurde. Aufgrund der Integration der sLRO Zellen in das paraxiale presomitische Mesoderm, dem Vorläufergewebe der Somiten, stellte sich die Frage, ob dies eine Verbindung zwischen diesen zwei Prozessen erklären könnte. Die Untersuchung von *Xenopus* Embryonen nach Manipulation von *dmrt2* zeigte, dass die Spezifizierung des paraxialen Mesoderms in der frühen Gastrula für die Ausbildung der sLRO Zellen ausschlaggebend ist. Über die Induktion des myogenen Transkriptionsfaktors *myf5* reguliert Dmrt2 die Spezifizierung des paraxialen Mesoderms und insbesondere der sLRO Zellen in *Xenopus*. Dies demonstrierte zum ersten Mal experimentell eine direkte Verbindung zwischen der frühen Somitogenese und der Lateralitätsdeterminierung und liefert eine erste Erklärung wie diese Prozesse zusammenhängen.

Directory

Affidavit	1
Abstract	2
Zusammenfassung	4
Introduction - Body axes specification in <i>Xenopus laevis</i>	8
Anteroposterior and dorsoventral axis development	8
Specification of the dorsoventral and anteroposterior axis	8
Induction of the Spemann Organizer	9
Function of the Spemann Organizer	10
The process of gastrulation.....	11
Neurulation forms the central nervous system	12
Left-right body axis development	12
The Nodal cascade	13
Leftward-fluid flow at the LRO breaks the bilateral symmetry	14
Specification of the superficial mesoderm.....	15
The planar cell polarity pathway	18
The core PCP pathway in vertebrates.....	18
PCP in cilia polarization	19
PCP regulates gastrulation and neural tube closure	20
Aim of this work	21
Original research Chapter I: AP- and DV-axis development	24
A novel role for the organizer gene Goosecoid as an inhibitor of Wnt/PCP-mediated convergent extension in <i>Xenopus</i> and mouse.....	25
Original research Chapter II:Left-right axis development	53
A conserved role for the Unconventional Myosin1d in Laterality Determination	54

<i>dmrt2</i> and <i>myf5</i> link early somitogenesis to left-right axis determination in <i>Xenopus laevis</i>	71
Discussion	106
The early function of <i>gooseoid</i> : establishment of the dorsoventral and anteroposterior axis by intervening with PCP signaling.....	106
Myosin1d links an ancestral symmetry breaking mechanism to the newly evolved leftward-flow	107
Myosin1d and symmetry breakage: a cytoskeletal function in laterality determination besides PCP signaling?.....	109
Sensory LRO cell fate depends on <i>myf5</i> downstream of <i>dmrt2</i>	113
Conclusion	115
References	116
Author's contribution	131
Curriculum vitae	132
Danksagung	135

Introduction - Body axes specification in *Xenopus laevis*

Anteroposterior and dorsoventral axes development

The fundamental body plan of the bilateria is attributed to the generation of the dorsoventral (back-belly) and anteroposterior (head-trunk) axis. Bilateria are defined by an external bilateral symmetry as the left and right side represent the mirror image of each other reflected from the midline along the anteroposterior axis. To generate this body plan the DV- and AP-axis has to be specified and established during early embryonic development.

Specification of the dorsoventral and anteroposterior axis

Already the unfertilized egg reveals asymmetries which divide the oocyte into an animal and a vegetal half. The animal part of this cell consists of highly condensed pigments that protect the embryo from UV radiation and cells derived thereof will later make up the prospective animal. In contrast, the vegetal hemisphere serves as a nutrition resource for the developing non-feeding embryo (Gilbert, 2010).

The dorsoventral (DV) axis, dividing the organism into belly and trunk, is specified during fertilization of the oocyte. Sperm binding onto the receptor in the animal half leads to the release of the nucleus and the centriole, which in turn initiates cytoskeletal rearrangement in the zygote. This induces a shift of maternal components from the vegetal region to the future dorsal side. The point of sperm entry hallmarks the DV axis by determining the ventral side with respect to the future dorsal side (Gilbert, 2010).

During fertilization the centriole provided by the sperm organizes the microtubules in a parallel manner in the vegetal part. This leads to separation of the cortical cytoplasm from the inner cytoplasm. In turn, cortical rotation is initiated, meaning a rotation about 30 degrees of the cortical cytoplasm. The parallel arrangement of the microtubules organizes the growing-ends in the animal dorsal region. The microtubule skeleton is thought to translocate at least two vegetally deposited maternal components of the canonical Wnt pathway, Dishevelled (Dvl) and the GSK3-binding protein (GBP). These components are transported to the dorsal side where they activate the canonical Wnt/ β -catenin pathway by inactivating the Glycogen-synthase-kinase 3 (GSK3). In an active state GSK3 phosphorylates the transcription factor β -catenin (Ctnnb1) and

thereby marks it for degradation. Due to loss of GSK3 activity Ctnnb1 is able to accumulate and to initiate gene transcription at the midblastula when the genome becomes activated by demethylation. This leads to the induction of the Spemann Organizer (SO), the primary body axis signaling center (Gilbert, 2010).

Induction of the Spemann Organizer

Fundamental experiments on the SO go back to Hans Spemann and Hilde Mangold at the beginning of the 20th century. Constriction experiments on salamanders at early cleavage stages gave rise to two identical siblings. Performing the same constriction experiments but perpendicular to the plane of the first cleavage led to a normal larvae and a so called “Bauchstück” - belly piece. These experiments demonstrated that nuclei of early blastomeres are identical and that there must be an early asymmetrically distributed cytoplasmic component that regulates axis induction. Spemann speculated that the so called grey crescent might be crucial for this process. The grey crescent arises during fertilization by cytoplasmic movements of the pigments at the future dorsal side of the early newt embryo. After the first cleavage both blastomeres contain a part of the grey crescent. He speculated that this region might be decisive for initiating gastrulation and that cell fate potency occurs during gastrulation. Ongoing transplanting experiments confirmed this hypothesis. Transplanting prospective epidermal cells of early gastrulae into the future neural tissue region of an early host gastrulae led the transplanted cells to become neural tissue and *vice versa*. The same experiment performed on late gastrulae stage embryos led to a completely different result as the transplanted cells exhibited an autonomous development as their prospective fate was already determined (Gilbert, 2010). After these insights Hans Spemann and Hilde Mangold performed their most spectacular experiment in 1924 for which they received the Nobel Prize in 1935. Transplanting experiments of the dorsal lip, the region where gastrulation starts, resulted in the formation of a secondary body axis e.g. a siamese twin when the dorsal lip was transplanted into the ventral half of a recipient embryo. These experiments highlighted that the cells of the dorsal lip are the organizing center for primary axis induction as those cells are able to induce a cell fate change in ventral tissue (Spemann & Mangold, 1924, Gilbert, 2010).

Since Spemann our knowledge on the molecular basis of SO induction has substantially increased. The induction of the SO depends at least on two important

processes. Cortical rotation after fertilization activates the Wnt signaling pathway by stabilizing Ctnnb1 in dorsal cells. After midblastula transition, dorsally accumulated Ctnnb1 interacts with the transcriptional repressor ubiquitous transcription factor Tcf3, transforming it to a transcriptional activator. This leads to the induction of the homeobox transcription factors *siamois* and *twin* in dorsal cells. In cooperation with the co-factor Smad2/4, Siamois and Twin activates the expression of the organizer genes *goosecoid (gsc)* and *xlim1*. For this cooperation to occur, Smad2/4 has to be activated in dorsal cells dependent on the transforming-growth factor- β (Tgf- β) signaling pathway. This activation step is provided by the maternal expression of the paracrine Tgf- β factors Gdf1 and Vegt in vegetal cells. Vegt induces the expression of Tgf- β proteins like Activin, Gdf3 and Nodal in endodermal cells. Through synergistic interaction of Vegt and Ctnnb1 a Nodal gradient is established along the DV axis. This results in a low ventral Nodal concentration that leads to ventral mesoderm and a high dorsal Nodal concentration that induces a dorsal mesodermal cell fate. In the most dorsal cells the Nodal ligands activate Smad2/4 by binding to its receptor. This leads to the cooperation of Twin, Siamois and Smad2/3 and to the induction of the SO by activating the expression of *gsc* and *xlim1*. Contrarily, Ctnnb1 is not active ventrally as it becomes degraded, leading to Tcf3 acting as transcriptional repressor (Gilbert, 2010).

Function of the Spemann Organizer

The function of the SO is to generate the dorsal structures of the embryo by regulating the activity of the Wnt and Bmp signaling pathway in a tightly controlled manner. It generates a DV Bmp gradient and an anteroposterior (AP) Wnt gradient by the secretion of antagonizing factors. Shortly after specification of the SO, Twin, Siamois and Smad2/4 induce the expression of the three Bmp-inhibitors *chordin*, *noggin* and *folliculin*. These antagonists become expressed in the dorsal lip and later on in the notochord. By interacting with Bmp2 and Bmp4, these secreted proteins block Bmp signaling by preventing ligand-receptor initiation. This step is important for the specification of the neuroectodermal tissue, since Bmp signaling induces epidermal cell fate. In the most anterior region that gives rise to the head and brain structures, the prechordal plate and the pharyngeal mesendoderm represent the leading edge of the dorsal lip. The pharyngeal mesendoderm expresses the Bmp/Wnt/Nodal

antagonists *cerberus* (Cer), *dickkopf* (Dkk), *frzbee* (Frzb) and *insulin-like growth factors* (IGFs). These proteins inhibit Wnt- and Bmp signaling in the most anterior region and enable head formation (Gilbert, 2010).

Summarizing, the tightly controlled regulation of Wnt- and Bmp signaling by the SO specifies anterior head structures by blocking both signals. In the posterior region it allows the induction of trunk structures by preventing Bmp but allowing Wnt signaling.

The process of gastrulation

Gastrulation is defined by a controlled cell-cell-movement of the three germ-layers into the correct position for further differentiation and development. During this process the mesoderm invaginates into the embryo until it lays down between the inner endodermal and the outer ectodermal cells. The process of gastrulation starts within 10 hours after fertilization with the SO forming at the dorsal lip (Gilbert 2010).

Shortly before gastrulation starts the pharyngeal endoderm implements a vegetal rotation causing a relocation to the blastocoel roof plate directly above the mesodermal cells. Subsequently the dorsal lip forms where the cells move into the embryo. To ensure this, the cells at the lip have to change their shape dramatically. They form polarized endodermal bottleneck cells that shift the main part of their cell into the embryo by constriction. Thereby they remain in contact with the superficial layer in a narrowed region. This cell change is crucial for forming the blastoporus and initiating gastrulation. By contacting the extracellular matrix, the bottleneck cells migrate first along the blastocoel roof plate and bring the pharyngeal endoderm towards the anterior region of the embryo. The enclosing mesoderm of the involuting marginal zone consisting of head and chorda mesoderm is passively pulled by the migrating cells. Before the involution of the marginal zone, the mesoderm changes its arrangement. Radial intercalation of the mesodermal cells forms a small layer of elongated cells along the AP axis. This process is called convergent extension (CE). At this time the bottleneck cells are no longer the driving force of gastrulation. By now the converging mesoderm is sliding the pharyngeal endoderm towards the anterior region of the embryo. Simultaneously the outer ectodermal cells migrate around the embryo by epiboly. In the course of this transformation the ectodermal cells raise their proliferation rate and deep cells integrate into each other to form a two-layered cell organization. Furthermore, epiboly supports the invagination and CE of the involuting mesodermal

zone as it provides the formation of fibrils by fibronectin that forms the extracellular matrix (Gilbert, 2010).

Neurulation forms the central nervous system

Enclosed to gastrulation the neurulation begins. Neurulation is defined by the formation and closure of the neural tube to form the central nervous system. After neural induction by the SO, the neural plates arise and thicken in a bilateral symmetric manner to form the neural folds. As a result the neural groove is formed in the embryonic midline that later on forms the lumen of the neural tube. At this time it segregates the left and right neural plate. The cells of the neural plate start to move towards each other to fuse and form the neural tube. This happens differently between the posterior and the anterior neural tube closure (NTC). NTC starts posteriorly in the region that forms the spinal cord and the hindbrain. In the first phase the cells of the neural folds start to grow thin and extend by radial intercalation and form a monolayer structure. These cells then migrate mediolaterally to fuse and form the posterior part of the neural tube (Keller et al., 1992). In the anterior region that forms the fore- and hindbrain NTC occurs without mediolateral CE and is driven by radial intercalation through apical constriction (Keller et al., 1992; Darken et al., 2002; Goto and Keller, 2002 Wallingford and Harland, 2002; Lindqvist et al., 2010; Prager et al., 2017; Gilbert, 2010).

Left-right body axis development

The left-right (LR) body axis is the last one that becomes established during embryogenesis. It is defined by the position of the visceral organs, like the liver laying on the right, the gut coiling asymmetrically through the body cavity and the lung which consist of two lobes on the left and three on the right side. This wildtype arrangement of the inner organs is determined as *situs solitus*. Misplacement of the inner organs can lead to various phenotypes like *situs inversus totalis*, meaning a complete mirror image, or heterotaxia (*situs ambiguus*) where at least one organ is affected in its position or structure that could cause severe diseases or lethality (Sutherland & Ware, 2009).

For setting up the arrangement of the visceral organs that are asymmetrically distributed in the coelom of external bilateral symmetric organisms, the symmetry has to be broken. This event takes place during neurulation, where a leftward-fluid flow in most vertebrates leads to the asymmetric induction of the highly conserved Nodal cascade that regulates laterality determination.

The Nodal cascade

The Nodal signaling pathway is highly conserved throughout the animal kingdom and participates in many processes such as mesoderm induction and differentiation, endoderm induction, stem cell maintenance and left-right axis determination in chordates (Quail et al., 2013).

Nodal ligands are cytokines which belong to the transforming-growth-factor beta (Tgf- β) family. The first Nodal ligand was identified in 1993 in mice by genetic screens with a rapid follow up of identification in zebrafish, chickens and frogs (Zhou et al., 1993, Toyama et al., 1995; Smith, 1995; Jones et al., 1996). Interestingly, in contrast to mice, chickens and humans, where only one ligand is present, lower vertebrates like *D. rerio* and *Xenopus* exhibit multiple Nodal ligands (Schier, 2003).

After secretion, Nodal ligands can act as long-range signals and thereby operate in a dose-dependent manner. Signaling occurs when Nodal binds to its receptor which is a complex of type II serine-threonine kinase receptors ActRII or ActRIIB and the type I receptor ActRIB/ALK4 (Reissmann et al., 2001, Yan et al., 2002, Yeo and Whitman, 2001). Furthermore, Nodal ligands need the EGF-CFC co-receptor for providing signaling as it ensures the specificity for interaction with the ActRIB receptor (Chen & Shen, 2004; Reissmann et al., 2001; Yeo and Whitman, 2001; Yan et al., 2002).

Binding of the ligand to its receptor leads to a downstream activation of Nodal signaling by phosphorylation of the receptor associated Smads (R-Smad) Smad2 and Smad3 (Massagué, 1998). In turn, phosphorylated Smad2/Smad3 form a complex with the mediator-Smad Smad4 and enter the nucleus. This complex then interacts with the co-transcription factors FoxH1 and Mixer to form a transcription initiation complex and induces the expression of Nodal target genes like *nodal1*, *lefty2*, *pitx2* or *foxa2* (Germain et al., 2000; Randall et al., 2004 Dickmeis et al., 2001; Whitman, 2001). By the induction of *lefty2*, Nodal activates its own negative feedback inhibitor. Lefty2 antagonizes Nodal signaling by interacting with the EGF-CFC co-receptor as well as

with Nodal itself. This interaction prevents the complex formation between receptor and ligand and limits *nodal* expression and signaling in time and space (Meno et al., 1999; Chen and Shen, 2004; Cheng et al., 2004). The homeobox transcription factor *pitx2*, however, continues to be expressed in left organ anlagen and is thought to govern asymmetric organ morphogenesis (Yoshioka et al., 1998; Logan et al., 1998; Shiratori et al., 2014).

To generate the asymmetric position of the visceral organs and thereby defining the LR body axis, the unilateral activation of the Nodal cascade on the left side is crucial. This is initiated in most vertebrates by a transient structure in the posterior part of the embryo that is defined as the left-right organizer (LRO). The LRO generates a leftward fluid flow which becomes translated into genetic information on the prospective left side of the embryo (Nonaka et al., 1998; Okada et al., 2005; Schweickert et al., 2007; Oteiza et al., 2008).

Leftward-fluid flow at the LRO breaks the bilateral symmetry

The LRO is a transient triangular ciliary structure in the posterior part of the archenteron of neurula stage embryos. The cilia of the central cells produce a leftward-fluid flow by rotating counterclockwise, which becomes sensed by the left flow-perceiving cells. The lateral LRO flanking cells express the Tgf- β /Wnt/Bmp antagonist *dand5*, *nodal1*, the RNA-binding protein *bicaudal1* (*bicc1*) and *gdf3* (*growth differentiation factor 3*) in a bilateral symmetric manner in preflow stages (st. 14 – 17) (Bell et al., 2003; Vonica & Brivanlou 2007; Vick 2009; Maisonneuve et al., 2009). Thereby Dand5 binds Nodal1 extracellularly and represses Nodal signaling on both sides of the early embryo (Piccolo et al., 1999; Vonica & Brivanlou 2007). This interaction has to be prevented on the left side for symmetry breakage and is initiated by the leftward flow (Blum et al., 2007; Schweickert et al., 2007; Schweickert et al., 2010). The mechanism of flow sensing can be explained by the two-cilia model (Tabin & Vogan 2003), where kinking of lateral non-motile cilia on the left side leads to calcium²⁺ (ca²⁺) influx by Pc2 into these cells (McGrath et al., 2003; Sarmah et al., 2005; Tanaka et al., 2005). However, ca²⁺ signaling is important for repressing *dand5* and in turn for the induction of the Nodal cascade (Yoshida et al., 2012; Takao et al., 2013). The exact mechanism behind this is up to now only partially understood. Sensing of flow on the left side leads to post-transcriptional repression of *dand5* via the proximal region of its 3'UTR which is

regulated by the RNA binding protein Bicc1. Thereby Bicc1 has two functions during the symmetry breakage event. In preflow stages, Bicc1 regulates the mRNA stability of *dand5* directly and of *nodal1* indirectly in lateral LRO cells. After the leftward-fluid flow occurred, Bicc1 interacts with a more distal region of the proximal part of the *dand5* 3'UTR that leads to post-transcriptional repression. This function of Bicc1 on the left side seems to be Ca^{2+} dependent (Getwan 2015; Maerker et al., 2020 in revision). Consequently, in post-flow stages, Dand5 activity on the left side is reduced and Nodal1 is released of repression (Fig. 1, (4)). Nodal1 then dimerizes with Gdf3 (Gdf1 in mouse) that initiates long-range signaling by the usage of sulfated proteoglycans in the extracellular matrix to be transferred to the left LPM (Rankin et al., 2000; Eimon & Harland, 2002; Vonica & Brivanlou, 2007; Tanaka et al., 2007; Oki et al., 2007; Marjoram & Wright, 2011; Peterson et al., 2013).. Here, Nodal1 induces its own feedback loop (Fig.1, (5)) and the expression of *pitx2* that triggers the asymmetric position of the visceral organs (Fig.1, (6) (Yoshioka et al., 1998; Logan et al., 1998; Shiratori et al., 2014).

To ensure the symmetry breaking mechanism operates correctly, the precursor tissue of the LRO, the superficial mesoderm (SM), has to be specified during early gastrulation.

Specification of the superficial mesoderm

The LRO of *Xenopus* arises from the SM which is part of the outer layer of the dorsal mesoderm anteriorly to the SO (Fig. 1, (1)). Those cells involute at the end of gastrulation and line up with the roof of the gastrocoel (Fig.1, (2)). This structure constitutes to the transient LRO until the superficial cells ingress into the noto- and hypochord and into the somites (Shook et al., 2004).

Crucial for the specification of the SM is the induction of the Forkhead box transcription factor J1 Foxj1 in early gastrulae. *foxj1* represents the master regulator gene for motile cilia and becomes induced by canonical Wnt and Fgf (fibroblast growth factor) signaling (Glinka et al., 1996; Smith et al., 1995; Stubbs et al., 2008; Yu et al., 2008; Walentek et al., 2013; Schneider et al., 2019). In early gastrula stage embryos, Wnt signaling orchestrates the induction of *nodal3*, both in the SO and the SM, in a Serotonin-dependent manner (Smith et al., 1995; Glinka et al., 1996; Beyer et al., 2012). Nodal3

synergizes with the ca^{2+} -channel Pc2 and induces together with Fgf signaling the expression of *foxj1* in SM (Vick et al., 2018; Schneider et al., 2019).

After specification of the SM the tissue invaginates into the embryo at the end of gastrulation and forms the transient LRO. The LRO consists of medial flow-generating cells that harbor motile, posterior polarized cilia that rotate counterclockwise (Antic et al., 2010). These cells are part of the superficial layer of the notochord and ingress into the hypo- and notochord after leftward flow. The flanking region of the LRO on the right and left side make up the sensory LRO (sLRO) cells, which are of somitic origin in *Xenopus* (Shook et al., 2004). These cells are characterized by non-polarized and immotile cilia which are thought to bend by flow and finally induce symmetry breakage (McGrath et al., 2003; Boskovski et al., 2013; Tavares et al., 2017). How the sLRO cells become specified and separated from the flow-generating cells is less understood. Recent studies demonstrated, that this process might depend on Fgf signaling, including an interaction with Pc2 (Schneider et al., 2019; Sempou et al., 2018).

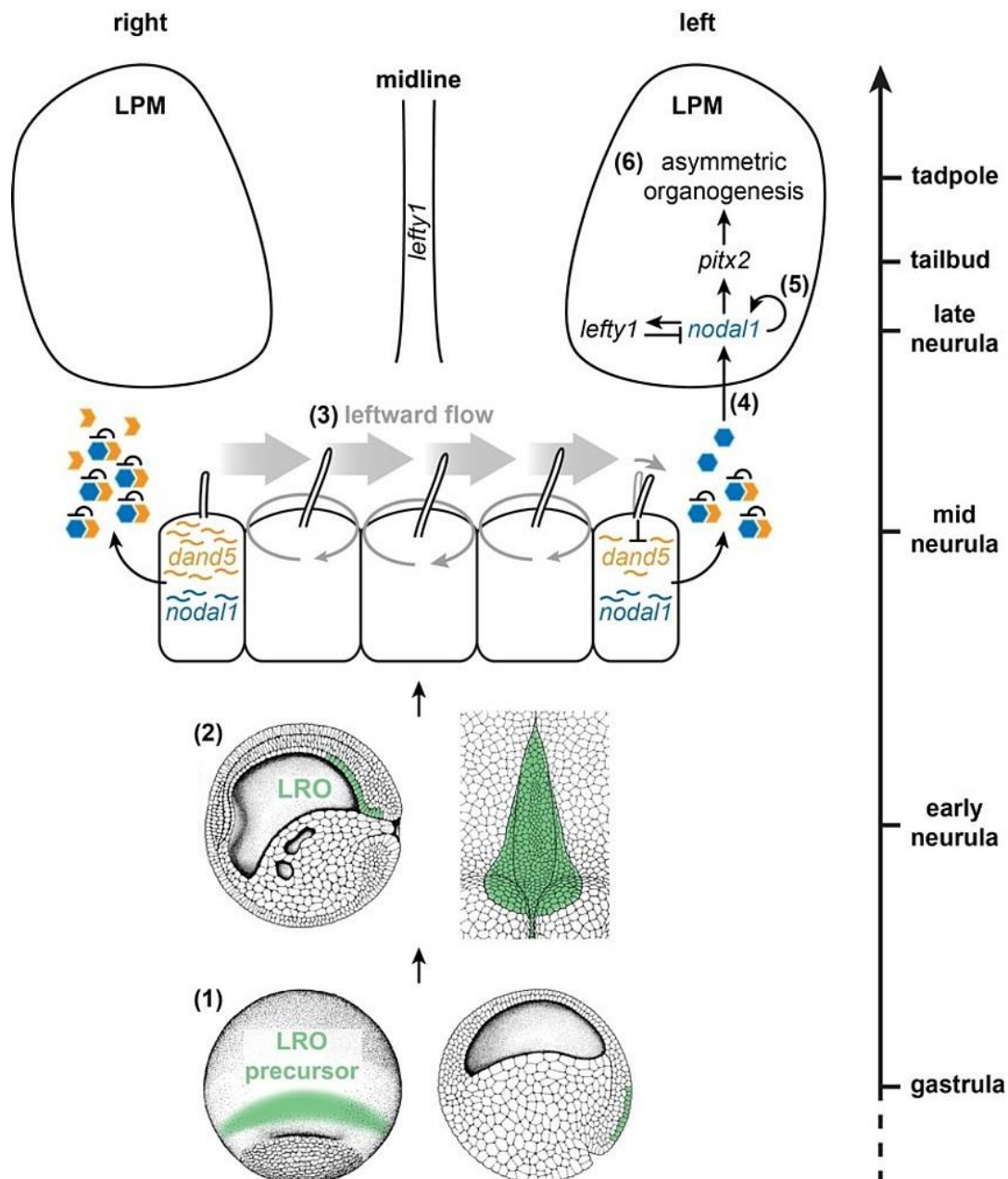


Figure 1: Symmetry breakage in *Xenopus laevis*

At onset of gastrulation, the SM (green) the precursor tissue of the *Xenopus* LRO, becomes specified in the dorsal midline (1). In course of gastrulation, the SM lines up the archenteron roof in the posterior part of the embryo and forms the ciliated LRO at early neurulation (2). At mid neurula, posterior polarized cilia produce a leftward-fluid flow (3) that becomes sensed by the left marginal cells. These cells express the Tgf- β growth factor *nodal1* (blue) and its antagonist the Tgf- β /Wnt/Bmp inhibitor *dand5* (yellow). Flow-sensing leads to loss of Dand5 activity on the left side. Nodal1 is released of repression and becomes transferred into the left lateral plate mesoderm (4). In the left LPM, Nodal1 activates its' own feedback loop (5) and the induction of *pitx2* that regulates asymmetric organogenesis (6). This process is prevented on the right side by the presence of Dand5 (Picture adapted from Blum & Ott, 2019).

The planar cell polarity pathway

Planar cell polarity (PCP) is defined by the orientation of a cell or cilia along a tissue axis in a specific direction. The polarity within a cell is important to coordinate cellular behavior like directed movement of cells or ciliary outgrowth and beating. A considerable example for oriented cellular migration is the process of gastrulation. Mesodermal cells become polarized and migrate towards the embryonic midline that leads to blastoporal closure, thinning and lengthening of the embryo. Besides the induction of polarity within a cell, PCP regulates the positioning of a cilium that is crucial for its function. Cilia can act as an antenna for the reception and transmission of extracellular signals that lead to a tissue and pathway dependent readout. Misregulation can impair sensing of extracellular signals, like e.g. the kinocilia in the inner ear resulting in deafness, or affect the transport of fluids like the circulation of the cerebrospinal fluid in the ventricle of the brain or mucociliary clearance in the lung (Littlewood & Müller, 2000; Worthington & Cathcart 1963; Antunes & Cohen 2007).

The generation of planar cell polarity is regulated by the intercellular asymmetric distribution of several key components of the PCP pathway. Initiating PCP can be regulated by the core PCP system throughout the animal kingdom and/or the global PCP/Dachsous/Fat system that is mainly characterized in *Drosophila*. The purpose of both systems is to polarize cells and tissues by interacting with extracellular cues (Axelrod, 2009; Goodrich & Strutt, 2011; Peng & Axelrod, 2012). It is not clarified if the core and the global PCP pathway act independently or facilitate each other. Current studies verified that they can act autonomously as well as cross talk by the global system that can promote the transport of Frizzled along microtubules (Casal et al., 2006; Brittle et al., 2012; Sagner et al., 2012; Merkel et al., 2014; Harumoto et al., 2010). Evidences for the existence of the global system in vertebrates occur but are less described, though protein conservation of this system in vertebrates suggests that they might act in a related way (Saburi et al., 2008; Saburi et al., 2012; Sharma & McNeil 2013; Wallingford 2012).

The core PCP pathway in vertebrates

The core PCP pathway, also known as Fz/PCP pathway, consists of 6 main players. Three of those are membrane-spanning proteins, the receptor Fz, the transmembrane

protein Vangl and the atypical cadherin Fmi. The other three, Dvl, Pk and Dg, form the cytoplasmic components of this pathway. Fz, Dvl and Dg are localized to the distal part of the cell, while Vangl and Pk are proximally and Fmi is symmetrically distributed (Vinson & Adler, 1987; Krasnow et al., 1995; Tree et al., 2002; Wolff & Rubin, 1998; Bastock et al., 2003; Das et al., 2002).

PCP can be regulated by long-range or short-range signaling. For long-range signaling non-canonical Wnt ligands like Wnt11 or Wnt5 have to bind to the intercellular cysteine-rich domain of Fz for pathway induction (Gao et al., 2011; Wu et al., 2013; Qian et al., 2007; Wallingford & Harland, 2001; Tada et al., 2000). Short-range signaling can occur in the absence of Wnt ligands. When Fmi is found between two neighboring cells they interact with each other, as well as when Fz is on the distal side of one cell with Vangl on the proximal side of the adjacent cell. In turn both complexes stabilize each other. Intracellularly, Dg and Pk have an antagonizing function while both are able to interact with Dvl. While Dg stabilizes the Fz/Dvl complex, Pk recruited to the membrane by Vangl, destabilizes Dvl activity. As a consequence an asymmetric distribution is arranged both on the proximal side of the cell by the presence of the Vangl/Pk complex and distally by the Fz/Dg/Dvl complex. This organization can either lead to cytoskeleton rearrangement or to a transcriptional response downstream of Dvl. For a cytoskeleton rearrangement, Dvl has to interact with several downstream factors of small GTPases of the Rho family (Rho, Rac and Cdc42), as the Rho-associated kinase Rok. This might be mediated by Daam1 (Marlow et al., 2002; Winter et al., 2001, Habas et al., 2001; Miller et al., 2011). In combination with JNK/MAPK and Jun-Fos transcription factors, Dvl is able to induce a transcriptional response (Boutros et al., 1998; Weber et al., 2000; Weber et al., 2008).

PCP in cilia polarization

The proper arrangement of cilia within a tissue or a cell is a major step to ensure functionality. PCP signaling provides actin assembly at the apical cortex and basal body (BB) orientation. In multiciliated cells like the *Xenopus* epidermis, an *in vivo* model for the human airway, Dvl is apically distributed and regulates actin assembly and the transport of BBs to the apical surface (Park et al., 2008). At the apical cell cortex the BBs exhibit two polarized structures, a posteriorly oriented basal foot and an anteriorly ciliary rootlet (Park et al., 2005; Park et al., 2006; Park et al., 2008). This orientation

allows axonemal outgrowth of cilia and structural support by anchoring to the sub-apical actin network (Werner et al., 2011).

In mono-ciliated cells like those of the LRO, the PCP pathway regulates the posterior polarization of cilia which is crucial for generating the leftward fluid flow. The core proteins Vangl and Pk localize anteriorly at the membrane in LRO cells of mice and *Xenopus*, while Dvl is distributed posteriorly (Antic et al., 2010; Hashimoto et al., 2010). Disruption of one of these components led to LR defects attributed to loss of cilia polarization within the LRO. In *Xenopus*, the upstream Wnt ligand Wnt11b seems to be crucial for cilia orientation in the LRO (Walentek et al., 2013). However, in mice the interaction of the non-canonical Wnt ligands Wnt5a/Wnt5b with their inhibitors of the Sfrp family (secreted frizzled related proteins) - both forming a gradient along the embryonic AP axis - restricts Wnt5a/Wnt5b expression posteriorly to the LRO cells. There it regulates BB docking and posterior polarization of cilia by the PCP pathway (Minegishi et al., 2017).

PCP regulates gastrulation and neural tube closure

The main driving force for gastrulation and neural tube closure is provided by PCP signaling that regulates apical constriction and CE. Gastrulation is initiated by the formation of endodermal bottleneck cells at the dorsal lip of the embryo that undergo apical constriction (Hardin & Keller, 1988). These cells elongate while they reduce their apical surface and shift their main part into the embryo. This process is regulated by actomyosin contractility and the core PCP protein Vangl2 in *Xenopus* (Lee & Harland, 2007; Ossipova et al., 2015). At the same time mesodermal cells start to migrate towards the embryonic midline in anterior direction by mediolateral intercalation. Before these cells start to migrate, they expose lamellipodia in random orientation. This rapidly changes in a bipolar manner by reorientation of the protrusions. The protrusions align towards the embryonic midline and towards the neighboring mesodermal cells. The connection between these cells enables the generation of traction force for mediolateral intercalation (Keller et al., 2000; Wallingford et al., 2002). The polarization and orientation of the lamellipodia in mesodermal cells and thereby CE depends on the localization of the core PCP proteins Dvl and Vangl2 in *Xenopus* (Wallingford et al., 2000; Goto & Keller, 2002, Park et al., 2005).

Even the attached neurulation requires PCP signaling along the AP axis in two different manners. Posteriorly, NTC is regulated by CE while anteriorly radial intercalation drives NTC. Radial intercalation is provided by apical constriction that requires the expression of Vangl2 at the apical tip. This distribution organizes the microtubule cytoskeleton apicobasally which allows cells to elongate by reducing the apical surface and enlarging the basal side. In turn these cells intercalate radially and close the anterior neural tube (Lee et al., 2007; Ossipova et al., 2015; Prager et al., 2017).

Aim of this work

One of the primary processes during early embryonic patterning is the establishment of the three body axes that form a bilateral symmetric organism. While the AP- and DV-axis are externally visible, the LR body axis is concealed since it is defined by the orientation of the internal organs. The aim of the present work was to address the function of *gooseoid* during AP- and DV- axis development and of *myosin1d* and *dmrt2* during LR body formation in *Xenopus laevis*.

The development of the AP- and DV-axis depends on the induction of the SO that represents the major signaling center for primary axis induction. A key regulator in the early SO is the transcriptional repressor of the *bicoid* subfamily of the paired homeobox family *gooseoid* (*gsc*). Gsc acts in a negative autoregulatory loop and ventral misexpression induces a secondary body axis. Surprisingly, the loss of function in frogs or mice had no impact on early development which compromised the early function of Gsc in axis development. Interestingly, overexpression of *gsc* in *Xenopus* and mice impaired the elongation of the notochord (Deissler, 2002; Andre, 2004; Ulmer, 2008, 2012). In addition, the *gsc* gain of function in *Xenopus* led to severe gastrulation and neural tube closure defects, while the function of the *Drosophila gsc* was restricted to secondary body axis induction (Ulmer 2008). These observations elevated the presumption that Gsc attained a novel function during vertebrate development in regulating PCP-mediated CE. This hypothesis should be analyzed *in vivo* by gain and loss of function experiments of *gsc* in the embryonic midline and neural tissue of *Xenopus* embryos. Combinatorial experiments with several factors of the Wnt/PCP pathway should clarify if Gsc interacts with PCP signaling. Further, analysis of explants that are attributed to elongation should highlight if the *gsc* GOF is able to repress PCP

ex vivo. These studies could be insightful for understanding the role of Gsc in the SO and during DV- and AP-axis patterning.

Two genes, *myosin1d* (*myo1d*) and *doublesex and mab3-related transcription factor 2* (*dmrt2*), have been recently identified to be involved in LR axis determination. The unconventional Myo1d, an actin-based motor protein, arranges the dextral orientation of the tubular organs in the invertebrate *Drosophila melanogaster* by interfering with adherens junctions and the core and global PCP pathway (Hozumi et al., 2006; González-Morales et al., 2015). This observation was exciting as the symmetry breaking mechanism in *Drosophila* occurs independently of leftward-flow and does not reflect asymmetric gene expression but rather dextral morphogenesis of tubular organs. The importance of the cytoskeleton for laterality determination had already been described for the several model organisms like the freshwater snail *Lymnaea stagnalis* or the chicken. Thus it was of high interest if Myo1d represents a component of the ancestral symmetry breaking mechanism that became conserved along invertebrates and vertebrates. The role of *myo1d* during LR determination should be analyzed in a vertebrate model organism where symmetry breakage is flow-dependent. Several loss of function approaches should highlight if Myo1d is involved in the arrangement of the inner organs and moreover if it intervenes with PCP signaling in *Xenopus laevis*.

The transcription factor Dmrt2 represents a gene of ancestral sex determination in *Drosophila* and *C.elegans* that became conserved across phyla. Besides this function, Dmrt2 was the first protein of the *dmrt* family identified to have a function besides sexual development (Meng et al., 1999). Recent studies in zebrafish showed that *dmrt2* is involved in somitogenesis and in laterality determination by regulating the expression of the *forkhead box transcription factor j1* (*foxj1*), the master regulator of motile cilia (Meng et al., 1999; Saude et al., 2005; Pinto et al., 2018). That these processes are linked has often been proposed as impaired somitogenesis can include laterality defects and *vice versa*. How this correlates has not been examined more in detail and became mostly explained by retinoic acid (RA) signaling that is thought to protect the somites from asymmetric cues derived from the LPM. We hypothesize, that Dmrt2 links these processes at the onset of gastrulation independently of RA. The lateral flow-sensing LRO cells in *Xenopus* are of somitic fate (Shook et al., 2004) and how they become specified and separated from the flow-generating cells is less understood. Based on the somitic origin of the sLRO cells and that mesodermal patterning is

important for specifying the SM, we speculate that the induction of the paraxial mesoderm might be crucial for the lateral sLRO cells. This step might be facilitated by *Dmrt2* that could regulate the early specification of the somitogenic lineage in the *Xenopus* gastrulae and thereby link somitogenesis to LR axis induction. The analysis of early paraxial mesodermal and laterality marker genes after *Dmrt2* depletion should elucidated if *dmrt2* associates with these processes and has a conserved function during symmetry breakage.

**Original research Chapter I:
AP- and DV-axis development**

**A novel role for the organizer gene Goosecoid as an inhibitor
of Wnt/PCP-mediated convergent extension in *Xenopus* and
mouse**

SCIENTIFIC REPORTS

OPEN

A novel role of the organizer gene *Gooseoid* as an inhibitor of Wnt/PCP-mediated convergent extension in *Xenopus* and mouse

Received: 01 August 2016
Accepted: 18 January 2017
Published: 21 February 2017

Bärbel Ulmer^{1,*,†}, Melanie Tingler^{1,*,†}, Sabrina Kurz^{1,*,†}, Markus Maerker^{1,*,†}, Philipp Andre¹, Dina Mönch¹, Marina Campione^{1,‡}, Kirsten Deißler¹, Mark Lewandoski², Thomas Thumberger^{1,§}, Axel Schweickert¹, Abraham Fainsod³, Herbert Steinbeißer⁴ & Martin Blum¹

Gooseoid (*Gsc*) expression marks the primary embryonic organizer in vertebrates and beyond. While functions have been assigned during later embryogenesis, the role of *Gsc* in the organizer has remained enigmatic. Using conditional gain-of-function approaches in *Xenopus* and mouse to maintain *Gsc* expression in the organizer and along the axial midline, neural tube closure defects (NTDs) arose and dorsal extension was compromised. Both phenotypes represent convergent extension (CE) defects, arising from impaired Wnt/planar cell polarity (PCP) signaling. Dvl2 recruitment to the cell membrane was inhibited by *Gsc* in *Xenopus* animal cap assays and key Wnt/PCP factors (*RhoA*, *Vangl2*, *Frickle*, *Wnt11*) rescued *Gsc*-mediated NTDs. Re-evaluation of endogenous *Gsc* functions in MO-mediated gene knockdown frog and knockout mouse embryos unearthed PCP/CE-related phenotypes as well, including cartilage defects in *Xenopus* and misalignment of inner ear hair cells in mouse. Our results assign a novel function to *Gsc* as an inhibitor of Wnt/PCP-mediated CE. We propose that in the organizer *Gsc* represses CE as well: *Gsc*-expressing prechordal cells, which leave the organizer first, migrate and do not undergo CE like the *Gsc*-negative notochordal cells, which subsequently emerge from the organizer. In this model, *Gsc* provides a switch between cell migration and CE, i.e. cell intercalation.

During development, invertebrate and vertebrate embryos alike elongate and narrow their anterior-posterior (AP) axis by convergent extension (CE). CE is driven by intercalation of bipolar cells perpendicular to the previously established AP axis, necessitating a perfect coordination between spatial cues and cellular behavior. In *Drosophila* it has been shown that positional AP information, encoded by *Eve*, *Runt* and localized *Toil*-receptor expression, is directly translated into germ band CE¹. Likewise, AP-patterning was shown to be directly linked to CE movements in explanted chordamesoderm of *Xenopus* embryos². Molecular cues, which control and orient CE relative to the AP axis, have not been described in vertebrate embryos. How the spatial patterning is maintained and reinforced in the highly dynamic environment of the elongating and developing vertebrate embryo has yet to be defined.

The vertebrate body plan is established during gastrulation through the activity of the primary embryonic organizer (Spemann organizer), a specialized group of cells located at the amphibian dorsal lip of the blastopore

¹University of Hohenheim, Garbenstr. 30, 70599 Stuttgart, Germany. ²Genetics of Vertebrate Development Section, Cancer and Developmental Biology Lab, National Cancer Institute, National Institutes of Health, Frederick, MD 21702, USA. ³Department of Developmental Biology and Cancer Research, Institute for Medical Research Israel-Canada, Hebrew University, Jerusalem 9112102, Israel. ⁴Institute of Human Genetics, University Hospital Heidelberg, Im Neuenheimer Feld 366, 69120 Heidelberg, Germany. [†]Present address: Department of Experimental Pharmacology and Toxicology, Cardiovascular Research Center, University Medical Center Hamburg-Eppendorf, 20246 Hamburg, Germany. [‡]Present address: CNR-Neuroscience Institute, Department of Biomedical Sciences, University of Padova, Italy. [§]Present address: Centre for Organismal Studies (COS) Heidelberg, Heidelberg University, Im Neuenheimer Feld 230, 69120 Heidelberg, Germany. *These authors contributed equally to this work. Correspondence and requests for materials should be addressed to M.B. (email: martin.blum@uni-hohenheim.de)

or homologous structures in other vertebrates (node in birds and mammals, embryonic shield in fish³). Organizer transplantation to the opposite, ventral side of the gastrula embryo induces the formation of a secondary axis, in which neighboring ventral cells adopt both a dorsal fate and undergo gastrulation movements⁴. Expression of the homeobox transcription factor gene *Gooseoid* (*Gsc*) marks Spemann's organizer in vertebrates and beyond^{5,6}. Upon ectopic expression on the ventral side, i.e. opposite to its normal site of action, *Gsc* efficiently induces the formation of secondary embryonic axes in *Xenopus*⁷. This remarkable ability to mimic Spemann's organizer in gain-of-function experiments is readily explained by its well characterized ability to transcriptionally repress target genes identified in mouse, frog and zebrafish, including *Wnt8a* and *BMP4* pathway components^{8–18}. In stark contrast, *Gsc* knockout mouse embryos lack gastrulation defects^{19,20}, as do frog and fish embryos with impaired *Gsc* function^{15,16,21,22}. This lack of a gastrulation phenotype is likely explained by functional redundancy with other factors expressed in the organizer, which await identification.

Yet there may be additional *Gsc* functions in the organizer. A number of studies suggested a general role of *Gsc* in cell migration during development and disease that is not explained by its role as a transcriptional repressor of BMP4 and Wnt8 targets. Lineage labeling and video microscopy of *Gsc*-injected embryos revealed enhanced anterior migration of posterior cells²³. *Gsc* was also able to enhance the migratory behavior of cultured embryonic frog head mesenchymal cells²⁴. In tumor cells, *Gsc* expression correlated with enhanced migratory activity as well²⁵. Together these data point to a possible role of *Gsc* in mediating cellular behavior.

The early embryonic expression pattern of *Gsc* in vertebrate embryos is in agreement with such a function. The initial transcription in the organizer tissue itself is very transient. As axial mesodermal cells (prechordal plate and notochord) begin to leave the organizer in rostral direction, *Gsc* expression remains active in prechordal cells but ceases in the resident organizer tissue and the notochord^{10,26,27}. Segregation of organizer-derived cells into these two cell populations is accompanied by differences in cell behavior and gene expression: *Gsc* marks the prechordal cells, characterized by single cell migration, while *Brachyury* is expressed and instrumental for CE in the notochord^{28–31}.

Based on this dichotomy we hypothesize that *Gsc* plays a role in prechordal cells to promote migration and to inhibit CE. In order to test this hypothesis, we performed conditional gain-of-function experiments in mouse and *Xenopus*. Our experiments resulted in CE-phenotypes in both species, including neural tube closure and axial elongation defects. Rescue of *Gsc*-induced CE phenotypes by co-expression of planar cell polarity (PCP) pathway components suggested a novel function of *Gsc* as a negative regulator of PCP-mediated CE. Loss-of-function experiments showed that *Gsc* impaired bipolar elongation of cells in Meckel's cartilage in *Xenopus* and affected the alignment of hair cells in the inner ear of *Gsc* knockout mouse embryos. Based on these results we propose a novel role of *Gsc* as inhibitor of PCP-mediated CE.

Results

Sustained *Gsc* expression along the axial midline interferes with CE and causes neural tube and blastopore closure defects in *Xenopus*.

Gsc expression in the organizer ceases with the exit of the first cell population, which migrates anteriorly and constitutes the prechordal mesoderm. Our hypothesis predicts that a sustained activity of *Gsc* along the subsequently emerging notochord interferes with the cellular behavior of these cells, namely CE. In order to ectopically express *Gsc* in a tightly controlled temporal and spatial manner, we employed a previously described inducible *Gsc* protein³². In short, a construct was used, in which the *Gsc* coding sequence was fused to the ligand binding domain of the glucocorticoid receptor (GR). In the absence of the synthetic ligand dexamethasone (dex), *Gsc*-GR localizes to the cytoplasm and remains inactive, while ligand addition results in a conformational change, nuclear entry and onset of *Gsc* function as a transcriptional repressor³². Functionality of the construct was demonstrated by dex treatment of ventrally injected specimens, which led to double axis induction in 14/24 cases, i.e. at frequencies described previously³² (not shown).

Targeting of *Gsc*-GR to the dorsal midline was achieved by microinjection of synthetic mRNA into the marginal region of the two dorsal blastomeres of the 4-cell embryo (Fig. 1A). Analysis of a co-injected lineage tracer confirmed delivery to the notochord and floor plate, which cannot be targeted separately in such experiments (not shown). No phenotypic changes were observed in the absence of dex (Fig. 1B,E), while ligand addition between cleavage and blastula stages (st. 6–9) resulted in a high percentage of embryos with neural tube closure defects (NTDs; Fig. 1C,E; Table S1). More severe blastopore closure defects (BPD³³) were observed as well (Fig. 1D,E; Table S1). In these cases, the dorsal midline was disrupted, which resulted in cup-shaped morphologies (Fig. 1D). The overall percentage of affected embryos dropped when dex was added during gastrulation, and very few malformations were recorded when *Gsc*-GR was activated during late gastrula/early neurula stages (Fig. 1E; Table S1 and data not shown). Development of BPD and NTD depended on the presence of the homeodomain (HD) as well as the paired-type DNA binding specificity of *Gsc* (lysine in position 50 of the HD), while the repression domain (eh1/GEH) was not required for NTD/BPD induction (Fig. 1E). A slight but non-significant delay in neural tube closure was observed in a proportion of specimens (not shown). Sustained *Gsc* expression along the dorsal midline thus interfered with blastopore and neural tube closure, processes known to depend on CE^{34,35}.

Xbra mRNA transcription serves as a readout of CE in the notochord, which narrows and lengthens concomitantly with neural tube closure³⁶. In order to assess whether notochordal CE was affected by sustained *Gsc* expression as well, we analyzed *Xbra* in less severely affected dex-treated specimens without BPD. In the absence of dex, the notochord was elongated and narrow during neurula stages. Activation of ectopic *Gsc* activity, however, resulted in shortened and widened *Xbra* expression domains (Fig. 1F–I), in agreement with CE defects in the notochord. While the expression level of *Xbra* in the notochord was not affected, we expected a repression of *Xbra* transcription by *Gsc* during gastrulation, in line with the reported role of *Gsc* as a repressor of *Brachyury* in the prechordal mesoderm^{10,11,13}. Analysis at late gastrula (stage 11) demonstrated that repression of *Xbra* in dex-treated specimens took place but was restricted to the injection site (Fig. 1K; 35/74, 47.3%). In the absence of

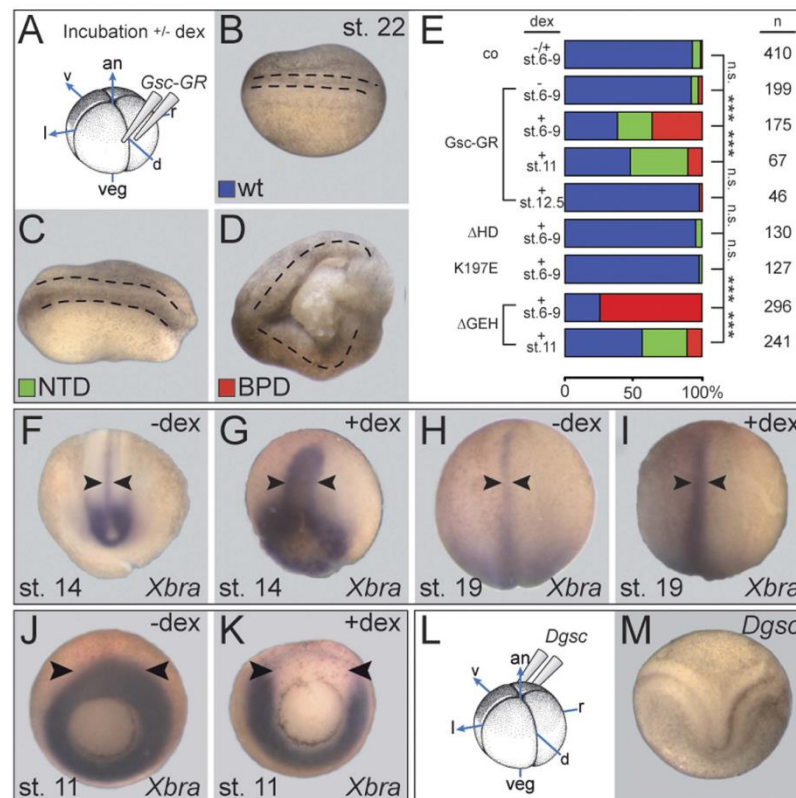


Figure 1. Gsc-mediated CE phenotypes in *Xenopus*. (A) Experimental design. Specimens were injected with *Gsc-GR* into the dorsal marginal region of the 4-cell embryo and cultured to the stages indicated, with or without addition of dex. (B–E) *Gsc-GR* induced NTD and BPD in whole embryos. Specimens were scored for wt appearance (blue; B), NTD (green; C) and BPD (red; D). Anterior is to the left in (B–D). (E) Compilation of results. Note that *Gsc-GR* caused CE phenotypes in a highly significant proportion of embryos, but only when activated before and during gastrulation. Note also that deletion of the homeodomain (Δ HD) or altering the DNA-binding specificity (K197E) prevented BPD/NTD-induction, while the repression domain GEH was not required for BPD/NTD. (F–I) Impaired CE of the notochord upon sustained dorsal *Gsc-GR* expression. Note that the notochord was wider and shorter in dex-treated (G,I) as opposed to untreated (F,H) specimens, both at stage 14 (F,G) and stage 19 (H,I). (J,K) Repression of *Xbra* transcription on the dorsal side upon *Gsc-GR* activation. (L,M) Double axis formation (M) following ventral injections of *Dgsc* mRNA into 4-cell *Xenopus* embryos (L).

dex, *Gsc-GR* injected embryos showed wildtype (wt) *Xbra* expression around the blastopore (arrowheads, Fig. 1J; 48/51, 94.1%).

In order to assess the effects of Gsc on CE in a semi-quantitative manner, we turned to Keller open-face explants, which have been used in the past to investigate notochord CE in *ex vivo* assays³⁷ (Fig. 2A). Dorsal marginal zone tissue was isolated at stage 10–10.5 from *Gsc-GR*-injected embryos, which were incubated in the presence or absence of dex from stage 6/7 onwards, and scored for CE when un-injected siblings reached stage 22 (Fig. 2A–C). CE was classified into three categories³⁸, with class 0 representing explants without elongation, class 1 containing elongated specimens, and class 2 explants which in addition displayed a constriction (Fig. 2B). In the absence of dex, more than 90% of explants elongated, with the majority of specimens falling into class 2 (36/51; 70.6%). In contrast, CE in dex-treated explants was severely compromised, with significantly reduced class 2 extensions (19/75), the relative majority of specimens elongating without constriction and about 25% not elongating at all (class 1; 36/75, 48%; Fig. 2C).

In order to investigate if and how sustained Gsc expression along the dorsal midline interfered with cell fate determination, i.e. with neural induction and mesodermal patterning, mRNA transcription of neural (*Ncam*) and

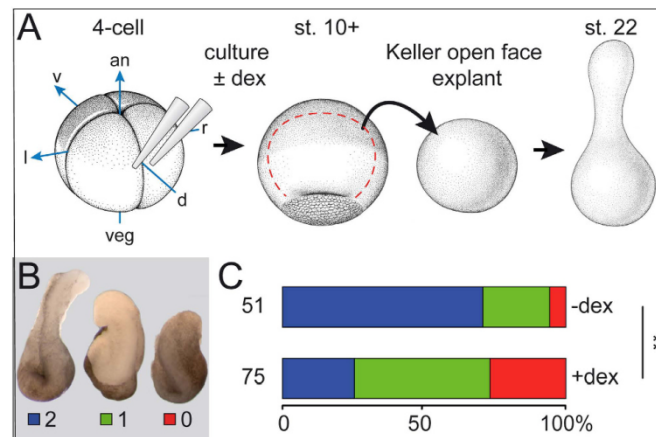


Figure 2. *Gsc* inhibits CE in Keller open face explants. (A–C) CE defects in Keller open face explants (schematically depicted in (A) upon activation of *Gsc-GR*. (B) Explants were classified as class 2 (blue) when extensions showed a constriction (left), as class 1 (green) when elongation occurred without constriction (middle), and as class 0 (red) when no elongation ensued (right)³⁸. an, animal; uninj., uninjected control; d, dorsal; l, left; r, right; v, ventral; veg, vegetal. (C) Summary of results.

somatic (*MyoD*) marker genes was analyzed. Both genes were expressed in specimens displaying BPDs upon dex treatment, even though somites did not epithelialize into the typical chevron-shaped patterns of control specimens (Fig. S1A–D). Sustained expression of *Gsc* on the dorsal side of *Xenopus* embryos thus did not interfere with specification of neural and mesodermal tissue, but inhibited CE in the notochord.

To analyze whether NTDs were caused by impaired CE as well, we investigated a potential role of *Gsc* in cell shape changes in the neuroectoderm. A prerequisite of CE is that cells polarize, i.e. elongate and adopt a bipolar morphology. *Gsc-GR* was targeted to the neuroectoderm by microinjecting synthetic mRNA to the A1 lineage of 8-cell embryos. Rhodamine dextran was co-injected as a lineage tracer, and injections were performed unilaterally in order to provide for an internal control on the un-injected contralateral side (Fig. 3A). Injected specimens were incubated until mid-neurula stages (stage 16), fixed and processed for cell shape assessment via phalloidin-staining of the actin cytoskeleton. In the absence of dex, cell morphologies appeared indistinguishable on both sides, while *Gsc* activation resulted in less elongated, rounder cells (Fig. 3B–D). To quantitate this effect, the length-to-width ratio was determined and expressed as elongation score, with a value of 1 representing a round cell and 0 a hypothetical elongated cell without width. The results from a representative specimen are depicted in Fig. 3E. On the *Gsc-GR* side a significant decrease of cells displaying a score of <0.5 was observed (14/105 or 13% on the *Gsc-GR* injected side, and 55/173 or 32% on the control side). In addition, unlabeled cells in between the injected rhodamine dextran-positive cells, which likely represent intercalation events, were observed on un-injected and untreated control sides (asterisks in Fig. 3B). Upon *Gsc* activation, no such unlabeled cells were found (Fig. 3C). In some explants, cell numbers were slightly (and non-significantly) reduced (not shown), however, cell proliferation and apoptosis were not affected by *Gsc-GR* activation (Fig. S2). The occasionally observed alterations of cell numbers may be caused by dex treatment, as previously reported³⁹. These results strongly suggest that NTDs in frog tadpoles were due to impaired CE as well, caused by a lack of bipolar cell polarization in *Gsc*-misexpressing neuroectodermal cells.

Finally, we wondered whether this novel function of *Gsc* as an inhibitor of CE was evolutionary conserved. *Gsc* represents an ancient member of the metazoan toolkit of animal embryogenesis which is present from radiata (cnidarians; hydra^{6,40}) to lophotrochozoans⁴¹, ecdysozoans (e.g. *Drosophila*) and deuterostomians alike. In all cases, the homeodomain and the N-terminal repression domain are highly conserved^{42,43}. We chose to analyze *Drosophila Gsc*, which was previously shown to be able to rescue the dorsal axis of UV-treated ventralized *Xenopus* embryos⁴⁴. In line with these experiments, *Dgsc* was able to induce double axis formation upon ventral injection (Fig. 1L, M; 24/25, 96%). Dorsal injections of *Dgsc*, however, had no effect on neural tube or blastopore closure (100/100, not shown), indicating that the novel function of *Gsc* described here as a repressor of CE arose later in evolution and may be independent of its function as a transcriptional repressor.

Expression of *Gsc* in the entire mouse primitive streak results in NTD and compromises axial extension. Next we wondered whether this novel role of *Gsc* to repress CE was conserved among the vertebrates. To investigate this possibility, we expressed *Gsc* in the entire primitive streak of mouse embryos using a conditional approach⁴⁵. Construct *T-Gsc* contained the 650 bp primitive streak enhancer of the mouse *Brachyury (T)* gene⁴⁶, followed by a floxed LacZ gene and the mouse *Gsc* coding sequence (Fig. 4A). Construct *mT-Gsc* was

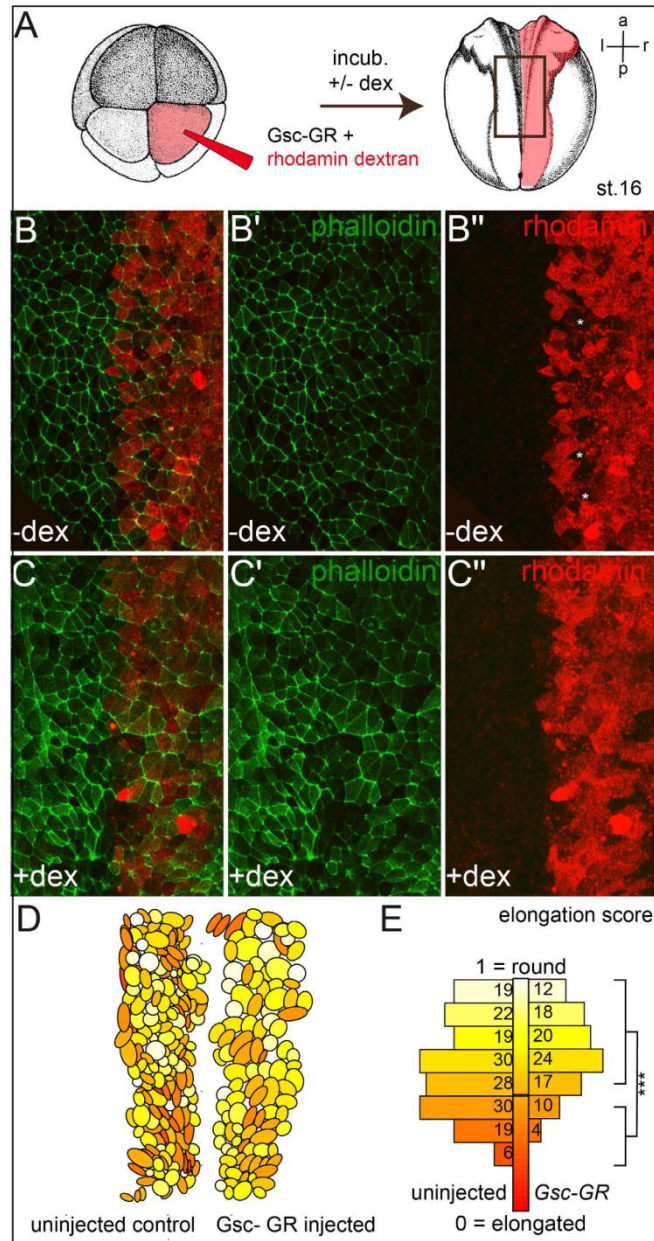


Figure 3. Gsc compromises bipolar elongation of neural plate cells. (A) Targeted injection scheme of *Gsc-GR* and lineage tracer (rhodamine red) into the right side of the neural plate (B,C). Drawings taken from Xenbase (www.xenbase.org/anatomy/alldevo.do)⁹⁷. (D,E) Analysis of cell elongation. The color gradient ranging from pale yellow (round, width = length, 1) to dark red (elongated, 0) exemplifies the change from bipolar cells on the un-injected (right) side towards rounded cells upon activation of *Gsc-GR* (D). (E) Significant decrease of percentage of elongated cells (elongation score < 1/2) after *Gsc-GR* misexpression. a, anterior; l, left; p, posterior; r, right.

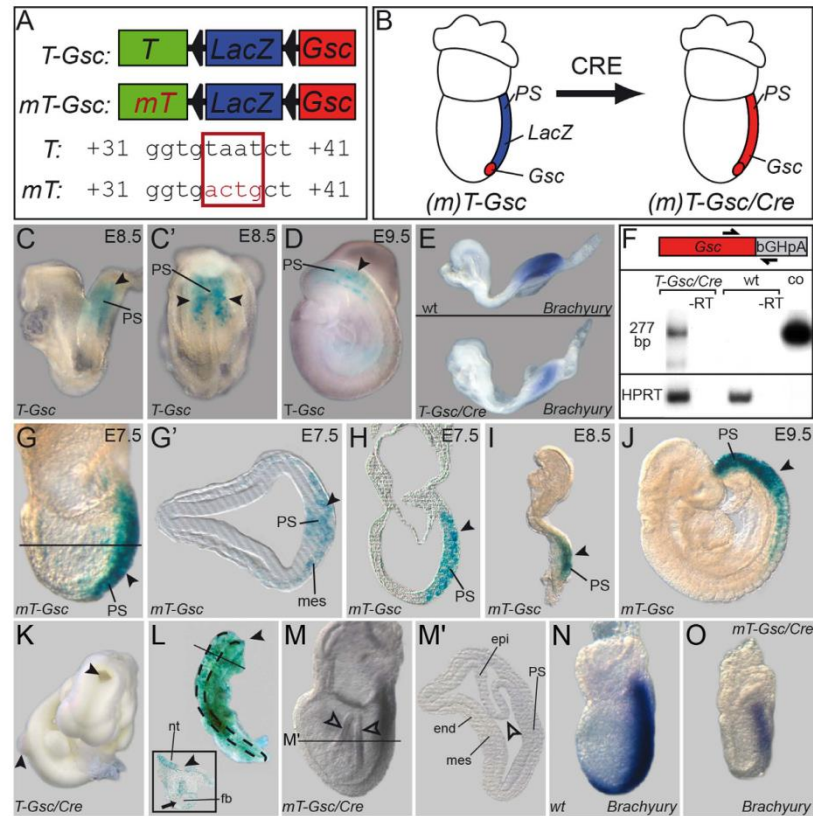


Figure 4. Gsc-mediated CE phenotypes in the mouse. Conditional misexpression of *Gsc* in the entire primitive streak of the mouse. (A) Constructs used to generate transgenic mouse lines. *T*, wt *Brachyury* streak enhancer; *mT*, mutant enhancer not repressed by *Gsc*; triangles, loxP sites. (B) Schematic depiction of *Gsc* (red) and *LacZ* (blue) expression at E7.5 before (left) and after (right) Cre-mediated recombination. (C,D) *LacZ* expression (arrowheads) in the primitive streak (PS) mesoderm of E8.5 (lateral view in C, posterior view in C') and E9.5 (D) *T-Gsc* embryos. (E) Reduced *Brachyury* mRNA expression upon transgene activation (*T-Gsc/Cre*, lower panel) compared to wt embryo (upper panel). (F) Detection of transgenic *Gsc* mRNA by RT-PCR from *T-Gsc/Cre* and wt E8.5 embryos. A 277 bp fragment specific for transgenic *Gsc* mRNA was amplified using a *Gsc* primer and a primer derived from the bovine growth hormone polyadenylation (bGHpA) signal present in the construct. Note that no signal was detected in wt embryos, and that a band identical in size to one amplified from the *T-Gsc* control plasmid was seen in *T-Gsc/Cre* embryos. (G–J) *LacZ* expression (arrowheads) in the PS mesoderm of E7.5 (G,H) plane of histological section G' indicated in (G), E8.5 (I) and E9.5 (J) *mT-Gsc* embryos. (K) Cranial and caudal NTD (arrowheads) in E10.5 *T-Gsc/Cre* embryo. (L) Craniorachischisis in chimeric E10.5 embryo generated from ES cells expressing *LacZ* and *Gsc*. Note that, except for the forebrain region (arrow; cross section shown in inset), the entire neural tube stayed open (arrowheads). (M) Malformation of *mT-Gsc/Cre* gastrula embryo. Note irregular folding of epiblast (open arrowheads). (M') Histological section at level indicated in (M). (N,O) Repression of *Brachyury* transcription in *mT-Gsc/Cre* (O) compared to wt (N) E7.5 embryos. end, endoderm; epi, epiblast; fb, forebrain; mes, mesoderm; nt, neural tube; PS, primitive streak.

identical, except that the *Gsc*-binding site in the *Brachyury* streak enhancer was mutated to prevent *Gsc*-mediated transgene repression¹¹. Thus, *T-Gsc* should result in moderate transgene expression, creating a scenario resembling the endogenous *Gsc* gene, where *Gsc* negatively autoregulates its own expression⁴⁷. *mT-Gsc*, in contrast, should allow for pronounced and sustained ectopic *Gsc* expression in the primitive streak mesoderm and descendants thereof. Transgenic *T-Gsc* mouse lines moderately expressed the *LacZ* reporter gene in the nascent primitive streak mesoderm from E7.5 onwards (Fig. 4C,D and data not shown). Much stronger *LacZ* staining was found in embryos of *mT-Gsc* lines, as expected (Fig. 4G–J).

To study the phenotypes induced by ectopic Gsc activity, mice were mated to the *deleter* line, which expresses the CRE-recombinase ubiquitously from blastocyst stages onwards⁴⁸ (Fig. 4B). First, the effects of moderate Gsc misexpression were assessed. Transgenic *T-Gsc* embryos analyzed from E7.0–E9.0 were morphologically indistinguishable from wt specimens (not shown). *Brachyury* expression in the primitive streak was reduced (Fig. 4E), demonstrating that the transgenic Gsc protein was functional. Transgenic Gsc expression was verified by RT-PCR (Fig. 4F). Phenotypic effects, however, were encountered in 44/197 (22.3%) of transgenic embryos analyzed at E9.5–E10.5. Affected specimens in all cases were characterized by cranial NTDs, while 10/44 in addition showed spina bifida (Fig. 4K). In order to prove the specificity of Gsc-induced NTDs, we generated chimeric mouse embryos by blastocyst injection of ES cells stably expressing Gsc and LacZ. Embryos were analyzed at E9.5–E10.5 to assess NTDs. In control chimeric embryos, derived from injection of ES cells expressing only LacZ, no NTDs were observed (not shown). *Gsc/LacZ* chimeras, in contrast, were characterized by a high percentage of NTDs which were encountered in 22/27 specimens (81.5%) generated in five experiments. Of these, two chimeric embryos were characterized by a lack of closure along the entire cranio-caudal axis except for the fore-brain region (craniorachischisis; Fig. 4L). Together these data demonstrated that NTDs induced from moderate level overexpression of Gsc in the primitive streak of transgenic *T-Gsc/Cre* embryos represented a Gsc-specific gain-of-function phenotype.

High level ectopic Gsc expression from Cre-mediated activation of *mT-Gsc* resulted in much earlier phenotypes. At E8.5 only very few but severely malformed embryos were recovered (not shown). E7.5 *mT-Gsc/Cre* embryos expressed various levels of Gsc transcripts. Compared to wt embryos, *mT-Gsc* specimens generally revealed Gsc expression domains that were more intensely stained and extended towards the caudal primitive streak (Fig. S3A–D). E7.5 specimens displayed a range of deficiencies that can roughly be grouped into two categories. A typical example of a mildly affected embryo, which was seen in about 60% of cases, is shown in Fig. 4M. The overall size did not differ significantly from wt, however, the epiblast appeared folded-up, which was more obvious in sections (arrowhead in Fig. 4M'). Primitive streak and mesoderm were clearly discernible. Severely affected embryos, in contrast, were characterized by egg cylinders that appeared hardly elongated at all and were approximately half the size of wt specimens (Fig. S3J,L).

The lack of axial elongation suggested that notochordal cells did not form or did not undergo CE. To investigate these options, E7.5 *mT-Gsc/Cre* embryos were analyzed morphologically, histologically and for marker gene expression. Scanning electron microscopy demonstrated that mutant embryos lacked the ciliated epithelium of the posterior notochord (PNC) at the distal tip of the egg cylinder, that is also known as ventral node²⁶ (Fig. S3E,F). The notochordal plate, i.e. the anterior extension of the PNC from which the notochord develops, was consistently absent in severely affected embryos as well (Fig. S3F and data not shown). To analyze axial mesoderm formation, the notochordal marker genes *Brachyury* and *Noto* were studied (Fig. 4N,O; Fig. S3G,H). Both genes were clearly down-regulated. Residual mRNAs were found in the primitive streak (*Brachyury*; Fig. 4O) and at the distal tip of the egg cylinder (*Noto*; Fig. S3H). No signals were observed anterior to the primitive streak. Thus, although mesoderm clearly arose in transgenic embryos (Fig. 4N), cells did not organize into PNC and notochordal plate during the course of gastrulation. Next, axis specification was analyzed, as Gsc acts as a potent inducer of secondary axes in *Xenopus*. Transcripts of *Otx2*, which marks the anterior pole (Fig. S3I), and *Fgf8*, which is expressed in the posterior part of the embryo (Fig. S3K), were found localized in the anterior and posterior half of the mutant egg cylinders as well (Fig. S3J,L). The AP-axis, therefore, was correctly specified in transgenic embryos, even in the most severe cases (Fig. S3J,L, and data not shown). Taken together, Gsc expression along the entire primitive streak of the mouse gastrula embryo impaired axial elongation, without affecting the patterning of embryonic tissues, and caused NTDs comparable to the BPDs and NTDs seen in *Xenopus*.

Gsc inhibits Wnt/PCP. CE in frog and mouse is regulated by non-canonical Wnt signaling, specifically the PCP pathway^{49–51}. One of the hallmarks of PCP signaling is the recruitment of Dvl2 to the plasma membrane^{52,53}, which is compromised when PCP signaling is impaired^{54,55}. We therefore wondered whether Gsc was able to interfere with Dvl2 localization. In *Xenopus*, a Dvl2-GFP fusion protein serves to investigate the subcellular localization in animal cap explant cultures⁵⁶. Upon expression of the Wnt receptor Fz7, Dvl2-GFP translocated from the cytoplasm to the plasma membrane (Fig. 5C,E). Animal caps represent a naïve stem cell-like tissue that can be differentiated into descendants of all three germ layers⁵⁷. As Gsc expression in the early vertebrate embryo is limited to mesodermal tissues^{58,59}, animal cap explants were injected with the mesoderm-inducing isoform of *Fgf8*, *Fgf8b*, which was verified by germ layer-specific marker gene expression⁶⁰ (Fig. S4). In order to assess whether Gsc impacted on Dvl2 subcellular localization, *Dvl2-GFP*, *fz7*, *fgf8* and *Gsc-GR* were coinjected into the animal region of 4–8 cell embryos, specimens were cultured in the presence or absence of dex until control embryos reached stage 10.5, when animal caps were excised and imaged (Fig. 5A). In the absence of dex, Dvl2-GFP relocated from the cytoplasm to the plasma membrane (Fig. 5B,E). When Gsc activity was induced following dex treatment, Dvl2-recruitment to the cell membrane was severely compromised (Fig. 5D,E; $p=0.002$). Gsc-GR acted in a cell-autonomous manner, as Dvl2 membrane localization was not affected in neighboring cells when *Gsc-GR* was only injected and activated in a subset of animal cap cells (Fig. 5F,G). These data demonstrated that in overexpression assays Gsc was clearly able to interfere with the recruitment of Dvl2 to the membrane as a prerequisite of non-canonical Wnt signaling and CE, in agreement with the observed gain-of-function phenotypes in mouse and frog.

Wnt/PCP pathway components rescue Gsc-induced NTD/BPD. Our hypothesis that Gsc interferes with Wnt/PCP signaling predicted that pathway components should be able to rescue the *Gsc-GR* induced gain-of-function phenotypes NTD and BPD *in vivo*. The downstream effector *RhoA* was assessed, which regulates CE by reorganization of the actin cytoskeleton⁶¹. A constitutively active (ca) construct was used as well as a dominant-negative (dn) form of *RhoA* (Paterson *et al.*⁹⁰). Both have been shown to induce BPD and NTD⁶¹, like

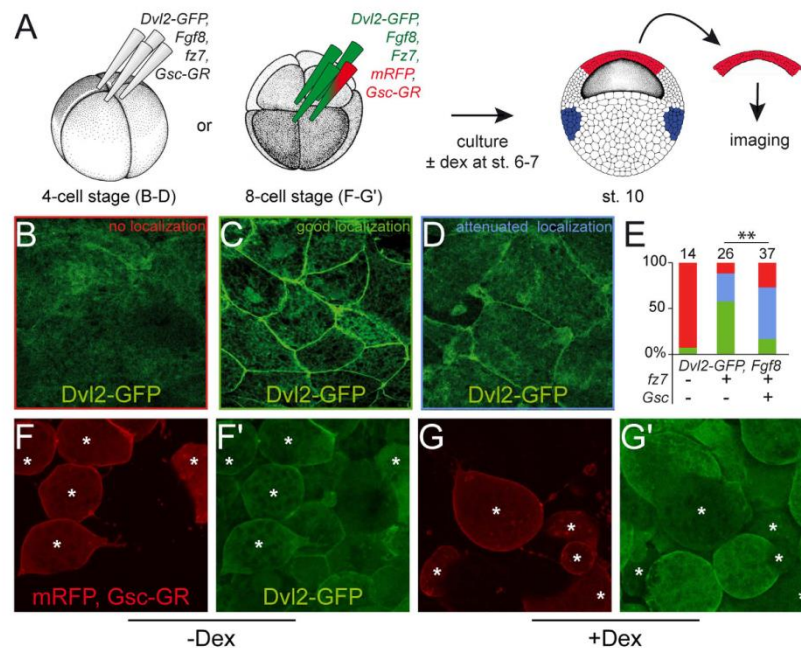


Figure 5. *Gsc-GR* inhibits membrane recruitment of *Dvl2*. (A) Co-injection of mRNAs as indicated into the animal region of all cells at the 4-cell stage or of selected cells at the 8-cell stage. Embryos were cultured \pm dex (added at st. 6/7), animal cap tissues were excised at stage 10 and subjected to live imaging. (B–E) Membrane localization of *Dvl2*-GFP was significantly impaired upon *Gsc-GR* activation. (B–D) Examples of specimens from the same batch of embryos and photographed with the same exposure times showing lack of localization (B; red), good (C; green) and attenuated localization (D; blue). (E) Quantification of results ($p = 0.002$). (F,G) Cell-autonomous effect of *Gsc-GR*. Injection of *Gsc-GR* in 1/4 animal cap cells at the 8-cell stage (cf. A) resulted in attenuation of *Dvl2*-GFP membrane recruitment upon dex treatment (cf. F' and G'). *mark *Gsc-GR*-injected cells, as revealed by fluorescence of lineage tracer mRFP.

most PCP components, which give rise to similar phenotypes upon gain- and loss-of-function⁶². In addition, the core PCP components *Vangl2* and *Prickle* were investigated, as they are required for subcellular localization of *Dvl2*^{63,64}. In addition, the potential of *Wnt11* and *Xbra* to rescue *Gsc*-mediated phenotypes was analyzed, as both are known to induce CE in *Xenopus*^{65,66}.

NTD and BPD were observed when *Gsc-GR* or any of the PCP components were injected into the dorsal marginal zone (Fig. 6). To test if and how *Gsc* interacted with PCP signaling, co-injection experiments were performed. *caRhoA* significantly decreased the percentage of malformed embryos induced by *Gsc-GR* (Fig. 6A; Table S1). In order to analyze whether *dnRhoA* enhanced the *Gsc* effects accordingly, both were co-expressed. High lethality of embryos prevented the quantitative analysis of the experiment (not shown). When the dosage of the injected *Gsc-GR* construct was lowered 2.5-fold, *dnRhoA* co-injection resulted in a significantly higher percentage of affected specimens as compared to the injection of *dnRhoA* alone (Fig. 6B; Table S1). As *RhoA* is a general modifier of actin cytoskeleton dynamics, we extended our study to core PCP pathway components. Co-injections of *Prickle* and *Vangl2* partially rescued the *Gsc*-induced phenotypes (Fig. 6C,D; Table S1). In addition, mouse *Brachyury* and *Xenopus Wnt11* were also able to partially revert *Gsc-GR* induced NTD and BPD (Fig. 6E,F; Table S1). In summary, these gain-of-function experiments demonstrated the potential of *Gsc* to act as a negative regulator of PCP-mediated CE, at least in the context of gain-of-function induced phenotypes.

Wnt/PCP phenotypes in *Gsc* morphant frog and mutant mouse embryos. In order to analyze whether the endogenous *Gsc* is involved in inhibition of Wnt/PCP-mediated CE as well, we re-investigated *Gsc* morphant frog embryos and knockout mouse specimens. In *Xenopus* we used a previously characterized *Gsc* MO²¹. Analysis of morphant tadpoles revealed that the eye distance was significantly reduced at stage 45 compared to uninjected control specimens (Fig. 7A,B). Co-injection of a full-length mouse *Gsc* cDNA construct, which was not targeted by the MO, partially rescued this phenotype, demonstrating the specificity of the MO (Fig. 7C). As during development the eye field is split by the prechordal plate, which expresses *Gsc*, we hypothesized that this population of migrating cells was affected in morphants. *Shh* mRNA transcription was analyzed,

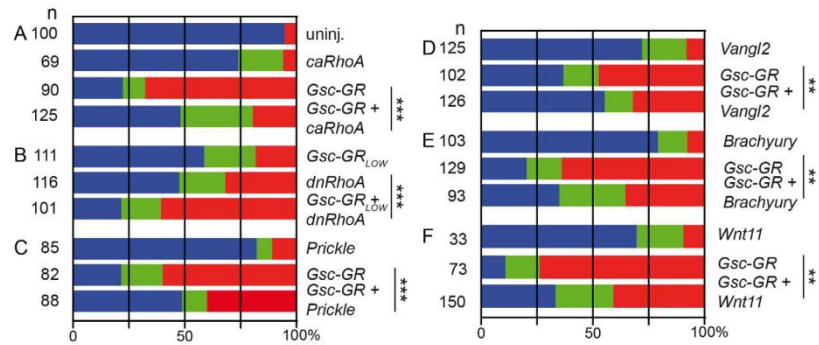


Figure 6. Rescue of Gsc-GR mediated NTD/BPD by Wnt/PCP pathway components. *Xenopus* embryos were injected with the indicated mRNAs into the dorsal marginal region of all cells at the 4-cell and cultured to stage 22. Dex was added when *Gsc-GR* was used. Specimens were scored for normal appearance (blue bars), NTD (green) and BPD (red). (A) constitutively active *RhoA*; (ca; A) dominant-negative (dn) *RhoA*; (C) *Prickle*; (D) *Vangl2*; (E) *Brachyury*; (F) *Wnt11*. Uninjected embryos (uninj.) served as controls. Note that rescue was observed upon co-injection of *Gsc-GR* with *ca-RhoA*, *Prickle*, *Vangl2*, *Brachyury* and *Wnt11*, while enhanced phenotypes were seen with co-injected *dn-RhoA*. As embryos in the latter combination showed high rates of lethality, the dose of injected *Gsc-GR* was reduced from 400 pg to 160 pg. Cf. Table S1 for numbers and statistics.

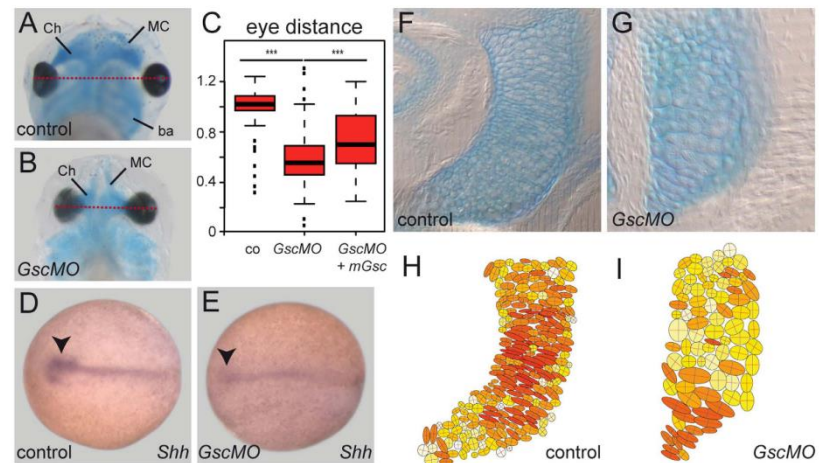


Figure 7. Prechordal plate and cartilage defects in *Gsc* morphant *Xenopus* tadpoles. (A–E) Prechordal plate defects. (A–C) Close-set eyes in *Gsc* morphants. Distance between left and right eye (red lines) was reduced in morphants. Arithmetic mean of control specimens was set to 1.0 in (C). Note that this phenotype was rescued by co-injection of a mouse *Gsc* cDNA construct. (D,E) *Shh* mRNA expression in control (D) and high dose *Gsc* morphant (E). Note that the prechordal plate (arrowheads) was severely reduced in morphants. (F–I) Cartilage phenotypes in *Gsc* morphant frog tadpoles. Cartilage was stained with alcian blue in wt (F,H) or *Gsc* morphant (G,I) tadpoles at stage 45. Shape of cartilage cells of was analyzed in frontal sections of embryos (F,G). (H,I) Cells were outlined with ImageJ and aspect ratios were calculated and visualized. Cell shapes are indicated by a color gradient from yellow to red, with round cells depicted in light yellow and elongated bipolar cells in deep red. Note that the majority of cartilage cells in *Gsc* morphants had lost their bipolar appearance.

which along the axial midline is expressed in the prechordal plate mesoderm and the floorplate of the neural tube. Figure 7(D,E) shows that the width of the anteriormost *Shh* expression domain, i.e. the expression in or above the prechordal plate, was narrowed, in line with the observed close-set eyes.

To analyze whether the notochord was expanded at the expense of the prechordal plate, which was previously suggested in experiments using antisense *Gsc* DNA expression constructs¹⁶, *Xbra* mRNA expression was investigated in morphant specimens. Surprisingly, the notochord appeared wider and shorter, as compared to wt specimen (Fig. S5). The aspect ratio, which was set to 1.0 in control specimens, was significantly reduced to 0.61 in morphants (Fig. S5C). As we had noted this particular phenotype in *Gsc* gain-of-function specimens (Fig. 1F–I), we wondered whether *Gsc* transcription was affected in *Gsc* morphants. The *Gsc* expression domain in morphants was indeed stronger and expanded both laterally and posteriorly towards the blastopore (Fig. S5G,H). This at first glance paradoxical finding, however, is in good agreement with our previous finding of a negative auto-regulatory feedback loop of *Gsc* on its own transcription⁶⁷. The analysis of MO-mediated *Gsc* loss-of-function phenotypes thus might be hampered by limiting MO-doses, which might be insufficient to prevent the translation of additional transcripts generated by the release of the negative autoregulatory *Gsc* feedback loop. When the MO doses were increased to counteract this possible effect, the length of the notochord was slightly expanded to an aspect ratio of 1.14 in morphants ($p = 0.0193$), an effect which was partially (and non-significantly) reversed by co-injection of the mouse rescue cDNA construct (aspect ratio 1.07; Fig. S5D–F). These tendencies may suggest that MO doses have, indeed, been limiting.

In addition to a reduced eye distance we noted that the morphology of the head cartilage was altered in *Gsc* morphant tadpoles at stage 45, in particular Meckel's cartilage and the ceratohyale (Fig. 7A,B,F–I). In mouse, *Gsc* is expressed in undifferentiated branchial arch mesenchyme and persists as these tissues undergo differentiation into head cartilage⁶⁸. Re-evaluating *Gsc* expression during late tadpole development revealed a like expression pattern in *Xenopus* as well (Fig. S6). As cartilage condensation involves CE^{69,70}, we wondered whether morphological alterations in morphants were reminiscent of PCP phenotypes. To that end we analyzed cellular morphologies of cartilage cells. While wt cells displayed predominantly bipolar morphologies (Fig. 7F,H), evaluation of length vs. width aspect ratios demonstrated loss of elongated cell shapes in morphants (Fig. 7G,I). This phenotype strikingly resembled the failure of Meckel's cartilage cells to elongate and intercalate in morphants of the PCP effectors *inturned* and *fuzzy*⁷⁰, suggesting that the cartilage phenotype in *Gsc* morphant tadpoles represented a PCP-phenotype as well.

Finally, we re-investigated *Gsc*-knockout mouse embryos for potential PCP/CE phenotypes. Besides the above-mentioned expression around condensing cartilage, the inner ear is the organ that has been particularly well characterized with respect to PCP in the mouse. As previously described, *Gsc* was expressed in the inner ear opposite the organ of Corti⁷¹ (Fig. 8A,B), and opposite the expression domain of the non-canonical Wnt ligand *Wnt5a*⁷² (Fig. 8B). Stereo- and kinocilia of outer and inner hair cells (OHC/IHC) display a distinctive planar cell polarity and are a well-known target of PCP-signaling⁷³. To investigate whether PCP of inner ear hair cells was altered in *Gsc* knockout embryos, E18.5 cochleas were isolated from wt and knockout specimens and analyzed for stereo- and kinocilia orientation. Phalloidin staining was used to highlight the actin cytoskeleton of the V-shaped stereocilia, and tubulin staining to visualize the axoneme of the kinocilium. In wt and heterozygous E18.5 specimens, stereo- and kinocilia of IHCs and OHCs align and point towards the periphery of the cochlea (Fig. 8C,E). In *Gsc* knock-out embryos, however, this orientation was disrupted (Fig. 8D,F). A quantification of average deviations from the normal perpendicular orientation revealed higher values in *Gsc* knockout specimens, which was significantly pronounced in outer hair cell row 3 (Fig. 8G, $p = 0.03$, $n = 390$) compared to wt littermates ($n = 308$). This result unequivocally demonstrated that *Gsc* knockout mouse embryos displayed a well-characterized Wnt/PCP phenotype as well. Taken together, our *Gsc* gain- and loss-of-function studies in frog and mouse embryos revealed a novel role of *Gsc* as an inhibitor of Wnt/PCP-mediated cell morphogenesis and behavior, in particular CE.

Discussion

A quarter of a century ago, the first description of *Gsc*'s potential to induce secondary axis formation set the starting point for an extremely productive molecular analysis of Spemann's organizer⁷. The apparent lack of gastrulation phenotypes in mutants and morphants reduced the perceived relevance of *Gsc* to being the best available marker of organizer tissue across the animal kingdom. Our present report of a novel function of *Gsc* as transcriptional inhibitor of Wnt/PCP-mediated CE not only offers a potential mechanism to understanding the various malformations of bone and cartilage in *Gsc* knockout mice (and human patients⁷⁴). It may as well assign a role for *Gsc* in the organizer-derived prechordal plate, namely to restrict CE to the notochord and to facilitate or enable the migration of the prechordal mesodermal cells. Our conditional gain-of-function analyses in frog and mouse clearly demonstrate the potential of *Gsc* to act as an inhibitor of Wnt/PCP-mediated CE. The analysis of loss-of-function phenotypes in both model systems supports such a role during embryonic development, although - admittedly - they represent in parts initial and preliminary characterizations. A key question, that remains unanswered, relates to the molecular mechanism of *Gsc* function in inhibiting Wnt/PCP. Two aspects, which our experiments touch upon, deserve further elaboration, namely whether this effect is cell- or non-cell autonomous and how novel target genes were recruited under the control of *Gsc*.

As mentioned in passing, it is not possible to target the axial mesoderm/notochord in *Xenopus* without at the same time delivering constructs to the floorplate of the neural tube. Thus, the observed NTDs could represent a cell-autonomous effect of ectopic *Gsc* expression. The cell-autonomous interference of *Gsc*-GR with Dvl2 membrane recruitment in animal caps (cf. Fig. 5F,G) supports this notion. In the conditional mouse experiments, however, ectopic *Gsc* expression was strictly limited to the primitive streak mesoderm, as the *Brachyury* streak enhancer is only active there⁴⁶. NTDs in mouse, therefore, cannot be caused by a cell-autonomous *Gsc* function. The same reasoning holds true for the inner ear: here *Gsc* is expressed opposite to the IHCs/OHCs at the organ of Corti that undergo PCP. Further, *Gsc* and the Wnt ligand *Wnt5a*, which has been shown to be the decisive ligand for the arrangement of these cells⁷⁵, are expressed in adjacent rather than the same cells, demonstrating that the

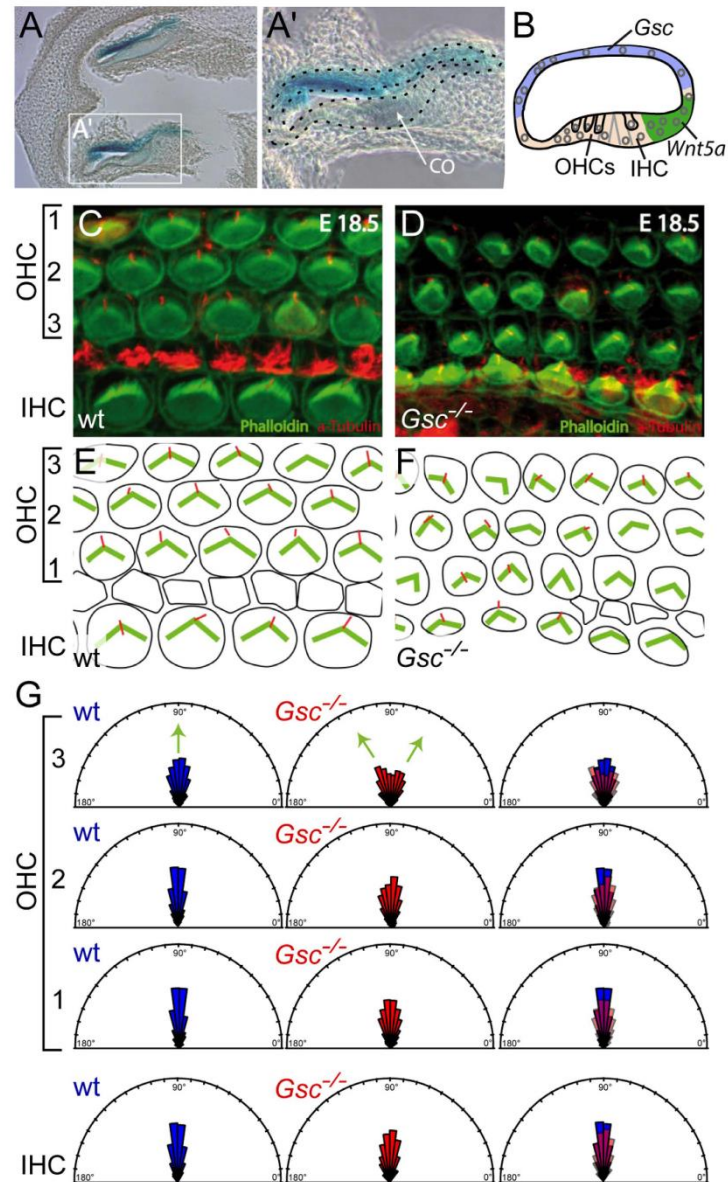


Figure 8. Disrupted alignment of outer hair cells (OHCs) in the cortical organ of *Gsc* knockout embryos. (A) *Gsc* transcription (blue) locates opposite of the cortical organ (CO). (B) Schematic depiction of *Gsc* expression in blue and *Wnt5a* expression in green. OHCs and inner hair cells (IHC) are highlighted by arrows. (C–G) Confocal imaging of kinocilia (red, tubulin) and stereocilia (green, phalloidin) in the cortical organ of *Gsc* knockout mouse embryos (D,F), compared to wt littermates (C,E) schematically depicted in (E,F). (G) Quantification of alignments, depicted as rose plots. According to the angle of deviations from the normal perpendicular orientation (90°), vectors were plotted in 11.25° sectors. The area of a sector represents the number of cells with this directionality. Note that significantly higher deviations from the normal perpendicular orientation (90°) were observed in OHC3 of *Gsc* knockout specimens (middle, red, $n = 390$) compared to wildtype littermates (left, blue, $n = 308$, $p = 0.03$).

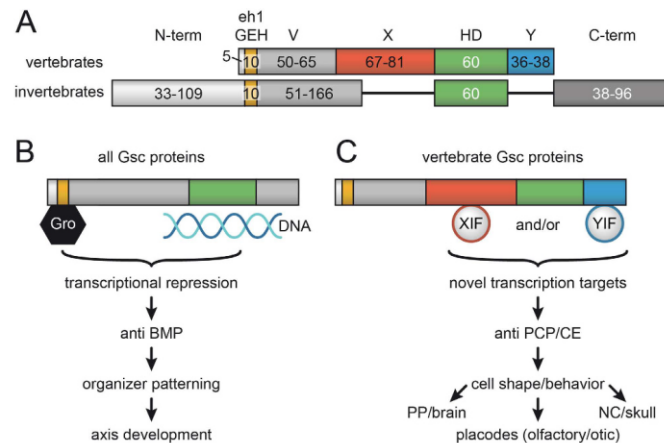


Figure 9. Vertebrate-specific Gsc functions: a model. (A) Domain structure of invertebrate and vertebrate Gsc proteins; numbers indicate ranges of amino acids. The engrailed homology (eh1/GEF) repression domain and the homeodomain (HD) are common to all Gsc proteins. Two highly conserved domains (X, Y) flanking the HD emerged at the base of the vertebrates. Note that invertebrates, besides lacking X/Y, possess variable length N- and C-terminal sequences and that the linker region between eh1/GEF and HD also varies greatly in length. (B) All Gsc proteins have the potential to act as transcriptional repressors through HD-binding to DNA and Groucho-recruitment to eh1/GEF. When assayed in *Xenopus*, *Drosophila* and vertebrate Gsc proteins act in organizer patterning and axis development through their conserved anti-BMP function. (C) Vertebrate Gsc proteins in addition affect cell shape and behavior through their anti PCP/CE function. We propose that X- and Y-domain interacting factors XIF and YIF function in recruiting novel transcriptional target genes under Gsc control. We further propose that this novel function of Gsc co-evolved with the vertebrate-specific novelties of an enlarged brain, skull and placodes, as vertebrate Gsc is expressed in the prechordal plate/floor plate of the diencephalon, neural crest mesenchyme and derivatives as well as otic vesicle/nasal cavity.

inner ear phenotype in the genetic knockout situation is the result of a non-cell autonomous effect of Gsc. It thus appears that context-dependently Gsc acts in a cell or non-cell autonomous manner to repress PCP/CE.

The inability of *Drosophila* Gsc to interfere with PCP/CE (while inducing double axis formation even more efficiently than *Xenopus* or mouse Gsc) indicates that this function either arose during vertebrate evolution or was lost in *Drosophila*. To approach this question, we compared Gsc protein sequences across the animal kingdom. In invertebrates, no conserved regions besides the highly conserved eh1/GEH domain and a basically invariant homeodomain (HD) were found, arguing against a loss of anti-PCP/CE activity in *Drosophila* (Fig. 9A, Fig. S7). The presence of eh1/GEH and HD in all Gsc sequences in addition suggests that all proteins should have the potential to act as transcriptional repressors in organizer patterning and axis development, at least when assayed in *Xenopus*, a function which is mediated through Gsc's well-documented anti-BMP function (Fig. 9B)^{16,76}. Vertebrate Gsc proteins in contrast possess two novel highly conserved domains flanking the HD, which we address as "X" and "Y" (Fig. 9A, Fig. S7). Interestingly, both domains are absent in the cephalochordate amphioxus, in which neither a cranium nor neural crest have evolved yet⁷⁷⁻⁷⁹, as well as in the lamprey, a primitive agnathan vertebrate that has neural crest but lacks jaws⁸⁰ (not shown). When databases were screened for sequences related to X and Y, exclusively vertebrate Gsc sequences were picked up (not shown). These data indicate that the anti-PCP/CE function evolved at the base of the vertebrates, likely together with the acquisition of domains X and/or Y (or parts thereof). We like to propose that X- and/or Y-interacting factors (XIF and YIF in Fig. 8C) recruited Gsc to novel target promoters, either by direct DNA-binding of XIF/YIF or through interaction with other DNA-binding proteins. Vertebrate-specific target genes could function directly upstream of PCP components. Alternatively, they may act in a parallel pathway that controls competence for Wnt/PCP signaling. Elucidating the molecular mechanisms will involve the identification of (1) target genes; (2) peptides mediating the vertebrate anti-PCP/CE function, for example by introducing X/Y sequences and fragments thereof into *Drosophila* Gsc and assaying recombinant genes in *Xenopus*; (3) XIF/YIF, for example through the identification of the interactome of identified peptides.

Relating the emergence of the anti-PCP/CE function at the base of the vertebrates to post-gastrulation expression patterns in the vertebrates reveals a potentially highly relevant coincidence: Gsc transcripts are found in (1) the prechordal plate and floor plate of the diencephalon; (2) branchial arch mesenchyme and derivatives (skull cartilage, tongue, etc.⁶⁸); (3) placodal derivatives (otic vesicle/organ of Corti, olfactory pit/nasal passage⁷¹, i.e. in tissues representing evolutionary novelties of the vertebrates⁸¹). It is tempting to speculate that Gsc was recruited into gene regulatory networks specific to these tissues to shape their morphogenesis by regulating cellular morphology and behavior.

In the light of this reasoning, an in-depth re-evaluation of the endogenous *Gsc* functions in the various vertebrates is in demand. While this manuscript was under review, two relevant studies were published. The analysis of otic vesicle differentiation in zebrafish morphants and TALEN-induced mutants revealed a function for *Gsc* in the delamination of neuroblasts, i.e. a process involving epithelial-to-mesenchymal transitions associated with cell shape changes and delamination/migration behavior⁸². Inner ear hair cell PCP was not investigated in this study. In *Xenopus*, aCRISPR/Cas9 approach to genome-editing of - among others - *Gsc* was reported and specimens were shown to display massive head defects, that were not further characterized⁸³ but in perfect agreement with the neural crest/skull phenotypes reported here. Genome editing should provide a powerful complementing means to the use of MOs for studying *Gsc* function, as applicable MO-doses may be the limiting factor in such experiments, based on the observed gain-of-function by loss-of-function, i.e. interference with the negative auto-regulatory feedback loop (cf. Fig. S5G,H). Even antisense RNA may prove useful in the future. The late Herbert Steinbeißer and colleagues previously injected such RNAs into the axial midline and noted that the notochord was expanded at the expense of the prechordal plate¹⁶. Unfortunately, this loss-of-function approach fell in disgrace⁸⁴ and the prechordal plate phenotype was never fully characterized.

The knockout mouse in any case deserves to be re-evaluated. When we analyzed *Gsc* expression domains during organogenesis stages, we found transcripts adjacent to tissues that elongate during development, which might involve PCP-mediated convergent extension. *Gsc* mRNA was for example found at the anterior tip of the tongue, in the arytenoid swellings and the palatal shelves⁷¹ (Fig. S8). The previously described limb bud expression fits to this proposal as well, as limb bud differentiation was identified as a PCP-dependent process as well^{85,86}.

Finally, the early embryonic expression pattern of *Gsc* in vertebrate embryos is in agreement with such a function. The first transcription in the organizer tissue itself is very transient. As axial mesodermal cells (prechordal plate and notochord) migrate out in rostral direction, *Gsc* is downregulated in the organizer, maintained in the prechordal cells and absent in the notochord^{10,26,27}. Segregation of organizer-derived cells into these two populations is accompanied by differences in cell behavior (single cell migration of the prechordal cells and CE in the notochord) and gene expression (*Gsc* in the prechordal and *Brachyury* in the notochordal mesoderm^{28-30,87,88}). *Gsc*, thus, may provide the switch between cell intercalation and cell migration by limiting CE to the notochord. 25 years after the first characterization of *Gsc* in the organizer, the fascination for this gene continues. Much has to be learned about its function in development and disease.

Methods

All methods were performed in accordance with the relevant guidelines and regulations.

Statement of approval of animal experimentation. Handling, care and experimental manipulations of mice were approved by the Regional Government Stuttgart, Germany (Vorhaben A379/12 ZO "Molekulare Embryologie"), according to German regulations and laws (§6, article 1, sentence 2, nr. 4 of the animal protection act).

Plasmids and construction of *Xenopus* expression vectors. K197E¹⁷ was obtained from Dan Kessler, Wnt11 constructs were from Kristen Kwan, Vangl2 from Ray Keller, and Prickle1 from Naoto Ueno. *Gsc*-GR has been described in ref. 89. Fgf8, Fz7, Dvl2-GFP, dnRhoA and caRhoA constructs were provided by the Steinbeißer laboratory.

The following PCR primers were used for cloning of deletion constructs ΔHD and ΔGEH: ΔHDfor 5'-ATATCGATGCGCTGCAAGGAGTCGCTGCTG-3', ΔHDrev 5'-CTGGACTCTGACAGTGGTCCTCGAGAT-3', ΔGEHfor 5'-ATATCGATGCGCTGCAAGGAGTCGCTGCTG-3', ΔGEHrev 5'-CTGGACTCTGACAGTGGTCCTCGAGAT-3'. The starting construct to clone T-*Gsc* was PML129 (vector backbone PGEM3, Promega), which contained the 658 bp *Brachyury* streak promoter, followed by a floxed LacZ cassette with triplicate polyadenylation signals to ensure that the downstream open reading frame is not part of the mRNA. To create construct T-*Gsc* the 771 bp *Gsc* coding sequence was inserted downstream, flanked by a 231 bp polyadenylation signal from the bovine growth hormone gene (from pRc/CMV, Invitrogen). Construct mT-*Gsc* was generated by mutating the *Brachyury* streak promoter 35 bp downstream of the transcriptional start site from TAAAT into ACTG¹⁴.

Generation of transient chimeric embryos. Two constructs were used to transfect mouse ES cells (line E14-KPA, kindly provided by Klaus Peter Knobloch, FMP, Berlin, Germany), a *Gsc* and a LacZ expression construct, which both used the human ubiquitin promoter. Stable lines were selected by co-transfection of the selection plasmid containing the PGK-neo cassette. Individual clones were characterized for transgene expression by RT-PCR analysis (pcubi-*Gsc* primer; see below). A clone displaying high expression levels was used in blastocyst injection experiments to derive transgenic embryos which were harvested at E9.5 and E10.5.

Generation of T-*Gsc* and mT-*Gsc* mouse lines and Cre-mediated transgene activation. Inserts of vectors were isolated by KpnI enzyme digestion and introduced by electroporation into E14-KPA and CJ7 cells (kindly provided by Thomas Gridley, Jackson Laboratory, USA), and cultured following standard procedures. After G418 selection (250 µg/ml), four transgenic clones were identified with T-*Gsc* and 28 clones with mT-*Gsc*, each containing single copy gene integration verified by Southern blot analysis. Reporter gene activity was tested by X-gal staining of mesodermally differentiated clones, which express *Brachyury*. Mesodermal differentiation was performed in hanging drop cultures in the presence of DMSO. Clones showing strong reporter gene activity were used to generate transgenic mice, which were derived from C57BL/6J blastocyst injections. Offspring of germ line-transmitting chimeric mice were screened for the presence of the T-*Gsc* transgene. Heterozygous mice were kept on a mixed background and mated to obtain homozygous animals. One line was obtained with T-*Gsc* and two lines with mT-*Gsc*. Transgenes were activated by crossing homozygous deleter females with homozygous T-*Gsc* or mT-*Gsc* males.

Genotyping of transgenic mice and embryos. DNA from embryos and tail biopsies was isolated using standard protocols. Primers and PCR conditions were as follows:

LacZ primer: a) 5'-TCAATCCGCCGTTTGTTC; 3'-CCGCCACATATCCTGATCTTCC; 280 bp, 55 °C b) 5'-GCAGTGCACGGCAGATACACACTT; 3'-CCCCATATGGAAACCGTCG; 510 bp, 55 °C; c) 5'-GGGACGGCGAATGAATGAATTA; 3'-CCCCATATGGAAACCGTCG; 160 bp, 55 °C;

Cre primer: a) 5'-CGCATAACCAGTAAAACAGCAT; 3'-GAAAGTCGAGTAGGCGTGTACG; 550 bp, 55 °C b) 5'-TAATCGCCATCTTCCAGCAG; 3'-GCTGGCTGGTGGCAGATGGCG; 650 bp, 55 °C; c) 5'-CAATTTACTGACCGTACAC; 3'-GCTGGCTGGTGGCAGATGGCG; 751 bp, 55 °C; Gsc-bGHPA primer: 5'-GTTCTGTACTGGTGTCTCG (in Exon3 of Gsc); 3'-GGCACCTTCCAGGGTCAAGG (in the polyadenylation signal of the bovine growth hormone); 277 bp, 63.5 °C; pcubi-Gsc 5'-CCACTAGTCCAGTGTGGTGG; 3'-GACGCAGGGCTGCGGGGGTC; 385 bp, 65 °C.

Manipulations of *Xenopus* embryos. For microinjections, drop size was calibrated to about 8 nl/injection. Embryo culture and microinjection followed standard procedures. mRNAs were prepared using the Ambion message machine kit. DsRed mRNA (1.6 ng mRNA/embryo) and rhodamine-B dextran (0.5–1.0 µg/µl; Molecular Probes) were used as lineage tracers. Unless indicated otherwise, 400 pg Xgsc-GR mRNA/embryo was injected³². Gsc-GR fusion protein was activated by the addition of 10 µg/ml dexamethasone at stage 6–8 (unless specified otherwise). Concentrations of injected mRNAs (transcribed from CS2⁺-expression vectors) were: constitutive active RhoA V14 (32–64 pg mRNA/embryo), dominant negative RhoA N19³⁰ (320 pg mRNA/embryo), *Prickle1*¹⁹¹ (1.8 ng/embryo), *Vangl2/Strab3* (400 pg/embryo), *T* (800 pg mRNA/embryo); cds of mouse *Brachyury*, and *Wnt11*²⁹ (80 pg mRNA/embryo). For knock-down experiments a coding morpholino was used (5'-GCTGAACATGCCAGAAGGCATCACC-3, Gene Tools LLC³¹). Statistical calculations were performed using Pearson's chi-square test comparing the number of affected embryos against the number of wt embryos (Statpages.com).

Manipulations of *Xenopus* explants. Keller open face explants were prepared as described^{37,87}, except that DFA medium was used. Animal cap assays were conducted according to Green, 1999. All cells of the 4-cell embryo were injected into the animal pole, dex was added at stage 6, where indicated, and the animal caps were cut at stage 9. Recombinant human Activin A (R&D Systems) was added immediately after cutting and the embryos were cultured until control specimens reached stage 22–30. For the Dvl2 localization assay, the following mRNAs, transcribed with the Ambion message machine from CS2⁺ vectors, were injected: a construct containing the C-terminal DEP-domain of Dvl2 fused to GFP (400 pg/cell; D9⁵⁶), *Frizzled7*⁷² (400 pg/cell), *Fgf8* (8.8 pg/cell), *Gsc-GR*³² (560 pg/cell). Explants were cultured until control siblings reached stage 10.5.

RT-PCR. Total RNA was isolated from animal cap explants at stage 10.5, and cDNAs were prepared using standard protocols. Primers used for amplification where from different exons to avoid genomic contamination. *EF1alpha* served as loading control. EF1α: for 5'-ACTGCCTTGATGATGACTCCTAG rev 5'-CAGATTGGTGCTGGATATGC; *Wnt11*: for 5'-TGACGGTCTAGTCCCTGACCA, rev 5'-GGT TGCAGCTGTCACCTACCA; *Xbra*: for 5'-CACAGTTTCATAGCAGTGACCG, rev 5'-TTCGTG AGTGTACGGACTGG.

Analysis of cell proliferation and apoptosis. Immunofluorescence was performed on whole-mount embryos, fixed for 1–2 hours at room temperature in 4% PFA for cell proliferation or in methanol/DMSO (4:1; Dent's solution) for assessment of apoptosis. Embryos were processed as previously published and according to standard procedures^{93,94}. Ethanol treatment (2.5%) served as positive control for the apoptosis assay. Primary antibodies: polyclonal rabbit anti-phospho-Histone H3 (Ser10; 1:700; Merck), monoclonal rabbit anti-caspase-3 Ab (1:150; 9665, Cell Signaling Technologies). Secondary antibody: Alexa Fluor 488-conjugated goat anti-rabbit (1:750, Invitrogen).

RNA *in situ* hybridization and histological analysis. *Xenopus* and mouse embryos were fixed in 4% PFA for 2 hrs and processed following standard protocols. Digoxigenin-labelled (Roche) RNA probes were prepared from linearized plasmids using SP6 or T7 RNA polymerase (Promega). *In situ* hybridization was performed as described⁹⁵. Cartilage was stained with 0.05% alcian blue followed by bleaching. For histological analysis embryos were embedded in gelatine-albumin and sectioned on a vibratome (30 µm).

Analysis of cell shape and gene expression domains. Aspect ratios of cell shape and gene expression domains as well as statistical significances were calculated by Mann-Whitney-U test in statistical R (R-Development-Core-Team, 2008). The whiskers of the box plots extend to maximal 1.5 × IQR, outliers are displayed as dots. Aspect ratio = major axis/minor axis. Major and minor are the primary and secondary axis of the best fitting ellipse.

Scanning Electron Microscopy. SEM analysis was performed following published protocols⁹⁶. In brief, embryos were dissected and immediately fixed in 2.5% glutaraldehyde in Soerensen's buffer (0.1M sodium phosphate buffer; pH 7.4). Specimens were postfixed in 1% OsO₄, critical point dried, sputter coated, and examined using a Zeiss DSM 940 A SEM (Oberkochen, Germany).

Analysis of the cortical organ. The inner ear of E18.5 embryos was dissected and fixed in 4% PFA for 2 days at 4 °C. Cochleae were opened for better accessibility and stained with a mouse monoclonal antibody directed against acetylated alpha tubulin (1:700; Sigma), Cy3-conjugated secondary polyclonal rabbit sheep anti

mouse antibodies (Sigma; 1:250) and Alexa Fluor® 488 Phalloidin (Molecular probes, 1:40) following standard procedures, and imaged using a Zeiss LSM Pascal 5 Confocal Laser Scanning Microscope.

To determine stereociliary bundle orientation, we used the angle measurement tool in ImageJ, measuring the angle between the line from the position of the kinocilium through the middle of the “V”-shaped stereocilia and a line parallel to the mediolateral axis. In perfectly aligned cells, this angle is 90°. A Wilcoxon rank sum test with continuity correction in statistical R (R-Development-Core-Team, 2008) was used for statistical analyses.

References

1. Paré, A. C. *et al.* A positional Toll receptor code directs convergent extension in *Drosophila*. *Nature* **515**, 523–527 (2014).
2. Ninomiya, H., Elinson, R. P. & Winklbauer, R. Antero-posterior tissue polarity links mesoderm convergent extension to axial patterning. *Nature* **430**, 364–367 (2004).
3. Blum, M. *et al.* Ciliation and gene expression distinguish between node and posterior notochord in the mammalian embryo. *Differentiation* **75**, 133–146 (2007).
4. Spemann, H. & Mangold, H. Über Induktion von Embryonalanlagen durch Implantation artfremder Organisatoren. *Archiv für Entwicklungsmechanik der Organismen* **100**, 599–638 (1924).
5. Blum, M. *et al.* Gastrulation in the mouse: the role of the homeobox gene *gooseoid*. *Cell* **69**, 1097–1106 (1992).
6. Broun, M., Sokol, S. & Bode, H. R. *Cngsc*, a homologue of *gooseoid*, participates in the patterning of the head, and is expressed in the organizer region of *Hydra*. *Development* **126**, 5245–5254 (1999).
7. Cho, K. W., Blumberg, B., Steinbeisser, H. & de Robertis, E. M. Molecular nature of Spemann's organizer: the role of the *Xenopus* homeobox gene *gooseoid*. *Cell* **67**, 1111–1120 (1991).
8. Christian, J. L. & Moon, R. T. Interactions between *Xwnt-8* and Spemann organizer signaling pathways generate dorsoventral pattern in the embryonic mesoderm of *Xenopus*. *Genes Dev* **7**, 13–28 (1993).
9. Fainsod, A., Steinbeisser, H. & de Robertis, E. M. On the function of BMP-4 in patterning the marginal zone of the *Xenopus* embryo. *EMBO J.* **13**, 5015–5025 (1994).
10. Artinger, M., Blitz, L., Inoue, K., Tran, U. & Cho, K. W. Interaction of *gooseoid* and *brachyury* in *Xenopus* mesoderm patterning. *Mech. Dev.* **65**, 187–196 (1997).
11. Boucher, D. M. *et al.* *Gooseoid* expression represses *Brachyury* in embryonic stem cells and affects craniofacial development in chimeric mice. **44**, 279–288 (2000).
12. Dixon Fox, M. & Bruce, A. E. Short- and long-range functions of *Gooseoid* in zebrafish axis formation are independent of *Chordin*, *Noggin* 1 and *Follistatin-like 1b*. *Development* **136**, 1675–1685 (2009).
13. Latinkic, B. V. & Smith, J. C. *Gooseoid* and *mix.1* repress *Brachyury* expression and are required for head formation in *Xenopus*. *Development* **126**, 1769–1779 (1999).
14. Latinkic, B. V. *et al.* The *Xenopus* *Brachyury* promoter is activated by FGF and low concentrations of activin and suppressed by high concentrations of activin and by paired-type homeodomain proteins. *Genes Dev* **11**, 3265–3276 (1997).
15. Seiliez, I., Thisse, B. & Thisse, C. *FoxA3* and *gooseoid* promote anterior neural fate through inhibition of *Wnt8a* activity before the onset of gastrulation. *Dev Biol* **290**, 152–163 (2006).
16. Steinbeisser, H., Fainsod, A., Niehrs, C., Sasai, Y. & de Robertis, E. M. The role of *gsc* and BMP-4 in dorsal-ventral patterning of the marginal zone in *Xenopus*: a loss-of-function study using antisense RNA. *EMBO J.* **14**, 5230–5243 (1995).
17. Yao, J. & Kessler, D. S. *Gooseoid* promotes head organizer activity by direct repression of *Xwnt8* in Spemann's organizer. *Development* **128**, 2975–2987 (2001).
18. Yasuo, H. & Lemaire, P. Role of *Gooseoid*, *Xnot* and *Wnt* antagonists in the maintenance of the notochord genetic programme in *Xenopus* gastrulae. *Development* **128**, 3783–3793 (2001).
19. Rivera-Pérez, J. A., Mallo, M., Gendron-Maguire, M., Gridley, T. & Behringer, R. R. *Gooseoid* is not an essential component of the mouse gastrula organizer but is required for craniofacial and rib development. *Development* **121**, 3005–3012 (1995).
20. Yamada, G. *et al.* Targeted mutation of the murine *gooseoid* gene results in craniofacial defects and neonatal death. *Development* **121**, 2917–2922 (1995).
21. Sander, V., Reversade, B. & de Robertis, E. M. The opposing homeobox genes *Gooseoid* and *Vent1/2* self-regulate *Xenopus* patterning. *EMBO J.* **26**, 2955–2965 (2007).
22. Ferreira, B., Artinger, M., Cho, K. & Niehrs, C. Antimorphic *gooseoids*. *Development* **125**, 1347–1359 (1998).
23. Niehrs, C., Keller, R., Cho, K. W. & de Robertis, E. M. The homeobox gene *gooseoid* controls cell migration in *Xenopus* embryos. *Cell* **72**, 491–503 (1993).
24. Luu, O., Nagel, M., Wacker, S., Lemaire, P. & Winklbauer, R. Control of gastrula cell motility by the *Gooseoid/Mix.1/Siamois* network: basic patterns and paradoxical effects. *Dev Dyn.* **237**, 1307–1320 (2008).
25. Hartwell, K. A. *et al.* The Spemann organizer gene, *Gooseoid*, promotes tumor metastasis. *Proc Natl Acad Sci USA* **103**, 18969–18974 (2006).
26. Blum, M. *et al.* Ciliation and gene expression distinguish between node and posterior notochord in the mammalian embryo. *Differentiation* **75**, 133–146 (2007).
27. Schulte-Merker, S. *et al.* Expression of zebrafish *gooseoid* and no tail gene products in wild-type and mutant no tail embryos. *Development* **120**, 843–852 (1994).
28. Winklbauer, R. Mesodermal cell migration during *Xenopus* gastrulation. *Dev Biol* **142**, 155–168 (1990).
29. Kwan, K. M. *Xbra* functions as a switch between cell migration and convergent extension in the *Xenopus* gastrula. *Development* **130**, 1961–1972 (2003).
30. Domingo, C. & Keller, R. Induction of notochord cell intercalation behavior and differentiation by progressive signals in the gastrula of *Xenopus laevis*. *Development* **121**, 3311–3321 (1995).
31. Yamada, T. Caudalization by the amphibian organizer: *brachyury*, convergent extension and retinoic acid. *Development* **120**, 3051–3062 (1994).
32. Shapira, E., Marom, K., Yelin, R., Levy, A. & Fainsod, A. A role for the homeobox gene *Xvex-1* as part of the BMP-4 ventral signaling pathway. *Mech. Dev.* **86**, 99–111 (1999).
33. Ewald, A. J., Peyrot, S. M., Tyszka, J. M., Fraser, S. E. & Wallingford, J. B. Regional requirements for Dishevelled signaling during *Xenopus* gastrulation: separable effects on blastopore closure, mesendoderm internalization and archenteron formation. *Development* **131**, 6195–6209 (2004).
34. Shih, J. & Keller, R. The epithelium of the dorsal marginal zone of *Xenopus* has organizer properties. *Development* **116**, 887–899 (1992).
35. Keller, R., Shook, D. & Skoglund, P. The forces that shape embryos: physical aspects of convergent extension by cell intercalation. *Phys Biol* **5**, 015007 (2008).
36. Keller, R. & Tibbetts, P. Mediolateral cell intercalation in the dorsal, axial mesoderm of *Xenopus laevis*. *Dev Biol* **131**, 539–549 (1989).
37. Sive, H. L., Grainger, R. M. & Harland, R. M. *Xenopus laevis* Keller Explants. *CSH Protoc* **2007**, pdb.prot4749–pdb.prot4749 (2007).

38. Kühl, M. *et al.* Antagonistic regulation of convergent extension movements in *Xenopus* by Wnt/beta-catenin and Wnt/Ca2+ signaling. *Mech. Dev.* **106**, 61–76 (2001).
39. McCulloch, C. A. & Tenenbaum, H. C. Dexamethasone induces proliferation and terminal differentiation of osteogenic cells in tissue culture. *Anat Rec* **215**, 397–402 (1986).
40. Matus, D. Q. *et al.* Molecular evidence for deep evolutionary roots of bilaterality in animal development. *Proc Natl Acad Sci USA* **103**, 11195–11200 (2006).
41. Lartillot, N., Le Gouar, M. & Adoutte, A. Expression patterns of fork head and gooseoid homologues in the mollusc *Patella vulgata* supports the ancestry of the anterior mesendoderm across Bilateria. *Dev. Genes Evol.* **212**, 551–561 (2002).
42. Mailhos, C. *et al.* *Drosophila* Gooseoid requires a conserved heptapeptide for repression of paired-class homeoprotein activators. *Development* **125**, 937–947 (1998).
43. Tessmar-Raible, K. & Arendt, D. Emerging systems: between vertebrates and arthropods, the Lophotrochozoa. *Curr. Opin. Genet. Dev.* **13**, 331–340 (2003).
44. Goriely, A. *et al.* A functional homologue of gooseoid in *Drosophila*. *Development* **122**, 1641–1650 (1996).
45. Lewandoski, M. Conditional control of gene expression in the mouse. *Nat. Rev. Genet.* **2**, 743–755 (2001).
46. Clements, D., Taylor, H. C., Herrmann, B. G. & Stott, D. Distinct regulatory control of the Brachyury gene in axial and non-axial mesoderm suggests separation of mesoderm lineages early in mouse gastrulation. *Mech. Dev.* **56**, 139–149 (1996).
47. Danilov, V., Blum, M., Schweickert, A., Campione, M. & Steinbeisser, H. Negative autoregulation of the organizer-specific homeobox gene gooseoid. *J. Biol. Chem.* **273**, 627–635 (1998).
48. Schwenk, E., Baron, U. & Rajewsky, K. A cre-transgenic mouse strain for the ubiquitous deletion of loxP-flanked gene segments including deletion in germ cells. *Nucleic Acids Res* **23**, 5080–5081 (1995).
49. Park, T. J., Gray, R. S., Sato, A., Habas, R. & Wallingford, J. B. Subcellular localization and signaling properties of Dishevelled in developing vertebrate embryos. *Current Biology* **15**, 1039–1044 (2005).
50. Wallingford, J. B. & Harland, R. M. Neural tube closure requires Dishevelled-dependent convergent extension of the midline. *Development* **129**, 5815–5825 (2002).
51. Ybot-Gonzalez, P. *et al.* Convergent extension, planar-cell-polarity signalling and initiation of mouse neural tube closure. *Development* **134**, 789–799 (2007).
52. Axelrod, J. D., Miller, J. R., Shulman, J. M., Moon, R. T. & Perrimon, N. Differential recruitment of Dishevelled provides signaling specificity in the planar cell polarity and Wingless signaling pathways. *Genes Dev* **12**, 2610–2622 (1998).
53. Wallingford, J. B. *et al.* Dishevelled controls cell polarity during *Xenopus* gastrulation. *Nature* **405**, 81–85 (2000).
54. Carreira-Barbosa, E. *et al.* Prickle 1 regulates cell movements during gastrulation and neuronal migration in zebrafish. *Development* **130**, 4037–4046 (2003).
55. Park, M. & Moon, R. T. The planar cell-polarity gene *sbm* regulates cell behaviour and cell fate in vertebrate embryos. *Nat Cell Biol* **4**, 20–25 (2002).
56. Rothbacher, U. *et al.* Dishevelled phosphorylation, subcellular localization and multimerization regulate its role in early embryogenesis. *EMBO J.* **19**, 1019–1022 (2000).
57. Green, J. In *Molecular Methods in Developmental Biology* 127, 1–14 (Humana Press, 1999).
58. Blum, M. *et al.* Gastrulation in the mouse: the role of the homeobox gene gooseoid. *Cell* **69**, 1097–1106 (1992).
59. Blumberg, B., Wright, C. V., De Robertis, E. M. & Cho, K. W. Organizer-specific homeobox genes in *Xenopus laevis* embryos. *Science* **253**, 194–196 (1991).
60. Fletcher, R. B., Baker, J. C. & Harland, R. M. FGF8 spliceforms mediate early mesoderm and posterior neural tissue formation in *Xenopus*. *Development* **133**, 1703–1714 (2006).
61. Tahinci, E. & Symes, K. Distinct functions of Rho and Rac are required for convergent extension during *Xenopus* gastrulation. *Dev Biol* **259**, 318–335 (2003).
62. Wang, Y. & Nathans, J. Tissue/planar cell polarity in vertebrates: new insights and new questions. *Development* **134**, 647–658 (2007).
63. Goto, T. & Keller, R. The planar cell polarity gene *strabismus* regulates convergence and extension and neural fold closure in *Xenopus*. *Dev Biol* **247**, 165–181 (2002).
64. Wallingford, J. B., Goto, T., Keller, R. & Harland, R. M. Cloning and expression of *Xenopus* Prickle, an orthologue of a *Drosophila* planar cell polarity gene. *Mech. Dev.* **116**, 183–186 (2002).
65. Conlon, E. L. & Smith, J. C. Interference with brachyury function inhibits convergent extension, causes apoptosis, and reveals separate requirements in the FGF and activin signalling pathways. *Dev Biol* **213**, 85–100 (1999).
66. Tada, M. & Smith, J. C. *Xwnt11* is a target of *Xenopus* Brachyury: regulation of gastrulation movements via Dishevelled, but not through the canonical Wnt pathway. *Development* **127**, 2227–2238 (2000).
67. Danilov, V., Blum, M., Schweickert, A., Campione, M. & Steinbeisser, H. Negative Autoregulation of the Organizer-specific Homeobox Gene gooseoid. *Journal of Biological ...* (1998).
68. Gaunt, S. J., Blum, M. & de Robertis, E. M. Expression of the mouse gooseoid gene during mid-embryogenesis may mark mesenchymal cell lineages in the developing head, limbs and body wall. *Development* **117**, 769–778 (1993).
69. Ahrens, M. I., Li, Y., Jiang, H. & Dudley, A. T. Convergent extension movements in growth plate chondrocytes require GPI-anchored cell surface proteins. *Development* **136**, 3463–3474 (2009).
70. Park, T. J., Haigo, S. L. & Wallingford, J. B. Ciliogenesis defects in embryos lacking *inturned* or *fuzzy* function are associated with failure of planar cell polarity and Hedgehog signaling. *Nat Genet* **38**, 303–311 (2006).
71. Gaunt, S. J., Blum, M. & de Robertis, E. M. Expression of the mouse gooseoid gene during mid-embryogenesis may mark mesenchymal cell lineages in the developing head, limbs and body wall. *Development* **117**, 769–778 (1993).
72. Munnamalai, V. & Fekete, D. M. Wnt signaling during cochlear development. *Semin Cell Dev Biol* **24**, 480–489 (2013).
73. Kelly, M. & Chen, P. Shaping the mammalian auditory sensory organ by the planar cell polarity pathway. *Int J Dev Biol* **51**, 535–547 (2007).
74. Parry, D. A. *et al.* SAMS, a syndrome of short stature, auditory-canal atresia, mandibular hypoplasia, and skeletal abnormalities is a unique neurocristopathy caused by mutations in Gooseoid. *Am. J. Hum. Genet.* **93**, 1135–1142 (2013).
75. Qian, D. *et al.* Wnt5a functions in planar cell polarity regulation in mice. *Dev Biol* **306**, 121–133 (2007).
76. Onichtchouk, D. *et al.* The *Xvent-2* homeobox gene is part of the BMP-4 signalling pathway controlling [correction of controlling] dorsoventral patterning of *Xenopus* mesoderm. *Development* **122**, 3045–3053 (1996).
77. Putnam, N. H. *et al.* The amphioxus genome and the evolution of the chordate karyotype. *Nature* **453**, 1064–1071 (2008).
78. Yu, J.-K. S. The evolutionary origin of the vertebrate neural crest and its developmental gene regulatory network – insights from amphioxus. *Zoology (Jena)* **113**, 1–9 (2010).
79. Yu, J.-K., Meulemans, D., McKeown, S. J. & Bronner-Fraser, M. Insights from the amphioxus genome on the origin of vertebrate neural crest. *Genome Res.* **18**, 1127–1132 (2008).
80. Shimeld, S. M. & Donoghue, P. C. J. Evolutionary crossroads in developmental biology: cyclostomes (lamprey and hagfish). *Development* **139**, 2091–2099 (2012).
81. Gans, C. & Northcutt, R. G. Neural crest and the origin of vertebrates: a new head. *Science* **220**, 268–273 (1983).
82. Kantarci, H., Gerberding, A. & Riley, B. B. Spemann organizer gene Gooseoid promotes delamination of neuroblasts from the otic vesicle. *Proc Natl Acad Sci USA* 201609146–16. doi: 10.1073/pnas.1609146113 (2016).

83. Blitz, I. L., Fish, M. B. & Cho, K. W. Y. Leapfrogging: primordial germ cell transplantation permits recovery of CRISPR/Cas9-induced mutations in essential genes. *Development* **143**, 2868–2875 (2016).
84. Blum, M., De Robertis, E. M., Wallingford, J. B. & Niehrs, C. Morpholinos: Antisense and Sensibility. *Dev. Cell* **35**, 145–149 (2015).
85. Gao, B. *et al.* Wnt signaling gradients establish planar cell polarity by inducing Vangl2 phosphorylation through Ror2. *Dev. Cell* **20**, 163–176 (2011).
86. Gros, J. *et al.* WNT5A/JNK and FGF/MAPK pathways regulate the cellular events shaping the vertebrate limb bud. *Curr. Biol.* **20**, 1993–2002 (2010).
87. Keller, R. & Winklbauer, R. In **27**, 39–89 (Elsevier, 1992).
88. Yamada, G. *et al.* Targeted mutation of the murine goosecoid gene results in craniofacial defects and neonatal death. *Development* **121**, 2917–2922 (1995).
89. Shapira, E., Marom, K., Levy, V., Yelin, R. & Fainsod, A. The *Xvex-1* antimorph reveals the temporal competence for organizer formation and an early role for ventral homeobox genes. *Mech. Dev.* **90**, 77–87 (2000).
90. Paterson, H. F. *et al.* Microinjection of recombinant p21rho induces rapid changes in cell morphology. *J. Cell Biol.* **111**, 1001–1007 (1990).
91. Takeuchi, M. *et al.* The prickle-related gene in vertebrates is essential for gastrulation cell movements. *Current Biology* **13**, 674–679 (2003).
92. Medina, A., Reintsch, W. & Steinbeisser, H. *Xenopus* frizzled 7 can act in canonical and non-canonical Wnt signaling pathways: implications on early patterning and morphogenesis. *Mech. Dev.* **92**, 227–237 (2000).
93. Tözser, J. *et al.* TGF- β Signaling Regulates the Differentiation of Motile Cilia. *Cell Reports* **11**, 1000–1007 (2015).
94. Sive, H. L., Grainger, R. M. & Harland, R. M. *Early development of Xenopus laevis* (2000).
95. Belo, J. A. *et al.* Cerberus-like is a secreted factor with neutralizing activity expressed in the anterior primitive endoderm of the mouse gastrula. *Mech. Dev.* **68**, 45–57 (1997).
96. Sulik, K. *et al.* Morphogenesis of the murine node and notochordal plate. *Dev. Dyn.* **201**, 260–278 (1994).
97. Karpinka, J. B. *et al.* Xenbase, the *Xenopus* model organism database; new virtualized system, data types and genomes. *Nucleic Acids Res.* **43**, D756–63 (2015).

Acknowledgements

This paper is dedicated to the memory of the late Herbert Steinbeißer, who passed away in 2014. He was involved in this project from its beginning in the 1990s; the Dvl2 membrane recruitment experiments in animal caps were performed in his laboratory. We thank all members of the Blum lab for continuous support and suggestions. Verena Andre, Andreas Faessler, Simone Kienle, Anna Schäfer and Susanne Seitz helped with some of the experiments. This work was supported by a grant from the Volkswagen Foundation to MB and a fellowship from the Landesgraduiertenförderung Baden-Württemberg to BU.

Author Contributions

M.B. conceived the project and supervised it throughout. B.U. performed the *Xenopus* experiments except for the *Gsc* mutant analysis in whole embryos, the apoptosis and proliferation analysis in *Gsc*-GR injected neural plates, the Dvl2 membrane localization assay to investigate the cell-autonomous *Gsc* function in animal caps, the expression analysis of *Xenopus Gsc* during organogenesis and the protein alignments of invertebrate and vertebrate *Gsc* sequences, which were performed by M.T., S.K. and M.M.; D.M. analyzed the inner ear phenotype in *Gsc* knockout mice; M.C. generated the T-*Gsc* mouse line; K.D. generated and analyzed the mT-*Gsc* mouse line together with P.A.; M.L. provided the conditional mouse expression system; T.T. analyzed the cartilage phenotype in *Gsc* morphants; A.F. suggested important experiments and helped with the interpretation of results; A.S. provided constant advice and helped with the interpretation and evaluation of data. H.S. was an invaluable advisor throughout the project; he suggested the animal cap experiments, which B.U. performed in his laboratory. M.B. and B.U. wrote the manuscript with input from A.F., A.S., M.T., S.K., M.M., M.C., M.L.

Additional Information

Supplementary information accompanies this paper at <http://www.nature.com/srep>

Competing financial interests: The authors declare no competing financial interests.

How to cite this article: Ulmer, B. *et al.* A novel role of the organizer gene *Goosecoid* as an inhibitor of Wnt/PCP-mediated convergent extension in *Xenopus* and mouse. *Sci. Rep.* **7**, 43010; doi: 10.1038/srep43010 (2017).

Publisher's note: Springer Nature remains neutral with regard to jurisdictional claims in published maps and institutional affiliations.



This work is licensed under a Creative Commons Attribution 4.0 International License. The images or other third party material in this article are included in the article's Creative Commons license, unless indicated otherwise in the credit line; if the material is not included under the Creative Commons license, users will need to obtain permission from the license holder to reproduce the material. To view a copy of this license, visit <http://creativecommons.org/licenses/by/4.0/>

© The Author(s) 2017

Supplementary Information

A novel role of the organizer gene *Goosecoild* as an inhibitor of Wnt/PCP-mediated convergent extension in *Xenopus* and mouse

Bärbel Ulmer^{1§+}, Melanie Tingler^{1§}, Sabrina Kurz^{1§}, Markus Maerker^{1§}, Philipp Andre¹, Dina Mönch¹, Marina Campione^{1*}, Kirsten Deißler¹, Mark Lewandoski², Thomas Thumberger^{1&}, Axel Schweickert¹, Abraham Fainsod³, Herbert Steinbeißer⁴ and Martin Blum^{1#}

¹University of Hohenheim, Garbenstr. 30, 70599 Stuttgart, Germany

²Genetics of Vertebrate Development Section, Cancer and Developmental Biology Lab, National Cancer Institute, National Institutes of Health, Frederick, MD 21702, USA

³Department of Developmental Biology and Cancer Research, Institute for Medical Research Israel-Canada, Hebrew University, Jerusalem 9112102, Israel

⁴Institute of Human Genetics, University Hospital Heidelberg, Im Neuenheimer Feld 366, 69120 Heidelberg, Germany

⁺Present address: Department of Experimental Pharmacology and Toxicology, Cardiovascular Research Center, University Medical Center Hamburg-Eppendorf, 20246 Hamburg, Germany.

^{*}Present address: CNR-Neuroscience Institute, Department of Biomedical Sciences, University of Padova, Italy

[&]Present address: Centre for Organismal Studies (COS) Heidelberg, Heidelberg University, Im Neuenheimer Feld 230, 69120 Heidelberg, Germany

[§]These authors contributed equally to the present work

[#]Corresponding author: martin.blum@uni-hohenheim.de

SUPPLEMENTARY INFORMATION

Supplemental Figures and Tables

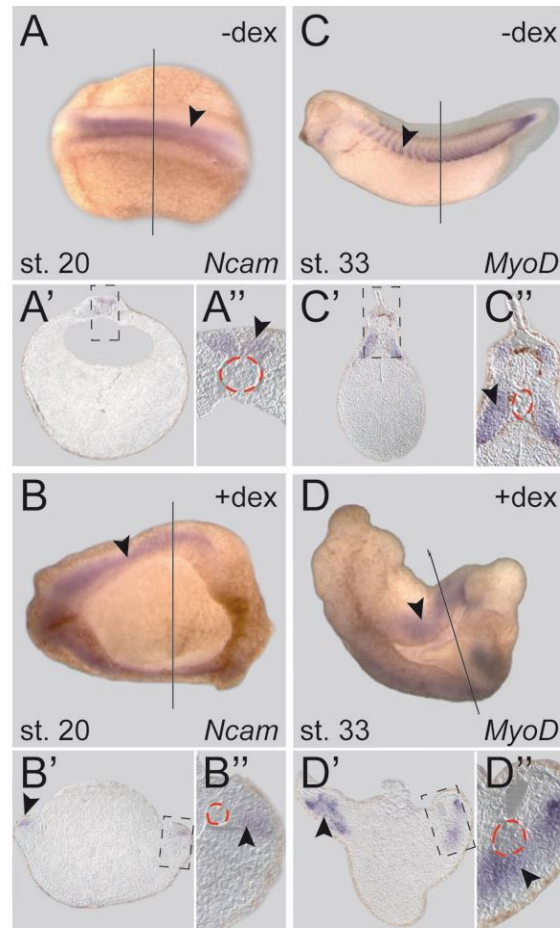


Fig. S1. Characterization of *Gsc-GR* mediated CE phenotypes in *Xenopus* embryos. Analysis of neural (*Ncam*; A, B) and paraxial mesodermal (somite; *MyoD*; C, D) marker gene expression in wildtype (-dex; A, C) and *Gsc-GR* expressing (+dex; B, D) embryos. Dex was added at stage 6-9, and embryos were analyzed for marker gene expression by whole-mount in situ hybridization following fixation at the stages indicated. Note that specification of examined tissues (arrowheads) was not affected. Solid lines indicate planes of sections, dashed boxes mark regions shown in higher magnification. Red dashed lines outline notochord.

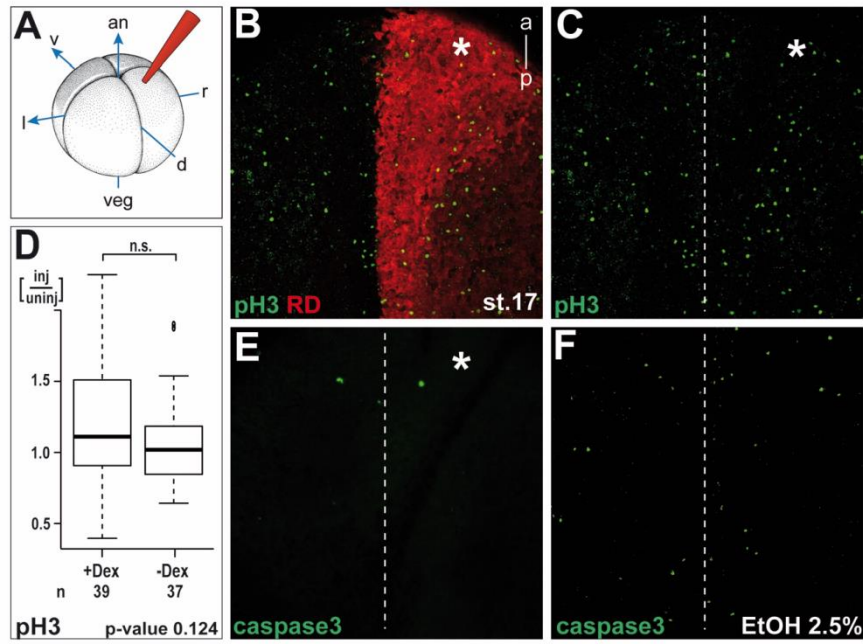


Fig. S2. Proliferation (A-D) and apoptosis (A, E, F) were unaffected upon *Gsc-GR* activation in the neuroectoderm. Embryos were unilaterally injected with *Gsc-GR* and lineage tracer rhodamine dextrane into the neuroectodermal (dorsal-animal) lineage at the 4-cell stage, dex was added (+Dex) or omitted (-Dex) between st.6-8, and specimens were cultured until stage 17. *, injected side. Proliferation and apoptosis were assessed by IF using an anti-pH3 (B, C) and anti-caspase3 antibodies (E, F), respectively. (D) Evaluation of proliferation. (F) Ethanol treatment at stage 13 (2.5%) served as a positive control for induction of apoptosis. Note that neither proliferation nor apoptosis were affected by *Gsc-GR* activation.

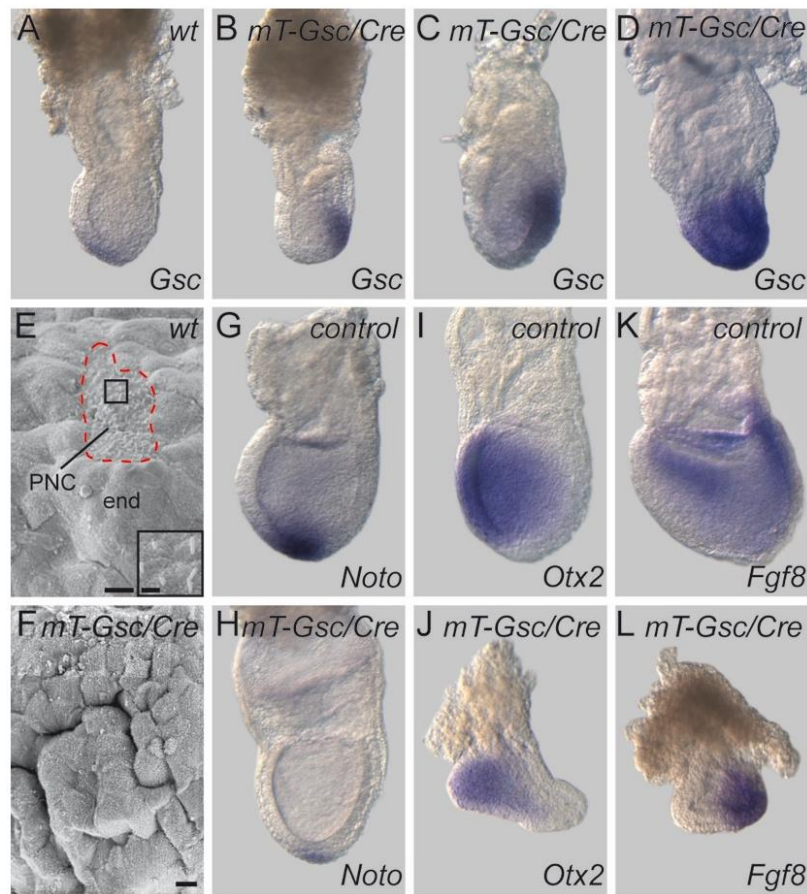


Fig. S3. Characterization of E7.5 *mt-Gsc/Cre* embryos.

(A-D) Variable degree of ectopic *Gsc* mRNA expression in E7.5 *mT-Gsc/Cre* embryos (B-D) compared to wildtype (A; wt).

(E, F) Scanning electron micrographs, revealing absence of ciliated epithelium of posterior notochord (PNC; outlined by dashed red line), and deep furrows in endodermal cell layer of *mt-Gsc/Cre* specimen (F) as compared to wt embryo (E). Detail of ciliated epithelium shown in higher magnification in inset of (E).

(G, H) Reduced *Noto* mRNA transcription in *mt-Gsc/Cre* (H) compared to wt (G) embryo.

(I-L) *Otx2* (I, J) and *Fgf8* (K, L) gene expression demonstrate normal anterior-posterior axis specification in *mT-Gsc/Cre* (J, L) compared to wt (I, K) embryos.

Scale bars in (E, F) represent 10 μm and 2 μm in inset of (E).

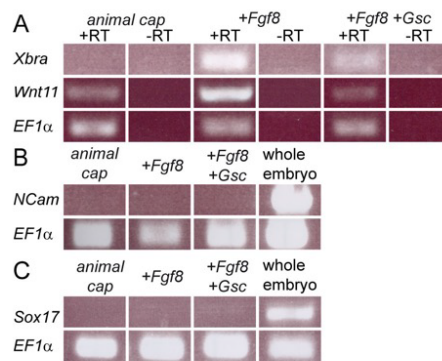


Fig. S4. Mesodermal differentiation of *Fgf8*-injected animal cap explants.

Semi-quantitative RT-PCR analysis of animal cap explants injected with *Gsc-GR* and/or *Fgf8*.

(A) *Fgf8* induces transcription of mesodermal marker genes *Xbra* und *Wnt11*.

(B, C) No induction of the neural marker *Ncam* (B) or the endoderm gene *Sox17* (C). Elongation factor 1 α (*EF1 α*) served as loading control.

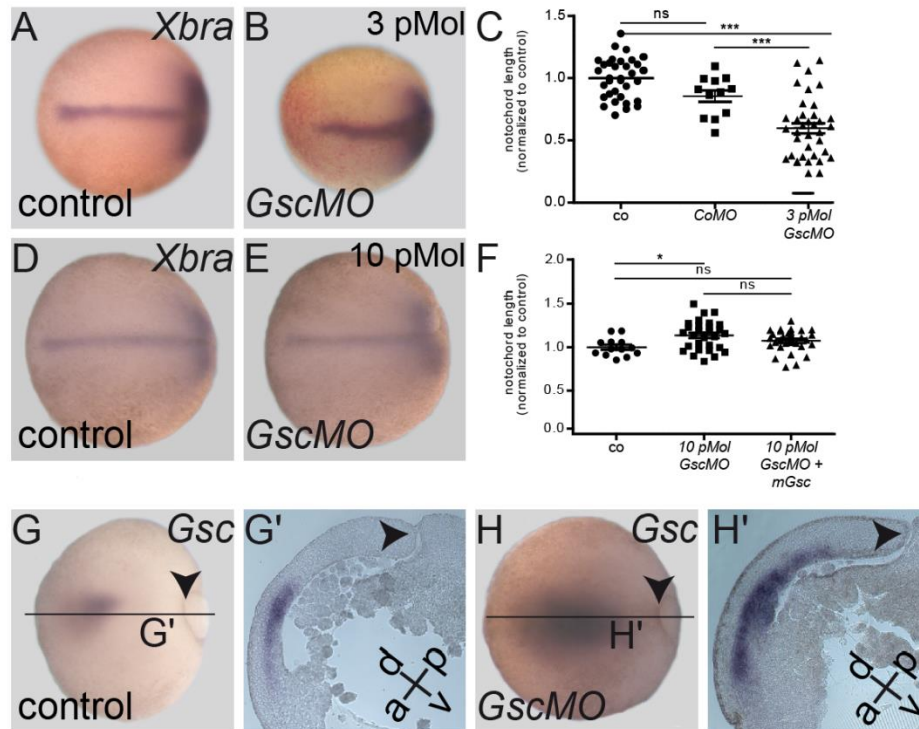


Fig. S5. CE phenotypes in *Gsc* morphant *Xenopus* embryos.

(A-C) Shorter and widened notochord as judged by *Xbra* mRNA expression in low dose *Gsc* morphant (B) as compared to control MO injected specimen (A). (C) Quantitative assessment of notochord lengths (normalized to control which was set to 1.0 in uninjected specimens).

(D-F) High dose injections of *GscMO* enhanced axis elongation. (D, E) *Xbra* mRNA expression in control un-injected embryo (co, D) and high dose *Gsc* morphant (E). (F) Quantification of notochord lengths in controls, high dose *Gsc* morphants and morphant specimens co-injected with a mouse *Gsc* cDNA construct.

(G, H) *Gsc* mRNA expression in low-dose *Gsc* morphants. (G, G') *Gsc* mRNA expression in control MO-injected neurula stage embryo. (H, H') Upregulated and expanded *Gsc* expression levels in *Gsc* morphant. Note that *Gsc* expression in morphant almost extended to the blastopore (arrowheads in G', H'). a, anterior; co, control un-injected; CoMO; control MO-injected; d, dorsal; p, posterior; v, ventral. Embryos shown with anterior to the left.

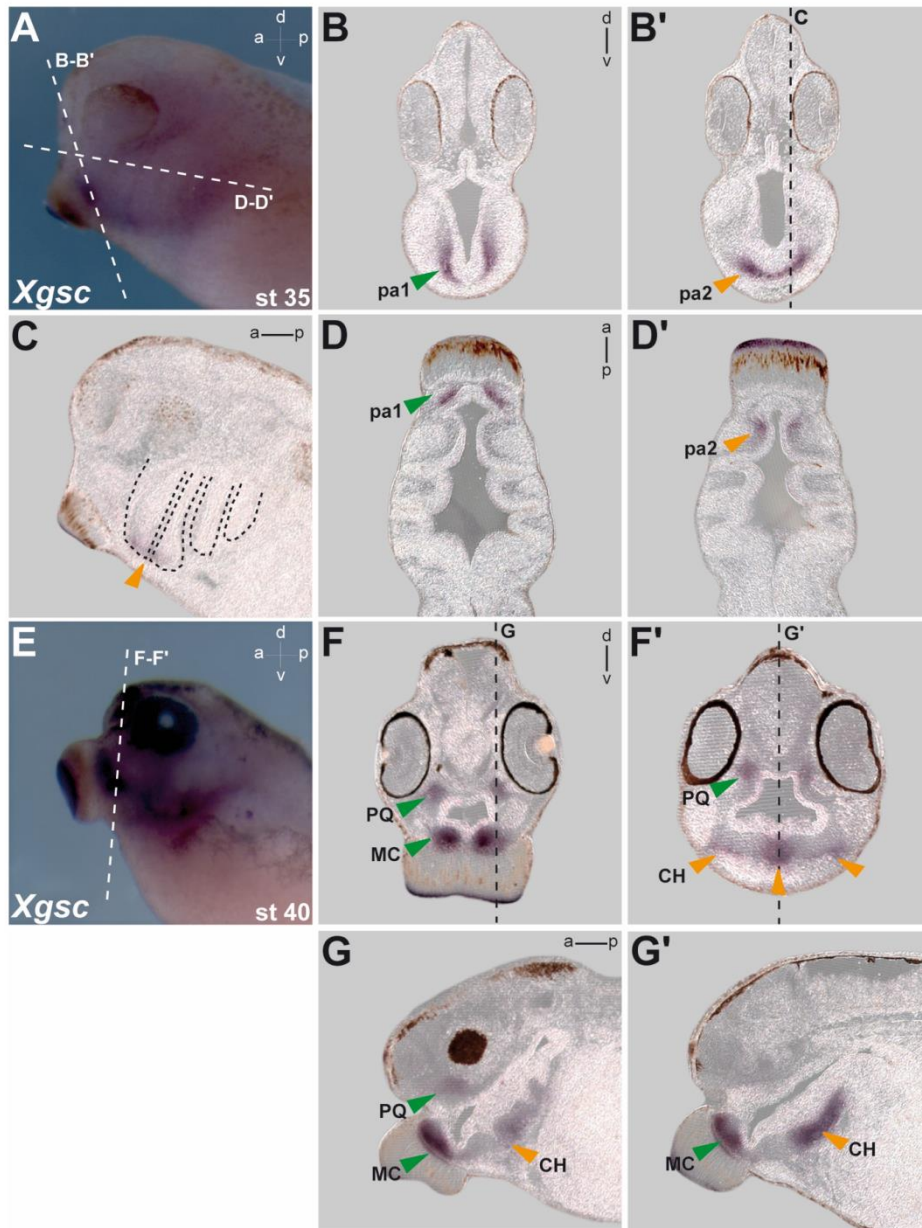


Fig. S6. *Gsc* expression in cranial neural crest and derived head cartilage. Whole-mount *in situ* hybridization of st. 35 (A-D) and st. 40 (E-G) tadpoles with a *Gsc*-specific antisense probe. Planes of histological vibratome sections are indicated by dashed lines. *Gsc* transcripts were found in pharyngeal arch (pa) mesenchyme and in differentiating cranial cartilage. Green arrowheads, pa1 and its derivatives palatoquadrate (PQ) and Meckel's cartilage (MC); orange arrowheads, pa2 and its derivative ceratohyal (CH).

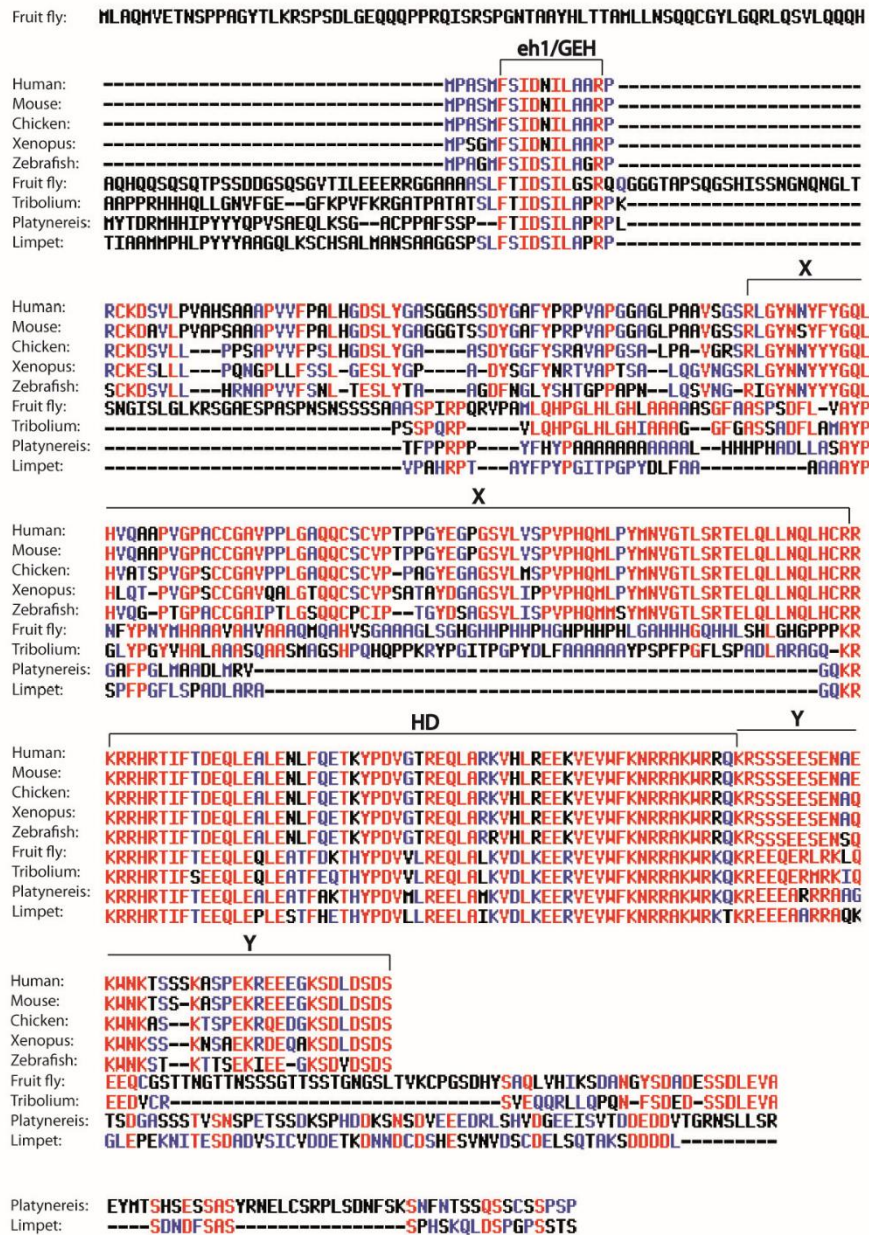


Fig. S7. Multiple sequence alignment of Gsc proteins. Note that the eH1- and homeodomains are very highly conserved throughout the animal kingdom. Two similarly highly conserved domains N- and C-terminal of the homeodomain, marked "X" and "Y", are specific for vertebrate Gsc protein sequences. The following sequences were used: human (NM_173849.2), mouse (NM_010351.1), chicken (NP_990662.1), *Xenopus* (XM_018231890.1), zebrafish (NM_131017.1), fruit fly (CAA64699.1), tribolium (XP_008198241.1), *Platynereis* (AJ289023.1), limpet (AJ507423.1). Alignments were generated using multalin (<http://multalin.toulouse.inra.fr/multalin/>).

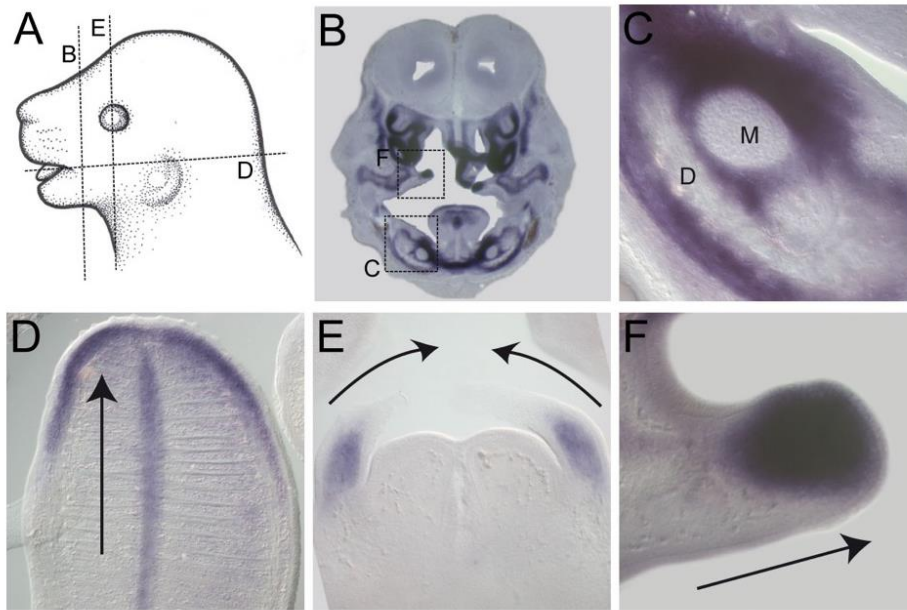


Fig. S8. *Gsc* expression adjacent to tissues undergoing elongation in E14.5 mouse embryos.

In situ hybridisation using a mouse *Gsc* antisense RNA probe on frontal and transversal vibratome section of E14.5 wildtype mouse embryos.

(A) Schematic depiction of sectional planes.

(B, C) *Gsc* transcripts localize to regions around Meckel's (M) cartilage and the developing *dentate*.

(D) *Gsc* was expressed at the tip of the tongue and the developing *septum linguae*. (E) *Gsc* transcript localization to the arytenoid swellings before fusion.

(F) *Gsc* expression in the mesenchyme of the palatal shelves.

	wt		BPD		NTD		n	n defects	p wt-defects Chi-Square
	n	%	n	%	n	%			
GscGR, 10 experiments									
uninjected controls with/without dex	267	93,0	3	1,0	17	5,9	287	20	
<i>GscGR</i> without dex	183	92,0	6	3,0	10	5,0	199	16	
<i>GscGR</i> + dex st 6-8	67	38,3	64	36,6	44	25,1	175	108	<10-4
<i>GscGR</i> + dex st 11	32	47,8	7	10,4	28	41,8	67	35	<10-4
<i>GscGR</i> + dex st 12,5	46	97,9	1	2,1		0,0	47	1	0,080
RhoAca, 4 experiments									
uninjected controls with/without dex	95	95,0	5	5,0	0	0,0	100	5	
<i>GscGR</i> without dex	20	80,0	1	4,0	4	16,0	25	5	
<i>GscGR</i> and <i>RhoAca</i> without dex	51	73,9	4	5,8	14	20,3	69	18	
<i>GscGr</i> with dex	20	22,2	61	67,8	9	10,0	90	70	
Rescue (<i>GscGR</i> and <i>RhoAca</i> with dex)	60	48,0	24	19,2	41	32,8	125	65	<10-4
RhoAdn, 4 experiments									
uninjected controls with dex	149	96,1	3	1,9	3	1,9	155	6	
<i>GscGR</i> 160 pg without dex	85	88,5	4	4,2	7	7,3	96	11	
<i>GscGr</i> 160 pg with dex	65	58,6	20	18,0	26	23,4	111	46	
<i>GscGR</i> and <i>RhoAdn</i> without dex	55	47,4	37	31,9	24	20,7	116	61	
Rescue (<i>GscGR</i> and <i>RhoAdn</i> with dex)	22	21,8	61	60,4	18	17,8	101	79	<10-4
Prickle, 4 experiments									
uninjected controls without dex	137	95,8	2	1,4	4	2,8	143	6	
<i>GscGR</i> without dex	70	93,3	5	6,7	0	0,0	75	5	
<i>GscGR</i> and <i>Prickle</i> without dex	70	82,4	9	10,6	6	7,1	85	15	
<i>GscGr</i> with dex	18	22,0	49	59,8	15	18,3	82	64	
Rescue (<i>GscGR</i> and <i>Prickle</i> with dex)	43	48,9	35	39,8	10	11,4	88	45	<10-4
Vangl2, 6 experiments									
uninjected controls without dex	115	95,8	0	0,0	5	4,2	120	5	
<i>GscGR</i> without dex	55	94,8	2	3,4	1	1,7	58	3	
<i>GscGR</i> and <i>Vangl2</i> without dex	90	72,0	10	8,0	25	20,0	125	35	
<i>GscGr</i> with dex	38	37,3	48	47,1	16	15,7	102	64	
Rescue (<i>GscGR</i> and <i>Vangl2</i> with dex)	70	55,6	40	31,7	16	12,7	126	56	0,006
T, 6 experiments									
uninjected controls without dex	131	94,9	2	1,4	5	3,6	138	7	
<i>GscGR</i> without dex	37	90,2	2	4,9	2	4,9	41	4	
<i>GscGR</i> and <i>T</i> without dex	82	79,6	8	7,8	13	12,6	103	21	
<i>GscGr</i> with dex	27	20,9	82	63,6	20	15,5	129	102	
Rescue (<i>GscGR</i> and <i>T</i> with dex)	53	35,3	44	29,3	53	35,3	150	97	0,008
Wnt11, 3 experiments									
uninjected controls	45	90,0	1	2,0	4	8,0	50	5	
<i>GscGR</i> without dex	20	80,0	4	16,0	1	4,0	25	5	
<i>GscGR</i> and <i>Wnt11</i> without dex	23	69,7	3	9,1	7	21,2	33	10	
<i>GscGR</i> with dex	8	11,0	54	74,0	11	15,1	73	65	
Rescue (<i>GscGR</i> and <i>Wnt11</i> with dex)	31	33,3	38	40,9	24	25,8	93	62	0,007

Table S1. *Gsc-GR* induced CE phenotypes and rescue by PCP components.

Raw data of experiments summarized in Figure 2. BPD, blastopore closure defect; NTD, neural tube closure defect. Statistical analyses were performed using StatPages.org.

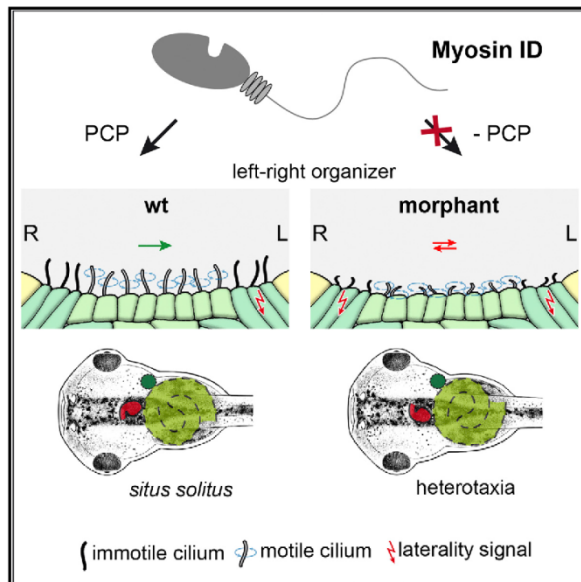
**Original research Chapter II:
Left-right axis development**

A conserved role for the Unconventional Myosin1d in Laterality Determination

Current Biology

A Conserved Role of the Unconventional Myosin 1d in Laterality Determination

Graphical Abstract



Authors

Melanie Tingler, Sabrina Kurz, Markus Maerker, ..., Janine M. LeBlanc-Straceski, Stéphane Noselli, Martin Blum

Correspondence

martin.blum@uni-hohenheim.de

In Brief

Tingler et al. show that myosin 1D is required for laterality in the frog *Xenopus*, namely for left-asymmetric gene expression and leftward flow. Myosin 1D acts through the planar cell polarity pathway, a key feature of asymmetric gonad and gut morphogenesis in *Drosophila*, suggesting a common evolutionary origin of arthropod and chordate laterality.

Highlights

- The unconventional myosin 1D is required for vertebrate left-right asymmetry
- Loss of *myo1d* causes aberrant leftward flow and laterality defects in *Xenopus*
- The function of myosin1D is mediated through the planar cell polarity pathway
- Myosin 1D links laterality in arthropods and chordates



Tingler et al., 2018, *Current Biology* 28, 810–816
 March 5, 2018 © 2018 Elsevier Ltd.
<https://doi.org/10.1016/j.cub.2018.01.075>

CellPress

A Conserved Role of the Unconventional Myosin 1d in Laterality Determination

Melanie Tingler,^{1,4} Sabrina Kurz,^{1,4} Markus Maerker,^{1,4} Tim Ott,^{1,4} Franziska Fuhl,^{1,4} Axel Schweickert,¹ Janine M. LeBlanc-Straceski,² Stéphane Noselli,³ and Martin Blum^{1,5,*}

¹University of Hohenheim, Institute of Zoology, Garbenstrasse 30, 70593 Stuttgart, Germany

²Department of Biology, Merrimack College, 315 Turnpike Street, North Andover, MA 01845, USA

³Université Côte d'Azur, CNRS, INSERM, Institut de Biologie Valrose, Parc Valrose, 06108 Nice, France

⁴These authors contributed equally

⁵Lead Contact

*Correspondence: martin.blum@uni-hohenheim.de

<https://doi.org/10.1016/j.cub.2018.01.075>

SUMMARY

Anatomical and functional asymmetries are widespread in the animal kingdom [1, 2]. In vertebrates, many visceral organs are asymmetrically placed [3]. In snails, shells and inner organs coil asymmetrically, and in *Drosophila*, genitalia and hindgut undergo a chiral rotation during development. The evolutionary origin of these asymmetries remains an open question [1]. Nodal signaling is widely used [4], and many, but not all, vertebrates use cilia for symmetry breaking [5]. In *Drosophila*, which lacks both cilia and Nodal, the unconventional myosin ID (*myo1d*) gene controls dextral rotation of chiral organs [6, 7]. Here, we studied the role of *myo1d* in left-right (LR) axis formation in *Xenopus*. Morpholino oligomer-mediated *myo1d* downregulation affected organ placement in >50% of morphant tadpoles. Induction of the left-asymmetric Nodal cascade was aberrant in >70% of cases. Expression of the flow-target gene *dand5* was compromised, as was flow itself, due to shorter, fewer, and non-polarized cilia at the LR organizer. Additional phenotypes pinpointed Wnt/planar cell polarity signaling and suggested that *myo1d*, like in *Drosophila* [8], acted in the context of the planar cell polarity pathway. Indeed, convergent extension of gastrula explant cultures was inhibited in *myo1d* morphants, and the ATF2 reporter gene for non-canonical Wnt signaling was down-regulated. Finally, genetic interference experiments demonstrated a functional interaction between the core planar cell polarity signaling gene *vangl2* and *myo1d* in LR axis formation. Thus, our data identified *myo1d* as a common denominator of arthropod and chordate asymmetry, in agreement with a monophyletic origin of animal asymmetry.

RESULTS AND DISCUSSION

The Unconventional myosinID Gene Is Required for LR Axis Formation in *Xenopus laevis*

We have previously shown that maternal and zygotic Myo1d is present in the *Xenopus* egg cell and throughout the first 3 days of embryogenesis [9], i.e., before, during, and after left-right (LR) symmetry breaking [5]. Zygotic mRNA expression was predominantly found in presomitic mesoderm and somites [9], tissues related to the *Xenopus* LR organizer (LRO) [5]. To assess a possible function of *myo1d* in *Xenopus* LR axis formation, an antisense morpholino oligomer (MO) was designed that targeted sequences overlapping the translational start site (AUG-MO). AUG-MO was injected at the 4-cell stage and targeted toward the LRO. Specimens were cultivated until they reached stages 24, 32, or 45 to investigate *nodal1* or *pitx2* expression and organ situs, respectively. Organ placement, as assessed by heart and gut looping as well as positioning of the gall bladder (Figure 1A), was significantly disturbed in specimens injected with AUG-MO (Figures 1B–1D). Likewise, left-asymmetric expression of *nodal1* and *pitx2* were disturbed in >70% of AUG-MO-injected morphants, with bilateral expression in the left and right lateral plate mesoderm (LPM) representing the most commonly observed defective pattern (Figures 1E and 1F; Figures S1A–S1H). Remarkably, AUG-MO caused phenotypes at very low doses (0.2 pmol or 3.3 ng per embryo). Furthermore, a scrambled mismatch MO (MM-MO) did not affect the laterality of injected embryos (Figures 1E and 1F). In addition, Myo1d protein was downregulated in morphant embryos, as shown by western blot analysis (Figure S1I). A full-length *myo1d* expression construct [10] that was not targeted by AUG-MO partially rescued left-asymmetric *nodal1* expression in the LPM (Figure 1E). Together, these experiments argue for MO specificity. Bilateral *nodal1/pitx2* expression, observed in the majority of LR-altered *myo1d* morphants (75%; cf. Figures 1E and 1F), also occurs when the midline barrier function is disturbed [11], i.e., when Nodal1 protein crosses from the left to the right side. However, the midline in *myo1d* morphants was normal, as shown by the wild-type expression pattern of the midline barrier gene *lefy1* (Figures S1J and S1K).

To confirm the MO-derived LR phenotypes, we created CRISPR/Cas9 F0 mutants in *Xenopus laevis*. Two guide RNAs were designed, targeting subdomains of the ATP-binding site



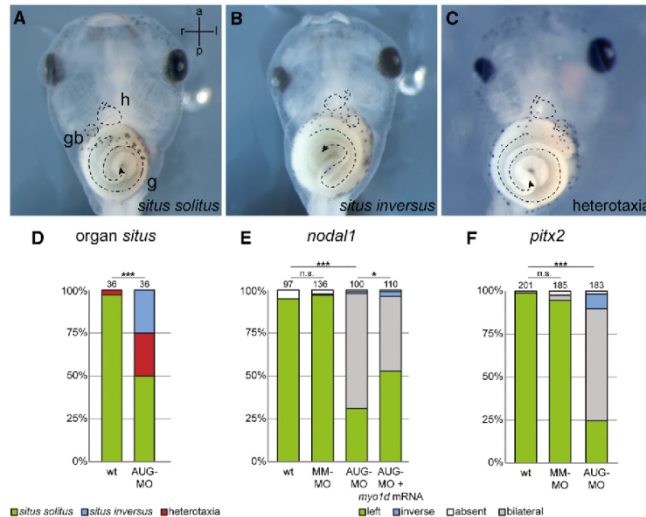


Figure 1. *myo1d* Is Required for LR Axis Formation in *Xenopus laevis*

(A–D) Organ situs in wild-type (A) and *myo1d* morphant tadpoles displaying situs inversus (B) and heterotaxia (C) at stage 45. g, gut; gb, gall bladder, h, heart.

(D) Quantification of organ situs analysis.

(E and F) Quantification of *nodal1* (E) and *pitx2* (F) expression patterns in wildtype embryos and specimens injected with MM-MO, AUG-MO or co-injected with AUG-MO and rescue mRNA. Numbers represent analyzed specimens, which were derived from 3 (D and E) and 5 (F) independent experiments. See also Figure S1.

(Figure 2A), which were separately co-injected together with Cas9 protein into 1-cell-stage embryos [12]. Both resulted in identical ranges of phenotypes (Figures 2B and 2C): at least half the embryos were severely malformed, with gastrulation and blastopore closure defects, preventing the analysis of marker gene expression. Importantly, these phenotypes were encountered upon the injection of high doses of AUG-MO as well (data not shown). The remaining injected F0 specimens were evaluated for *pitx2* expression. About 60% lacked asymmetry and showed absent or bilateral *pitx2* expression (Figure 2D); remarkably, these embryos were also stunted, i.e., revealed a convergence extension phenotype (Figure 2C). The remaining specimens appeared normal and displayed left-asymmetric *pitx2* expression (Figures 2C and 2D). F0 *myo1d* mutants thus closely resembled *myo1d* morphants, as in both cases asymmetric marker gene expression was lost. Differences were recorded, however, namely that in morphants, Nodal cascade gene expression was bilateral in the vast majority of cases, while it was absent or bilateral in mutants. Although we lack a conclusive explanation at this time, beyond realizing that gene knockdowns differ from mosaic F0 mutants, genome editing provided additional proof of MO specificity, as in both cases the same quality of LR defect was observed, i.e., loss of asymmetry. In summary, these experiments demonstrated a role for *myo1d* in LR axis formation in *Xenopus*.

***myo1d* Is Required for LRO Morphogenesis and Leftward Flow**

Induction of the left-asymmetric Nodal cascade in the LPM of the 2-day embryo is preceded by several well-defined morphogenetic and molecular steps, beginning with the specification of the LRO precursor, the so-called superficial mesoderm (SM), which forms caudal to the Spemann organizer at mid-gastrula stages [5, 13] (Figure S2A). The SM was not affected in *myo1d*

morphants, as demonstrated by the expression of marker genes *foxj1* and *wnt11b* [14] (Figures S2B–S2E). The LRO in the frog is represented by the transient ciliated epithelium of the gastrocoel roof plate (GRP), which forms at the dorsal-posterior end of the primitive gut when SM cells involute during gastrulation [13, 15] (Figure S2A). We investigated whether the GRP had correctly formed in *myo1d* morphants using a Tektin isoform marker gene; *tekt2* expression was unaffected (Figures S2F and S2G), indicating that a GRP had formed. LRO function of the GRP arises when cilia develop and polarize in the central region of the GRP. As they become motile, they produce a leftward flow of extracellular fluids [16], which, presumably, is sensed by peripheral GRP cells harboring non-polarized and immotile cilia [1, 5].

To assess GRP morphogenesis, dorsal explants were prepared and analyzed for cilia by immunofluorescence (IF) using an antibody against acetylated alpha-tubulin. Figures 3A–3E show that, although cilia were present in morphant GRPs, ciliation was markedly altered. Cilia were significantly shorter, showed reduced polarization to the posterior pole of cells (a prerequisite of leftward flow), and were reduced in number (Figures 3F–3H). To determine if the flow itself was compromised, the transport of fluorescent microbeads was assessed using high-speed videography [16]. Time-lapse movies of GRPs show that flow was indeed disordered in *myo1d* morphants compared to wild-type specimens (Movie S1). Evaluation of flow parameters confirmed this disruption, with significantly reduced flow velocity and directionality in *myo1d* morphant specimens (Figures 3I and 3J). Importantly, some individual beads showed inverted movement, i.e., from left to right (Movie S1), in agreement with the observed predominant bilateral induction of asymmetric LPM marker genes (cf. Figures 1E and 1F). Leftward flow induces asymmetric LPM gene expression by downregulating the Nodal repressor *dand5* in lateral GRP cells (i.e., the purported flow sensor cells), where this gene is co-expressed with *nodal1* [17]. Expression of both genes was analyzed in dorsal explants isolated at post-flow stages (stage 19). Figures 3K–3O show that *nodal1* was unaffected in morphants, while *dand5* asymmetries were lost due to bilateral downregulation of mRNA expression. Expression of the

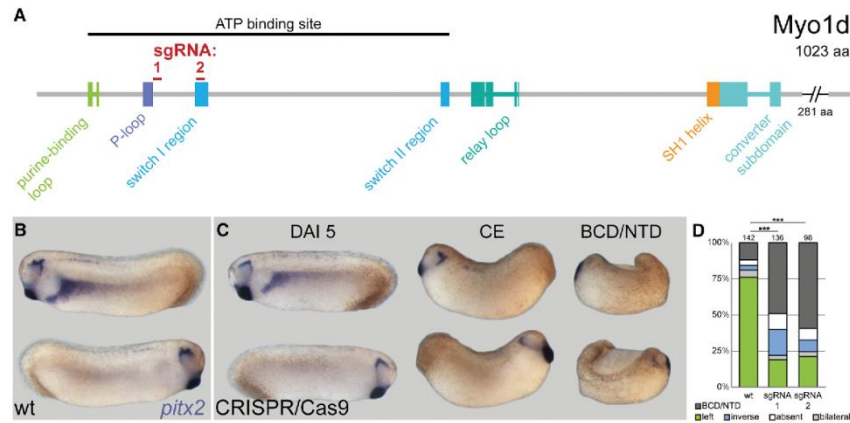


Figure 2. Laterality Defects in Genome-Edited F0 *myo1d* Mutant Tadpoles

(A) Schematic depicting Myo1d protein structure (sgRNA sites indicated). (B and C) Appearance and *pitx2* gene expression in WT (B) and F0 *myo1d* mutant (C) tadpoles. (D) Compilation of *pitx2* expression patterns. BCD, blastopore closure defect; NTD, neural tube closure defect. Note that mutant embryos with WT appearance showed WT *pitx2* expression in the left LPM, while stunted specimens with a convergent extension (CE) phenotype lacked expression or displayed mRNA expression on both sides.

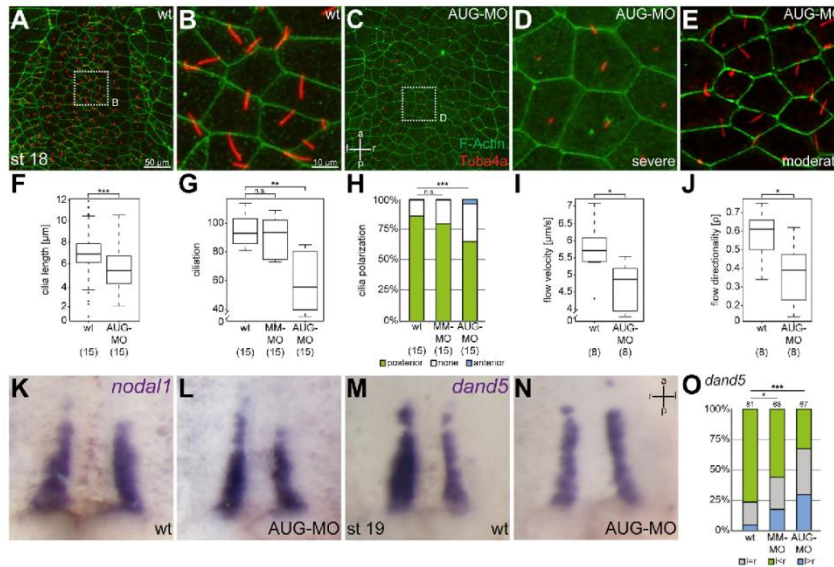
transforming growth factor β (TGF- β) gene *gdf3*, the functional frog homolog of the Nodal agonist *Gdf1* in mouse, was unaltered in morphants (Figures S2H and S2I). In summary, these results demonstrated that *myo1d* was required for GRP morphogenesis and leftward flow and that downregulation of this conserved unconventional myosin resulted in a loss of molecular asymmetries and, consequently, a high frequency of heterotaxia (*situs ambiguus*) and *situs inversus* in morphant tadpoles (Figure 1).

PCP Defects in *myo1d* Morphant Frog Embryos

In *Drosophila*, *myo1d* interacts with both the global (Dachsous/Fat) and core (Frizzled/Wnt) PCP pathways to control chiral morphogenesis of the adult hindgut [8]. In the course of analyzing *myo1d* morphant *Xenopus* embryos, we noted a number of LR-unrelated developmental defects that have been linked to altered PCP signaling. First, the apical surface of GRP cells appeared enlarged in morphants as compared to wild-type (WT), suggesting a defect in apical constriction of involuting SM cells (cf. Figures 2A–2E). Apical constriction during gastrulation and neural tube closure is under the control of PCP [18]. Quantification of 25 cells each from 15 WT and 15 morphant embryos revealed that, on average, the cell surface in *myo1d* morphants was increased by 25% (Figure 4A). Second, neural tube closure was delayed in morphant embryos, i.e., the neural tube was still open at stage 18 when it had just closed in wild-type specimens (Figure 4B; Figures S3A and S3B; Movie S2). Delayed neural tube closure has been reported in the frog upon knockdown of *dishevelled2* (*dsh2*) and characterized as a convergent-extension (CE) defect that fails to narrow the midline [19]. In mouse embryos lacking one or both copies of the core PCP gene *vangl2*, the same phenotype was described [20]. Third, the ciliation of

multi-ciliated cells (MCCs) in the larval skin of *myo1d* morphants was delayed. Ciliation of MCCs was much reduced on the morphant side of unilaterally injected stage 24 embryos, compared to the uninjected contralateral side (Figure S3C). No differences were recorded at stage 32, i.e., this phenotype represented a transient delay in MCC differentiation and apical intercalation (data not shown). MCC function was directly assessed by tracking fluorescent microbeads added to tadpoles. Figure 4C and Movies S3 and S4 demonstrate that defects observed at stage 24 were no longer present at stage 32 (data not shown). Such a transient delay in cilia extension of MCCs has previously been described upon *Foxn4* loss of function in *Xenopus* [21], and radial cell intercalation of MCC has been linked to PCP proteins Vangl2, Prickle3, and Disheveled [22]. Finally, the stunted appearance of F0 mutants with disturbed *pitx2* expression was reminiscent of a CE phenotype as well (cf. Figure 2C). Together, this evidence hinted at a more general role of *myo1d* in PCP signaling and CE.

To investigate *myo1d* function in the context of a well-established CE-Wnt/PCP assay, we employed Keller open-face explants [23]. Dorsal marginal zone tissue was isolated at stage 10–10.5 from WT and *myo1d* morphant embryos, and it was scored for CE when un-manipulated siblings reached stage 22 (Figure 4C). CE was classified into three categories, with class 0 representing explants without elongation, class 1 containing elongated specimens, and class 2 explants being those that were elongated and displayed a constriction (Figure 4C). While more than 90% of WT explants elongated, with the relative majority of specimens falling into class 2 (23/54, 43%), CE was severely compromised in *myo1d* morphants, with significantly reduced class 2 extensions (6/44), the relative majority of specimens elongating without constriction, and about 25% not



elongating at all (class 1, 24/44, 61%; Figure 4C). Finally, an *ATF2*-based luciferase reporter was analyzed to monitor non-canonical Wnt signaling in *Xenopus* [24]. The reporter gene, alone or in combination with different concentrations of *myo1d* AUG-MO, was injected into the neural lineage at the 4-cell stage, neural plate explants were prepared at stage 14/15, and luciferase activity was recorded (Figure S3D). Compared to WT specimens, the reporter gene activity was dose-dependently downregulated in morphants (Figure S3D). In summary, these analyses of LR-unrelated phenotypes demonstrated that *myo1d* acted on non-canonical Wnt/PCP signaling and CE in the broader sense.

Functional Interaction between the Core PCP Signaling Gene *vangl2* and *myo1d* in LR Axis Formation in *Xenopus*

Finally, we asked whether PCP signaling and *myo1d* interacted during LR axis specification. Knockdown of the core PCP gene *vangl2* in *Xenopus* has been shown to disrupt cilia polarization

and LPM *nodal1* expression [25]. For gene knockdown of *vangl2*, a combination of two previously characterized antisense MOs was injected [26]. To analyze the potential genetic interaction of *vangl2* and *myo1d*, MO doses were reduced such that individual knockdowns resulted in greatly attenuated phenotypes. When MOs were co-injected, LR phenotypes were observed, as documented for the expression of LPM *pitx2* (Figure 4D). These experiments unequivocally showed that *myo1d* was required for PCP-dependent determination of the LR axis in *Xenopus* in much the same way as in the fruit fly *Drosophila* [8]. A possible role of *myo1d* has been previously addressed by over-expression of a full-length expression construct [10]. Injections of high amounts of synthetic *myo1d* mRNAs (≥ 5 ng) resulted in 15% of specimens with heterotaxia, but the mechanism of action was not addressed in this study [10]. We were not able to reproduce this result; it is a hallmark of non-canonical Wnt signaling and PCP, however, that both gain- and loss-of-function manipulations result in qualitatively similar phenotypes [27].

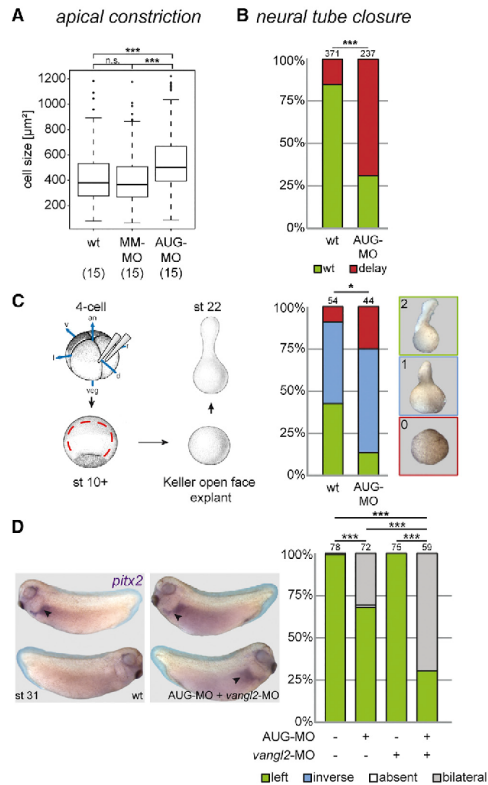


Figure 4. Functional Interaction between *myo1d* and PCP

(A and B) Morphant specimens displayed enhanced apical surfaces of GRP cells at stage 18 (A) and delayed neural tube closure at stage 18 (B). (C) Convergent extension defects in Keller open-face explants of *myo1d* morphants at stage 22.

(D) Co-injection of *myo1d* AUG-MO with two antisense MOs directed against *vangl2* (at sub-phenotypic doses each) disrupted LR axis formation, as determined by expression of *pitx2* in the LPM. Numbers represent analyzed specimens, which were derived from 3 independent experiments for apical constriction defects of GRP cells, 7 experiments for neural tube closure delay, and 4 experiments for *myo1d* and *vangl2* interaction during LR axis formation. To determine the cell surface area, 25 cells from a central part of the GRP were analyzed in each case. See also Figure S3 and Movies S2, S3, and S4.

The evolutionary origin of animal asymmetries has been controversially discussed in recent years [1, 28–30]. While morphological and functional asymmetries have been described in most phyla [1], there is no single common mechanism that accounts for asymmetric development. The Nodal cascade genes *nodal*, *lefty*, and *pitx2* are present and required for asymmetric development in lophotrochozoans (such as snails) and deuterostomes (sea urchins, uro- and cephalochordates as well as vertebrates), but they have not been described in ecdy-

sozoans [1]. Cilia-driven leftward fluid flow at the LR organizer is a hallmark of some, but not all, chordates [1], and *Drosophila* as the sole ecdysozoan species studied in depth lacks Nodal and cilia but uses *Myo1d*, PCP, and the Hox gene *Abd-B* [7, 8] to achieve laterality. This diversity has been taken as evidence of multiple independent evolutionary pathways to establish LR asymmetry [31, 32].

Our finding of a role of *myo1d* in *Xenopus* LR development represents the first demonstration of a common denominator of ecdysozoan and deuterostome/chordate asymmetries. Interestingly, actomyosin-dependent asymmetric heart morphogenesis has recently been shown to depend on a right-sided instructive pathway that involves BMP signaling and, as a target, the homeobox gene *prx1* [33]. It has been proposed that this BMP-*Prx1*-actomyosin pathway is suggestive of a conserved role in laterality determination during bilaterian evolution [33], a notion that is fully supported by our data. Future studies will address the question of whether or not *myo1d* is involved in this pathway. Additionally, we uncovered a conserved link between PCP and *myo1d* in establishing LR asymmetry in flies and frogs. Interestingly, these results can be further generalized, as LR defects were also encountered in morphant and mutant CRISPR/Cas9 zebrafish embryos (S.N. and Max Furthauer, personal communication). Defects in zebrafish included shorter and mispolarized cilia, LRO morphogenetic defects, and aberrant leftward flow, resulting in absent Nodal cascade gene induction and organ situs distortions, and, most significantly, a genetic interaction with *vangl2* as well (S.N. and Max Furthauer, personal communication).

In conclusion, our data are consistent with a monophyletic origin of animal organ asymmetries. It may be beneficial to investigate other mechanisms of invertebrate asymmetries in vertebrate model organisms in the future (for which the frog *Xenopus* is particularly well suited [34]), such as the role of Hox genes, which may be involved in placing the LRO at the correct anterior-posterior position during development.

STAR★METHODS

Detailed methods are provided in the online version of this paper and include the following:

- KEY RESOURCES TABLE
- CONTACT FOR REAGENT AND RESOURCE SHARING
- EXPERIMENTAL MODEL AND SUBJECT DETAIL
- METHOD DETAILS
 - Plasmid construction
 - Immunofluorescence staining
 - Flow-analysis
 - Luciferase Assay
 - CRISPR/Cas9 mediated genome editing
 - Monoclonal Antibody Preparation
 - Western blot analysis
- QUANTIFICATION AND STATISTICAL ANALYSIS
 - Statistical analysis

SUPPLEMENTAL INFORMATION

Supplemental Information includes three figures and four movies and can be found with this article online at <https://doi.org/10.1016/j.cub.2018.01.075>.

ACKNOWLEDGMENTS

We are grateful to Michael Levin for sharing a full-length *myo1d* expression construct and to Susanne Bogusch, whose expert help was instrumental to cloning the rescue vector. Work in the Blum lab has been supported by DFG grants BL-285/9 and BL-285/10. S.K. and T.O. have been recipients of fellowships from the Landesgraduiertenförderung Baden-Württemberg. S.K. was also funded by the Federal Ministry of Education and Research (01PL11003), project Humboldt relocated. J.M.L.-S. gratefully acknowledges several students in her 1998–2015 Molecular Biology and Biotechnology and Directed Research courses, especially G. Angelini, K. Ganser, S. Saldí, N. McIver, and B. Sickler; the Merrimack College Faculty Development Grant Program; Murray Fellowship; Yassini Award; NSF-RUI 0077516; and B. Bement, A. Sokac, S. Sokol, and members of his laboratory. Work in the Noselli lab was supported by grants from ANR (DRO-ASY ANR-13-BSV2-006, DroZeMyo, and LABEX SIGNALIFE ANR-11-LABX-0028-01).

AUTHOR CONTRIBUTIONS

M.B., M.T., A.S., and S.N. designed experiments. M.T., S.K., M.M., F.F., and J.M.L.-S. conducted experiments, with T.O. performing the CRISPR/Cas9 genome editing. M.B. wrote the manuscript with help from M.T., A.S., S.N., and J.M.L.-S.

DECLARATION OF INTERESTS

The authors declare no competing interests.

Received: October 19, 2017

Revised: January 1, 2018

Accepted: January 24, 2018

Published: February 22, 2018

REFERENCES

- Blum, M., Feistel, K., Thumberger, T., and Schweickert, A. (2014a). The evolution and conservation of left-right patterning mechanisms. *Development* **141**, 1603–1613.
- Coutelis, J.B., González-Morales, N., Géminard, C., and Noselli, S. (2014). Diversity and convergence in the mechanisms establishing L/R asymmetry in metazoa. *EMBO Rep.* **15**, 926–937.
- Grimes, D.T., and Burdine, R.D. (2017). Left-Right Patterning: Breaking Symmetry to Asymmetric Morphogenesis. *Trends Genet.* **33**, 616–628.
- Shiratori, H., and Hamada, H. (2014). TGF β signaling in establishing left-right asymmetry. *Semin. Cell Dev. Biol.* **32**, 80–84.
- Blum, M., Schweickert, A., Vick, P., Wright, C.V.E., and Danilchik, M.V. (2014b). Symmetry breakage in the vertebrate embryo: when does it happen and how does it work? *Dev. Biol.* **393**, 109–123.
- Hozumi, S., Maeda, R., Taniguchi, K., Kanai, M., Shirakabe, S., Sasamura, T., Spéder, P., Noselli, S., Aigaki, T., Murakami, R., and Matsuno, K. (2006). An unconventional myosin in *Drosophila* reverses the default handedness in visceral organs. *Nature* **440**, 798–802.
- Spéder, P., Adám, G., and Noselli, S. (2006). Type 1D unconventional myosin controls left-right asymmetry in *Drosophila*. *Nature* **440**, 803–807.
- González-Morales, N., Géminard, C., Lebreton, G., Cerezo, D., Coutelis, J.-B., and Noselli, S. (2015). The Atypical Cadherin Dachsous Controls Left-Right Asymmetry in *Drosophila*. *Dev. Cell* **33**, 675–689.
- LeBlanc-Straceski, J.M., Sokac, A., Bement, W., Sobrado, P., and Lemoine, L. (2009). Developmental expression of *Xenopus* myosin 1d and identification of a *myo1d* tail homology that overlaps TH1. *Dev. Growth Differ.* **51**, 443–451.
- McDowell, G.S., Lemire, J.M., Paré, J.-F., Cammarata, G., Lowery, L.A., and Levin, M. (2016). Conserved roles for cytoskeletal components in determining laterality. *Integr. Biol.* **8**, 267–286.
- Meno, C., Shimono, A., Saijoh, Y., Yashiro, K., Mochida, K., Ohishi, S., Noji, S., Kondoh, H., and Hamada, H. (1998). *lefty-1* is required for left-right determination as a regulator of *lefty-2* and nodal. *Cell* **94**, 287–297.
- Nakayama, T., Blitz, I.L., Fish, M.B., Odeleye, A.O., Manohar, S., Cho, K.W.Y., and Grainger, R.M. (2014). Cas9-based genome editing in *Xenopus tropicalis*. *Methods Enzymol.* **546**, 355–375.
- Shook, D.R., Majer, C., and Keller, R. (2004). Pattern and morphogenesis of presumptive superficial mesoderm in two closely related species, *Xenopus laevis* and *Xenopus tropicalis*. *Dev. Biol.* **270**, 163–185.
- Walentek, P., Schneider, I., Schweickert, A., and Blum, M. (2013). *Wnt11b* is involved in cilia-mediated symmetry breakage during *Xenopus* left-right development. *PLoS ONE* **8**, e73646.
- Blum, M., Andre, P., Muters, K., Schweickert, A., Fischer, A., Bitzer, E., Bogusch, S., Beyer, T., van Straaten, H.W.M., and Viebahn, C. (2007). Ciliation and gene expression distinguish between node and posterior notochord in the mammalian embryo. *Differentiation* **75**, 133–146.
- Schweickert, A., Weber, T., Beyer, T., Vick, P., Bogusch, S., Feistel, K., and Blum, M. (2007). Cilia-driven leftward flow determines laterality in *Xenopus*. *Curr. Biol.* **17**, 60–66.
- Schweickert, A., Vick, P., Getwan, M., Weber, T., Schneider, I., Eberhardt, M., Beyer, T., Pachur, A., and Blum, M. (2010). The nodal inhibitor *Coco* is a critical target of leftward flow in *Xenopus*. *Curr. Biol.* **20**, 738–743.
- Ossipova, O., Chuykin, I., Chu, C.-W., and Sokol, S.Y. (2015b). *Vangl2* cooperates with *Rab11* and *Myosin V* to regulate apical constriction during vertebrate gastrulation. *Development* **142**, 99–107.
- Wallingford, J.B., and Harland, R.M. (2002). Neural tube closure requires Dishevelled-dependent convergent extension of the midline. *Development* **129**, 5815–5825.
- Ybot-Gonzalez, P., Savery, D., Gerrelli, D., Signore, M., Mitchell, C.E., Faux, C.H., Greene, N.D.E., and Copp, A.J. (2007). Convergent extension, planar-cell-polarity signalling and initiation of mouse neural tube closure. *Development* **134**, 789–799.
- Campbell, E.P., Quigley, I.K., and Kintner, C. (2016). *Foxn4* promotes gene expression required for the formation of multiple motile cilia. *Development* **143**, 4654–4664.
- Ossipova, O., Chu, C.-W., Fillatre, J., Brott, B.K., Itoh, K., and Sokol, S.Y. (2015a). The involvement of PCP proteins in radial cell intercalations during *Xenopus* embryonic development. *Dev. Biol.* **408**, 316–327.
- Sive, H.L., Grainger, R.M., and Harland, R.M. (2007). *Xenopus laevis* Keller Explants. *CSH Protoc.* **2007**, pcb.prot4749.
- Ohkawara, B., and Niehrs, C. (2011). An ATF2-based luciferase reporter to monitor non-canonical Wnt signaling in *Xenopus* embryos. *Dev. Dyn.* **240**, 188–194.
- Antic, D., Stubbs, J.L., Suyama, K., Kintner, C., Scott, M.P., and Axelrod, J.D. (2010). Planar cell polarity enables posterior localization of nodal cilia and left-right axis determination during mouse and *Xenopus* embryogenesis. *PLoS ONE* **5**, e8999.
- Prager, A., Hagenlocher, C., Ott, T., Schambony, A., and Feistel, K. (2017). *hmmr* mediates anterior neural tube closure and morphogenesis in the frog *Xenopus*. *Dev. Biol.* **430**, 188–201.
- Wang, Y., and Nathans, J. (2007). Tissue/planar cell polarity in vertebrates: new insights and new questions. *Development* **134**, 647–658.
- Boorman, C.J., and Shimeld, S.M. (2002). The evolution of left-right asymmetry in chordates. *BioEssays* **24**, 1004–1011.
- Thompson, H., Shaw, M.K., Dawe, H.R., and Shimeld, S.M. (2012). The formation and positioning of cilia in *Ciona* intestinalis embryos in relation to the generation and evolution of chordate left-right asymmetry. *Dev. Biol.* **364**, 214–223.
- Nakamura, T., and Hamada, H. (2012). Left-right patterning: conserved and divergent mechanisms. *Development* **139**, 3257–3262.



31. Okumura, T., Utsuno, H., Kuroda, J., Gittenberger, E., Asami, T., and Matsuno, K. (2008). The development and evolution of left-right asymmetry in invertebrates: lessons from *Drosophila* and snails. *Dev. Dyn.* 237, 3497–3515.
32. Vandenberg, L.N., and Levin, M. (2013). A unified model for left-right asymmetry? Comparison and synthesis of molecular models of embryonic laterality. *Dev. Biol.* 379, 1–15.
33. Ocaña, O.H., Coskun, H., Minguillón, C., Murawala, P., Tanaka, E.M., Galcerán, J., Muñoz-Chápuli, R., and Nieto, M.A. (2017). A right-handed signalling pathway drives heart looping in vertebrates. *Nature* 549, 86–90.
34. Duncan, A.R., and Khokha, M.K. (2016). *Xenopus* as a model organism for birth defects—Congenital heart disease and heterotaxy. *Semin. Cell Dev. Biol.* 57, 73–79.

STAR★METHODS

KEY RESOURCES TABLE

REAGENT or RESOURCE	SOURCE	IDENTIFIER
Antibodies		
Mouse monoclonal anti acetylated α -tubulin	Sigma	T6793
Anti-mouse IgG (whole molecule) F(ab') ₂ fragment-Cy3	Sigma	C2181
Anti-mouse IgG (H+L), CF 405S	Sigma	SAB4600023
Alexa Fluor 488 Phalloidin	Invitrogen	A12379
Alexa Fluor 555 Phalloidin	Invitrogen	A34055
Chemicals, Peptides, and Recombinant Proteins		
Pfu DNA Polymerase	Promega	M7745
Cas9 with NLS	PNA BIO	CP01-50
FluoSpheres Carboxylate-Modified Microspheres, 0.5 μ m, yellow-green fluorescent (505/515)	Invitrogen	F8813
Human chorionic gonadotropin (hCG)	Sigma	C0809-1VL
PureProteome NHS Flexibind Magnetic Beads	Milipore	LSKMAGA02
Laemmli sample buffer 2x	Sigma	S3401
Critical Commercial Assays		
MEGAscript T7 Transcription Kit	Thermo Fisher Scientific	AM1354
MEGAclear Transcription Clean-Up Kit	Thermo Fisher Scientific	AM1908
innuPREP DOUBLEpure Kit	Analytik Jena	845-KS-5050050
Ni-NTA affinity purification column	QIAGEN	N/A
EDTA-free Protease Inhibitor Cocktail	Roche	000000011873580001
Dual-Luciferase® Reporter Assay System	Promega	E1910
Experimental Models: Cell Lines		
BL21 Star One Shot cells	Invitrogen	C602003
Experimental Models: Organisms/Strains		
<i>Xenopus laevis</i> (female, male)	Nasco	https://www.enasco.com/xenopus/
Oligonucleotides		
sgRNA-RO: AAAAGCACCGACTCGGTGCCACTTTTTCAAGT TGATAACGGACTAGCCTTATTTAACTTGCTATTCTAGCT CTAAAAC	Merck	N/A
T7:sgRNA 1-FO: GCAGCTAATACGACTCACTATAGGTACT GCATGATGTACTTACGTTTTAGAGCTAGAAATAGCAAG	Merck	N/A
T7:sgRNA 2-FO: GCAGCTAATACGACTCACTATAGGGTT GTCGTTACGATTCTGTCTTTAGAGCTAGAAATAGCAAG	Merck	N/A
myo1d forward primer [5' ATCCATGGCGGAACAAAGAGG GGCTGC 3']	Sigma	N/A
myo1d reverse primer [5' ATTCTAGATTAATTGGCTGGAAC ACTGAG 3']	Sigma	N/A
Software and Algorithms		
Adobe Suite CS6: Photoshop and Illustrator	Adobe	N/A
ImageJ/Fiji	N/A	https://fiji.sc/
AxioVision 4.6	Zeiss	N/A
Zen 2012 Blue edition	Zeiss	https://www.zeiss.com
Statistical R-Gui	N/A	https://www.r-project.org/
RStudio	N/A	https://www.rstudio.com/

(Continued on next page)



Continued		
REAGENT or RESOURCE	SOURCE	IDENTIFIER
Other		
pET100/D-TOPO vector	Invitrogen	N/A
myo1d AUG-MO [5' TGCAGCCCTCTTGTCCGCCATGT 3']	GeneTools	N/A
myo1d mismatch-MO [5' TGGACCCCGTCTTCTCCCC CATGT 3']	GeneTools	N/A
Axioplan2 imaging microscope	Zeiss	N/A
Zeiss LSM 700	Zeiss	N/A
GloMax® Explorer System	Promega	N/A
AxioCam H5m video camera	Zeiss	N/A
Xenbase	N/A	https://xenbase.org
PubMed	N/A	https://www.ncbi.nlm.nih.gov/pubmed/

CONTACT FOR REAGENT AND RESOURCE SHARING

Further information and requests for resources and reagents should be directed to and will be fulfilled by the Lead Contact, Martin Blum (martin.blum@uni-hohenheim.de).

EXPERIMENTAL MODEL AND SUBJECT DETAIL

For *in vivo* studies, *Xenopus laevis* was used as model organism. Frogs were obtained from Nasco (901 Janesville Avenue PO Box 901 Fort Atkinson). Handling, care and experimental manipulations of animals was approved by the Regional Government Stuttgart, Germany (Vorhaben A379/12 ZO “Molekulare Embryologie”), according to German regulations and laws (§6, article 1, sentence 2, nr. 4 of the animal protection act). Animals were kept at the appropriate condition (pH=7.7, 20°C) at a 12 h light cycle in the animal facility of the Institute of Zoology of the University of Hohenheim. Female frogs (4-20 years old) were stimulated with 25-75 units of human chorionic gonadotropin (hCG; Sigma), depending on weight and age, that was injected subcutaneously one week prior to oviposition. On the day prior to ovulation, female frogs were injected with 300-700 units of hCG. Eggs were collected into a petri dish by careful squeezing of the females, followed by *in vitro* fertilization. Sperm of male frogs was gained by dissecting of testes that were stored at 4°C in 1x MBSH (Modified Barth’s Saline with HEPES).

METHOD DETAILS

Plasmid construction

The *myo1d*-CS2+ construct was a gift of Dr. Michael Levin (Tufts University). For generation of a rescue construct, *myo1d* was cloned into the CS2+ myc-tag vector that contained 5 myc sequences at the N terminus. The following primers were used for cloning:

myo1d forward primer: 5' ATCCATGGCGGAACAAGAGGGGCTGC 3'
myo1d reverse primer: 5' ATTCTAGATTAATTGGCTGGAACACTGAG 3'

For *in vitro* synthesis of mRNA using the Ambion sp6 message kit, the plasmid was linearized with NotI.

Immunofluorescence staining

For immunofluorescence staining, embryos were fixed in 4% PFA for 1h at RT on a rocking platform, followed by 2 washes in calcium- and magnesium-free PBS (PBS⁻) for 15 min each. For staining of GRP explants, embryos were dissected using a scalpel into anterior and posterior halves. Posterior halves (GRP explants) were collected and transferred to a 24 well plate and washed twice for 15 min in PBS⁻. GRP-explants and whole embryos were blocked for 2h at RT in CAS-Block diluted 1:10 in PBS⁻. The blocking reagent was replaced by antibody solution (anti acetylated tubulin antibody, diluted 1:700 in CAS-Block) and incubated overnight at 4°C. In the morning, the antibody solution was removed and explants/embryos were washed twice for 15 min in PBS⁻. Finally, the secondary antibody (diluted 1:1000 in CAS-Block) was added together with Phalloidin (1:200) and incubated for a minimum of 3h at RT. Before photo documentation, embryos or explants were shortly washed in PBS⁻ and transferred onto a microscope slide.

Flow-analysis

For analysis of leftward flow, dorsal posterior GRP-explants were dissected from stage 16/17 embryos in 1x MBSH [16]. GRP-explants were placed in a Petri dish containing fluorescent microbeads (diameter 0.5 µm; diluted 1:2500 in 1xMBSH) and incubated for a few seconds. Explants were transferred to a microscope slide which was prepared with Vaseline to create a small chamber

e2 Current Biology 28, 810–816.e1–e3, March 5, 2018

that contained fluorescent microbead solution; a coverslip was carefully pressed on to seal the chamber. Time lapse movies of leftward flow were recorded using an AxioCam HSm video camera (Zeiss) at 2 frames per second for 1 min using an Axioplan2 imaging microscope (Zeiss). For flow analysis, two open-source programs, ImageJ and statistical-R, were used. Using the Particle-Tracker plug-in from ImageJ, leftward flow was analyzed and particle movement was measured. Directionality and velocity of fluorescent microbeads were calculated using statistical-R.

Luciferase Assay

Luciferase reporter assays were carried out using the Promega Dual-Luciferase® Reporter Assay System. Embryos were injected at the 4-cell stage with AUG-MO, ATF2-luciferase DNA and Renilla DNA into the dorsal animal blastomeres, and neural tissue was dissected at stage 14/15 (cf. Figure S3D for a schematic depiction of the procedure [24]). Neural tissue was transferred into a 1.5 mL Eppendorf tube and the 0.1xMBSH buffer was removed, leaving the tissue moistened. The tissue was lysed and homogenized in 100 µl 1x passive lysis-buffer by pipetting the suspension up and down, followed by a 15 min incubation at RT. The lysate was centrifuged for 2 minutes at 14 000 rpm and the upper phase was transferred into a new tube. The lysate was re-centrifuged and two 25 µl aliquots (technical duplicates) were transferred into a 96well plate. 75 µl 1x Luciferase assay substrate was added through the GloMax® Explorer System and the luminescence was measured. This step was repeated with 75 µl 1x Stop and Glow reagents. To calculate the relative luciferase units (RLU in [%]) the ratio between luciferase and Renilla values was calculated and correlated to the wt control, which we set to 100%.

CRISPR/Cas9 mediated genome editing

sgRNA templates (under T7 promoter control) were generated using Pfu polymerase-mediated primer extension following *in vitro* synthesis (4 h) of the sgRNAs [12]. Prior to use, sgRNAs were denatured at 70°C for 2 min and immediately chilled on ice. Cas9 protein and sgRNAs were mixed and incubated at 37°C for 5 min to allow RNP formation. Zygotes were dejellied 20 min post fertilization and immediately injected with 8 nL of RNP mix. Injected embryos were cultivated for 12 h at 25°C to enhance cutting efficiency, followed by transfer to ambient temperature (20°C) until stage 28 was reached, when specimens were fixed for phenotypic analysis.

Monoclonal Antibody Preparation

A monoclonal antibody, Mab4E12, was raised against the tail polypeptide NARNSNQFVSRNSNE (aa834-847) of the *Xenopus laevis* myosin 1d L homolog (GenBank Accession Number AF540952.1) by AbPro, Woburn, MA, USA. A 828 bp tail region that included amino acids R729-N1007 was amplified by PCR from a cDNA clone optimized for expression in *E. coli* (GenScript), pXIMyo1d-opt, using the primers (Forward: CACCGCCGTTATAAAGTTAAAAGT; Reverse: TTATTAGTTTGCCGGAACAGACAG), and cloned into the pET100/D-TOPO vector (Invitrogen) to create pXIMyo1d-optTail2D. BL21 Star One Shot cells (Invitrogen) were transformed with this vector and expression of the 35 kDa fusion protein consisting of the myo1d tail and N terminus 6X His-tag was induced with IPTG. Cells were harvested after 1.5 hr of induction and the fusion protein was affinity purified using Ni-NTA affinity purification column from a cleared lysate under denaturing conditions (QIAGEN). The affinity purified tail polypeptide was cross-linked to PureProteome NHS Flexibind Magnetic Beads (Millipore), and Mab4E12 was purified following the manufacturer's instructions.

Western blot analysis

Embryos were injected at the 1-4 cell stage with 1 ng of MO and cultivated until stage 28. The antisense morpholino, AUG-MO, [5' TGCAGCCCCTCTGTTCCGCCATGT 3'] overlapped the start codon (underlined) of *myo1d*. The control mismatch morpholino MM-MO, [5' TGGACCCCTCTCTTCCGCCATGT 3'] was identical to the AUG-MO except for the five C/G mismatches (underlined and indicated by bold lettering). Embryo lysates were made by homogenizing 1 embryo in 20 µl of 4°C lysis buffer (50 mM Tris pH 8.0, 150 mM NaCl, 0.5% NP40 0.5 ml, 0.5% Triton X-100 0.5 ml, 1 mM EGTA) plus cOmplete, Mini, EDTA-free Protease Inhibitor Cocktail (Roche) and centrifuging at 13.000 x g for 10 min to remove cellular debris followed immediately by mixing the supernatant 1:1 with 2x Laemmli SDS sample buffer (SIGMA). Embryo lysates in Laemmli sample buffer were boiled for 5 min, snap cooled on ice, and spun to remove debris before loading onto gels. Bio-Rad Precision Plus Kaleidoscope markers and half-embryo equivalents were loaded per lane on Bio-Rad 4%–20% polyacrylamide precast gels at 100 V. Western blots were prepared using the Trans-Blot SD. Semi-Dry Transfer Cell at 15 V for 45 min. Blots were air-dried, blocked in 5% non-fat dry milk in TBS, rinsed and incubated in the affinity purified 4E12 monoclonal antibody at a concentration of 5 µg in 10 mL TBS overnight at 4°C. Blots were washed in TBS, re-blocked in 10% non-fat dry milk in TBS, rinsed and incubated with goat anti-mouse horseradish peroxidase (HRP) conjugated anti-mouse IgG (Jackson Labs) at 1:10.000 dilution for 1 hr at RT. After rinsing with TBS, chemiluminescent detection was performed using a peroxide-luminol/enhancer solution (Pierce) and GeneSnap image acquisition software on a SynGene gel documentation system.

QUANTIFICATION AND STATISTICAL ANALYSIS

Statistical analysis

Statistical calculations of marker gene expression patterns and cilia distribution were performed using Pearson's chi-square test (Bonferroni corrected) in statistical R. For statistical calculation of ciliation, cilia length, cell size, flow velocity and directionality Wilcoxon-Match-Pair test was used (RStudio).

Current Biology, Volume 28

Supplemental Information

A Conserved Role of the Unconventional

Myosin 1d in Laterality Determination

Melanie Tingler, Sabrina Kurz, Markus Maerker, Tim Ott, Franziska Fuhl, Axel Schweickert, Janine M. LeBlanc-Straceski, Stéphane Noselli, and Martin Blum

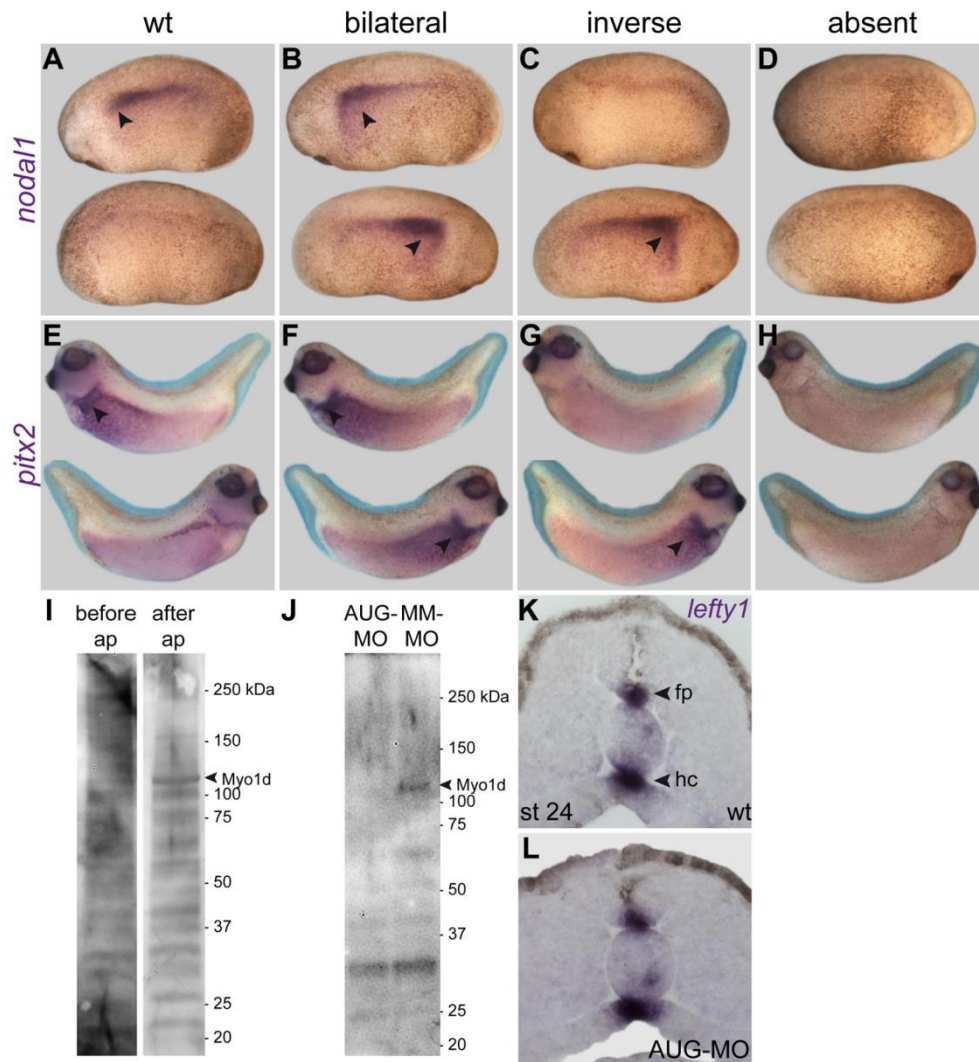


Figure S1. *Myo1d* is required for LR axis formation, Related to Figure 1.

(A-H) *nodal1* (A-D) and *pitx2* (E-H) expression in wildtype (A, E) and *myo1d* morphant (B-D, F-H) embryos, as determined by WM-ISH with antisense probes for *nodal1* (A-D) and *pitx2* (E-H).

(I, J) Downregulation of Myo1d protein in *myo1d* morphants. (I) Tadpole lysates were probed with Mab4E12 before (left) and after (right) affinity purification (ap). (J) Embryos were injected at the 2-4 cell stage with 1 ng of AUG-MO or an antisense MO containing 5 mismatches (MM-MO). Affinity purified Mab4E12 was used to probe western blots containing lysates from stage 28 embryos.

(K, L) *Lefty1* mRNA expression in wildtype (K) and *myo1d* morphant (L) specimen, as shown by transversal histological sections of WM-ISH stained embryos at stage 24. fp, floor plate; hc, hypochord; MM-MO, mismatch MO.

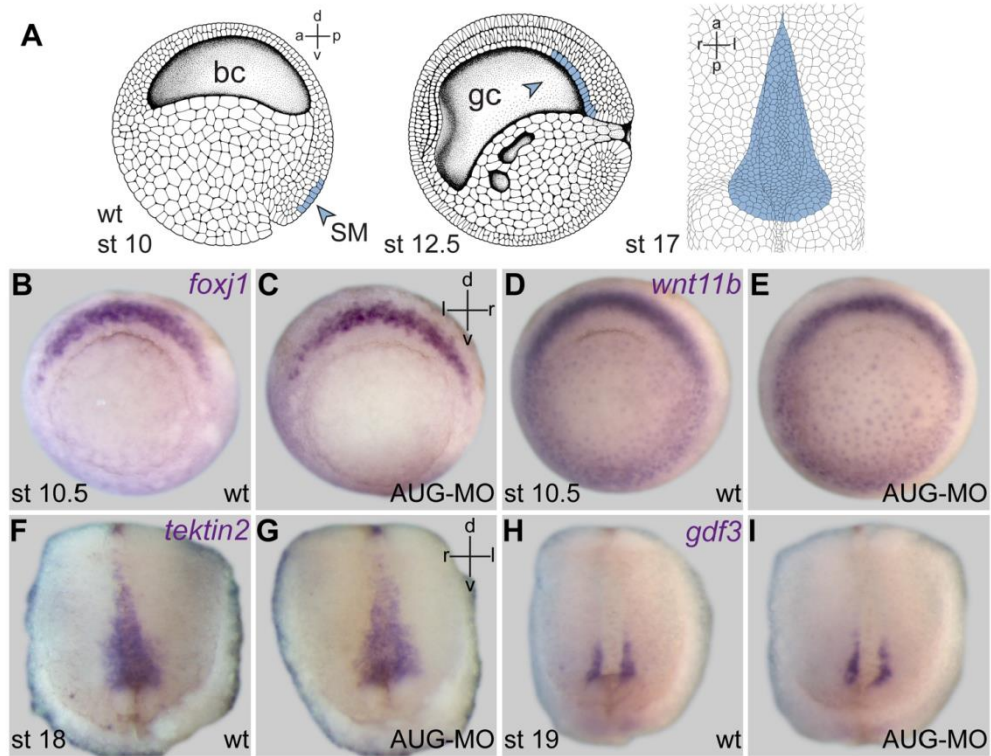


Figure S2. Marker gene expression in the superficial mesoderm (SM) and gastrocoel roof plate (GRP) of wildtype and *myold* morphant embryos, Related to Figure 3.

(A) Development of the LRO at the *Xenopus* gastrocoel roof: the SM involutes during gastrulation to give rise to the GRP during early neurulation, which is shown in a dorsal explant in a ventral view on the right (blue); modified from [S1]. (B-E) Expression of *foxj1* (B, C) and *wnt11b* (D, E) in the SM of wt (B, D) and *myold* morphant (C, E) embryos at stage 10.5. (F-I) Expression of *tektin2* (F, G) and *gdf3* (H, I) in the GRP of dorsal explants isolated from wt (F, H) and *myold* morphant embryos (G, I) at stage 18 (G, H) and 19 (H, I).

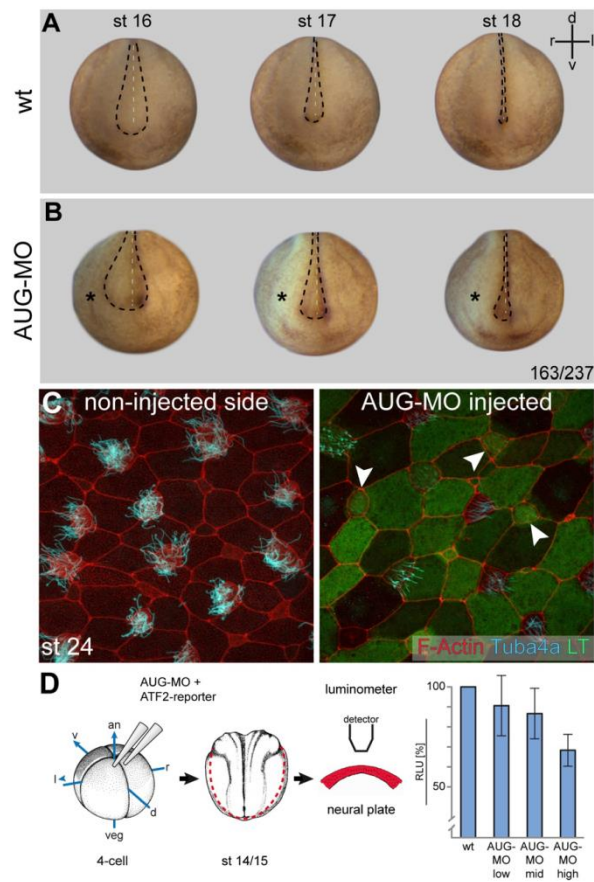


Figure S3. PCP defects in *myo1d* morphant *Xenopus* embryos, Related to Figure 4.

(A, B) Neural tube closure delay. Embryos were injected with AUG-MO at the 4-cell stage on the right side. Progress of neural tube closure in unilaterally injected embryos (B) was recorded at stages 16, 17 and 18, when the neural tube in wildtype uninjected specimens (A) had closed. *, injected side. Dashed lines outline neural folds. Please cf. also Movie S3.

(C) Ciliation of skin multi-ciliated cells (MCCs) at stage 24 in specimen unilaterally injected with AUG-MO at the 4-cell stage. Left: control side; right: MO-injected side. LT, lineage tracer fluorescein dextrane. Please cf. also Movies S4 +5.

(D) Dose-dependent inhibition of the ATF2-based luciferase reporter to monitor non-canonical Wnt signaling. AUG-MO, the ATF2-reporter gene and Renilla luciferase were injected into the neural lineage at the 4-cell stage, and specimens were cultured until stage 14/15. Neural plate tissue was dissected and analyzed for reporter gene activity. RLU, relative luciferase units (\pm standard error).

Supplemental References

[S1] Tisler, M., Thumberger, T., Schneider, I., Schweickert, A., and Blum, M. (2017). Leftward Flow Determines Laterality in Conjoined Twins. *Curr. Biol.* 27, 543–548.

Supplemental Movies

Original Movie legends from Current Biology

Movie S1. Leftward Flow in WT and myo1d Morphant Embryos, Related to Figure 3

Dorsal explant was prepared at stage 16/17, fluorescent microbeads were added and cilia-driven bead transport was recorded at a frame rate of 2 frames per second. Left: wildtype embryo; right: morphant specimen. Movie plays at 5 x real time. Note that in the morphant, individual beads were also transported from left to right

Movie S2. Delay of Neural Tube Closure in myo1d Morphants, Related to Figure 4

Embryos were unilaterally injected with AUG-MO at the 4-cell stage. Time lapse movie was recorded from stage 14 to stage 19 at 2 frames per minute. Injected side is marked by an asterisk. Jerks in the middle of the sequence were caused by manual re-positioning of the specimens. Movie plays at 900 x real time. Note that neural tube closure in the morphant specimen proceeds at reduced velocity on the injected sides.

Movie S3. Bead Transport along the Larval Skin of a WT Specimen at Stage 24, Related to Figure 4

Bead transport along the anterior-posterior axis of a wildtype embryo, incubated in culture medium containing fluorescent microbeads, was recorded at 10 frames per second. Movie plays at real time.

Movie S4. Compromised Bead Transport along the Larval Skin of a myo1d Morphant Specimen at Stage 24, Related to Figure 4

AUG-MO was injected into the ventral right blastomere at the 4-cell stage and embryos were cultured until stage 24. Bead transport along the anterior-posterior axis, incubated in culture medium containing fluorescent microbeads, was recorded at 10 frames per second. Note that bead transport on the injected side (*) was slowed down. Movie plays at real time.

***dmrt2* and *myf5* link early somitogenesis to left-right axis
determination in *Xenopus laevis***

dmrt2* and *myf5* link early somitogenesis to left-right axis determination in *Xenopus laevis

Melanie Tingler, Axel Schweickert, Martin Blum

University of Hohenheim, Garbenstr. 30, 70599 Stuttgart, Germany

Abstract

The left-right (LR) body axis of vertebrates and thus the position of the inner organs is set up by a highly conserved embryonic process. In most vertebrates the left positional information is manifested during neurulation by the so called left-right organizer (LRO). The LRO depicts a transient ciliated epithelia and generates a cilia-driven leftward fluid flow which breaks the bilateral symmetry of the early embryo. This flow is thought to be sensed by the ciliated cells of the left LRO margin and translated into post-transcriptional repression of the Tgf- β /Wnt/Bmp antagonist *dand5*. Subsequently the co-expressed Tgf- β growthfactor Nodal1 is released of Dand5 repression and transfers to the left lateral plate mesoderm. There Nodal1 induces the Nodal cascade which is composed of a positive feedback loop, the feedback inhibitor lefty and the expression of the homeobox gene *pitx2* that drives asymmetric organogenesis.

The transcription factor of the doublesex and mab3-related family, Dmrt2, was mainly studied during sexual development of invertebrates and vertebrate somitogenesis. We show that *dmrt2* impacted on 2 essential functions during symmetry breakage in the African clawed frog *Xenopus laevis*. Using morpholino mediated knock-down of *dmrt2* we revealed that LRO ciliation was broadly affected as well as *nodal1* mRNA expression was absent in sensory LRO cells. These observations were accompanied by a strong mRNA reduction in early gastrulae of two transcription factors, *foxj1* the master control gene of motile cilia and the somitogenesis promoting factor *myf5*.

We demonstrate that *myf5* is required for left-right (LR) asymmetry via specifying sensory LRO cells. Myf5 acted downstream of Dmrt2 as *dmrt2* morphants were rescued by *myf5* mRNA. Therefor *dmrt2* is needed for LRO ciliation as well as for the specification of the lateral flow-perceiving cells. We show for the first time that the basic embryonic processes of symmetry breakage and somitogenesis are tightly linked.

Introduction

Heterotaxia syndrome is a rare disease affecting the asymmetric position of the inner organs with a prevalence of 1:10 000 (Lin et al., 2014). It can be manifested as *situs ambiguus* resulting in the misplacement of some but not all inner organs across the left-right body axis or in *situs inversus totalis* defined as the complete mirror image arrangement of the visceral organs. While *situs inversus totalis* has no clinical impact on patients, heterotaxia can result in severe malformation (isomerism) and malfunction of the inner organs (Sutherland & Ware, 2009). The determination of the LR body axis requires breakage of the initial bilateral symmetry in the early embryo. The first detectable asymmetry is a leftward fluid flow in fish, frog and mouse neurulae. This asymmetric event is generated by a transient ciliary structure in the posterior embryonic midline which is termed the left-right organizer (LRO; posterior notochord or node in mouse, Kupffer's vesicle -KV- in fish and gastrocoel roof plate -GRP- in frog) (Nonaka et al., 1998; Okada et al., 2005; Schweickert et al., 2007; Oteiza et al., 2008). Midline LRO cells harbor motile, posteriorly polarized monocilia that rotate in a counterclockwise manner (Antic et al., 2010). Thereby these cilia produce a directional leftward-fluid flow that is sensed by cells which project non-motile cilia and bilaterally flank the flow-generating area (McGrath et al., 2003; Nonaka et al., 2005; Boskovski et al., 2013; Tavares et al., 2017). These laterally positioned, sensory LRO (sLRO) cells express the secreted Tgf- β /Wnt/Bmp antagonist *dand5* and the Tgf- β morphogen *nodal1* in a bilaterally symmetric pattern prior to flow (Marques et al., 2004; Vonica & Brivanlou 2007; Schweickert et al., 2010). Because of Dand5, Nodal1 protein is prevented from being transferred to the lateral plate mesoderm (LPM) and to activate its own feedback loop (Hashimoto et al., 2004; Vonica & Brivanlou 2007). This situation changes due to the leftward-fluid flow when left cells perceive the flow. Although the sensing mechanism has not been fully unraveled a cilia based process is generally accepted. Bending of sensory cilia by leftward flow represents one hypothesis of flow sensing. In this setting, a ciliary localized mechano-sensor based on the calcium channel Polycystin-2 triggers calcium²⁺ (ca²⁺) influx (McGrath et al., 2003; Yoshida et al., 2012). Asymmetric ca²⁺ spikes have been demonstrated in zebrafish and mouse (Yuan et al., 2015; McGrath et al., 2003; Takao et al., 2013). How ca²⁺ influences the downstream process is currently not known. In any scenario, Nodal1 is flow dependently released of Dand5 repression, transfers to and promotes its own feedback loop in the left LPM. In addition, Nodal1 induces the transcription of its feedback

inhibitor *lefty* in *Xenopus* and the homeobox transcription factor *pitx2*. Pitx2 then drives the asymmetric development of most inner organs (Meno et al., 1998; Yoshioka et al., 1998; Logan et al., 1998; Meno et al., 1999; Cheng et al., 2000). This asymmetric Nodal cascade is highly conserved across vertebrates e.g. chick, mouse or *Xenopus* and represents the major signal that regulates the establishment of the LR body axis in vertebrates (Levin et al., 1995; Lowe et al., 1996; Collignon et al., 1996).

The symmetry breakage event requires the induction of the LRO that starts with its specification and morphogenesis. In early frog gastrulae, the LRO precursor tissue is called the superficial mesoderm (SM). The SM contains superficial cells which are positioned anteriorly to Spemann Organizer. It can be detected by the transcription of the forkhead box transcription factor *foxj1*, the master regulator for motile cilia development. SM specification depends on a tightly controlled network, including canonical Wnt and downstream Fibroblast growth factor (Fgf) signaling (Glinka et al., 1996; Smith, 1995; Stubbs et al., 2008; Walentek et al., 2013; Schneider et al. 2019; Vick et al., 2018). Since *foxj1* should mark motile cilia harboring, flow-generating (fg) cells, it is currently unclear how the flow-sensing cell identity, containing non-motile cilia, is established. Besides the difference in cilia polarization and motility, fgLRO and sLRO cells differentiate into distinct cell fates. In post-flow stages fgLRO cells integrate into the embryonic midline i.e. the notochord, while the flanking sLRO cells contribute to the paraxial mesoderm i.e. the somites (Shook et al., 2004).

Several reports demonstrated that disrupting somitogenesis in frog, fish or mice often resulted into LR-defects and interestingly also *vice versa*. A network of pathways including Wnt, Notch and Fgf signaling and the t-box gene transcription factor Tbx6 are shared by both processes (Chapman et al., 1996; Watabe-Rudolph et al., 2002; White et al., 2003; Hadjantonakis et al., 2008).

Like Tbx6, the transcription factors of the doublesex and mab3-related family, Dmrt2, had been implicated in LR determination and somitogenesis. This gene family is evolutionary highly conserved and represents proteins that are involved in sex determination in invertebrates and vertebrates. It originates from *doublesex (dsx)* in *Drosophila melanogaster* and from *C. elegans male-abnormal 3 (mab3)* and is based on the presence of an unusual cysteine-rich zinc binding DNA-binding domain, called the DM-domain (Raymond et al. 1998; Erdman & Burtis, 1993). This domain is highly conserved across the animal kingdom while further sequences of the Dmrt proteins show high variations (Voff et al., 2003).

dmrt2 was the first family member gene that was described to have a function apart from sexual development (Meng et al., 1999). In zebrafish, chick and mouse it plays a major role during early somitogenesis i.e. specification, differentiation and/or synchronization of segmentation (Meng et al., 1999; Saúde et al., 2005; Seo et al., 2006; Liu et al., 2009; Sato et al., 2010). In 2005 Leonor Saúde and colleagues found a first hint for a possible connection between *dmrt2* and left-right axis establishment in chick embryos. At st.4 Hamburger and Hamilton (HH) *dmrt2* was bilateral symmetrical expressed in Hense's node, the LRO in chick, and became transiently enriched on the left side of Hense's node until 7HH (Saúde et al., 2005). They further confirmed in gain and loss of function experiments in zebrafish that LR establishment is perturbed by randomized expression of *nodal1*, *lefty* and *pitx2* without affecting the embryonic midline. After the discovery of the fish-specific duplication of *dmrt2* in 2008 which allows neofunctionalization it was possible to distinguish between the specific functions of *dmrt2a* and *dmrt2b* (Zhang 2003; Zhou et al., 2008). Both proteins are involved in LR symmetry breakage and somitogenesis through different pathways (Liu et al., 2009). Characterization of the ancestral *dmrt2a* in more detail revealed that the master control gene for motile cilia, *foxj1*, is a target gene (Pinto et al., 2018).

Here we report that *dmrt2* function during symmetry breakage is conserved in *Xenopus laevis*. Dmrt2 regulates two important functions during LRO morphogenesis in the early gastrulae. Correlating to zebrafish, Dmrt2 intervenes in the induction of *foxj1* in the SM and hence controls ciliogenesis of the LRO. Next, it specifies the paraxial mesoderm as it activates *tbx6* and *myf5* expression in early gastrulae. We demonstrated that this step is crucial for setting up the flow-sensing network as the Dmrt2-mediated induction of *myf5* is important for specifying the sLRO cells.

Our results provide an early function of the paraxial mesoderm for the specification of the flow-sensing LRO area and link early somitogenesis to left-right axis establishment.

Results

***dmrt2* has 3 isoforms and shows a broad expression pattern**

We examined the expression pattern of *dmrt2* during *Xenopus laevis* development to detect LR relevant expression domains (Fig. S1). Maternal transcripts were not detected by *in situ* hybridization and RT-PCR (not shown). A first weak and diffused expression pattern could be observed in early gastrula stage embryos (st.10.5) in the mesoderm surrounding the blastoporus (Fig. S1A). At late gastrulation (st. 12) the expression of *dmrt2* is concentrated to the elongating notochord (Fig. S1B). During early neurulation *dmrt2* expression starts in the epidermis and later stages retain this domain (Fig. S1, C-F). Additionally, expression arises in the lateral mesoderm attached to the presomitic mesodermal border and dispersed along the notochord (Fig. S1C). Interestingly, we detected *dmrt2* expression in hemisections of late neurulae (Fig. S1D) only in the posterior part of the notochord (Fig. S1D'). This *dmrt2* positive region contains the LRO of *Xenopus*. Transversal sectioning revealed that the expression is distributed over the whole posterior notochord, including the central flow-generating LRO (fgLRO) cells (Fig.S1D''). Early tailbud stage (st. 21) showed a broad expression in the presomitic mesodermal region and in epidermal cells (Fig. S1E). In late tailbud stage (st. 34, Fig. S1F) the expression stays stable in the epidermis where it might be restricted to a subtype of ion-secreting cells, the tail-organizer, the dermomyotom (Fig. S1F''), the proctodaeum and to a part of the abdominal hypaxial muscle anlagen.

The analysis of the *dmrt2* expression pattern of during *Xenopus* development suggests a function during somitogenesis and left-right axis determination, which would be consistent with other model organism. Of note, sequence comparison and EST analysis indicated that the *Xenopus dmrt2* gene might be expressed in different isoforms (Fig. S1G, H). Based on the available data we generated specific primers for each isoform and performed PCR analysis on cDNA of st. 33 tadpoles (Fig. S1H) produced with dTT-oligomers. We identified a full length transcript with 1587 base pairs (bp). It contains the sequence of all 4 exons, including its 5'UTR in exon 1 and 2, the 3'UTR in exon 4 and the highly conserved DNA-binding domain, the DM-domain, in exon 2. A region in exon 4, that we termed as "U-domain" for "unknown domain", shows high sequence conservation within vertebrates (Fig. S1G). Alternative splicing and intron retention generated a second isoform with 579 bp that represents the smallest *dmrt2* isoform we identified. As isoform 2 consists of the first and second exon it also

includes the DM-domain as well as additional 129 bp of coding sequence formally derived from intron 2 (Fig. S1G). A third isoform was identified which lacks the DNA-binding domain but includes the conserved U-domain. The open reading frame of this one starts in contrast to the other isoforms with exon 4 and has 960 bp coding sequence (CDS).

By now we were not able to clarify which distal regions belong to the 5' and 3'UTRs of the three different isoforms. Also we were not able to differentiate between expression pattern of each individual isoform during *Xenopus* development (Fig. S1, A-F). The designed *in situ* hybridization probe for *dmrt2* includes the whole sequence between exon 1 and exon 4 and thus should recognize all 3 isoforms. Interestingly, existence of the third isoform only in other vertebrates like e.g. primates, bird or minke whales might point out a conserved function during somitogenesis.

The expression pattern of *dmrt2* in *Xenopus* suggests a conserved *dmrt2* function during vertebrate development. These functions could be isoform and stage dependent. Especially the expression pattern in the LRO (Fig. S1, D-D'') was of interest as this implicated an involvement of *dmrt2* during LR axis establishment in *Xenopus*, too.

Loss of *dmrt2* led to left-right defects and impaired ciliogenesis

The results of the expression analysis revealed a first hint for a function of *dmrt2* during symmetry breakage in *Xenopus* as it was expressed in the central LRO cells in neurulae. As the specificity of morpholino oligomers (MO) is highly discussed during the last years we tried to use the advantage of the CRISPR/Cas9 system. Thereby we generated F0 knock-out embryos with high indel efficiency (90 %) by injecting a *dmrt2* sgRNA targeting the DM-domain in exon 2 and Cas9 protein into one-cell stage embryos (Fig. S2A). Unfortunately we were not able to analyze LR marker genes in the LRO or the LPM as most of these embryos, so called *dmrt2* crispants, had severe gastrulation defects (Fig. S2C, D).

As consequence of the severe gastrulation defects seen in *dmrt2* crispants we decided to take advantage of a MO in a tightly controlled manner for any further investigations. Like in *dmrt2* crispants, a high amount of *dmrt2*-MO led to gastrulation defects (not shown) wherefore we titrated the amount of MO to a concentration that did not perturb gastrulation. Then, we analyzed exemplarily the expression of two organizer marker

genes, *chordin* (Fig. S3A, A') and *gooseoid* (Fig. S3B, B'), as well as the mesodermal marker gene, *t-box gene t (tbxt)* (Fig. S3C, C'). The loss of *dmrt2* in the applied concentration demonstrated that the analyzed marker genes were not affected and allowed further investigations.

We started to analyze the expression of the LR marker gene *pitx2* that is only expressed in the left LPM of wildtype embryos (Fig. 1A). After unilaterally left KD of *dmrt2*, the *pitx2* expression in the LPM was absent in 60 % of the embryos (Fig. 1B, C). We were able to partially restore it by co-expressing the full length mRNA of *dmrt2*, demonstrating that the MO induced KD was specific.

Next, we checked the morphogenesis of the LRO in mid-neurulae. By adding fluorescent microbeads to the LRO in dorsal posterior explants at st. 17 we measured the leftward fluid flow in control embryos (Fig. 1D) and *dmrt2* morphants (Fig. 1E) to quantify flow velocity (Fig. 1F) and directionality (Fig. 1G). Leftward-fluid flow was heavily impaired in morphants (Fig. 1E) as both, directionality (Fig. 1G) and velocity (Fig. 1F) were affected.

As the defective flow in neurulae could be the result of reduced *foxj1* levels in the SM as well as *foxj1* is a *dmrt2a* target gene in zebrafish (Pinto et al., 2018), we analyzed the specification of the SM (Fig. 1, H-J). In comparison to wildtype controls embryos (Fig. 1H, J), the depletion of *dmrt2* strongly reduced *foxj1* in the SM in 85 % of the embryos (Fig. 1I, J). Subsequently and for the proof of principle, we stained the LRO with an antibody against acetylated α -tubulin (Tuba4a) to visualize cilia and stained the F-actin cytoskeleton to mark the cell borders (Fig. 1, K-L"). The central fgLRO cells (Fig. 1K, K') and the flanking lateral sLRO cells (Fig. 1K, K'') can be clearly distinguished in LROs of untreated embryos (Fig. 1K). Measurement of ciliary length revealed an average of 6 μm and cilia were posteriorly polarized (Fig. 1K, K', M). In contrast, after unilateral left KD of the *dmrt2*, depicted by green lineage tracer, cilia were abnormal with respect to positioning and ciliary length (Fig. 1L-M), as they were unpolarized (Fig. 1L') and reduced to about 3 μm (Fig. 1M). Interestingly, the loss of *dmrt2* completely erased the sLRO cells (Fig. 1L''). This indicated that Dmrt2 has an axial and a paraxial function. In the midline it acts on LRO ciliogenesis by regulating *foxj1* expression in the SM. The loss of the border between the fgLRO and the sLRO opens the question if sLRO cells are specified and if *dmrt2* influences the patterning of the paraxial mesoderm as sLRO cells are of somitic origin.

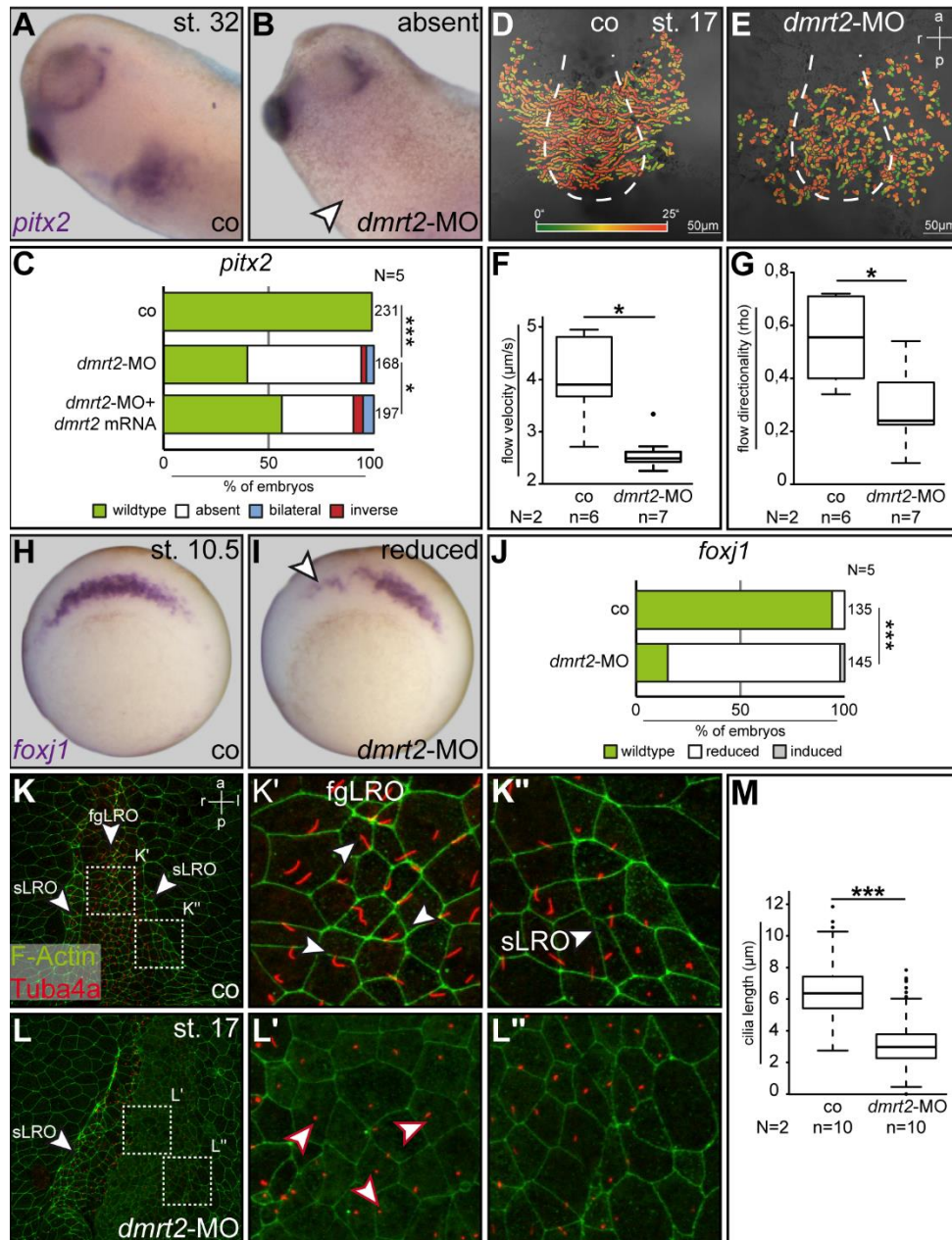


Figure 1: Loss of *dmrt2* impaired laterality determination and LRO morphogenesis

The LR marker gene *pitx2* was expressed in the left LPM in untreated control siblings (A, C). After unilaterally left KD of *dmrt2*, *pitx2* in the left LPM was absent (B) in 60 % of the embryos (C). Co-expressing the full length *dmrt2* mRNA reduced the amount of LR defects up to 40 % (C). Analysis of the LRO morphogenesis in *dmrt2* morphants strongly revealed that leftward-fluid flow is perturbed (E) in velocity (F) and directionality (G) in comparison to wildtype control embryos (D, F, G). *foxj1* that became expressed in the SM in wildtype embryos (H, J) was reduced in *dmrt2* morphants (I, J). Fluorescence staining of the LRO for F-actin and Tuba4a manifested that fgLRO cells harbored mispolarized and shortened cilia after *dmrt2* KD (shown by green lineage tracer) (L, L', M) and loss of sensory LRO cells (L'').

asterisk mark the injected side; a=anterior; co=control; fgLRO=flow-generating left-right organizer; l=left; p=posterior; r=right; sLRO= sensory left-right organizer;

Dmrt2 regulates paraxial mesoderm patterning

The immunofluorescence staining revealed that sLRO cells are affected in *dmrt2* morphants. Therefore we stained for the LR marker gene *nodal1* that is expressed in a bilateral symmetric fashion in wildtype embryos (Fig. 2A). After depletion of Dmrt2, the *nodal1* expression domain was completely erased in 50 % of the embryos (Fig. 2B, D) and could be partially restored by co-expressing *dmrt2* (Fig. 2C, D). Of note, targeting the right-side of the embryo resulted in the same outcome (not shown).

As sLRO cells in *Xenopus* are of somitic origin (Shook et al., 2004), we asked whether paraxial mesoderm patterning was affected. We investigated the expression of two myogenic marker genes at the onset of gastrulation, namely *tbx6* (Fig. 2, E-H) and *myf5* (Fig. 2, I-L). We noted that both, *tbx6* (Fig. 2F, H) and *myf5* (Fig. 2, J-L) expression were strongly reduced after *dmrt2* KD. Co-injecting the *dmrt2* mRNA was able to restore the *tbx6* expression in mesodermal cells (Fig. 2G, H).

These observations told us that the specification of the sLRO cells was lost in *dmrt2* morphants. Due to their contribution to the paraxial mesoderm which was strongly affected after loss of Dmrt2, this suggested that paraxial mesoderm patterning in *Xenopus* might be linked to symmetry breakage.

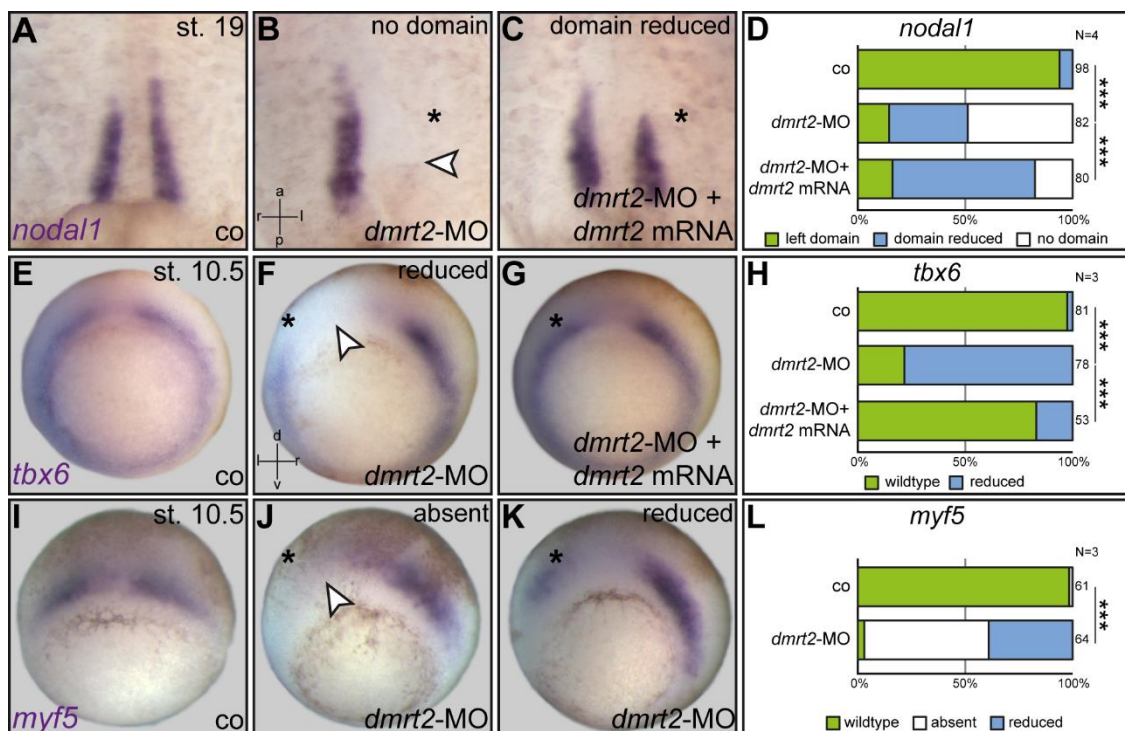


Figure 2: sLRO cells and paraxial mesoderm patterning are lost in *dmrt2* morphants

In wildtype embryos, *nodal1* became expressed in a bilateral symmetric manner in the LRO (A). Morpholino-mediated KD of *dmrt2* led to complete loss of the sLRO expression domain (B, D) that could

partially be restored by co-injecting *dmrt2* mRNA (C, D). Analysis of *tbx6* (E-H) and *myf5* (I-L) in early gastrulae demonstrated that paraxial mesoderm patterning was affected. *tbx6* was reduced on the targeted side (F, H) and was significantly rescued upon co-expressing *dmrt2* (G, H). The angle-wing like expression pattern of *myf5* (I) was lost (J) or reduced (K) in *dmrt2* morphants (L).

asterisk mark the injected side; a=anterior; co=control; l=left; p=posterior r=right

Paraxial mesoderm patterning is important for sLRO cell specification

Based on the observation that *dmrt2* influences paraxial mesoderm patterning, we wanted to know if these can be linked experimentally to symmetry breakage in *Xenopus*. First of all, we asked whether *myf5* (Fig. S4A) and *tbx6* (Fig. S4B) are expressed in the frog LRO. *In situ* hybridization and transversal sectioning of neurula stage embryos demonstrated that both were expressed in the lateral sLRO cells (Fig. S4A', B'). As *myf5* is a direct target gene of Dmrt2 in mice and of Tbx6 in *Xenopus*, we wondered if *tbx6* could restore *myf5* expression in *dmrt2* morphants (Sato et al., 2010; Li et al., 2006). Again, the loss of *dmrt2* led to absent *myf5* expression in 60 % of the embryos on the targeted side (Fig. 3B, D). Co-injecting *tbx6* in *dmrt2* morphants significantly rescued the loss of *myf5* in early gastrulae (Fig. 3C, D). Ongoing we checked for *nodal1* in the LRO (Fig. 3, E-H). While the *dmrt2* morphants mainly showed a completely loss of the *nodal1* domain (Fig. 3F, H), siblings that were co-injected with *tbx6* had a partially restored *nodal1* expression (Fig. 3G, H).

Next, we investigated if manipulation of the paraxial mesoderm itself affects laterality determination. As the early angle-wing like expression pattern of *myf5* could remark the future position of the sLRO cells, we decided to use a translation blocking morpholino against *myf5*. The unilateral left loss of *myf5* phenocopied the *dmrt2* morphants. The *nodal1* expression domain was absent in the LRO in about 50 % after *myf5* KD (Fig. 3J, L) which could be rescued by co-expressing *myf5* mRNA (Fig. 3K, L), demonstrating MO specificity. In addition, analysis of *pitx2* in the LPM (Fig. 3, M-P) confirmed the importance of *myf5* for symmetry breakage. In contrast to wildtype control siblings that showed left-sided expression in the LPM (Fig. 3M, P), *myf5* morphants lacked the *pitx2* pattern (Fig. 3N, P).

These results showed that the specification of the paraxial mesoderm is crucial for symmetry breakage in *Xenopus*.

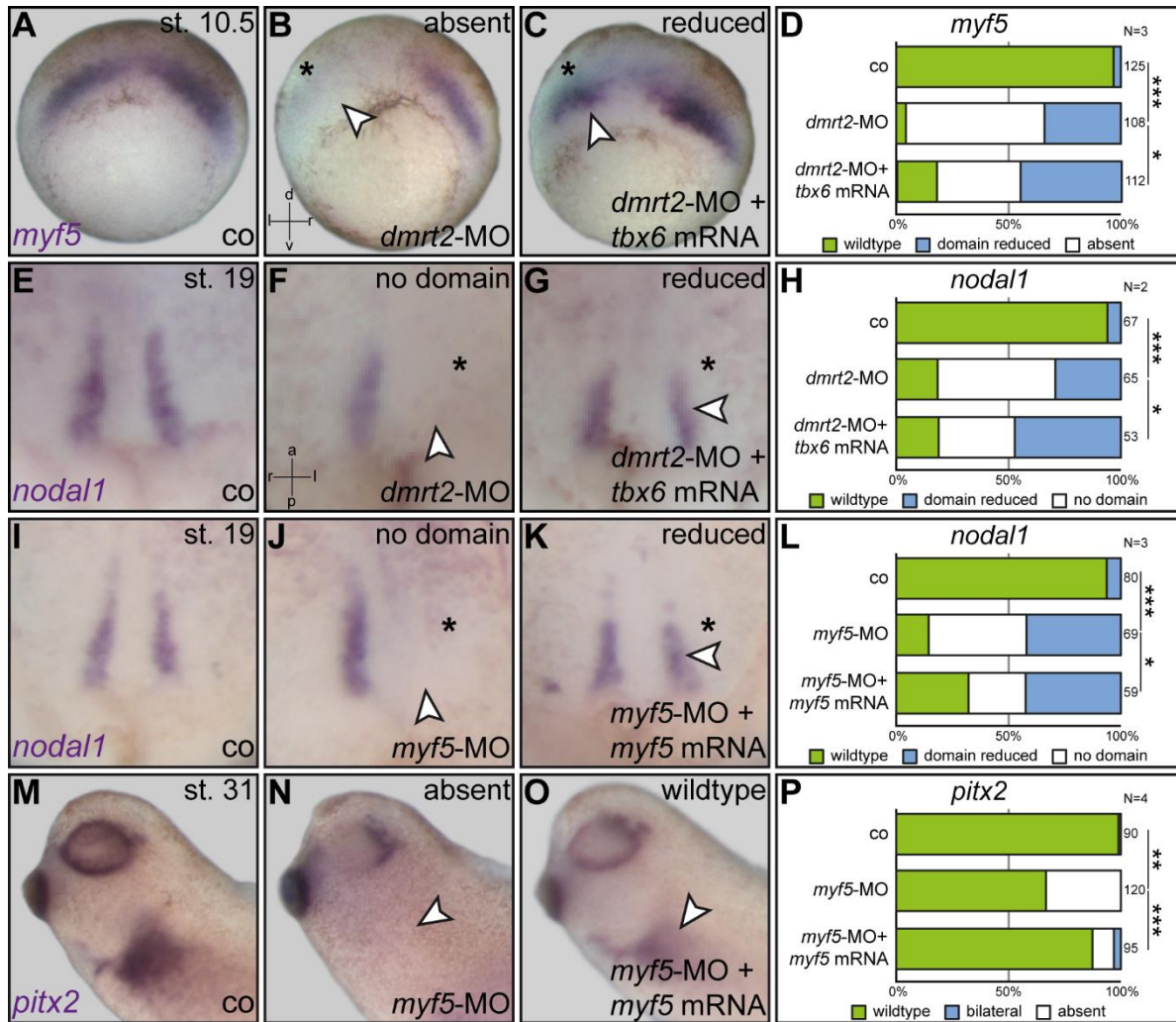


Figure 3: Paraxial mesoderm patterning is important for laterality determination

Wildtype control embryos showed the angle-wing like expression pattern of *myf5* in early gastrulae (A). Depletion of *Dmrt2* strongly impaired *myf5* expression (B, D) that could be restored by co-expressing *tbx6* (C, D). In neurula (E-H), the erased *nodal1* domain in the LRO of *dmrt2* morphants (F) was rescued upon on expressing *tbx6* mRNA (G, H). Blocking the translation of *myf5* (I-P) phenocopied the *dmrt2* morphants. *nodal1* was absent in the LRO (J, L) and the LPM lacked *pitx2* expression (N, P). Co-expressing *myf5* mRNA in *myf5* morphants restored the wildtypic situation of *nodal1* (K, L) and *pitx2* (O, P) in those siblings.

asterisk mark the injected side; a=anterior; co=control; d=dorsal; l=left; p=posterior; r=right; v=ventral

Myf5 specifies sLRO cells downstream of Dmrt2

Last, we asked if *Dmrt2* and *Myf5* act in the same pathway on sLRO specification. Therefore we performed epistatic experiments (Fig. 4, A-G) with suboptimal *dmrt2* and *myf5* MO doses and analyzed *nodal1* (Fig.4, A-D) in the LRO and *pitx2* expression in the LPM (Fig.4, E-G). These experiments showed, that both were stronger affected if

the MOs were injected together than alone. Single low dose injection of each led to a reduced *nodal1* domain in the LRO (Fig. 4B, D), while the combination of both erased the expression (Fig. 4C, D). Corresponding to this, the single loss of either *dmrt2* or *myf5* had a weak impact on *pitx2* in the LPM (Fig. 4G). The parallel KD of both strongly compromised *pitx2* resulting in absent expression on the left side (Fig. 4F, G). This indicates that *myf5* and *dmrt2* act together in the same process.

Finally, to further strengthen this possible interaction between Myf5 and Dmrt2 during sLRO cell specification and laterality determination, we tried to rescue the *dmrt2*-MO with *myf5* mRNA (Fig. 4, H-N). The depletion of Dmrt2 revealed a complete loss of *nodal1* in 65 % of the embryos (Fig. 4I, K). The co-expression of *myf5* in *dmrt2* morphants restored the *nodal1* domain (Fig. 4J) with 90 % of the embryos showing a wildtypic pattern again in the LRO (Fig. 4K). Additionally, *pitx2* that was absent in all morphant embryos (Fig. 4M, N) could be rescued in 45 % of the embryos (Fig. 4N). This showed that Dmrt2 specifies the sLRO of *Xenopus* in a *myf5* dependent manner.

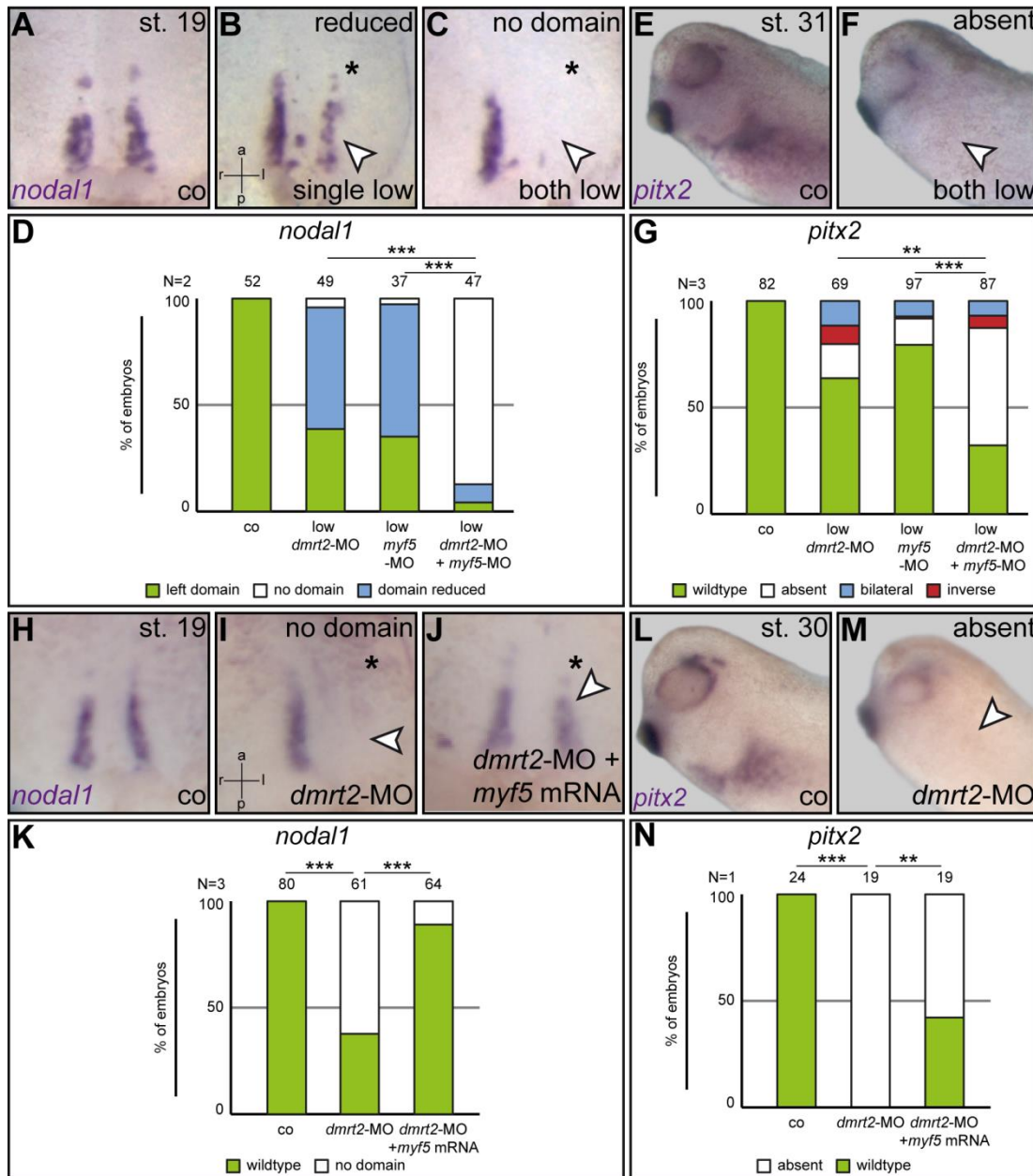


Figure 4: Myf5 specifies sLRO cells downstream of Dmrt2

Epistatic experiments with suboptimal doses of *dmrt2*- and *myf5*-MO showed that single injection had a weak impact on *nodal1* in the LRO (B, D). Combining both revealed a complete loss of the *nodal1* domain in 90 % of the embryos (C, D). Analysis of *pitx2* confirmed this observation (G) as the single loss of one component had a weak impact in the LPM (G) in comparison to the combined loss of function that lacked *pitx2* expression (F) in 70 % of the embryos (G). *nodal1* (H-K) and *pitx2* expression in *dmrt2* morphants (I, M) could be restored by co-expressing *myf5* mRNA (K, N).

Asterisk mark the injected side; a=anterior; co=control; l=left; p=posterior; r=right

Discussion

The intrinsic chirality of the inner organs is crucial for their proper function. Malformations that occur in humans during embryonic development can engender organ dysfunction or be lethal. Therefore it is indispensable that the bilateral symmetry gets broken properly to initiate asymmetric organ morphogenesis. In most vertebrates, the mechanism of symmetry breakage is constituted by a cilia-driven leftward fluid flow (Nonaka et al., 1998; Okada et al., 2005; Schweickert et al., 2007; Oteíza et al., 2008). Importantly, flow directionality needs to be perceived and translated into molecular pathways which fix laterality. Thus somitic sLRO cells are of utmost relevance for LR development.

These events require the specification of the transient LRO that has been extensively studied during the last years. However, the mechanism that specifies and separates the lateral sensory LRO cells, which are of somitic nature in *Xenopus*, was less examined. Recent studies showed that this process involves Fgf signaling (Sempou et al., 2018; Schneider et al., 2019).

A current study identified *dmrt2* as a novel regulator of symmetry breakage in zebrafish. Here, *Dmrt2* regulates the expression of *foxj1* and the synchronized segmentation of the somites (Saúde et al., 2005; Pinto et al., 2018). These observations gave a first hint that *dmrt2* could be involved in the specification of the somitic LRO sensor cells and thereby provided the basis of this work.

***dmrt2* expression pattern points to a conserved function among vertebrates**

First, we examined the expression pattern of *dmrt2* during *Xenopus laevis* development. Expression was restricted to the notochord, the intermediate mesoderm, the ionocytes and the somites which recapitulated the already described functions of *dmrt2* during LR establishment, kidney development, ionocyte specification in the human airway epithelia and somite differentiation, respectively (Meng et al., 1999; Saúde et al., 2005; Pinto et al., 2018; Öunap et al., 2004; Han et al., 2010; Deprez et al., preprint; Bouman et al., 2018; Seo et al., 2006;). This pointed to an overall conserved function of *dmrt2* in vertebrates.

Moreover, it turned out that *dmrt2* is expressed in 3 different isoforms in *Xenopus laevis*. Further investigations have to analyze the function of each during *Xenopus laevis* development and to proof the existence of additional isoforms as the human *dmrt2*

encodes for 6 variants (Ottolenghi et al., 2000). We suggest that these isoforms act in a tightly controlled network and can regulate target genes stage- and tissue-dependently in a combinatorial manner. Of note, the homologous gene *dsx* becomes alternatively spliced in *Drosophila* (Burtis & Baker, 1989). Both isoforms possess two oligomerization domains and act on the same target gene but with different effect (An et al., 1996, Erdman et al., 1996). The *dsx^M* splice variant acts as transcriptional activator leading to male differentiation, while the *dsx^F* represses the target gene (Coschigano & Wensink 1993). Additionally, Dmrt proteins generally have the competence to bind DNA as monomers, homo- or heterodimers and can operate in a feedback loop (Murphy et al., 2007, Pinto et al., 2018). This shows that the regulatory machinery of *dmrt2* is sophisticated. Future work has to characterize if *Xenopus* Dmrt2 operates in a related mechanism. Identification of the transactivation domain, as well as functional studies of oligodimerization domains and especially of the vertebrate specific U-domain would be valuable, as we propose that the latter is important for the function of Dmrt2 during symmetric somitogenesis that arose within vertebrates.

Dmrt2 links early somitogenesis to symmetry breakage

However, decisive for the high frequency LR defects in *Xenopus* morphant embryos seem not to be the result of a reduction of *foxj1* expression in early gastrulae. It turned out that the co-expression of *myf5* after *dmrt2* KD manifested the specification of the sLRO cells. This was proven by the loss of *myf5* that phenocopied the *dmrt2* KD and led to impaired *pitx2* and *nodal1* expression. Additionally, epistatic experiments showed that both genes act in the same signaling pathway. This confirms that the specification of the sLRO cells depends on the induction of the myogenic lineage. How *dmrt2* and *myf5* cooperate exactly needs to be evaluated.

We propose that Dmrt2 acts downstream or parallel of Fgf signaling during paraxial mesoderm patterning in early gastrulae. Fgf signaling is imperatively necessary for this process, as well as for the specification of sLRO cells and the induction of *foxj1* in the SM (Sempou et al., 2018; Schneider et al., 2019). The Fgf8 ligand operates in a positive feedback loop with Tbx6 that in turn directly regulates the induction of *myf5*, *wnt8* and *fgf8* independently of Tbx6 (Fletcher & Harland 2008; Li et al., 2006). Likewise the loss of *dmrt2* affected *tbx6* and *myf5* expression without affecting *tbxt*, the patterning of the SM and the specification of the sLRO cells reinforcing our idea.

Interestingly, *Myf5* activates *myod1* expression that deals in a feedback loop inducing the expression of *tbx6*. Thereby, *Myod1* is able to induce *tbx6* but it is not sufficient for the activation of *myf5*, demonstrating the complex regulation machinery of *myf5* that might include additional regulators (Maguire et al., 2012). This is in agreement with our data as we were able to rescue *tbx6* expression but not *myf5* in gastrulae. Of note, we found that *myod1* was reduced in *dmrt2* morphants and in turn, the overexpression of *myod1* in animal caps was able to induce *dmrt2* (not shown). Additionally, *myf5* and *nodal1* expression in *dmrt2* morphants were rescued by co-expressing *tbx6*, supporting the hypothesis that *dmrt2* is part of this early signaling cascade. A function for *tbx6* in symmetry breakage had already been reported in mice. *tbx6* KO mice harbored node ciliogenesis defects and lacked the perinodal signaling (Hadjantonakis et al., 2008). It would be interesting, if *myf5* or *myod1* KO mice show laterality defects as well. Surprisingly, the KO of *dmrt2* in mice led to disturbed epithelialization and differentiation defects of the somites but not to LR defects (Seo et al., 2006; Lourenço et al., 2010). We propose that the *dmrt2* KO mice have to be evaluated in more detail. As the human *dmrt2* gene encodes for 6 isoforms that are the result of alternative splicing, a bicistronic transcript and the usage of an initial transcriptional start site (Ottolenghi et al., 2000), we speculated that even mice could exhibit several isoforms. The *dmrt2* null KO mice were produced by targeting the DM-Domain in the second exon and thereby could still possess some functional isoforms that could be important for symmetry breakage.

Summarizing, there are several indications that strengthening the implication of *Dmrt2* to be part of this tightly controlled early somitogenic pathway in *Xenopus*.

***Dmrt2* could integrate Bmp, Wnt or Notch signaling**

Another scenario could be an interaction with Bone morphogenic protein (Bmp) or Wnt signaling. Studies in zebrafish demonstrated, that *dmrt2* becomes reciprocally regulated by Bmp and Sonic hedgehog (Shh) signaling (Meng et al., 1999). In the early *Xenopus* gastrulae, Bmp generates a dorsoventral gradient that specifies dose-dependently the mesodermal tissues. Thereby it restricts *Wnt8* activity to the dorsolateral margins where *Wnt8* activates the expression of *myf5* in the paraxial mesoderm (Dosch et al., 1997, Maroma et al., 1999). Contrary to this, Bmp signaling represses *myf5* in the ventral mesoderm by inducing *vent1* (Dosch et al., 1997; Polli &

Amaya 2002). The interaction of *Dmrt2* with *Bmp* or downstream *Wnt* signaling could be necessary for the induction or restriction of *myf5* expression to the dorsolateral mesoderm. Additionally, short- and long-range signaling of *Bmp* ligands depends on the composition of the extracellular matrix (ECM) (Jones 1996, Dosch et al., 1997; Ohkawara et al., 2002). *Dmrt2* regulates the expression of ECM proteins in the somites of mice. Therefore, it is possible that *Dmrt2* indirectly controls the transport of *Bmps* during *Xenopus* gastrulation or interacts with *Bmp* signaling in controlling *myf5* expression (Seo et al., 2006).

A last attractive interplay could occur with the Notch signaling pathway. Like the depletion of *Dmrt2*, disturbing Notch signaling impairs LR determination by ablating *nodal1* and *dand5* expression in the sLRO cells (Raya et al., 2003; Przemeczek et al., 2003; Tavares et al., 2017; Sakano et al., 2010; Krebs et al., 2003; Gourronc et al., 2007; Lopes et al., 2010; Boskovski et al., 2013 Kitajima et al., 2013). Further, it regulates ciliogenesis in the LRO by determining the switch between motile flow generating and immotile sensory cilia (Boskovski et al., 2013; Tavares et al., 2017). As *dmrt5* is a direct Notch target gene in *Xenopus* (Parlier et al., 2013) it remains to be tested if *dmrt2* is a Notch target gene as well.

Dmrt2 functions during somitogenesis in vertebrates

The base of the present work was the identification of the *Dmrt2* function during laterality determination and somitogenesis in zebrafish. A general contribution of *Dmrt2* in the somitic pathway might be conserved along vertebrates but with different regulatory functions. In mice, *dmrt2* is specifically expressed in the dermomyotom of the somites and represents a downstream target of the basic helix-loop-helix transcription factor *Tcf15* (also known as *Paraxis*) and of the paired box transcription factor *Pax3* (Rowton et al., 2013, Sato et al., 2010). The KO of *dmrt2* led to severe skeletal malformations which in turn were early lethal as neonates are not able to breath (Seo et al., 2006). Related phenotypes were observed in *myf5* and *tbx6* KO mice, implicating that the pathways overlap (Gensch et al., 2008; White et al., 2003). Of note, this and the early signaling cascade during paraxial mesoderm patterning in *Xenopus*, strengthening the presumption that *Dmrt2*, *Tbx6* and *Myf5* interact in the same pathway.

In *dmrt2* KO mice, the dermomyotom and myotome of the somites, which give rise to the dermis and muscles, failed to epithelialize as Laminin1, a component of the ECM, was reduced (Seo et al., 2006). This impacted mesenchymal-to-epithelial transition, a process that is necessary for somite compartmentalization. Moreover, skeletal structures which arise from the sclerotome were strongly impaired in *dmrt2* KOs, demonstrating that Dmrt2 is able to act cell-autonomously (Seo et al., 2006). This might occur by its impact on *myf5* in the myotom that has been shown to be a direct Dmrt2 target gene, which in turn induces the expression of *Pdgfa*, *Fgf2* and *Fgf6* ligands that act on the sclerotome beneath (Seo et al., 2006; Sato et al., 2010; Tallquist et al., 2000; Grass et al., 1996, Fraidenraich et al., 2000).

In comparison, in zebrafish Dmrt2 seems to regulate the epithelialization of the somites as well (Meng et al., 1999) and moreover the synchronized segmentation of the paraxial mesoderm into the metameric structure of the somites (Lourenço et al., 2010). This process occurs before somite differentiation and starts in a temporal and spatial proximity with the transfer of the asymmetric signal into the left LPM. Therefore, and as both processes share the same signaling pathways, the protection of the PSM from asymmetric signals came into focus. Several studies indicated that this might be provided by retinoic acid (RA) in vertebrates (Vermot & Pourquié, 2005; Sirbu & Duester, 2006; Brend & Holley, 2009).

Based on our findings, we suggest, contrary to the hypothesis in zebrafish, that Dmrt2 is not important for the protection of the somites from asymmetric cues but rather for the correct specification of the PSM that takes place much earlier than somite segmentation.

The evolution of sLRO cells

The origin and the ultimate fate of the sLRO cells in other model organisms had been less examined. In frog, signals from the Spemann Organizer specify the LRO at the onset of gastrulation by patterning the precursor tissue (Glinka et al., 1996; Smith, 1995; Stubbs et al., 2008; Walentek et al., 2013; Schneider et al. 2019; Vick et al., 2018). The mechanism that makes the difference between the fgLRO and the sLRO cells had not been identified so far. After leftward flow, sensory cells of the *Xenopus* LRO ingress into the somites while the fgLRO cells become part of the notochord (Shook et al., 2004). Likewise the cells of KV in zebrafish seem to become part of the

tail mesoderm e.g. muscles, and notochord (Melby et al., 1996). In contrast, in mice the flow-sensing crown cells migrate into the posterior part of the notochord after the symmetry breaking event (Yamanaka et al., 2007). A contribution to the somites of sLRO cells had only been described for *Xenopus* so far.

Interestingly, the *nodal* and *dand5* expressing cells in amphioxus, as well as in sauropsida like turtles, geckos and the chick, are part of the PSM (Kajikawa et al., 2020; Otto et al., 2014). In comparison, in mammals like mice, rabbit, cattle or the pig those cells contribute to axial or subchordal mesodermal cells (Schröder et al., 2015). This implicated that the origin of the flow-perceiving cells emanates from the PSM, which became lost with the evolution of mammals. We speculate that the establishment of the bilateral symmetric structure of the somites might represent a possible explanation. Nodal signaling regulates the overall asymmetric development in amphioxus and blocking of Nodal signaling led to symmetrisation of the embryo (Soukup et al., 2015). This is in agreement with studies in vertebrates, where it had been demonstrated that the PSM has to be protected from asymmetric cues derived from the LRO to form bilateral symmetric somites (Vermot & Pourquié, 2005; Sirbu & Duester, 2006; Brend & Holley, 2009). This process seems to be regulated by RA signaling that defines somite boarder formation. Of note, manipulating RA signaling in amphioxus did not influence somitogenesis (Bertrand et al., 2015), indicating that this function arose within vertebrates.

Based on the current data, we speculate that RA regulates the symmetric formation of the somite boarders, but its function in protection from asymmetric cues seems to be enigmatic. Further, if a related mechanism might be existent, it seems to be restricted to non-mammalian vertebrates for several reasons: The *nodal1* and *dand5* expressing cells in mammals are part of the embryonic midline and do not contribute to the PSM like it was identified in other vertebrate model organisms (Schröder et al., 2015; Yamanaka et al., 2007; Kajikawa et al., 2020; Otto et al., 2014). As the transfer of the asymmetric Nodal signal from the LRO to the LPM is not well characterized, it remains if this signal gets in any contact with the PSM in mammals. A recent study in mice identified, that Nodal moves towards the LPM by crossing the endodermal cells which are tightly apposed to the mouse LRO (Saund et al., 2012). Irrespectively to how Nodal becomes transferred to the LPM, the PSM does not respond to Nodal signaling and shows no expression of its receptor Cryptic and its downstream co-transcription factor Foxh1 (reviewed in Hamada & Tam, 2014), which calls the function of RA into doubt.

In addition, a direct interaction of RA with Nodal signaling has not been reported so far. Moreover, the hypothesis that RA shields the PSM from asymmetric cues is reposed on a few studies. A tightly controlled evaluation of this mechanism would be insightful. Studies in *Xenopus* revealed that RA is important for mesoderm patterning in early gastrulae (Janesick et al., 2018). It is of note, that the expression pattern of *aldh1a2*, which is coding for the enzyme that catalyzes the synthesis of RA, resembles the expression pattern of *myf5* in early gastrulae of *Xenopus* embryos (Bowes et al., 2010). The study by Janesick and colleagues demonstrated that RA affects somitogenesis much early than the synchronized segmentation takes place. Analysis of LR marker genes in RA deficient *Xenopus* morphants would be helpful to understand if RA signaling in *Xenopus* is associated to symmetry breakage. Interestingly, in mice and zebrafish incubations with RA or an RA antagonist, impaired laterality determination (Huang et al., 2011; Chazaud et al., 1999). This is in conflict with loss of *aldh1a2* function experiments in zebrafish and mice that did not impair LR asymmetry but somitogenesis (Vermot & Pouquié, 2005; Kawakami et al., 2005). It is conceivable that, like in *Xenopus*, RA regulates paraxial mesoderm patterning in other vertebrates. This could depict a possible explanation for the connection between symmetry breakage and somitogenesis, as both processes share the same signaling pathways. Summarizing, up to now, there are several indications that are contradiction to a RA-shielding mechanism. Further studies would be insightful to understand the role of RA signaling during early development and the evolution of the sLRO cells and somitogenesis.

Myf5 specifies sLRO cells downstream of Dmrt2

The decisive Dmrt2 Myf5 axis in the process of sLRO cell specification is a novelty. The angle-wing like expression pattern of *myf5* in the early gastrulae flanking the axial mesoderm already depicted the position of the future sLRO cells. Of note, this is conflicting with the results from Shook and colleagues who showed that the LRO arises from the superficial mesoderm only (Shook et al., 2004). The expression of *myf5*, however, is restricted to the deep mesodermal cells underneath the superficial layer (not shown) indicating that Myf5 may act non-cell autonomous. The capability of Myf5 to act non-cell autonomous was previously described in the somites where it induces the expression of several ligands like Fgf4, Fgf6 and Pdgfa (platelet-derived growth

factor A) in the myotom that act on the sclerotome beneath (Tallquist et al., 2000; Grass et al., 1996, Fraidenraich et al., 2000). A related mechanism might be in charge in the early gastrulae to engender the specification of sLRO and to separate them from the medial flow-generating cells. Additionally, transplantation experiments demonstrated that signals from the deep mesoderm are crucial for the specification of the lateral sLRO cells (not shown, unpublished observation).

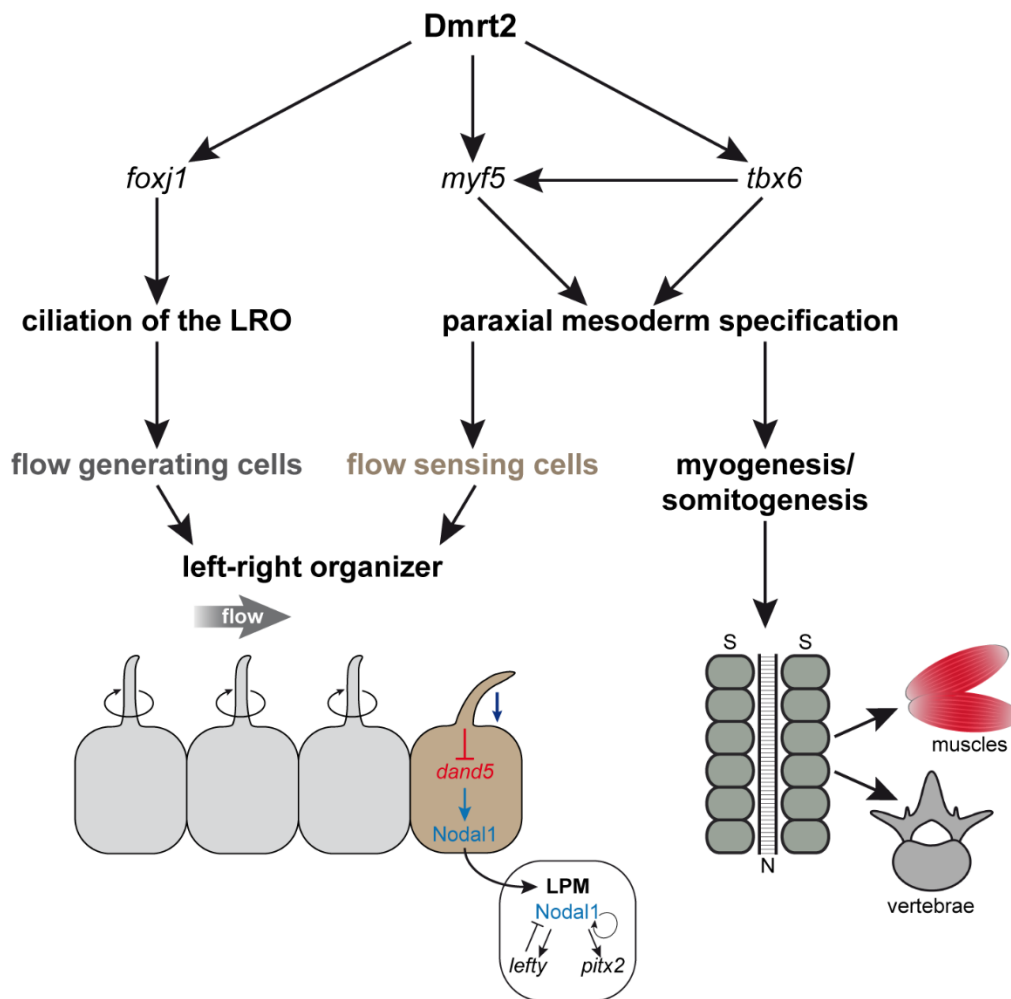


Figure 5: Dmrt2 regulates symmetry breakage and early somitogenesis in *Xenopus laevis*

Dmrt2 intervenes in two processes during symmetry breakage. It specifies the LRO by inducing *foxj1* in the SM that gives rise to the ciliated epithelium of the LRO (left panel). Simultaneously, it activates *tbx6* and *myf5* expression in the early gastrulae, leading to the specification of the paraxial mesoderm (right panel). This step is important for early myogenesis and somitogenesis as later on the metameric somites differentiate and form the muscles and vertebrae of the embryo. Additionally, paraxial mesodermal expression of *myf5* is important for symmetry breakage. Myf5 induces the lateral flow-sensing cell fate. This leads to separation of the sLRO cells from the flow-generating midline cells. This step is important since the sLRO are able to recognize the leftward flow and to translate this signal into the activation of the Nodal cascade on the left side. N=notochord; S=somites

In conclusion, we found that the involvement of *dmrt2* during symmetry breakage and somitogenesis is conserved in *Xenopus*. *Dmrt2* activates *foxj1* and initiates ciliogenesis of the LRO (Fig. 5, left panel). The induction of the paraxial mesoderm by regulating *tbx6* and *myf5* expression is important for somitogenesis (Fig. 5, right panel). This step is also indispensable for symmetry breakage in *Xenopus* as the sLRO cell fate depends on the activation of *myf5*. This links early somitogenesis to LR axis determination for the first time experimentally.

Material & Methods

Experimental model and subject

Xenopus laevis was used as model organism for *in vivo* studies. Frogs were obtained from Nasco (901 Janesville Avenue PO Box 901 Fort Atkinson) and were treated in accordance to German Regulations and laws approved by the Regional Government Stuttgart. Female frogs were primed with 30-50 units of human chorionic gonadotropin (hCG, SigmaAldrich) approximately 3-5 days prior to oviposition. The day prior to ovulation, frogs were injected with 300-600 units hCG, depending on weight and size. Eggs were collected into a petri dish by carefully squeezing and *in vitro* fertilized. Sperm of male frogs was gained by dissecting of testes.

Microinjection and morpholino sequences

Microinjections were performed with a volume of 4nl into the left dorsal marginal region of 4 and 8-cell stage embryos. Morpholinos (GeneTools) were injected at a concentration of 1pMol.

dmrt2-MO: 5' TGCCTTCATCTCGTACATCTCCAGC 3'

myf5-MO: 5' ACCATCTCCATTCTGAATAGTGCTG 3'

Primer and cloning of *dmrt2*

The probe for *dmrt2* was designed by using a forward primer containing the sequence of the 5'UTR in the first exon and a reverse primer with the sequence of 4th exon. Sequence was cloned into the pGEM T-easy vector system, linearized with SacII and synthetic antisense mRNA was transcribed by sp6 RNA polymerase.

Primer for *in situ* hybridization of *dmrt2*:

Forward Primer: TCCCACCACTAAGGGAACTG

Reverse Primer: TTTTCAAGATGTGCCTGCTG

For rescue experiments *dmrt2* was cloned into cs2⁺ vector using the following primers:

Forward primer:

ATCGGGATCCTTAGAAATGTATGAAATGAAAGCGCCTGCTGCCCCATCCTCTTC
CTCGT

Reverse Primer:

ATCCATCGATGTTACTGACTAGAACGCTTGACTGTTGTTGAGGG

Plasmid was linearized by SacII and mRNA was transcribed using the InVitrogen mMessage mMachine sp6 kit according to user instructions. For rescue experiments 50 – 100 ng/μg were injected.

For the identification of the three *dmrt2* isoforms the following primers were used:

Isoform 1 forward: CAAAGCCCAGCATCACAGAG
 Isoform 1 reverse: TAGGGCTGCTTTGTGACCTC
 Isoform 2 forward: CTCTTCCTCGTCCAACCCTT
 Isoform 2 reverse: TGTACATTGGAGAGGGCAGA
 Isoform 3 forward: ACTTTGTAAGCATGCTGTGTG
 Isoform 3 reverse: TAGGGCTGCTTTGTGACCTC

***tbx6* and *myf5* constructs**

The *tbx6* gain of function construct was a gift from Hideho Uchiyama. *myf5* in pBSK⁺ was a gift from Gawantka. For gain of function experiments, *myf5* was cloned into cs2⁺ by restriction digest using EcoRI.

myf5 rescue construct was cloned into cs2⁺ by the following primers:
 Forward primer: ATATCGATATGGAAATGGTTGACAGTTGTCCTTC
 Reverse Primer: ATGGAAATGGTTGACAGTTGTCCTTC

The *tbx6* and the *myf5* plasmids were linearized with NotI and mRNA transcribed using the Invitrogen mMessage mMachinE sp6 kit according to user instructions. A concentration of 30 ng/μl *tbx6* mRNA, 60 ng/μl *myf5* mRNA and 50 ng/μl *myf5* rescue mRNA were used for experiments.

CRISPR/Cas9 genome editing

CRISPR/Cas9 genome editing was carried out as described in Tingler et al., 2018. Embryos were injected at 1-cell stage.

Sequence for *dmrt2* sgRNA:

TAATACGACTCACTATAGGGCCAGGTGCAGGAACCCACGTTTTAGAGCTAGAA

Leftward-fluid flow analysis and immunofluorescence staining

Immunofluorescence staining and leftward-fluid flow analysis was carried out as described in Tingler et al., 2018.

Acknowledgement

We thank Hideho Uchiyama for sharing the *tbx6* overexpressing constructs with us and all members of the Blum lab for discussing and advices.

References

- An W., Cho S., Ishii H., Wensink P.C. (1996). "Sex-specific and non-sex-specific oligomerization domains in both of the doublesex transcription factors from *Drosophila melanogaster*". *Molecular Cellular Biology*, Vol. 16, Issue 6, 3106-3111
- Antic D., Stubbs J.L., Suyama K., Kintner C., Scott M.W., Axelrod J.D. (2010). "Planar Cell Polarity Enables Posterior Localization of Nodal Cilia and Left-Right Axis Determination during Mouse and *Xenopus* Embryogenesis". *PLoS One*, Vol. 5, Issue 2
- Bertrand S., Aldea D., Oulion S., Subirana L., de Lera A.R., Somorjai I., Escriva H. (2015). "Evolution of the Role of RA and FGF Signals in the Control of Somitogenesis in Chordates". *PLoS One*, Vol. 10, Issue 9
- Boskovski M.T., Yuan S., Pedersen N.B., goth C.K., Makova S., Clausen H., Brueckner M., Khokha M. K. (2013). "The heterotaxy gene GALNT11 glycosylates Notch to orchestrate cilia type and laterality". *Nature*, Vol. 504, 456 – 459
- Bouman A., Waisfisz Q., Admiraal J., van de Loo M., van Rijn R.R., Micha D., Oostra R., Mathijssen I.B. (2018). "Homozygous DMRT" variant associates with severe rib malformations in a newborn". *American Journal of Medical Genetics Part A*, Vol. 176, Issue 5, 1216-1221
- Bowes J.B., Snyder K.A., Segerdell E., Jarabek C.J., Azam K., Zorn A.M., Vite P.D. (2010). "Xenbase: gene expression and improved integration". *Nucleic acids research*, Vol. 38 (suppl) 1, 607-612
- Brend T., Holley S.C. (2009). "Balancing segmentation and laterality during vertebrate development". *Seminars in Cell & Developmental Biology*, Vol. 20, 472–478
- Burtis K.C., Baker B.S. (1989). "Drosophila doublesex Gene Controls Somatic Sexual Differentiation by Producing Alternatively Spliced mRNAs Encoding Related Sex-Specific Polypeptides". *Cell* Vol. 56, 997 – 1010
- Chapman D.L., Agulnik I., Hancock S., Silver L.M., Papaioannou V.E. (1996). "Tbx6, a mouse T-Box gene implicated in paraxial mesoderm formation at gastrulation". *Developmental Biology*, Vol. 180, Issue 2. 534-542
- Chazaud C., Chambon P., Dolle P. (1999). "Retinoic acid is required in the mouse embryo for left-right asymmetry determination and heart morphogenesis". *Development*, Vol. 126, 2589-2596
- Cheng A.M., Thisse B., Thisse C., Wright C.V. (2000). "The lefty-related factor Xatv acts as a feedback inhibitor of nodal signaling in mesoderm induction and L-R axis development in *Xenopus*". *Development*, Vol. 127, 1049 – 1061
- Collignon J., Varlet I., Robertson E.J. (1996). "Relationship between asymmetric nodal expression and the direction of embryonic turning". *Nature*, Vol. 381, 155-158.
- Coschigano K.T., Wensink P.C. (1993). "Sex-specific transcriptional regulation by the male and female doublesex proteins of *Drosophila*". *Genes & Development*, Vol. 7, 42 – 54
- Deprez M., Zaragosi L., Truchi M., Ruiz Garcia S., Arguel M., Lebrigrand K., Paquet A., Peer D., Marquette C., Leroy S., Barbry P. (2020). "A single-cell atlas of the human healthy airways". *bioRxiv preprint*
- Dosch R., Gawantka V., Delius H., Blumenstock C., Niehrs C. (1997). "Bmp-4 acts as a morphogen in dorsoventral mesoderm patterning in *Xenopus*". *Development* 124, 2325 – 2334
- Erdman S.E., Burtis K.C. (1993). "The *Drosophila* doublesex proteins share a novel zinc finger related DNA binding domain". *The EMBO Journal*, Vol. 12, No. 2, 527 – 535
- Erdman S.E., Chen H.J., Burtis K.C. (1996). "Functional and genetic characterization of the oligomerization and DNA binding properties of the *Drosophila* doublesex proteins". *Genetics*, Vol. 144, Issue 4, 1639-1652
- Fletcher R.B., Harland R.M. (2008). "The role of FGF signaling in the establishment and maintenance of mesodermal gene expression in *Xenopus*". *Developmental Dynamics* 237, 1243 - 1254
- Fraidenraich D., Iwahori A., Rudnicki M., Basilico C. (2000). "Activation of fgf4 gene expression in the myotomes is regulated by myogenic bHLH factors and by sonic hedgehog". *Developmental Biology*, Vol. 225, 392 – 406
- Gensch N., Borchardt T., Schneider A., Riethmacher D., Braun T. (2008). "Different autonomous myogenic cell populations revealed by ablation of Myf5-expressing cells during mouse embryogenesis". *Development*, Vol. 135, 1597-1604
- Glinka A., Delius H., Blumenstock C., Niehrs C. (1998). "Combinatorial signalling by Xwnt-11 and Xnr3 in the organizer epithelium". *Mechanism of development*, Vol. 60, Issue 2, 221-231
- Gourronc F., Ahmad N., Nedza N., Eggleston T., Rebagliati M. (2007). "Nodal activity around Kupffer's vesicle depends on the T-box transcription factors notail and spadetan and on notch signaling". *Developmental Dynamics*, Vol. 236, 2131 – 2146
- Grass S., Arnold H.H., Braun T. (1996). "Alterations in somite patterning of Myf-5-deficient mice; a possible role for FGF-4 and FGF-6". *Development* 122, 141 - 150

- Hadjantonakis A., Pisano E., Papaioannou V.E. (2008). "Tbx6 regulates left/right patterning in mouse embryos through effects on nodal cilia and perinodal signaling". *PLoS One*, Vol. 3, Issue 6
- Hamada H., Tam P.P.L. (2014). "Mechanisms of left-right asymmetry and patterning: driver, mediator and responder". *F1000Prime Reports*
- Han W.T., Marlow L.A., von Roemeling C.A., Cooper S.J., Kreinest P., Wu K., Luxon B.A., Sinha M., Anastasiadis P.Z., Copland J.A. (2010). "Pathway Signature and Cellular Differentiation in Clear Cell Renal Cell Carcinoma". *PLoS One*, Vol. 5, Issue 5
- Hashimoto H., Rebagliati M., Ahmad N., Muraoka O., Kurokawa T., Hibi M., Suzuki T. (2004). "The Cerberus/Dan-family protein Charon is a negative regulator of Nodal signaling during left-right patterning in zebrafish". *Development*, Vol. 137, 1741 – 1753
- Huang S., Ma J., Liu X., Zhang Y., Luo L. (2011). "Retinoic Acid Signaling Sequentially Controls Visceral and Heart Laterality in Zebrafish". *The Journal of Biological Chemistry*, Vol. 286, No. 32, 28533-28543
- Janesick A., Tang W., Shioda T., Blumberg B. (2018). "RAR γ is required for mesodermal gene expression prior to gastrulation in *Xenopus*". *Development*, Vol. 145, Issue 18
- Jones C.M., Armes N., Smitz J.C. (1996). "Signalling by TGF-beta family members: short-range effects of Xnr-2 and BMP-4 contrast with the long-range effects of activating". *Current Biology*, Vol.6, Issue 11, 1468 – 1475
- Kajikawa E., Horo U., Ide T., Mizuno K., Minegishi K., Hara Y., Ikawa Y., Nishimura H., Uchikawa M., Kiyonari H., Kuraku S., Hamada H. (2020). "Nodal paralogues underlie distinct mechanisms for visceral left-right asymmetry in reptiles and mammals". *Nature Ecology & Evolution*, Vol. 2, 261-269
- Kawakami Y., Raya Á., Raya R.M., Rodríguez-Esteban C., Belmonte J.C.I. (2005). "Retinoic acid signalling links left-right asymmetric patterning and bilaterally symmetric somitogenesis in the zebrafish embryo". *Nature* Vol. 435
- Kitajima K., Oki S., Ohkawa Y., Sumi T., Meno C. (2013). "Wnt signaling regulates left-right axis formation in the node of mouse embryo". *Developmental Biology*, Vol. 380, Issue 2, 222-232
- Krebs L.T., Iwai N., Nonaka S., Welsh I.C., Lan Y., Jiang R., Saijoh Y., O'Brien T.P., Hamada H., Gridley T. (2003). "Notch signaling regulates left-right asymmetry determination by inducing Nodal expression". *Genes & development*, Vol. 17, Issue 10, 1207-1212
- Levin M., Johnson R.L., Sterna C.D., Kuehn M., Tabin C. (1995). "A molecular pathway determining left-right asymmetry in chick embryogenesis". *Cell*, Vol. 82, 803 – 814
- Li H.Y., Bourdelas A., Carron C., Gomez C., Boucaut J.C., Shi D.L. (2006). "FGF8, Wnt8 and Myf5 are target genes of Tbx6 during anteroposterior specification in *Xenopus* embryo". *Developmental Biology* 290, 470 - 481
- Lin A.E., Krikov S., Riehle-Colarusso T., Frías J.L., Belmont J., Anderka M., Geva T., Getz K.D., Botto L.D., National Birth Defects Prevention Study (2014). "Laterality Defects in the National Birth Defects Prevention Study (1998-2007): Birth Prevalence and Descriptive". *American Journal of medical genetics*, Vol. 164, Issue 10, 2581 – 2591
- Liu S., Li Z., Gui J.F. (2009). "Fish-Specific Duplicated *dmt2b* Contributes to a Divergent Function through Hedgehog Pathway and Maintains Left-Right Asymmetry Establishment Function". *PLoS One*, Vol. 4, Issue 9
- Logan M., Pagán-Westphal S.M., Smith D.M., Paganessi L., Tarbin C.J. (1998). "The transcription factor Pitx2 mediates situs-specific morphogenesis in response to left-right asymmetric signals". *Cell*, Vol. 94, Issue 3, 3007 – 317
- Lopes S.S., Lourenço R., Pacheco L., Moreno N., Kreiling J., Saúde L. (2010). "Notch signalling regulates left-right asymmetry through ciliary length control". *Development*, Vol. 137, 3625 – 3632
- Lourenço R., Lopes S., Saúde L. (2010). "Left-right function of *dmt2* genes is not conserved between zebrafish and mouse". *PLoS One*, Vol. 5, Issue 12
- Lowe L.A., Supp D.M., Sampath K., Yokoyama T., Wright C.V.E., Potter S.S., Overbeek P., Kuehn M.R. (1996). "Conserved left-right asymmetry of nodal expression and alterations in murine situs inversus". *Nature*, Vol. 381
- Maguire R.J., Isaacs H.V., Pownall M.E. (2012). "Early transcriptional targets of MyoD link myogenesis and somitogenesis". *Developmental Biology* 371, 256 - 268
- Maroma K., Fainsod A., Steinbeisser H. (1999). "Patterning of the mesoderm involves several threshold response to BMP-4 and Xwnt-8". *Development* 87
- Marques S., Borges A.C., Silva A.C., Freitas S., Cordenonsi M., Belo J.A. (2004). "The activity of the nodal antagonist Cerl-2 in the mouse node is required for correct L/R body axis". *Genes & Development*, Vol. 18, 2342 - 2347
- McGrath J., Somlo S., Makova S., Tian X., Brueckner M. (2003). "Two Populations of Node Monocilia Initiate Left-Right Asymmetry in the Mouse". *Cell*, Vol. 114, Issue 1, 61-73
- Melby A.E., Warga R.M., Kimmel C.B. (1996). "Specification of cell fates at the dorsal margin of the zebrafish gastrula". *Development* 122, 2225-2237

- Meng A., Moore B., Tang H., Yuan B., Lin S. (1999). "A Drosophila doublesex-related gene, terra, is involved in somitogenesis in vertebrates". *Development* 126, 1259-1268
- Meno C., Gritsman K., Ohishi S., Ohfuji Y., Heckscher E., Mochida K., Shimono A., Kondoh H., Talbot W.S., Robertson E.J., Schier A.F., Hamada H. (1999). "Mouse Lefty2 and zebrafish antivin are feedback inhibitors of nodal signaling during vertebrate gastrulation". *Molecular Cell*, Vol. 4, Issue 3, 287 – 298
- Meno C., Shimono A., Saijoh Y., Yashiro K., Mochida K., Ohishi S., Noji S., Kondoh H., Hamada H. (1998). "lefty-1 is required for left-right determination as a regulator of lefty-2 and nodal". *Cell*, Vol. 94, 287 – 297
- Murphy M.W., Zarkower D., Bardwell V.J. (2007). "Vertebrate DM domain proteins bind similar DNA sequences and can heterodimerize on DNA". *BMC Molecular Biology*, Vol. 7, Issue 58
- Nonaka S., Tanaka Y., Okada Y., Takeda S., Harada A., Kanai Y., Kido M., Hirokawa N. (1998). "Randomization of left-right asymmetry due to loss of nodal cilia generating leftward flow of extraembryonic fluid in mice lacking KIF3B motor protein". *Cell*, Vol. 95, 829 – 837
- Nonaka S., Yoshida S., Watanabe D., Ikeuchi S., Goto T., Mashall W.F., Hamada H. (2005). "De novo formation of left-right asymmetry by posterior tilt of nodal cilia". *PLoS Biology*, Vol. 3, Issue 8
- Ohkawara B., Iemura S., ten Dijke P., Ueno N. (2002). "Action range of BMP is defined by its N-terminal basic amino acid core". *Current Biology*, Vol.12, Issue 3, 205 - 209
- Okada Y., Takeda S., Tanaka Y., Belmonte J.I., Hirokawa N. (2005). "Mechanism of nodal flow: a conserved symmetry breaking event in left-right axis determination". *Cell*, Vol. 121, 633 – 644
- Oteiza P., Köppen M., Concha M.L., Heisenberg C.P. (2008). "Origin and shaping of the laterality organ in zebrafish". *Development*, Vol. 135, 2807 – 2813
- Otto A., Pieper T., Viebahn C., Tsikolia N. (2014). "Early Left-Right Asymmetries During Axial Morphogenesis in the Chick Embryo". *Genesis*, Vol. 52, 614-625
- Ottolenghi C., Veitia R., Barbieri M., Fellous M., McElreavey K. (2000). "The Human Doublesex-Related Gene, *DMRT2*, Is Homologous to a Gene Involved in Somitogenesis and Encodes a Potential Bicistronic Transcript". *Genomics*, Vol. 64, 179 – 186
- Önup K., Uibo O., Zordania R., Kiho L., Ilus T., Öiglane-Shlik E.O., Bartsch O. (2004). "Three Patients With 9p Deletions Including *DMRT1* and *DMRT2*: A Girl With XY Complement, Bilateral Ovaries, and Extreme Growth Retardation, and Two XX Females With Normal Pubertal Development". *American Journal of Medical Genetics*, Vol. 130a, Issue 4, 415-423
- Parlier D., Moers V., Van Campenhout C., Preillon J., Leclère L., Saulnier A., Sirakov M., Busengdal H., Kricha S., Marine J.C., Rentzsch F., Bellefroid E.J. (2013). "The *Xenopus* doublesex-related gene *Dmrt5* is required for olfactory placode neurogenesis". *Developmental Biology*, Vol. 373, Issue 1, 39 – 52
- Pinto R.A., Almeida-Santos J., Lourenço R., Saúde L. (2018). "Identification of *Dmrt2a* downstream genes during zebrafish early development using a timely controlled approach". *BMC Developmental Biology*
- Polli M., Amaya E. (2002). "A study of mesoderm patterning through the analysis of the regulation of *Xmyf-5* expression". *Development* 129, 2917 - 2927
- Przemeck G.K., Heinzmann U., Beckers J., Hrabé de Angelis M. (2003). "Node and midline defects are associated with left-right development in *Delta1* mutant embryos". *Development*, Vol. 130, 3 – 13
- Raya A., Kawakami Y., Rodríguez-Esteban C., Büscher D., Koth C.M., Itoh T., Morita M., Raya R.M., Dubova I., Bessa J. G., de la Pompa J.L., Izpisua Belmonte J. C. (2003). "Notch activity induces Nodal expression and mediates the establishment of left-right asymmetry in vertebrate embryos". *Genes & Development*, Vol. 17, 1213 - 1218
- Raymond C.S., Shamu C.E., Shen M.M., Seifert K.J., Hirsch B., Hodgkin J., Zarkower D. (1998). "Evidence for evolutionary conservation of sex-determining genes". *Nature*, Vol. 391
- Rowton M., Ramos P., Anderson D.M., Rhee J.M., Cunliffe H.E., Rawls A. (2013). "Regulation of Mesenchymal-to-Epithelial Transition by *PARAXIS* During Somitogenesis". *Developmental Dynamics*, Vol. 242, 1332-1344
- Sakano D., Kato A., Parikh N., McKnight K., Terry D., Stefanovic B., Kato Y. (2010). "BCL6 canalizes Notch-dependent transcription, excluding Mastermind-like1 from selected target genes during left-right patterning". *Developmental Cell*, Vol. 16, 450 – 462
- Sato T., Rocancourt D., Marques L., Thorsteindóttir S., Buckingham M. (2010). "A *Pax3/Dmrt2/Myf5* Regulatory Cascade Functions at the Onset of Myogenesis". *PLoS Genetics*, Vol. 6, Issue 4
- Saúde L., Lourenço R., Gonçalves A., Palmeirim I. (2005). "*terra* is a left-right asymmetry gene required for left-right synchronization of the segmentation clock". *Nature Cell Biology*, Vol. 7, No. 9
- Saund R.S., Kanai-Azuma M., Kanai Y., Kim I., Lucero M.T., Saijoh Y. (2012). "Gut endoderm is involved in the transfer of left-right asymmetry from the node to the lateral plate mesoderm in the mouse embryo". *Development*, Vol. 139, Issue 13, 2426-2435

- Schneider I., Kreis J., Schweickert A., Blum M., Vick P. (2019). "A dual function of FGF signaling in *Xenopus* left-right axis formation". *Development* 146
- Schröder S.S., Tsikolia N., Weizbauer A., Hue I., Viebahn C. (2015). "Paraxial Nodal Expression Reveals a Novel Conserved Structure of the Left-Right Organizer in Four Mammalian Species". *Cells Tissues Organs*, Vol. 201, 77–87
- Schweickert A., Weber T., Beyer T., Vick P., Bogusch S., Feistel K., Blum M. (2007). "Cilia-driven leftward flow determines laterality in *Xenopus*". *Current Biology*, Vol. 17, 60 – 66
- Schweickert A., Vick P., Getwan M., Weber T., Schneider I., Eberhardt M., Beyer T., Pachur A., Blum M. (2010). "The Nodal Inhibitor *Coco* Is a Critical Target of Leftward Flow in *Xenopus*". *Current Biology*, Vol.20, 738 – 743
- Sempou E., Lakhani O.A., Amalray S., Khokha M.K. (2018). "Candidate Heterotaxy Gene *FGFR4* Is Essential for Patterning of the Left-Right Organizer in *Xenopus*". *Frontiers in Physiology*, Vol. 9, Article 1705
- Seo K.W., Wang Y., Kokubo H., Kettlewell J.R., Zarkower D.A., Johnson R.L. (2006). "Targeted disruption of the DM domain containing transcription factor *Dmrt2* reveals an essential role in somite patterning". *Developmental Biology* 290
- Shook D.R., Majer C., Keller R. (2004). "Pattern and morphogenesis of presumptive mesoderm in closely related species, *Xenopus laevis* and *Xenopus tropicalis*". *Developmental Biology* 270, 163 – 185
- Sirbu I.O., Duester G. (2006). "Retinoic-acid signalling in node ectoderm and posterior neural plate directs left-right patterning of somitic mesoderm". *Nature Cell Biology*, Vol. 8, Issue 3, 271-277
- Smith J.C. (1995). "Mesoderm-inducing factors and mesodermal patterning". *Current opinion in cell biology*, Vol. 7 Issue 6. 856-861
- Soukup V., Yong L.W., Lu T., Huang S., Kozmik Z., Yu J. (2015). "The Nodal signaling pathway controls left-right asymmetric development in amphioxus". *EvoDevo*, Vol. 6
- Stubbs J.L., Belmonte J.C., Kintner C. (2008). "The forkhead protein *Foxj1* specifies node-like cilia in *Xenopus* and zebrafish embryos". *Nature Genetics*, Vol. 40, Issue 12, 1454-1460
- Sutherland M.J., Ware S.M. (2009). "Disorders of Left-Right Asymmetry: Heterotaxy and Situs Inversus". *American Journal of Medical Genetics Part C (Seminars in Medical Genetics)*, 307-317
- Takao D., Nemoto T., Abe T., Kiyonari H., Kajjura-Kobayashi H., Shiratori H., Nonaka S. (2013). "Asymmetric distribution of dynamic calcium signals in the node of mouse embryo during left-right axis formation". *Developmental Biology*, Vol 376, Issue 1, 23-30
- Tallquist D., Weismann K.E., Hellström M. (2000). "Early myotome specification regulates *PDGFA* expression and axial skeleton development". *Development* 127, 5059 - 5070
- Tavares B., Jacinto R., Sampaio P., Pestana S., Pinto A., Vaz A., Roxo-Rosa M., Gardner R., Lopes T., Schilling B., Henry I., Saúde L., Lopes S.S. (2017). "Notch/Her12 signalling modules motile/immotile cilia ratio downstream of *Foxj1a* in zebrafish left-right organizer". *eLife*, Vol. 6
- Tingler M., Kurz S., Maerker M., Ott T., Fuhl F., Schweickert A., LeBlanc-Straceski, Noselli S., Blum M. (2018). "A Conserved Role of the Unconventional *Myosin1d* in Laterality Determination". *Current Biology*, Vol. 28
- Vermot J., Pourquié O. (2005). "Retinoic acid coordinates somitogenesis and left-right patterning in vertebrate embryos". *Nature*, Vol. 435, 215-220
- Vick P., Kreis J., Schneider I., Tingler M., Getwan M., Thumberger T., Beyer T., Schweickert A., Blum M. (2018). "An Early Function of *Polycystin-2* for Left-Right Organizer Induction in *Xenopus*". *iScience* Vol. 27, Issue 2, 76-85
- Volff J., Zarkower D., Bardwell V.J., Schartl M. (2003). "Evolutionary Dynamics of the DM Domain Gene Family in Metazoans". *Journal of Molecular Evolution*, Vol. 57, 241-249
- Vonica A., Brivanlou A.H. (2007). "The left-right axis is regulated by the interplay of *Coco*, *Xnr1* and *derrière* in *Xenopus* embryos". *Developmental Biology*, Vol. 303, 281 – 294
- Walentek P., Schneider I., Schweickert A., Blum M. (2013). "Wnt11b is involved in cilia-mediated symmetry breakage during *Xenopus* left-right development". *PLoS ONE* 8, e73646
- Watabe-Rudolph M., Schlautmann N., Papaioannou V.E., Gossler A. (2002). "The mouse rib-vertebrae mutation is a hypomorphic *Tbx6* allele". *Mechanism of Development*, Vol. 119, Issue 2, 251-256
- White P.H., Farkas D.R., McFadden E.E., Chapman D.L. (2003). "Defective somite patterning in mouse embryos with reduced levels of *Tbx6*". *Development*, Vol. 130, 1681-1690
- Yamanaka Y., Tamplin O.J., Beckers A., Gossler A., Rossant J. (2007). "Live Imaging and Genetic Analysis of Mouse Notochord Formation Reveals Regional Morphogenetic Mechanisms". *Developmental Cell*, Vol. 13, 884–896

Yoshida, S., Shiratori, H., Kuo, I.Y., Kawasumi, A., Shinohara, K., Nonaka, S., Asai, Y., Sasaki, G., Belo, J.A., Sasaki, H., Nakai, J., Dworniczak, B., Ehrlich, B.E., Pennekamp, P., Hamada, H., (2012). "Cilia at the node of mouse embryos sense fluid flow for left-right determination via Pkd2". *Science*, Vol. 338, 226–231

Yoshioka H., Meno C., Koshida K., Sugihara M., Itoh H., Ishimaru Y., Inoue T., Ohuchi H., Semina E.V., Murray J.C., Hamada H., Noji S. (1998). "Pitx2, a bicoid-type homeobox gene, is involved in a lefty-signaling pathway in determination of left-right asymmetry". *Cell*, Vol. 94, Issue 3, 299 – 305

Yuan S., Zhao L., Brueckner M., Sun Z. (2015). "Intraciliary Calcium Oscillations Initiate Vertebrate Left-Right Asymmetry". *Current Biology*, Vol. 25, 556-567

Zhang J. (2003). "Evolution by gene duplication: an update". *Trends in Ecology & Evolution*, Vol. 18, Issue 6, 292 – 298

Zhou X., Li Q., Lu H., Chen H., Guo Y., Cheng H., Zhou R. (2008). "Fish specific duplication of Dmrt2: Characterization of zebrafish Dmrt2b". *Biochimie*, Vol. 90, Issue 6, 878 – 887

Supplemental Information

dmrt2* and *myf5* link early somitogenesis to left-right axis determination in *Xenopus laevis

Melanie Tingler, Axel Schweickert, Martin Blum

University of Hohenheim, Garbenstr. 30, 70599 Stuttgart, Germany

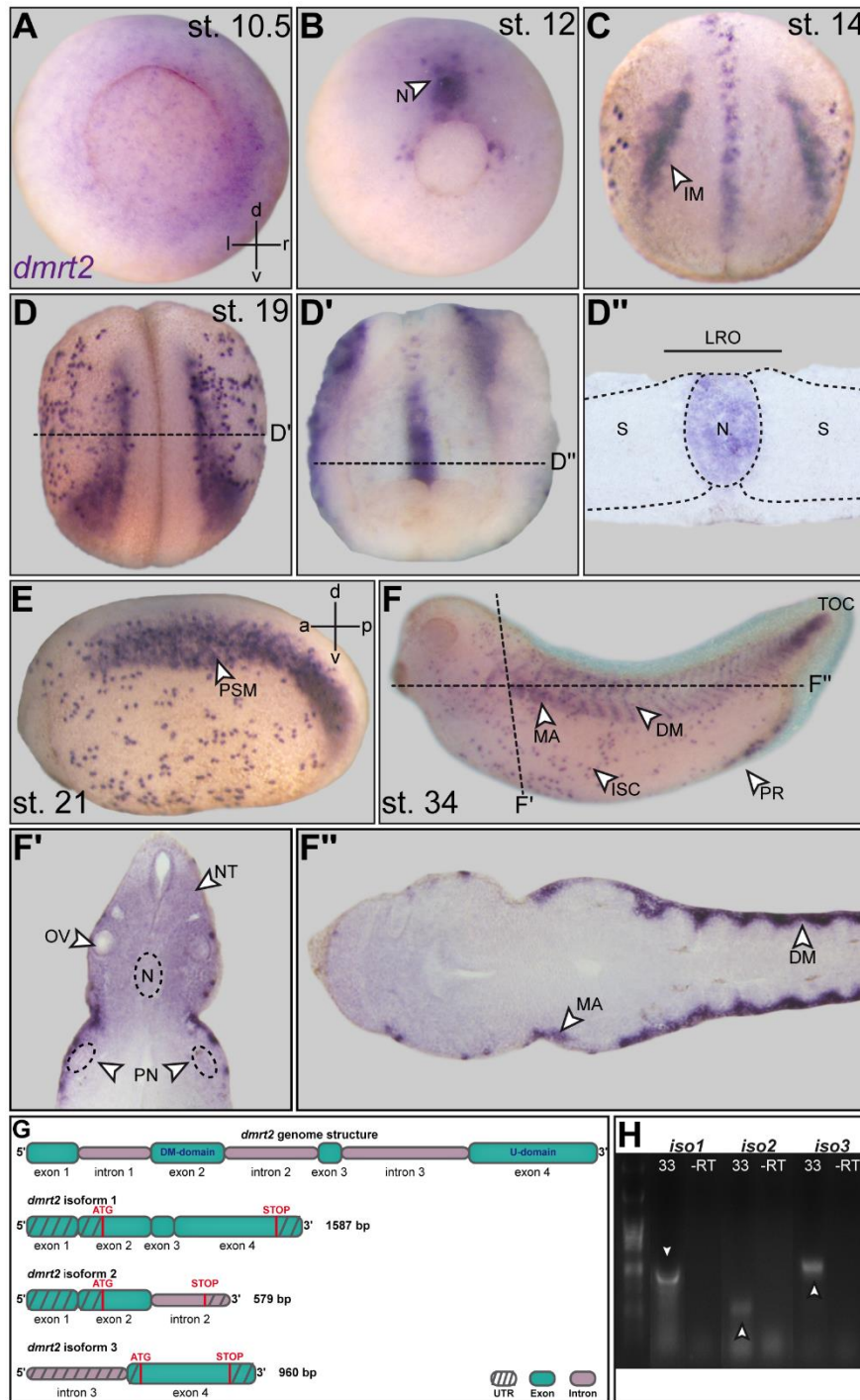


Figure S1: Expression analysis of *dmrt2* during *Xenopus* development

RNA *in situ* hybridization was conducted using a full length *dmrt2* probe. *dmrt2* showed no maternal expression and was first detectable in early gastrula stage embryos in the mesoderm surrounding the blastoporus (**A**). During the course of gastrulation, *dmrt2* got restricted to the elongating notochord (**B**) and the intermediate mesoderm attached to the PSM with onset of neurulation (**C**, **D**). Furthermore expression started in a subset of epidermal cells. Hemi-sections (**D'**) of late neurula stage embryos (**D**) displayed *dmrt2* expression in the posterior part of the notochord. Transversal sections demonstrated that the expression was part of the flow-generating LRO cells (**D''**). At early tailbud stages, *dmrt2* was detected in the PSM region and the epidermis (**E**). In late tailbuds,

stage 34 (**F**) the expression was pronounced to the muscle anlagen, the dermomyotom (**F'**), the tail organizing center and the proctodaeum (**F**).

(**G**) The genomic structure of *dmrt2* consists of 4 exons and 3 introns. By alternative splicing or via an alternative transcriptional start site, 3 different isoforms are made. The full length isoform, *isoform 1*, contains all 4 exons with the DNA-binding domain (DM-domain) in exon 2 and the U-domain in exon 4. In contrast, the second isoform, *isoform 2*, has an extended exon 2 with a distinct stop codon. The third isoform, *isoform 3*, has an alternative start-codon in the 4th exon and may lack upstream exons.

(**H**) PCR-analysis of oligo-dTT cDNA from st. 33 embryos displayed that all isoforms were expressed in *Xenopus laevis*. Concerning the specific primer we used, we identified a 822bp fragment specific for *isoform 1*, a 506bp fragment specific for *isoform 2* and a 1028bp fragment specific for *isoform 3*.

a=anterior; d=dorsal; DM=dermomyotom; IM=intermediate mesoderm; ISC=ion-secreting cells; l=left; LRO=left-right organizer; MA=muscle anlagen; N=notochord; NT=neural tube; OV=optic vesicle; p=posterior; PN=pronephric tubule; PR=proctodaeum; PSM=presomitic mesoderm; r=right; - RT=without reverse transcriptases; S=somite TOC=tail organizing center;

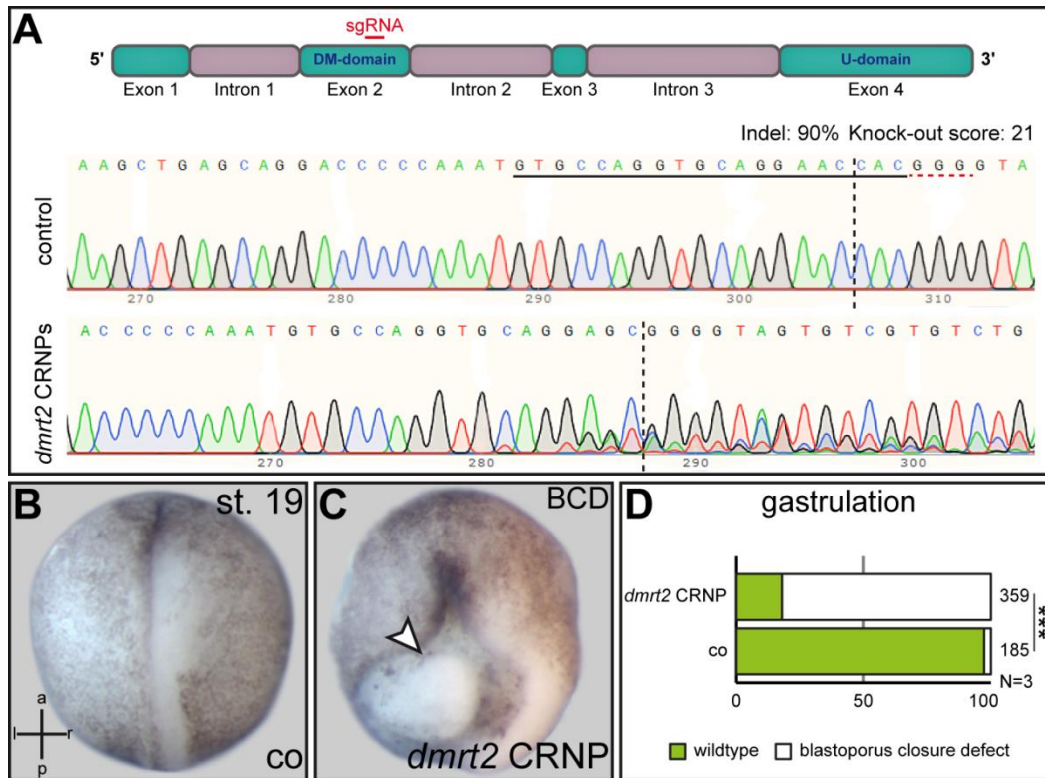


Figure S2: *dmrt2* crispants had severe gastrulation defects

CRISPR/Cas9 mediated genome editing of *dmrt2* showed a high cutting efficiency of 90 % but a low KO score of 24 % (A). Cultivating crispants to late stages (B) was no possible as they displayed severe gastrulation defects (C) in about 75 % of the embryos (D).

Black line in (A) marks the sequence of the sgRNA. Red dotted line represents the PAM (GGG) sequence for Cas9 and the vertical black dotted line the position of the double-strand breakage. BCD=blastoporus closure defect; co=control; CRNP=Cas ribonucleoprotein;

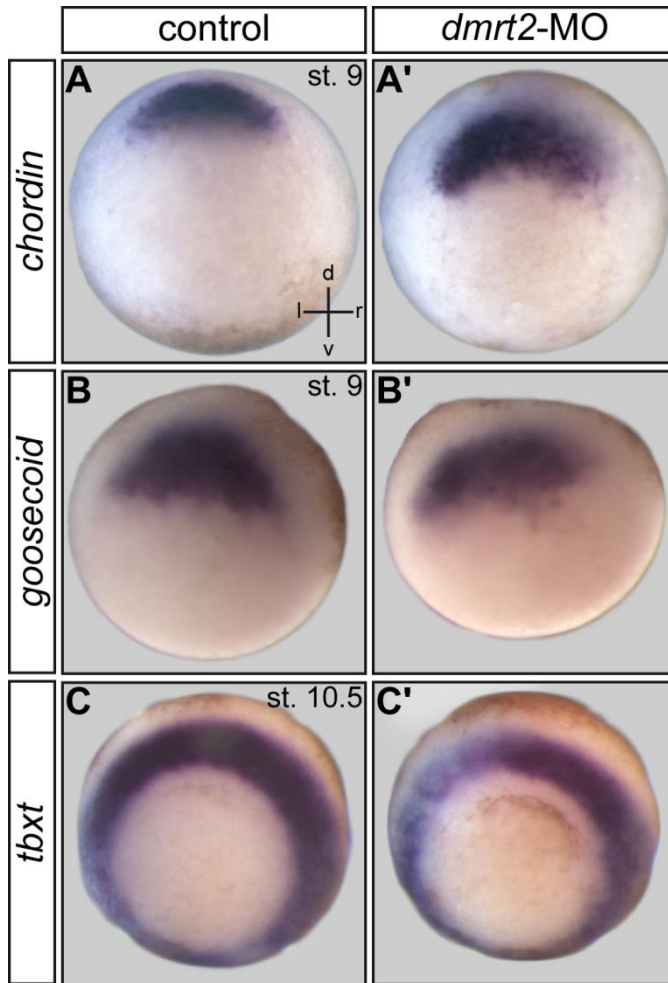


Figure S3: Early organizer and mesodermal marker genes were not affected in *dmrt2* morphants
The Spemann Organizer marker genes *chordin* (**A**) and *goosecoid* (**B**) were not perturbed in *dmrt2* morphants (**A'**, **B'**). Also, specification of the mesoderm analyzed by the expression of *tbxt* (**C**) was not influenced by the loss of *dmrt2* (**C'**).

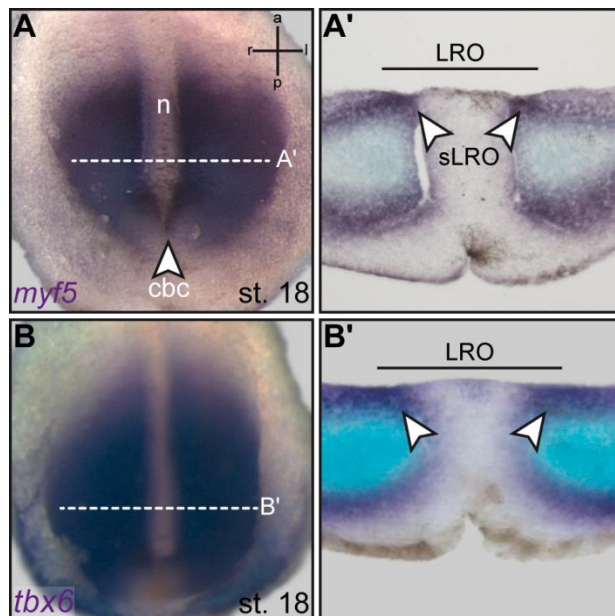


Figure S4: *myf5* and *tbx6* are expressed in sLRO cells

In situ hybridization for *myf5* (**A**) and *tbx6* (**B**) showed that both were expressed in the posterior presomitic mesoderm in neurula stage (st. 18) embryos. Transversal sectioning demonstrated that *myf5* (**A'**) and *tbx6* (**B'**) expression was restricted to the presomitic mesoderm, including the lateral sLRO cells. cbc=circular blastoporal collar; LRO=left-right organizer; sLRO=sensory left-right organizer;

Discussion

The generation of a bilateral symmetric organism requires the correct establishment and development of the three main body axes. In *Xenopus*, the DV-axis is determined by the sperm entry point and gets established during gastrulation. This depends on the action of the SO that represents the primary body axis signaling center. Gastrulation puts the three germ layers in their final position for further differentiation. Therefore, it is important that PCP driven gastrulation movements translocate the head organizer to the prospective anterior region of the embryo. This allows defined head and tail formation and generates the AP axis. Gastrulation also creates the gastrocoelic lumen, the place where the left-right organizer (LRO) is established.

The early function of *gooseoid*: establishment of the dorsoventral and anteroposterior axis by intervening with PCP signaling

Previous studies demonstrated that the loss of *gsc* function in mice and *Xenopus* had no impact on early developmental processes what compromised the early function of *gsc* in the SO (Rivera-Perez et al., 1995; Yamada et al., 1995; Sander et al., 2007). Interestingly, the *gsc* gain of function (GOF) with a vertebrate construct strongly affected gastrulation and neurulation in *Xenopus* embryos, while *Drosophila gsc* was only capable for primary axis induction (Ulmer 2008, Ulmer 2012). These observations elevated the presumption that the vertebrate *gsc* obtained a new function during evolution by regulating PCP signaling.

In the present study, we could confirm an inhibitory mechanism of Gsc on the PCP signaling pathway. Several experimental approaches which included *gsc* misexpression in different tissues that undergo PCP dependent CE demonstrated that these processes were inhibited in the presence of Gsc. Keller open face explants failed to elongate and blastoporus as well as neural tube closure was compromised. Additionally, membrane-recruitment of Dishevelled 2 (Dvl2), an intracellular component of the Wnt/PCP pathway, was cell-autonomously inhibited by Gsc, demonstrating that Gsc negatively influences PCP signaling. Rescue experiments by overexpressing components of the core PCP pathway or by *tbxt* or *wnt11b* approved this hypothesis. The results further explained late developmental defects seen in *gsc*

morphants *in vivo*. Depletion of Gsc in *Xenopus* led to severe head malformations that were attributed to prechordal plate (PP) and cartilage defects. This impaired separation of the eye field and the elongation and condensation of the ceratohyale and Meckel's cartilage. Recent studies by Blitz and colleagues confirmed these observations in *Xenopus tropicalis* as *gsc* mutant tadpoles showed a dramatical loss of head structures (Blitz et al. 2016). Interestingly, *gsc* KO mice showed that in the inner ear the PCP dependent alignment of the cortical hair cells' stereocilia was disturbed in a non-cell autonomously fashion. Sequence comparison of Gsc from invertebrates and vertebrates identified two novel domains. These domains are closely attached to the homeodomain (HD) and are vertebrate specific. The function of these domains remains unclear but it is likely that they are responsible for the interaction of Gsc with the PCP pathway, as these structural and functional features of Gsc arose within vertebrates. Analysis if these domains recruit Gsc directly or in combination with several co-factors to novel target genes that act upstream or parallel to PCP signaling would be insightful.

This study is in agreement with the early expression pattern of *gsc* and elucidated its early function. At the beginning of gastrulation *gsc* is expressed in the SO and has a short timeframe of overlapping expression with *tbxt* (Artinger et al., 1997). This rapidly changes as Gsc represses *tbxt* and in turn segregates the axial mesoderm into the head (prechordal plate; PP) and trunk (notochord) mesoderm (Artinger et al., 1997; Boucher et al., 2000; Latinkic & Smith, 1999). Consequently, Gsc restricts *tbxt* expression to notochord where *Tbxt* induces the Wnt/PCP ligand *wnt11b* (Conlon & Smith, 1999; Tada & Smith, 2000). This mediates thinning and lengthening of the embryo by PCP-mediated CE of the notochord. In contrast, in the *gsc*-positive cells of the PP, PCP signaling is prevented and single cell migration enabled, allowing the AP- and DV-axis to form.

Myosin1d links an ancestral symmetry breaking mechanism to the newly evolved leftward-flow

A novel regulator in the field of PCP signaling and LR axis determination is the unconventional Myosin1d (Myo1d). Myo1d is an Actin-based motor protein that led to disturbed Vangl1 localization and ciliation defects in tracheal and ependymal cells of KO rats, demonstrating that Myo1d interacts with PCP signaling (Hegan et al., 2015).

Interestingly, in the invertebrate *Drosophila melanogaster*, mutants of the homologous gene *myo31df* depict laterality defects (Spéder et al., 2006). These observations were exiting, as *Drosophila* represents a basal bilateral symmetric model organism of the ecdysozoa that harbors no leftward-fluid flow and no asymmetric Nodal signaling. The arrangement of the inner tubular organs in *Drosophila* is induced by the intrinsic chirality of the actomyosin cytoskeleton that initiates dextral rotation of the genital plate and the hindgut (Hozumi et al., 2006; Spéder et al., 2006; Juan et al., 2018).

In *myo1d* mutants the counterclockwise sinistral rotation was predominant and led to complete *situs inversus*. This highlighted that *myo1d* in *Drosophila* acts like *inversin* (*iv*) in the mouse and represents the second identified *situs inversus* gene (Spéder et al., 2006). The underlining mechanism requires the interaction of Myo1d with adherens junctional components like β -catenin and cadherins that leads to PCP-mediated rotation (Spéder et al., 2006; Petzoldt et al., 2012; González-Morales et al., 2015).

Like *Drosophila*, several model organisms that lack cilia use the cytoskeleton for symmetry breakage suggesting an important role for the cytoskeletal organization in the ancestral machinery of laterality determination. Predominant examples can be found along all phyla and are well studied in snails, annelids or the chick. In the freshwater snail *Lymnaea stagnalis* shell coiling defines the LR body axis. This occurs without a classical LRO and is regulated by the cytoskeleton dynamic at early cleavage stages (Shibazaki et al., 2004; Kuroda 2014). Maternal *formin* mRNA might be crucial for this dynamics (Davison et al., 2016; Kuroda et al., 2016). Formin interacts with actin filaments, orients the spindle apparatus and thereby regulates spiral cleavage between the 3rd to 5th cell division (Goode & Eck, 2007; Davison et al., 2016; Kuroda et al., 2016; Abe & Kuroda 2019). This determines the handedness of shell coiling later on by activating Nodal signaling (Grande & Patel, 2009). In comparison, in birds like the chick, symmetry breakage occurs without a cilia-mediated leftward-fluid flow and is interceded by leftward rotation of Hensen's node, the chick LRO (Cui et al., 2009; Gros et al., 2009). Even this cellular rearrangement requires a cytoskeleton dynamic that leads to the activation of the Nodal signaling cascade on the left-side and determines organ chirality in the chick.

The studies in *Drosophila* demonstrated that *myo1d* is a gene of the ancestral symmetry breaking mechanism by interacting with the actin cytoskeleton. It is highly conserved across the animal kingdom and studying *myo1d* function during LR determination in snails or chick would be of high interest. To achieve insights into a

possible conservation of *myo1d* in laterality determination in vertebrates we asked whether *myo1d* affects organ handedness in *Xenopus laevis* and interferes with the cytoskeleton.

Several loss of function approaches using morpholino-mediated KD and CRISPR/Cas9-mediated KO of *myo1d* in *Xenopus* confirmed that *myo1d* acts during LR establishment and PCP signaling. Thus Myo1d regulates laterality, which is conserved between flies and frogs. The reduction of Myo1d activity strongly impaired PCP-mediated processes. Neural tube closure was delayed and the LRO exhibited severe morphological defects. The cells of the LRO had an enlarged apical surface accompanied by shortened and non-polarized cilia. These morphological defects compromised the directionality and velocity of the leftward flow and led to laterality defects in morphant tadpoles. Epistatic experiments with the core PCP protein VanGogh-like 2 (Vangl2) demonstrated that the defects can be directly linked to an interaction of Myo1d with PCP signaling.

Coincident, studies performed in zebrafish by our collaborator Stéphané Noselli corroborated our findings further confirming the conservation of *myo1d* function in laterality determination (Juan et al., 2018).

This work showed that the ancestral symmetry breaking mechanism is evolutionary linked to the newly evolved leftward flow by the interaction of Myo1d with the cytoskeleton.

Myosin1d and symmetry breakage: a cytoskeletal function in laterality determination besides PCP signaling?

The present study pointed out that laterality defects after *myo1d* depletion depended on defective PCP signaling in *Xenopus* embryos. Surprisingly, unpublished preliminary experiments implicated that this interaction might be secondary for the impairment of symmetry breakage. We found that loss of *myo1d* function strongly disturbed LR-establishment by specifically targeting the right side of the embryo (Fig. 2A). This is in disagreement with PCP signaling as the underlying cause of the observed laterality defects as flow on the right side is dispensable for symmetry breakage (Vick et al., 2009). Additionally a bilateral symmetric *pitx2* expression was predominant in *myo1d* morphants, what is atypically for PCP-based laterality disturbance as this leads to randomized *pitx2* pattern (Antic et al. 2010). We found that embryos with impaired flow,

by adding methylcellulose to the archenteron, can be rescued upon left-sided *myo1d* loss of function (Fig. 2B). This strongly implicated, that Myo1d may constitute a second flow-dependent target which is repressed like *Dand5*. It remains open what might be the main function of *myo1d* during LR induction.

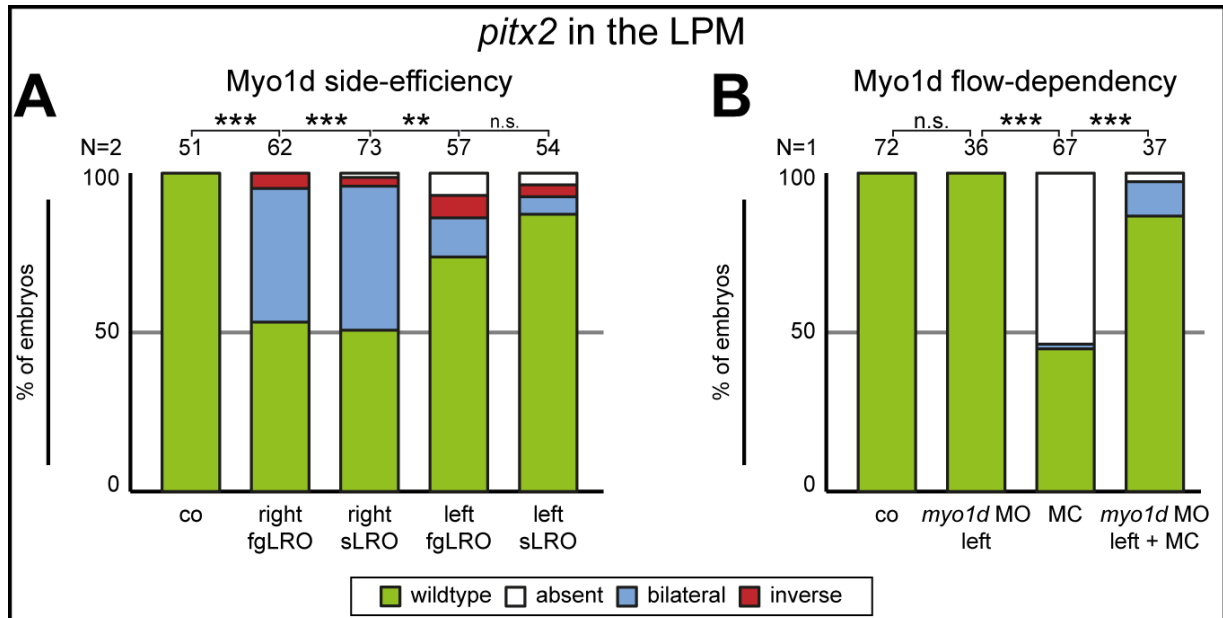


Figure 2: Myo1d is a leftward-fluid flow target.

(A) KD of *myo1d* led to left-right defects regarding the expression of *pitx2* in the LPM. A right-sided loss of function was more efficient than a left-sided one. There was no difference between targeting the right flow-generating fpLRO or the lateral sensory LRO (sLRO) cells. Targeting the fpLRO cells on the left side had a weak impact on *pitx2*, which could be explained by a weak impact on PCP signaling.

(B) Prevention of left-ward flow by adding methylcellulose (MC) to the archenteron led to loss of *pitx2* expression in the LPM. Simultaneously left-sided loss of *myo1d* rescued the laterality defects
fgLRO=flow-generating left-right organizer; MC=methylcellulose; sLRO=sensory left-right organizer;

Based on our new findings we speculate that a missing link between the ca^{2+} influx and the loss of *Dand5* activity is represented by Myo1d. We propose that Myo1d transports *dand5* mRNA to the apical surface in lateral sLRO cells during preflow stages. At the apical side the mRNA of *dand5* is translated and the protein becomes secreted to the extracellular space. The apical release of *Dand5* leads to interaction with *Nodal1* extracellularly and to prevention of *Nodal* signaling on the left and right side. This situation changes due to the leftward flow. Flow becomes sensed on the left margin and leads to ca^{2+} influx via the ciliary axonem. The ca^{2+} influx is recognized by the second messenger molecule Calmodulin (Cam) that in turn binds to the Myo1d light chain that contains two Calmodulin binding motifs (IQ motifs) (Hammer, 1994;

Coluccio, 1997). This binding negatively influences the Myo1d function that might become inactivated or lead to cytoskeletal rearrangement and consequently to loss of apical *dand5* transport. Consequently, *dand5* mRNA becomes enriched basally and apical translation, secretion and extracellular inhibition of Nodal1 is prevented (Fig. 3). There are several indications that are in agreement with our model and can support this idea. First, we identified, that Myo1d seemed to be repressed flow-dependently. Only depletion on the right side led to bilateral symmetric *pitx2* expression, while the gain of function neither on the left nor on the right side had any impact on laterality determination. Moreover, blocking leftward flow that leads to loss of Nodal signaling can be rescued by left-sided reduction of Myo1d.

Next, it was shown in mice that a relocalization of *dand5* mRNA in sLRO cells takes place and is necessary for symmetry breakage. At pre-flow stages *dand5* is distributed along the apical membrane in left and right sensory cells. After the leftward flow, the localization of *dand5* mRNA only on the left side changed and it became enriched basally (Nakamura et al., 2012). This allocation might be explained as many mRNAs become located and translated closely to the place of action (Wilhelm & Vale, 1993; Hesketh, 1996; Kislaukis et al., 1994; Simmonds et al., 2001; St Johnston, 1995; Wilkie & Davis, 2001; Mingle et al., 2005). Additionally, apical protein localization of Dand5 in the mouse node has been reported (Inácio et al., 2013). That Myosins are generally able to transport cargos like proteins or mRNAs, was shown for e.g. the Megalin receptor or the *actin-related protein 2/3* mRNA (Naccache et al., 2006; Hartman & Spudich 2012; Mingle et al., 2005). Finally, *myo1d* constructs that lack the IQ motifs in *Drosophila* were not able to restore the wildtypic situation in *myo1d* mutants. This demonstrated the necessity of the interaction of Cam with Myo1d to regulate its function (Spéder et al., 2006). In addition, the Cam-dependent regulation of Myo1d activity was demonstrated for the rat Myo1d in cell culture experiments. Upon binding of ca^{2+} -activated Cam to Myo1d the ATPases activity of the Myo1d motor domain was inhibited (Köhler et al., 2005). The importance of ca^{2+} for the regulation of Myosin activity was further demonstrated for Myosin1c (Myo1c) in inner hair cells. Due to mechanical disruption, the cell tension in these cells changes and ion channels in stereocilia induce a ca^{2+} influx. Myo1c perceives the tension, interacts with adhesion proteins leading to closure of the ion channels to provide responsiveness to new stimuli. During this process the Myo1c activity itself seems to become regulated through its IQ motifs by the ca^{2+} influx (Siemens et al., 2004; Gillespie & Müller 2009;

Hartman et al., 2011; Zadro et al., 2009; Phillips et al., 2006; Adamek et al., 2008 & 2010). This regulatory mechanism reminds on the situation during flow-sensing in the LRO.

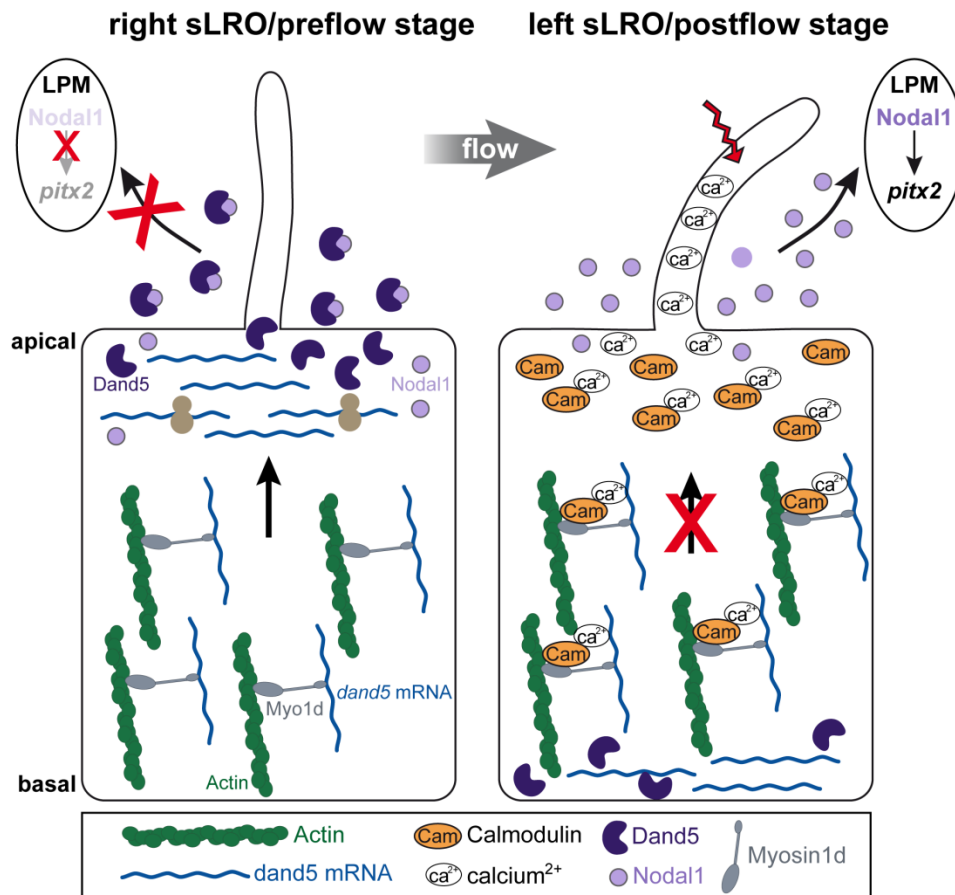


Figure 3: Leftward-flow leads to Ca²⁺-dependent inactivation of apical *dand5* mRNA transport by Myo1d.

In the case of the symmetry breaking event, Myo1d transports the mRNA of *dand5* to the apical surface on the right and left-side of the LRO during preflow-stages. Thereby it admits the apical translation and secretion of Dand5. In turn, Dand5 represses Nodal1 activity in the extracellular space and prevents Nodal signaling. Upon leftward-flow, the bending of cilia on the left side leads to Ca²⁺ influx and to Calmodulin activation. The activated Calmodulin binds to the IQ-motifs of Myo1d and inhibits the transport of *dand5* mRNA to the apical surface. This leads to basal localization of *dand5* mRNA and to the loss of apical translation and secretion. Nodal1 is released of repression, becomes transferred to left lateral plate mesoderm and induces the expression of *pitx2* and thereby asymmetric organ morphogenesis. In contrast, Myo1d is still active on the right side and transports the *dand5* mRNA to the apical surface. As result, Nodal1 is repressed on the right side by Dand5 and the bilateral symmetry has broken by left-sided activation of the Nodal cascade.

In summary we were able to show that the function of Myo1d in symmetry breakage is conserved across the animal kingdom. Based on our new preliminary findings, it has

to be examined in more detail how Myo1d influences symmetry breakage and if this occurs by regulating a spacial change of *dand5* mRNA. Besides the allocation of *myo1d* as the second identified *situs inversus* gene in at least *Drosophila*, we identified Myo1d to be the second identified protein whose function is directly flow-dependent. Our data affirm the hypothesis that Myo1d connects an ancestral cilia-independent mechanism of symmetry breakage to the newly evolved leftward-flow.

Sensory LRO cell fate depends on *myf5* downstream of *dmrt2*

The mechanism of symmetry breakage in most vertebrates requires a directional leftward-fluid flow that becomes sensed by the left marginal cells of the LRO. For the translation of this asymmetrically stimuli it is absolutely essential that the lateral sensory LRO (sLRO) cells are specified and separated from the flow-generating cells. The mechanism behind is less understood and needs further investigations.

Recent studies identified *dmrt2* as another factor to be involved in laterality determination and somitogenesis in zebrafish (Meng et al., 1999; Saude et al., 2005). That these processes are intertwined has been proposed but how they correlate has not been analyzed in more detail. Based on the affiliation of sLRO cells to the somites in *Xenopus* (Shook et al., 2004), it was of high interest if this could link these two processes by *dmrt2* and provide new insights into the origin and specification of the sLRO cells.

In the present work we showed that the function of Dmrt2 is conserved in *Xenopus*. Depletion of *dmrt2* led to frequent laterality defects that could be attributed to a complete loss of the *nodal1* expression domain within the LRO. Analysis of early marker genes depicted that the specification of the SM was disturbed and moreover, the patterning of the paraxial mesoderm (PM) that gives rise to the somites was strongly affected. The loss of the angle-wing like expression pattern of *myf5* in the PM in early gastrulae thereby was of high interest, as this patterning could remark the prospective position of sLRO cells. Surprisingly, LR defects were rescued up on expressing *myf5* in *dmrt2* morphants so that the *nodal1* domain in the LRO was restored. Manipulations of *myf5* confirmed these results as those siblings mimic the *dmrt2* LOF phenotype. Besides *myf5*, also the expression of the t-box gene transcription factor 6, *tbx6*, in the PM was impaired. In turn, co-expressing *tbx6* in *dmrt2* morphants rescued *myf5* and laterality defects.

These results showed that *Dmrt2* is part of the early somitogenic signaling pathway in *Xenopus* by specifying the paraxial mesoderm. It highlighted that this process is crucial for the symmetry breakage event as it induces the flow-perceiving cells of the LRO. Interestingly the emergence of the sLRO cells from the PM seems to be lost during evolution as those cells contribute to the notochord or subchordal cells in mammals like e.g. mice or rabbit (Schröder et al., 2015). This demonstrates that mammals only share the same signaling pathways for both processes while non-mammals further share partially the same morphological structures. It remains unclear why the PM cell fate of the sLRO was lost during the evolution of mammals. To further understand the evolution of sLRO cells and the connection between LR determination and somitogenesis, the analysis of the flow-perceiving cells in several vertebrate model organisms would be insightful

Finally, we found *dmrt2* to become expressed in three putative isoforms that could act stage- and tissue-dependently on regulating target genes in a combinatorial manner. The ability of Dmrt proteins to act as monomers, homo- or heterodimers in mice and the identification of a feedback loop of *dmrt2* in zebrafish suggest a tightly controlled interaction network of *dmrt2* that needs to be investigated in more detail (Murphy et al., 2007; Pinto et al., 2018). Of note, the human *dmrt2* gene encodes for 6 isoforms that are the result of alternative splicing, a bicistronic transcript and an alternatively transcriptional start site in the second intronic region. Therefore it is likely that more isoforms exist in *Xenopus* that could be able to regulate or antagonize the function of each other (Ottolenghi et al., 2000). We speculate that the identified isoforms of *dmrt2* in *Xenopus* regulate different processes that could represent a further explanation how one gene could affect several developmental processes.

In summary, this work enlightened a link between somitogenesis and symmetry breakage in *Xenopus*. It showed that the function of *dmrt2* is conserved in *Xenopus*, where it regulates the specification of the SM axial and the induction of the lateral PM. The lateral downstream activation of *myf5* in the PM is important for the specification of the flow-perceiving LRO cells. This demonstrated for the first time experimentally that early somitogenesis is linked to laterality determination in *Xenopus*.

Conclusion

The present collection functionally characterized the three conserved genes *gsc*, *myo1d* and *dmrt2* during axis determination in *Xenopus laevis*.

The analyzed genes retained their ancestral role during embryonic development and moreover in the case of *gsc* and *dmrt2* these genes gained new functions in the light of evolution.

Across the animal kingdom, the organizer gene *gsc* is able to induce a secondary body axis. By the insertion of the two novel domains that arose within vertebrates *Gsc* achieved a novel function in regulating PCP signaling cell- and non-cell autonomously. A related modification can be observed for *dmrt2*. The ancestral function of *dmrt2* is based on influencing sexual development in invertebrates and vertebrates that is provided by the highly conserved DM-domain. With development of the vertebrates, *dmrt2* attained a novel conserved domain with unknown function. Simultaneously it gained the ability to intervene with somitogenesis suggesting that the new structural and functional features correlate. In the case of *myo1d*, this study highlighted that not only gene function but also their involvement in developmental processes became conserved across the phyla.

References

- Abe M., Kuroda R. (2019). "The development of CRISPR for a mollusk establishes the formin *Lsdia1* as the long-sought gene for snail dextral/sinistral coiling". *Development*, Vol. 146
- Adamek N., Coluccio L.M., Geeves M.A. (2008). "Calcium sensitivity of the cross-bridge cycle of Myo1c, the adaptation motor in the inner ear". *PNAS*, Vol. 105, Issue 15, 5710-5715
- Adamek N., Lieto-Trivedi A., Geeves M.A., Coluccio L.M. (2010). "Modification of loop 1 affects the nucleotide binding properties of Myo1c, the adaptation motor in the inner ear". *Biochemistry*, Vol. 49, Issue 5, 958-971
- Ahrens M.J., Li Y., Jiang H., Dudley A.T. (2009). "Convergent extension movements in growth plate chondrocytes require gpi-anchored cell surface proteins". *Development* 136, 3463–3474
- An W., Cho S., Ishii H., Wensink P.C. (1996). "Sex-specific and non-sex-specific oligomerization domains in both of the doublesex transcription factors from *Drosophila melanogaster*". *Molecular Cellular Biology*, Vol. 16, Issue 6, 3106-3111
- Antic D., Stubbs J.L., Suyama K., Kintner C., Scott M.W., Axelrod J.D. (2010). "Planar Cell Polarity Enables Posterior Localization of Nodal Cilia and Left-Right Axis Determination during Mouse and *Xenopus* Embryogenesis". *PLoS One*, Vol. 5, Issue 2
- Andre, P. (2004). „Analyse von Gastrulationsdefekten nach Fehlexpression von gooseoid im Primitivstreifen der Maus“. Universität Hohenheim.
- Antunes M.C., Cohen N.A. (2007). "Mucociliary clearance – a critical upper airway host defense mechanism and methods of assessment". *Current Opinion in Allergy & Clinical Immunology*, 5-10
- Artinger M., Blitz I., Inoue K., Tran U., Cho K.W. (1997). "Interaction of gooseoid and brachyury in *Xenopus* mesoderm patterning". *Mech. Dev.* 65, 187–196
- Axelrod J.D. (2009). "Progress and challenges in understanding planar cell polarity signaling". *Seminars in Cell & Developmental Biology*, 964-971
- Axelrod J.D., Miller J.R., Shulman J.M., Moon R.T., Perrimon N. (1998). "Differential recruitment of Dishevelled provides signaling specificity in the planar cell polarity and Wingless signaling pathways". *Genes & Development* 12, 2610–2622
- Bastock R., Strutt H., Strutt D. (2003). "Strabismus is asymmetrically localised and binds to Prickle and Dishevelled during *Drosophila* planar polarity patterning". *Development*, Vol. 130, Issue 13, 3007-3014
- Bell E., Muñoz-Sanjuán I., Altmann C.R., Vonica A., Brivanlou A.H. (2003). "Cell fate specification and competence by Coco, a maternal BMP, TGFbeta and Wnt inhibitor". *Development*, Vol. 130, Issue 7, 1381-1389
- Belo J.A., Bouwmeester T., Leyns L., Kertesz N., Gallo M., Follettie M., de Robertis E.M. (1997). "Cerberus-like is a secreted factor with neutralizing activity expressed in the anterior primitive endoderm of the mouse gastrula". *Mechanisms of development* 68, 45–57
- Bertrand S., Aldea D., Oulion S., Subirana L., de Lera A.R., Somorjai I., Escriva H. (2015). "Evolution of the Role of RA and FGF Signals in the Control of Somitogenesis in Chordates". *PLoS One*, Vol. 10, Issue 9
- Beyer T., Danilchick M., Thumberger T., Vick P., Tisler M., Schneider I., Bogusch S., Andre P., Ulmer B., Walentek P., Niesler B., Blum M., Schweickert A. (2012). "Serotonin signaling is required for Wnt-dependent GRP specification and leftward flow in *Xenopus*". *Current Biology*, Vol. 22, Issue 1, 33-39
- Blitz I.L., Fish M.B., Cho K.W.Y. (2016). "Leapfrogging: primordial germ cell transplantation permits recovery of CRISPR/Cas9-induced mutations in essential genes". *Development* 143, 2868–2875
- Blumberg B., Wright C.V., de Robertis E.M., Cho K.W. (1991). "Organizer-specific homeobox genes in *Xenopus laevis* embryos". *Science* 253, 194–196
- Blum M., Andre P., Muders K., Schweickert A., Fischer A., Bither E., Bogusch S., Beyer T., van Straaten H.W.N., Viebahn C. (2007). "Ciliation and gene expression distinguish between node and posterior notochord in the mammalian embryo". *Differentiation* 75, 133–146
- Blum M., Feistel K., Thumberger T., Schweickert A. (2014). „The evolution and conservation of left-right patterning mechanisms“. *Development* 141, 1603–1613

- Blum M., Gaunt S.J., Cho K.W., Steinbeisser H., Blumberg B., Bittner D., De Robertis E.M. (1992). "Gastrulation in the mouse: the role of the homeobox gene goosecoid". *Cell* 69, 1097–1106
- Blum M., Ott T. (2019). "Mechanical strain, novel genes and evolutionary insights: news from the frog left-right organizer". *Current Opinion in Genetics & Development*, Vol. 56, 8-14
- Blum M., Schweickert A., Vick P., Wright C.V.E., Danilchik M.V. (2014). "Symmetry breakage in the vertebrate embryo: when does it happen and how does it work?". *Developmental Biology* 393, 109–123
- Boorman C.J., Shimeld S.M. (2002). "The evolution of left-right asymmetry in chordates". *BioEssays* 24, 1004–1011
- Boskovski M. T., Yuan S., Pedersen N. B., goth C. K., Makova S., Clausen H., Brueckner M., Khokha M. K. (2013). "The heterotaxy gene GALNT11 glycosylates Notch to orchestrate cilia type and laterality". *Nature*, Vol. 504, 456 – 459
- Boucher D.M., Schäffer M., Deissler K., Moore C.A., Gold J.D., Burdsal C.A., Meneses J.J., Pedersen R.A., Blum M. (2000). "Goosecoid expression represses Brachyury in embryonic stem cells and affects craniofacial development in chimeric mice". *The international journal of developmental biology* 44, 279–288
- Bouman A., Waisfisz Q., Admiraal J., van de Loo M., van Rijn R.R., Micha D., Oostra R., Mathijssen I.B. (2018). "Homozygous DMRT2 variant associates with severe rib malformations in a newborn". *American Journal of Medical Genetics Part A*, Vol. 176, Issue 5, 1216-1221
- Boutros M., Paricio N., Strutt D.I., Mlodzik M. (1998). "Dishevelled activates JNK and discriminates between JNK pathways in planar polarity and wingless signaling". *Cell*, Vol. 94, Issue 1, 109-118
- Bowes J.B., Snyder K.A., Segerdell E., Jarabek C.J., Azam K., Zorn A.M., Vite P.D. (2010). "Xenbase: gene expression and improved integration". *Nucleic acids research*, Vol. 38 (suppl) 1, 607-612
- Brend T., Holley S.C. (2009). "Balancing segmentation and laterality during vertebrate development". *Seminars in Cell & Developmental Biology*, Vol. 20, 472–478
- Brittle A., Thomas C., Strutt D. (2012). "Planar polarity specification through asymmetric subcellular localization of Fat and Dachshous". *Current Biology*, Vol. 22, Issue 10, 907-914
- Broun M., Sokol S., Bode H.R. (1999). "Cngsc, a homologue of goosecoid, participates in the patterning of the head, and is expressed in the organizer region of Hydra". *Development* 126, 5245–5254
- Burtis K.C., Baker B.S. (1989). "Drosophila doublesex Gene Controls Somatic Sexual Differentiation by Producing Alternatively Spliced mRNAs Encoding Related Sex-Specific Polypeptides". *Cell* Vol. 56, 997 – 1010
- Campbell E.P., Quigley I.K., Kintner, C. (2016). "Foxn4 promotes gene expression required for the formation of multiple motile cilia". *Development* 143, 4654–4664
- Carreira-Barbosa F., Concha M.L., Takeuchi N., Ueno N., Wilson S.W., Tada M. (2003). "Prickle 1 regulates cell movements during gastrulation and neuronal migration in zebrafish". *Development* 130, 4037–4046
- Casal J., Lawrence P.A., Struhl G. (2006). "Two separate molecular systems, Dachshous/Fat and Starry night/Frizzled, act independently to confer planar cell polarity". *Development*, Vol. 133, 4561-4572
- Chapman D.L., Agulnik I., Hancock S., Silver L.M., Papaioannou V.E. (1996). "Tbx6, a mouse T-Box gene implicated in paraxial mesoderm formation at gastrulation". *Developmental Biology*, Vol. 180, Issue 2. 534-542
- Chazaud C., Chambon P., Dolle P. (1999). "Retinoic acid is required in the mouse embryo for left-right asymmetry determination and heart morphogenesis". *Development*, Vol. 126, 2589-2596
- Chen C., Shen M.M. (2004). "Two modes by which Lefty proteins inhibit nodal signaling". *Current Biology*, Vol.6, Issue 4, 618-624
- Cheng A. M., Thisse B., Thisse C., Wright C. V. (2000). "The lefty-related factor Xatv acts as a feedback inhibitor of nodal signaling in mesoderm induction and L-R axis development in Xenopus". *Development*, Vol. 127, 1049 – 1061
- Cheng S.K., Olale F., Brivanlou A.H., Schier A.F. (2004). "Lefty blocks a subset of TGFbeta signals by antagonizing EGF-CFC coreceptors". *PLoS Biology*, Vol. 2, Issue 2
- Cho K.W., Blumberg B., Steinbeisser H., de Robertis E.M. (1991). "Molecular nature of Spemann's organizer: the role of the Xenopus homeobox gene goosecoid". *Cell* 67, 1111–1120
- Christian J.L., Moon R.T. (1993). "Interactions between Xwnt-8 and Spemann organizer signaling pathways generate dorsoventral pattern in the embryonic mesoderm of Xenopus". *Genes Dev* 7, 13–28

- Clements D., Taylor H.C., Herrmann B.G., Stott D. (1996). "Distinct regulatory control of the Brachyury gene in axial and non-axial mesoderm suggests separation of mesoderm lineages early in mouse gastrulation". *Mechanisms of development* 56, 139–149
- Collignon J., Varlet I. and Robertson E. J. (1996). "Relationship between asymmetric nodal expression and the direction of embryonic turning". *Nature*, Vol. 381, 155-158
- Coluccio L.M. (1997). "Myosin I". *The American journal of physiology*
- Conlon F.L., Smith J.C. (1999). "Interference with brachyury function inhibits convergent extension, causes apoptosis, and reveals separate requirements in the FGF and activin signalling pathways". *Developmental Biology* 213, 85–100
- Coschigano K. T., Wensink P. C. (1993). "Sex-specific transcriptional regulation by the male and female doublesex proteins of *Drosophila*". *Genes & Development*, Vol. 7, 42 – 54
- Coutelis J.B., González-Morales N., Géminard C., Noselli S. (2014). "Diversity and convergence in the mechanisms establishing L/R asymmetry in metazoan". *The EMBO Report* 15, 926–937
- Cui C., Little C.D., Rongish B.J. (2009). "Rotation of Organizer Tissue Contributes to Left-Right Asymmetry". *The Anatomical Record* 292, 557-564
- Danilov V., Blum M., Schweickert A., Campione M., Steinbeisser H (1998). "Negative autoregulation of the organizer-specific homeobox gene goosecoid". *The Journal of biological chemistry* 273, 627–635
- Darken R.S., Scola A.M., Rakeman A.S., Das G., Mlodzik M., Wilson P.A. (2002). "The planar polarity gene *trabismus* regulates convergent extension movements in *Xenopus*". *EMBO J.*, Vol. 21, 976-985
- Das G., Reynolds-Kenneally J., Mlodzik M. (2002). "The atypical cadherin *Flamingo* links *Frizzled* and *Notch* signaling in planar polarity establishment in the *Drosophila* eye". *Developmental Cell*, Vol. 2, Issue 5, 655-666
- Davison A., McDowell G.S., Holden J.M., Johnson H.F., Koutsovoulos G.D., Liu M., Hulpiau P., Van Roy F., Wade C.M., Banerjee R., Yang F., Chiba S., Davey J.W., Jackson D.J., Levin M., Blaxter M.L. (2016). "Formin Is Associated with Left-Right Asymmetry in the Pond Snail and the Frog". *Current Biology*, Vol. 26, 654-660
- Deissler, K. (2002). „Konditionale ubiquitäre Expression des Homeoboxgens *goosecoid* im Primitivstreifen der Maus“. Universität Hohenheim
- Deprez M., Zaragosi L., Truchi M., Ruiz Garcia S., Arguel M., Lebrigrand K., Paquet A., Peer D., Marquette C., Leroy S., Barbry P. (2020). "A single-cell atlas of the human healthy airways". *bioRxiv preprint*
- Dickmeis T., Aanstad P., Clark M., Fischer N., Herwig R., Mourrain P., Blader P., Rosa F., Lehrach H., Strähle U. (2001). "Identification of nodal signaling targets by array analysis of induced complex probes". *Developmental Dynamics*, Vol. 222, Issue 4, 571-580
- Dixon Fox M., Bruce A.E.E. (2009). "Short- and long-range functions of *Goosecoid* in zebrafish axis formation are independent of *Chordin*, *Noggin 1* and *Follistatin-like 1b*". *Development* 136, 1675–1685
- Domingo C., Keller R. (1995). "Induction of notochord cell intercalation behavior and differentiation by progressive signals in the gastrula of *Xenopus laevis*". *Development* 121, 3311–3321
- Dosch R., Gawantka V., Delius H., Blumenstock C., Niehrs C. (1997). "*Bmp-4* acts as a morphogen in dorsoventral mesoderm patterning in *Xenopus*". *Development* 124, 2325 – 2334
- Duncan A.R., Khokha M.K. (2016). "*Xenopus* as a model organism for birth defects-Congenital heart disease and heterotaxy". *Seminars in cell & developmental biology* 51, 73–79
- Eimon P.M., Harland R.M. (2002). "Effects of heterodimerization and proteolytic processing on *Derrière* and *Nodal* activity: implications for mesoderm induction in *Xenopus*". *Development*, Vol. 129, Issue 13, 3089-3103
- Erdman S. E., Burtis K. C. (1993). "The *Drosophila* doublesex proteins share a novel zinc finger related DNA binding domain". *The EMBO Journal*, Vol. 12, No. 2, 527 – 535
- Erdman S.E., Chen H.J., Burtis K.C. (1996). "Functional and genetic characterization of the oligomerization and DNA binding properties of the *Drosophila* doublesex proteins". *Genetics*, Vol. 144, Issue 4, 1639-1652
- Ewald A.J., Peyrot S.M., Tyszka J.M., Fraser S.E., Wallingford J. B. (2004). "Regional requirements for *Dishevelled* signaling during *Xenopus* gastrulation: separable effects on blastopore closure, mesendoderm internalization and archenteron formation". *Development* 131, 6195–6209

- Fainsod A., Steinbeisser H., de Robertis E.M. (1994). "On the function of BMP-4 in patterning the marginal zone of the *Xenopus* embryo". *EMBO J.* 13, 5015–5025
- Ferreiro B., Artinger M., Cho K., Niehrs C. (1998). "Antimorphic goosecooids". *Development* 125, 1347–1359
- Fletcher R.B., Baker J.C., Harland R.M. (2006). "FGF8 spliceforms mediate early mesoderm and posterior neural tissue formation in *Xenopus*". *Development* 133, 1703–1714
- Fletcher R.B., Harland R.M. (2008). "The role of FGF signaling in the establishment and maintenance of mesodermal gene expression in *Xenopus*". *Developmental Dynamics* 237, 1243 – 1254
- Fraidenraich D., Iwahori A., Rudnicki M., Basilico C. (2000). "Activation of *fgf4* gene expression in the myotomes is regulated by myogenic bHLH factors and by sonic hedgehog". *Developmental Biology*, Vol. 225, 392 – 406
- Gans C., Northcutt R.G. (1983). "Neural crest and the origin of vertebrates: a new head". *Science* 220, 268–273
- Gao B., Song H., Bishop K., Elliot G., Garrett L., English M.A., Andre P., Robinson J., Sood R., Minami Y., Economides A.N., Yang Y. (2011). "Wnt signaling gradients establish planar cell polarity by inducing Vangl2 phosphorylation through Ror2". *Developmental Cell* 20, 163–176
- Gaunt S.J., Blum M., de Robertis E.M. (1993). "Expression of the mouse goosecooid gene during mid-embryogenesis may mark mesenchymal cell lineages in the developing head, limbs and body wall". *Development* 117, 769–778
- Gensch N., Borchardt T., Schneider A., Riethmacher D., Braun T. (2008). "Different autonomous myogenic cell populations revealed by ablation of *Myf5*-expressing cells during mouse embryogenesis". *Development*, Vol. 135, 1597-1604
- Germain S., Howell M., Esslemont G.M., Hill C.S. (2000). "Homeodomain and winged-helix transcription factors recruit activated Smads to distinct promoter elements via a common Smad interaction motif". *Genes & Development*, Vol. 14, 435-451
- Getwan M. (2015). "Analyse des Flow-abhängigen Symmetriebruchs im Frosch *Xenopus*: die Funktion des Nodal-Inhibitors *Coco*"
- Gilbert S.F. (2010). "Developmental Biology, 9th edition". Sinauer Associates, Inc.
- Gillespie P.G., Müller U. (2009). "Mechanotransduction by hair cells: models, molecules, and mechanisms". *Cell*, Vol. 139, Issue 1, 33-44
- Glinka A., Delius H., Blumenstock C., Niehrs C. (1996). "Combinatorial signalling by *Xwnt-11* and *Xnr3* in the organizer epithelium". *Mechanism of development*, Vol. 60, Issue 2, 221-231
- Goodrich L.V., Strutt D. (2011). "Principles of planar polarity in animal development". *Development*, Vol. 138, 1877-1892
- González-Morales N., Géminard C., Lebreton G., Cerezo D., Coutelis J.B., Noselli, S. (2015). "The Atypical Cadherin *Dachsous* Controls Left-Right Asymmetry in *Drosophila*". *Developmental Cell* 33, 675–689
- Goode B.L., Eck M.J. (2007). "Mechanism and Function of Formins in the Control of Actin Assembly". *Annual Review of Biochemistry*, Vol. 76, 593-627
- Goriely A., Stella M., Coffinier C., Kessler D., Mailhos C., Dessain S., Desplan C. (1996). "A functional homologue of goosecooid in *Drosophila*". *Development* 122, 1641–1650
- Goto T., Keller R. (2002). "The planar cell polarity gene *strabismus* regulates convergence and extension and neural fold closure in *Xenopus*". *Developmental Biology* 247, 165–181
- Gourronc F., Ahmad N., Nedza N., Eggleston T., Rebagliati M. (2007). "Nodal activity around Kupffer's vesicle depends on the T-box transcription factors *notail* and *spadetan* and on notch signaling". *Developmental Dynamics*, Vol. 236, 2131 – 2146
- Grande C., Patel N.H. (2009). "Nodal signalling is involved in left-right asymmetry in snails". *Nature*, 457, 1007-1011
- Grass S., Arnold H. H., Braun T. (1996). "Alterations in somite patterning of *Myf-5*-deficient mice: a possible role for FGF-4 and FGF-6". *Development*, Vol. 122, 141 – 150
- Green J. (1999) in "Molecular Methods in Developmental Biology". Humana Press Vol. 127, 1–14
- Grimes D.T., Burdine R.D. (2017). "Left-Right Patterning: Breaking Symmetry to Asymmetric Morphogenesis". *Trends in genetics* 33, 616–628
- Gros J., Feistel K., Viebahn C., Blum M., Tabin C.J. (2009). "Cell Movements at Hensen's Node Establish Left/Right Asymmetric Gene Expression in the Chick". *Science*, Vol. 324, Issue 5929, 941-944

- Gros J., Hu J.K., Vinegoni C., Feruglio P.F., Weissleder R., Tabin C.J. (2010). "WNT5A/JNK and FGF/MAPK pathways regulate the cellular events shaping the vertebrate limb bud". *Current Biology* 20, 1993–2002
- Habas R., Kato Y., He X. (2001). "Wnt/Frizzled activation of Rho regulates vertebrate gastrulation and requires a novel Formin homology protein Daam1". *Cell*, Vol. 107, Issue 7, 843-854
- Hadjantonakis A., Pisano E., Papaioannou V.E. (2008). "Tbx6 regulates left/right patterning in mouse embryos through effects on nodal cilia and perinodal signaling". *PLoS One*, Vol. 3, Issue 6
- Hamada H., Tam P.P.L. (2014). "Mechanisms of left-right asymmetry and patterning: driver, mediator and responder". *F1000Prime Reports*
- Hammer J.A. (1994). "The structure and function of unconventional myosins: A review". *Journal of Muscle Research & Cell Motility* 15, 1–10
- Han W.T., Marlow L.A., von Roemeling C.A., Cooper S.J., Kreinest P., Wu K., Luxon B.A., Sinha M., Anastasiadis P.Z., Copland J.A. (2010). "Pathway Signature and Cellular Differentiation in Clear Cell Renal Cell Carcinoma". *PLoS One*, Vol. 5, Issue 5
- Hardin J., Keller R. (1988). "The behavior and function of bottle cells during gastrulation of *Xenopus laevis*". *Development*, Vol. 103, 211-230
- Hartman M.A., Finan D., Sivaramakrishnan S., Spudich J.A. (2011). "Principles of unconventional myosin function and targeting". *Annual Review of Cell & Developmental Biology*, Vol. 27, 133-155
- Hartman M.A., Spudich J.A. (2012). "The myosin superfamily at a glance". *Journal of Cell Science*, Vol. 125, 1627-1632
- Hartwell K.A., Muir B., Reinhardt F., Carpenter A.E., Sgroi D.C., Weinberg R.A. (2006). "The Spemann organizer gene, *Gooseoid*, promotes tumor metastasis". *Proceedings of the National Academy of Science of the USA* 103, 18969–18974
- Harumoto T., Ito M., Shimada Y., Kobayashi T.J., Ueda H.R., Lu B., Uemura T. (2010). "Atypical cadherins *Dachsous* and *Fat* control dynamics of noncentrosomal microtubules in planar cell polarity". *Developmental Cell*, Vol. 19, Issue 3, 389-401
- Hashimoto H., Rebagliati M., Ahmad N., Muraoka O., Kurokawa T., Hibi M., Suzuki T. (2004). "The Cerberus/Dan-family protein *Charon* is a negative regulator of Nodal signaling during left-right patterning in zebrafish". *Development*, Vol. 137, 1741 – 1753
- Hashimoto M., Hamada H. (2010). "Translation of anterior-posterior polarity into left-right polarity in the mouse embryo". *Current Opinion in Genetics & Development*, Vol. 20, Issue 4, 433-437
- Hegan P.S., Ostertag E., Geurts A.M., Mooseker M.S. (2015). "Myosin Id Is Required for Planar Cell Polarity in Ciliated Tracheal and Ependymal Epithelial Cells". *Cytoskeleton*, Vol. 72, Issue 10, 503-516
- Hesketh, J.E. (1996). "Sorting of messenger RNAs in the cytoplasm: mRNA localization and the cytoskeleton". *Experimental Cell Research*, Vol. 225, Issue 2, 219-236
- Hozumi S., Maeda R., Taniguchi K., Kanai M., Shirakabe S., Sasamura T., Spéder P., Noselli S., Aigaki T., Murakami R., Matsuno K (2006). "An unconventional myosin in *Drosophila* reverses the default handedness in visceral organs". *Nature* 440, 798–802
- Huang S., Ma J., Liu X., Zhang Y., Luo L. (2011). "Retinoic Acid Signaling Sequentially Controls Visceral and Heart Laterality in Zebrafish". *The Journal of Biological Chemistry*, Vol. 286, No. 32, 28533-28543
- Inácio J.M., Marques S., Nakamura T., Shinohara K., Meno C., Hamada H., Belo J.A. (2013). "The Dynamic Right-to-Left Translocation of *Cerl2* Is Involved in the Regulation and Termination of Nodal Activity in the Mouse Node". *PLoS One*, Vol. 1, Issue 3,
- Janesick A., Tang W., Shioda T., Blumberg B. (2018). "RARγ is required for mesodermal gene expression prior to gastrulation in *Xenopus*". *Development*, Vol. 145, Issue 18
- Jones C.M., Armes N., Smitz J.C. (1996). "Signalling by TGF-beta family members: short-range effects of *Xnr-2* and *BMP-4* contrast with the long-range effects of *activin*". *Current Biology*, Vol.6, Issue 11, 1468 – 1475
- Juan T., Géminard C., Coutelis J., Cerezo D., Polès S., Noselli S., Fürthauer M. (2018). "Myosin1D is an evolutionarily conserved regulator of animal left-right asymmetry". *Nature Communications*, Vol. 9
- Kajikawa E., Horo U., Ide T., Mizuno K., Minegishi K., Hara Y., Ikawa Y., Nishimura H., Uchikawa M., Kiyonari H., Kuraku S., Hamada H. (2020). "Nodal paralogues underlie distinct mechanisms for visceral left–right asymmetry in reptiles and mammals". *Nature Ecology & Evolution*, Vol. 2, 261-269

- Kantarci H., Gerberding A., Riley B.B. (2016). "Spemann organizer gene Goosecoid promotes delamination of neuroblasts from the otic vesicle". *Proceedings of the National Academy of Science of the USA* 201609146–16
- Karpinka J.B., Fortriede J.D., Burns K.A., James-Zorn C., Ponferrada V.G., Lee J., Karimi K., Zorn A.M., Vize P.D. (2015). „Xenbase, the *Xenopus* model organism database; new virtualized system, data types and genomes". *Nucleic Acids Research* 43, D756–63
- Kawakami Y., Raya Á., Raya R.M., Rodríguez-Esteban C., Belmonte J.C.I. (2005). "Retinoic acid signalling links left–right asymmetric patterning and bilaterally symmetric somitogenesis in the zebrafish embryo". *Nature* Vol. 435
- Keller R., Davidson L., Edlung A., Elul T., Ezin M., Shook D., Skoglund P. (2000). "Mechanisms of convergence and extension by cell intercalation". *Philosophical Transactions of the Royal Society of London Series B Biological Science*, 897-922
- Keller R., Shih J., Sater A. (1992). "The cellular basis of the convergence and extension of the *Xenopus* neural plate". *Developmental Dynamics*, Vol. 193, Issue 2, 199-217
- Keller R., Shook D., Skoglund P. (2008). "The forces that shape embryos: physical aspects of convergent extension by cell intercalation". *Physical Biology* 5
- Keller, R., Tibbetts P. (1989). "Mediolateral cell intercalation in the dorsal, axial mesoderm of *Xenopus laevis*". *Developmental Biology* 131, 539–549
- Keller R., Winklbauer R. (1992). "Cellular Basis of Amphibian Gastrulation". *Current Topics in developmental biology* 27, 39–89 (Elsevier, 1992)
- Kelly M., Chen P. (2007). "Shaping the mammalian auditory sensory organ by the planar cell polarity pathway". *The International journal of developmental biology* 51, 535–547
- Kislauskis E.H., Zhu X., Singer R.H. (1994). "Sequences responsible for intracellular localization of beta-actin messenger RNA also affect cell phenotype". *Journal of Cell Biology*, Vol. 127, No. 2, 441-451
- Kitajima K., Oki S., Ohkawa Y., Sumi T., Meno C. (2013). "Wnt signaling regulates left-right axis formation in the node of mouse embryos". *Developmental Biology* 380, Issue 2, 222-232
- Köhler D., Struchholz S., Bähler M. (2005). "The two IQ-motifs and Ca²⁺/calmodulin regulate the rat myosin 1d ATPase activity". *The FEBS Journal*, Vol. 272, Issue 9, 2189-2198
- Krasnow R.E., Wong L.L., Adler P.N. (1995). "Dishevelled is a component of the frizzled signaling pathway in *Drosophila*". *Development*, Vol. 121, Issue 12, 4095-4102
- Krebs L.T., Iwai N., Nonaka S., Welsh I.C., Lan Y., Jiang R., Saijoh Y., O'Brien T.P., Hamada H., Gridley T. (2003). "Notch signaling regulates left-right asymmetry determination by inducing Nodal expression". *Genes & development*, Vol. 17, Issue 10, 1207-1212
- Kuroda R. (2014). "How a Single Gene Twists a Snail". *Integrative and Comparative Biology*, Vol. 54, Issue 4, 677-687
- Kuroda R., Fujikura K., Abe M., Hosoiri Y., Asakawa S., Shimizu M., Umeda S., Ichikawa F., Takahashi H. (2016). "Diaphanous Gene Mutation Affects Spirial Cleavage and Chirality in Snails". *Scientific Reports*, Vol. 6
- Kühl M., Geis K., Sheldahl L.C., Pukrop T., Moon R.T., Wedlich D. (2001). "Antagonistic regulation of convergent extension movements in *Xenopus* by Wnt/beta-catenin and Wnt/Ca²⁺ signaling". *Mechanisms of Development* 106, 61–76
- Kwan K.M., Kirschner M.W. (2003). "Xbra functions as a switch between cell migration and convergent extension in the *Xenopus* gastrula". *Development* 130 1961–1972
- Lartillot N., Le Gouar M., Adoutte A. (2002). "Expression patterns of fork head and goosecoid homologues in the mollusc *Patella vulgata* supports the ancestry of the anterior mesendoderm across Bilateria". *Development Genes and Evolution* 212, 551–561
- Latinkic B.V., Smith J C. (1999). "Goosecoid and mix.1 repress Brachyury expression and are required for head formation in *Xenopus*". *Development* 126, 1769–1779
- LeBlanc-Straceski J.M., Sokac A., Bement W., Sobrado P., Lemoine L. (2009). "Developmental expression of *Xenopus* myosin 1d and identification of a myo1d tail homology that overlaps TH1". *Developmental, growth & differentiation* 51, 443–451
- Lee J., Harland R.M. (2007). "Actomyosin contractility and microtubules drive apical constriction in *Xenopus* bottle cells". *Developmental Biology*, Vol. 311, 40-52

- Lee C., Scherr H.M., Wallingford J.B. (2007). "Shroom family proteins regulate γ -tubulin distribution and microtubule architecture during epithelial cell shape change". *Development*, Vol. 134, 1431-1441
- Levin M., Johnson R. L., Sterna C. D., Kuehn M., Tabin C. (1995). "A molecular pathway determining left-right asymmetry in chick embryogenesis". *Cell*, Vol. 82, 803 – 814
- Lewandoski M. (2001). "Conditional control of gene expression in the mouse". *Nature Reviews. Genetics*. 2, 743–755
- Li H.Y., Bourdelas A., Carron C., Gomez C., Boucaut J.C., Shi D.L. (2006). "FGF8, Wnt8 and Myf5 are target genes of Tbx6 during anteroposterior specification in *Xenopus* embryo". *Developmental Biology* 290, 470 - 481
- Lin A. E., Krikov S., Riehle-Colarusso T., Frías J. L., Belmont J., Anderka M., Geva T., Getz K. D., Botto L. D., National Birth Defects Prevention Study (2014). "Laterality Defects in the National Birth Defects Prevention Study (1998-2007): Birth Prevalence and Descriptive". *American Journal of medical genetics*, Vol. 164, Issue 10, 2581 – 2591
- Lindqvist M., Horn Z., Bryja V., Schulte G., Papachristou P., Ajima R., Dyberg C., Arenas E., Yamaguchi T.P., Lagercrantz H., Ringstedt T. (2010). "Vang-like protein 2 and Rac1 interact to regulate adherens junctions". *Journal of Cell Science*, Vol. 123, 472-483
- Littlewood Evans A., Müller U. (2000). "Stereocilia defects in the sensory hair cells of the inner ear in mice deficient in integrin α 8 β 1". *Nature Genetics* 24, 424-428
- Liu S., Li Z., Gui J. F. (2009). "Fish-Specific Duplicated *dmt2b* Contributes to a Divergent Function through Hedgehog Pathway and Maintains Left-Right Asymmetry Establishment Function". *PLoS One*, Vol. 4, Issue 9
- Logan M., Pagán-Westphal S. M., Smith D. M., Paganessi L., Tarbin C. J. (1998). "The transcription factor *Pitx2* mediates situs-specific morphogenesis in response to left-right asymmetric signals". *Cell*, Vol. 94, Issue 3, 3007 – 317
- Lopes S. S., Lourenço R., Pacheco L., Moreno N., Kreiling J., Saúde L. (2010). "Notch signalling regulates left-right asymmetry through ciliary length control". *Development*, Vol. 137, 3625 – 3632
- Lourenço R., Lopes S., Saúde L. (2010). "Left-right function of *dmt2* genes is not conserved between zebrafish and mouse". *PLoS One*, Vol. 5, Issue 12
- Lowe L. A., Supp D. M., Sampath K., Yokoyama T., Wright C. V. E., Potter S. S., Overbeek P., Kuehn M. R. (1996). "Conserved left-right asymmetry of nodal expression and alterations in murine situs inversus". *Nature*, Vol. 381
- Luu O., Nagel M., Wacker S., Lemaire P., Winklbauer R. (2008). "Control of gastrula cell motility by the Goosecoid/Mix.1/Siamois network: basic patterns and paradoxical effects". *Developmental Dynamics* 237, 1307–1320
- Maerker M., Getwan M., Dowdle M.E., Pelliccia J.L., McSheene J.C., Yartseva V., Minegishi K., Vick P., Giraldez A.J., Hamada H., Burdine R.D., Sheets M.D., Schweickert A., Blum M. (2002). "Bicc1 and dicer regulate left-right patterning through post-transcriptional control of the Nodal-inhibitor *dand5*". *in Revision*
- Maguire R.J., Isaacs H.V., Pownall M.E. (2012). "Early transcriptional targets of MyoD link myogenesis and somitogenesis". *Developmental Biology* 371, 256 - 268
- Mailhos C., André S., Mollereau B., Goriely A., Hemmati-Brivanlou A., Desplan C. (1998). "Drosophila Goosecoid requires a conserved heptapeptide for repression of paired-class homeoprotein activators". *Development* 125, 937–947
- Maisonneuve C., Guilleret I., Vick P., Weber T., Andre P., Beyer T., Blum M., Constam D.B. (2009). "Bicaudal C, a novel regulator of Dvl signaling abutting RNA-processing bodies, controls cilia orientation and leftward flow". *Development*, Vol. 136, Issue 17, 3019-3030
- Marjoram L., Wright C. (2011). "Rapid differential transport of Nodal and Lefty on sulfated proteoglycan-rich extracellular matrix regulates left-right asymmetry in *Xenopus*". *Development*, Vol. 138, 475 – 485
- Marlow F., Topczewski J., Sepich D., Solnica-Krezel L. (2002). "Zebrafish Rho kinase 2 acts downstream of Wnt11 to mediate cell polarity and effective convergence and extension movements". *Current Biology*, Vol. 12, Issue 11, 876-884
- Maroma K., Fainsod A., Steinbeisser H. (1999). "Patterning of the mesoderm involves several threshold response to BMP-4 and Xwnt-8". *Development* 87
- Marques S., Borges A. C., Silva A. C., Freitas S., Cordenonsi M., Belo J. A. (2004). "The activity of the nodal antagonist Cerl-2 in the mouse node is required for correct L/R body axis". *Genes & Development*, Vol. 18, 2342 - 2347
- Massagué J. (1998). "TGF- β SIGNAL TRANSDUCTION". *Annual Review of Biochemistry*

- Matus D.Q., Pang K., Marlow H., Dun C.W., Thomsen G.H., Martindale M.Q. (2006). "Molecular evidence for deep evolutionary roots of bilaterality in animal development". *Proceedings of the National Academy of Science of the USA* 103, 11195–11200
- McCulloch C.A., Tenenbaum H.C. (1986). "Dexamethasone induces proliferation and terminal differentiation of osteogenic cells in tissue culture". *The Anatomical Record* 215, 397–402
- McDowell G.S., Lemire J.M., Paré J.F., Cammarata G., Lowery L.A., Levin M. (2016). "Conserved roles for cytoskeletal components in determining laterality". *Integrative Biology: quantitative biosciences from nano to macro* 8, 267–286
- McGrath J., Somlo S., Makova S., Tian X., Brueckner M. (2003). "Two Populations of Node Monocilia Initiate Left-Right Asymmetry in the Mouse". *Cell*, Vol. 114, Issue 1, 61-73
- Medina A., Reintsch W., Steinbeisser H. (2000). "Xenopus frizzled 7 can act in canonical and non-canonical Wnt signaling pathways: implications on early patterning and morphogenesis". *Mechanisms of development*. 92, 227–237
- Melby A.E., Warga R.M., Kimmel C.B. (1996). "Specification of cell fates at the dorsal margin of the zebrafish gastrula". *Development* 122, 2225-2237
- Meng A., Moore B., Tang H., Yuan B., Lin S. (1999). "A Drosophila doublesex-related gene, terra, is involved in somitogenesis in vertebrates". *Development* 126, 1259-1268
- Meno C., Gritsman K., Ohishi S., Ohfuji Y., Heckscher E., Mochida K., Shimono A., Kondoh H., Talbot W. S., Robertson E. J., Schier A. F., Hamada H. (1999). "Mouse Lefty2 and zebrafish antivin are feedback inhibitors of nodal signaling during vertebrate gastrulation". *Molecular Cell*, Vol. 4, Issue 3, 287 – 298
- Meno C., Shimono A., Saijoh Y., Yashiro K., Mochida K., Ohishi S., Noji S., Kondoh H., Hamada H. (1998). "lefty-1 is required for left-right determination as a regulator of lefty-2 and nodal". *Cell*, Vol. 94, 287 – 297
- Merkel M., Sagner A., Gruber F.S., Etourney R., Blasse C., Myers E., Eaton S., Jülicher F. (2014). "The balance of prickle/spiny-legs isoforms controls the amount of coupling between core and fat PCP systems". *Current Biology*, Vol. 24, Issue 18, 2111-2123
- Miller R.K., de la Torre Canny S.G., Jang C., Cho K., Ji H., Wagner D.S., Jones E.A., Habas R., McCreary P.D. (2011). "Pronephric tubulogenesis requires Daam1-mediated planar cell polarity signaling". *Journal of the American Society for Nephrology*, Vol. 22, Issue 9, 1654-1664
- Minegishi K., Hashimoto M., Ajima R., Takaoka K., Shinohara K., Ikawa Y., Nishimura H., McMahon A.P., Willert K., Okada Y., Sasaki H., Shi D., Fujimori T., Ohtsuka T., Igarashi Y., Yamaguchi T.P., Shimono A., Shiratori H., Hamada H. (2017). "A Wnt5 Activity Asymmetry and Intercellular Signaling via PCP Proteins Polarize Node Cells for Left-Right Symmetry Breaking". *Developmental Cell*, Vol. 40, Issue 5, 439-452
- Mingle L.A., Okuhama N.N., Shi J., Singer R.H., Condeelis J., Liu G. (2005). "Localization of all seven messenger RNAs for the actin-polymerization nucleator Arp2/3 complex in the protrusions of fibroblasts". *Journal of Cell Science* 118, 2425-2433
- Munnamalai V., Fekete D.M. (2013). "Wnt signaling during cochlear development". *Seminars in cell & developmental biology* 24, 480–489
- Murphy M.W., Zarkower D., Bardwell V.J. (2007). "Vertebrate DM domain proteins bind similar DNA sequences and can heterodimerize on DNA". *BMC Molecular Biology*, Vol. 7, Issue 58
- Naccache S.N., Hasson T., Horowitz A. (2006). "Binding of internalized receptors to the PDZ domain of GIPC/synectin recruits myosin VI to endocytic vesicles". *PNAS*, Vol 103, Issue 34, 12735-12740
- Nakamura T., Hamada, H. (2012). "Left-right patterning: conserved and divergent mechanisms". *Development* 139, 3257–3262
- Nakamura T., Saito D., Kawasumi A., Shinohara K., Asai Y., Takaoka K., Dong F., Takamatsu A., Belo J. A., Mochizuki A., Hamada H. (2012). "Fluid flow and interlinked feedback loops establish left-right asymmetric decay of Cer12 mRNA". *Nature Communications*, Vol. 3, Issue 1322
- Nakayama T., Blitz I.L., Fish M.B., Odeleye A.O., Manohar S., Cho K.W.Y., Grainger, R.M. (2014). "Cas9-based genome editing in *Xenopus tropicalis*". *Methods in Enzymology* 546, 355–375
- Niehrs C., Keller R., Cho K.W., de Robertis E.M. (1993). "The homeobox gene goosecoid controls cell migration in *Xenopus* embryos". *Cell* 72, 491–503
- Ninomiya H., Elinson R.P., Winklbauer R. (2004). "Antero-posterior tissue polarity links mesoderm convergent extension to axial patterning". *Nature* 430, 364–367

- Nonaka S., Tanaka Y., Okada Y., Takeda S., Harada A., Kanai Y., Kido M., Hirokawa N. (1998). "Randomization of left-right asymmetry due to loss of nodal cilia generating leftward flow of extraembryonic fluid in mice lacking KIF3B motor protein". *Cell*, Vol. 95, 829 – 837
- Nonaka S., Yoshida S., Watanabe D., Ikeuchi S., Goto T., Mashall W. F., Hamada H. (2005). "De novo formation of left-right asymmetry by posterior tilt of nodal cilia". *PLoS Biology*, Vol. 3, Issue 8
- Ocaña O.H., Coskun H., Minguillón C., Murawala P., Tanaka E.M., Galcerán J., Muñoz-Chápuli R., Nieto M.A. (2017). "A right-handed signalling pathway drives heart looping in vertebrates". *Nature* 549, 86–90
- Ohkawara B., Iemura S., ten Dijke P., Ueno N. (2002). "Action range of BMP is defined by its N-terminal basic amino acid core". *Current Biology*, Vol.12, Issue 3, 205 - 209
- Ohkawara B., Niehrs C. (2011). "An ATF2-based luciferase reporter to monitor non-canonical Wnt signaling in *Xenopus* embryos". *Developmental Dynamics* 240, 188–194
- Okada Y., Takeda S., Tanaka Y., Belmonte J. I., Hirokawa N. (2005). "Mechanism of nodal flow: a conserved symmetry breaking event in left-right axis determination". *Cell*, Vol. 121, 633 – 644
- Oki S., Hashimoto R., Okui Y., Shen M. M., Mekada E., Otani H., Saijoh Y., Hamada H. (2007). "Sulfated glycosaminoglycans are necessary for Nodal signal transmission from the node to the left lateral plate in the mouse embryo". *Development*, Vol. 134, 3893 – 3904
- Okumura, T., Utsuno H., Kuroda J., Gittenberger E., Asami T., Matsuno K. (2008). "The development and evolution of left-right asymmetry in invertebrates: lessons from *Drosophila* and snails". *Developmental Dynamics* 237, 3497–3515
- Onichtchouk D., Gawantka V., Dosch R., Delius H., Hirschfeld K., Blumenstock C., Niehrs C. (1996). "The *Xvent-2* homeobox gene is part of the BMP-4 signalling pathway controlling [Correction of controlling] dorsoventral patterning of *Xenopus* mesoderm". *Development* 122, 3045–3053
- Ossipova O., Chu C.W., Fillatre J., Brott B.K., Itoh K., Sokol, S.Y. (2015). "The involvement of PCP proteins in radial cell intercalations during *Xenopus* embryonic development". *Developmental Biology* 408, 316–327
- Ossipova O., Chuykin I., Chu C., Sokol S.Y. (2015). "Vangl2 cooperates with Rab11 and Myosin V to regulate apical constriction during vertebrate gastrulation". *Development* 142, 99-107
- Oteiza P., Köppen M., Concha M. L., Heisenberg C. P. (2008). "Origin and shaping of the laterality organ in zebrafish". *Development*, Vol. 135, 2807 – 2813
- Otto A., Pieper T., Viebahn C., Tsikolia N. (2014). "Early Left-Right Asymmetries During Axial Morphogenesis in the Chick Embryo". *Genesis*, Vol. 52, 614-625
- Ottolenghi C., Veitia R., Barbieri M., Fellous M., McElreavey K. (2000). "The Human Doublesex-Related Gene, *DMRT2*, Is Homologous to a Gene Involved in Somatogenesis and Encodes a Potential Bicistronic Transcript". *Genomics*, Vol. 64, 179 – 186
- Óunap K., Uibo O., Zordania R., Kiho L., Ilus T., Öiglane-Shlik E.O., Bartsch O. (2004). "Three Patients With 9p Deletions Including *DMRT1* and *DMRT2*: A Girl With XY Complement, Bilateral Ovaries, and Extreme Growth Retardation, and Two XX Females With Normal Pubertal Development". *American Journal of Medical Genetics*, Vol. 130a, Issue 4, 415-423
- Paré A.C., Vichas A., Fincher C.T., Mirman Z., Farrel D.L., Mainieri A., Zallen J.A. (2014). "Toll receptor code directs convergent extension in *Drosophila*". *Nature* 515, 523–527
- Park M., Moon R.T. (2002). "The planar cell-polarity gene *stbm* regulates cell behaviour and cell fate in vertebrate embryos". *Nature Cell Biology* 4, 20–25
- Park T.J., Gray R.S., Sato A., Habas R., Wallingford J.B. (2005). "Subcellular localization and signaling properties of *dishevelled* in developing vertebrate embryos". *Current Biology* 15, 1039–1044
- Park T.J., Haigo S.L., Wallingford J.B. (2006). "Ciliogenesis defects in embryos lacking *inturned* or *fuzzy* function are associated with failure of planar cell polarity and Hedgehog signaling". *Nature genetics* 38, 303–311
- Park T.J., Mitchel B.J., Abitua P.B., Kintner C., Wallingford J.B. (2008). "Dishevelled controls apical docking and planar polarization of basal bodies in ciliated epithelial cells". *Nature genetics*, Vol. 40, Issue 7, 871-879
- Parlier D., Moers V., Van Campenhout C., Preillon J., Leclère L., Saulnier A., Sirakov M., Busengdal H., Kricha S., Marine J. C., Rentzsch F., Bellefroid E. J. (2013). "The *Xenopus* doublesex-related gene *Dmrt5* is required for olfactory placode neurogenesis". *Developmental Biology*, Vol. 373, Issue 1, 39 – 52

- Parry D.A., Logan C.V., Stegmann A.P.A., Abdelhamed Z.A., Calder A., Khan S., Bonthron D.T., Clowes V., Sheridan E., Ghali N., Chudley A.E., Dobbie A., Strumpel C.T.R.M., Johnson C.A. (2013). "SAMS, a syndrome of short stature, auditory-canal atresia, mandibular hypoplasia, and skeletal abnormalities is a unique neurocristopathy caused by mutations in Goosecoid". *American Journal of human genetics* 93, 1135–1142
- Paterson H.F., Self A.J., Garrett M.D., Just I., Aktories K., Hall A. (1990). "Microinjection of recombinant p21rho induces rapid changes in cell morphology". *The Journal of cell biology* 111, 1001–1007
- Peng Y., Axelrod J.D. (2012). "Asymmetric protein localization in planar cell polarity: mechanisms, puzzles, and challenges". *Current Topics in Developmental Biology*, 101, 33-53
- Peterson A.G., Wang X., Yost H.J. (2013). „Dvr1 transfers left-right asymmetric signals from Kupffer's vesicle to lateral plate mesoderm in zebrafish". *Developmental Biology*, Vol. 382, 198 – 208
- Petzoldt A.G., Coutelis J., Géminard C., Spéder P., Suzanne M., Cerezo D., Noselli S. (2012). "DE-Cadherin regulates unconventional Myosin ID and Myosin IC in *Drosophila* left-right asymmetry establishment". *Development*, Vol. 139, Issue 10, 1874-1884
- Phillips K.R., Tong S., Goodyear R., Richardson G.P., Cyr J.L. (2006). "Stereociliary Myosin-1c Receptors Are Sensitive to Calcium Chelation and Absent from Cadherin 23 Mutant Mice". *Journal of Neuroscience*, Vol. 26, Issue 42, 10777–10788
- Piccolo S., Agius E., Leyns L., Bhattacharyya S., Grunz H., Bouwmeester T., De Robertis E.M. (1999). "The head inducer Cerberus is a multifunctional antagonist of Nodal, BMP and Wnt signals". *Nature* 397, 707-710
- Pinto R.A., Almeida-Santos J., Lourenço R., Saúde L. (2018). "Identification of Dmrt2a downstream genes during zebrafish early development using a timely controlled approach". *BMC Developmental Biology*
- Polli M., Amaya E. (2002). "A study of mesoderm patterning through the analysis of the regulation of Xmyf-5 expression". *Development* 129, 2917 - 2927
- Prager A., Hagenlocher C., Ott T., Schambony A., Feistel K. (2017). "hmmr mediates anterior neural tube closure and morphogenesis in the frog *Xenopus*". *Developmental Biology* 430, 188–201
- Przemeck G. K., Heinzmann U., Beckers J., Hrabé de Angelis M. (2003). "Node and midline defects are associated with left-right development in Delta1 mutant embryos". *Development*, Vol. 130, 3 – 13
- Putnam N.H., Butts T., Ferrier D.E.K., Furlong R.F., Hellsten U., Kawashima T., Robinson-Rechavi M., Shoguchi E., Terry A., Yu J., Benito-Gutiérrez E.L., Dubchak I., Garcia-Fernández J., Gibson-Brown J.J., Grigoriev I.V., Horton A.C., de Jong P.J., Jurka J., Kapitonov V.V., Kohara Y., Kuroki Y., Lindquist E., Lucas S., Osoegawa K., Pennacchio L.A., Salamov A.A., Satou Y., Sauka-Spengler T., Schmutz J., Shin-I T., Toyoda A., Bronner-Fraser M., Fujiyama A., Holland L.Z., Holland P.W.H., Satoh N., Rokhsar D.S. (2008). "The amphioxus genome and the evolution of the chordate karyotype". *Nature* 453, 1064–1071
- Qian D., Jones C., Rzadzinska A., Mark S., Zhang X., Steel K.P., Dai X., Chen P. (2007). "Wnt5a functions in planar cell polarity regulation in mice". *Developmental Biology* 306, 121–133
- Quail D.F., Siegers G.M., Jewer M., Postovi L. (2013). "Nodal signalling in embryogenesis and tumorigenesis". *The International Journal of Biochemistry & Cell Biology*, Vol. 45, Issue 4, 885-899
- Randall R.A., Howell M., Page C.S., Daly A., Bates P.A., Hill C.S. (2004). "Recognition of phosphorylated-Smad2-containing complexes by a novel Smad interaction motif". *Molecular and Cellular Biology*, Vol. 24, 1106-1121
- Rankin C.T., Bunton T., Lawler A.M., Lee S.J. (2000). "Regulation of left-right patterning in mice by growth/differentiation factor-1". *Nature Genetics* 24, 262-265
- Raya A., Kawakami Y., Rodríguez-Esteban C., Büscher D., Koth C. M., Itoh T., Morita M., Raya R.M., Dubova I., Bessa J. G., de la Pompa J.L., Izpisua Belmonte J. C. (2003). "Notch activity induces Nodal expression and mediates the establishment of left-right asymmetry in vertebrate embryos". *Genes & Development*, Vol. 17, 1213 - 1218
- Raymond C.S., Shamu C.E., Shen M.M., Seifert K.J., Hirsch B., Hodgkin J., Zarkower D. (1998). "Evidence for evolutionary conservation of sex-determining genes". *Nature*, Vol. 391
- Reissmann E., Jörnvall H., Blokzijl A., Andersson O., Chang C., Minchiotti G., Persico M.G., Ibáñez C.F., Brivanlou A.H. (2001). "The orphan receptor ALK7 and the Activin receptor ALK4 mediate signaling by Nodal proteins during vertebrate development". *Genes & Development*, Vol. 15, 2010-2022
- Rivera-Pérez J.A., Mallo M., Gendron-Maguire M., Gridley T., Behringer R.R. (1995). "Goosecoid is not an essential component of the mouse gastrula organizer but is required for craniofacial and rib development". *Development* 121, 3005–3012

- Rothbächer U., Laurent M.N., Deardorff M.A., Klein P.S., Cho K.W., Fraser S.E. (2000). "Dishevelled phosphorylation, subcellular localization and multimerization regulate its role in early embryogenesis". *The EMBO Journal* 19, 1010–1022
- Rowton M., Ramos P., Anderson D.M., Rhee J.M., Cunliffe H.E., Rawls A. (2013). "Regulation of Mesenchymal-to-Epithelial Transition by PARAXIS During Somitogenesis". *Developmental Dynamics*, Vol. 242, 1332-1344
- Saburi S., Hester I., Fischer E., Pontoglio M., Eremina V., Gessler M., Quaggin S.E., Harrison R., Mount R., McNeil H. (2008). "Loss of Fat4 disrupts PCP signaling and oriented cell division and leads to cystic kidney disease". *Nature Genetics*, 40, 1010-1015
- Saburi S., Hester I., Goodrich L., McNeil H. (2012). "Functional interactions between Fat family cadherins in tissue morphogenesis and planar polarity". *Development*, Vol. 139, Issue 10, 1806-1820
- Sagner A., Merkel M., Aigouy B., Gaebel J., Brankatschk M., Jülicher F., Eaton S. (2012). "Establishment of global patterns of planar polarity during growth of the *Drosophila* wing epithelium". *Current Biology*, Vol. 22, Issue 14, 1296-1304
- Sakano D., Kato A., Parikh N., McKnight K., Terry D., Stefanovic B., Kato Y. (2010). "BCL6 canalizes Notch-dependent transcription, excluding Mastermind-like1 from selected target genes during left-right patterning". *Developmental Cell*, Vol. 16, 450 – 462
- Sander V., Reversade B., de Robertis E.M. (2007). "The opposing homeobox genes Goosecoid and Vent1/2 self-regulate *Xenopus* patterning". *The EMBO Journal*. 26, 2955–2965
- Sarmah B., Latimer A. J., Appel B., Wente S.R. (2005). "Inositol polyphosphates regulate zebrafish left-right asymmetry". *Developmental Cell*, Vol. 9, Issue 1, 133-145
- Sato T., Rocancourt D., Marques L., Thorsteindóttir S., Buckingham M. (2010). "A Pax3/Dmrt2/Myf5 Regulatory Cascade Functions at the Onset of Myogenesis". *PLoS Genetics*, Vol. 6, Issue 4
- Saúde L., Lourenço R., Gonçalves A., Palmeirim I. (2005). "*terra* is a left–right asymmetry gene required for left–right synchronization of the segmentation clock". *Nature Cell Biology*, Vol. 7, No. 9
- Saund R.S., Kanai-Azuma M., Kanai Y., Kim I., Lucero M.T., Saijoh Y. (2012). "Gut endoderm is involved in the transfer of left-right asymmetry from the node to the lateral plate mesoderm in the mouse embryo". *Development*, Vol. 139, Issue 13, 2426-2435
- Schier A.F. (2003). "Nodal signaling in vertebrate development". *Annual Review of cell and developmental biology*, Vol. 19, 589-621
- Schneider I., Kreis J., Schweickert A., Blum M., Vick P. (2019). "A dual function of FGF signaling in *Xenopus* left-right axis formation". *Development* 146
- Schröder S.S., Tsikolia N., Weizbauer A., Hue I., Viebahn C. (2015). "Paraxial Nodal Expression Reveals a Novel Conserved Structure of the Left-Right Organizer in Four Mammalian Species". *Cells Tissues Organs*, Vol. 201, 77–87
- Schulte-Merker S., Hammerschmidt M., Beuchle D., Cho K.W., de Robertis E.M., Nüsslein-Volhard C. (1994). "Expression of zebrafish goosecoid and no tail gene products in wild-type and mutant no tail embryos". *Development* 120, 843–852
- Schweickert A., Weber T., Beyer T., Vick P., Bogusch S., Feistel K., Blum M. (2007). "Cilia-driven leftward flow determines laterality in *Xenopus*". *Current Biology*, Vol. 17, 60 – 66
- Schweickert A., Vick P., Getwan M., Weber T., Schneider I., Eberhardt M., Beyer T., Pachur A., Blum M. (2010). "The Nodal Inhibitor *Coco* Is a Critical Target of Leftward Flow in *Xenopus*". *Current Biology*, Vol.20, 738 – 743
- Schwenk F., Baron U., Rajewsky K. (1995). "A cre-transgenic mouse strain for the ubiquitous deletion of loxP-flanked gene segments including deletion in germ cells". *Nucleic Acids Research* 23, 5080–5081
- Seilliez I., Thisse B., Thisse C. (2006). "FoxA3 and goosecoid promote anterior neural fate through inhibition of Wnt8a activity before the onset of gastrulation". *Developmental Biology* 290, 152–163
- Sempou E., Lakhani O. A., Amalray S., Khokha M. K. (2018). "Candidate Heterotaxy Gene FGFR4 Is Essential for Patterning of the Left-Right Organizer in *Xenopus*". *Frontiers in Physiology*, Vol. 9, Article 1705
- Seo K.W., Wang Y., Kokubo H., Kettlewell J.R., Zarkower D.A., Johnson R.L. (2006). "Targeted disruption of the DM domain containing transcription factor Dmrt2 reveals an essential role in somite patterning". *Developmental Biology* 290
- Shapira E., Marom K., Yelin R., Levy A., Fainsod A. (1999). "A role for the homeobox gene *Xvex-1* as part of the BMP-4 ventral signaling pathway". *Mechanism of Development* 86, 99–111

- Sharma P., McNeil H. (2013). "Fat and Dachsous cadherins". *Progress in Molecular Biology and Translational Science*, Vol. 116, 215-235.
- Shibazaki Y., Shimizu M., Kuroda R. (2004). "Body Handedness Is Directed by Genetically Determined Cytoskeletal Dynamics in the Early Embryo". *Current Biology*, Vol. 14, 1462-1467
- Shih J., Keller R. (1992). "The epithelium of the dorsal marginal zone of *Xenopus* has organizer properties". *Development* 116, 887-899
- Shimeld S.M., Donoghue P.C.J.(2012). "Evolutionary crossroads in developmental biology: cyclostomes (lamprey and hagfish)". *Development* 139, 2091-2099
- Shiratori H., Hamada H. (2014). "TGF β signaling in establishing left right asymmetry". *Seminars in cell and developmental biology* 32, 80-84
- Shook D.R., Majer C., Keller, R. (2004). "Pattern and morphogenesis of presumptive superficial mesoderm in two closely related species, *Xenopus laevis* and *Xenopus tropicalis*". *Developmental Biology* 270, 163-185
- Siemens J., Lillo C., Dumont R.A., Reynolds A., Williams D.S., Gillespie P.G., Müller U. (2004). "Cadherin 23 is a component of the tip link in hair-cell stereocilia". *Nature*, 428, 950-955
- Simmonds A.J., dos Santos G., Livne-Bar I., Krause H.M. (2001). "Apical Localization of wingless Transcripts Is Required for Wingless Signaling". *Cell*, Vol. 105, Issue 2, 197-207
- Sirbu I.O., Duester G. (2006). "Retinoic-acid signalling in node ectoderm and posterior neural plate directs left-right patterning of somitic mesoderm". *Nature Cell Biology*, Vol. 8, Issue 3, 271-277
- Sive H. L., Grainger R.M., Harland R. M. (2007). „*Xenopus laevis* Keller Explants". *CSH Protoc* 2007, pdb.prot4749-pdb.prot4749
- Smith J.C. (1995). „Mesoderm-inducing factors and mesodermal patterning". *Current opinion in cell biology*, Vol. 7 Issue 6. 856-861
- Soukup V., Yong L.W., Lu T., Huang S., Kozmik Z., Yu J. (2015). "The Nodal signaling pathway controls left-right asymmetric development in amphioxus". *EvoDevo*, Vol. 6
- Stubbs J.L., Belmonte J.C., Kintner C. (2008). "The forkhead protein *Foxj1* specifies node-like cilia in *Xenopus* and zebrafish embryos". *Nature Genetics*, Vol. 40, Issue 12, 1454-1460
- Spéder, P., Adám, G., Noselli S. (2006). "Type II unconventional myosin controls left-right asymmetry in *Drosophila*". *Nature* 440, 803-807
- Spemann H., Mangold H (1924). „Über Induktion von Embryonalanlagen durch Implantation artfremder Organisatoren". *Archiv für Entwicklungsmechanik der Organismen* 100, 599-638
- Steinbeisser H., Fainsod A., Niehrs C., Sasai Y., de Robertis E.M. (1995). „The role of *gsc* and BMP-4 in dorsal-ventral patterning of the marginal zone in *Xenopus*: a loss-of-function study using antisense RNA". *The EMBO Journal* 14, 5230-5243
- Sulik K., Dehart D.B., Iangaki T., Carson J.L., Vrablic T., Gesteland K., Schoenwolf G.C. (1994). "Morphogenesis of the murine node and notochordal plate". *Developmental Dynamics* 201, 260-278
- Sutherland M.J., Ware S.M. (2009). "Disorders of Left-Right Asymmetry: Heterotaxy and Situs Inversus". *American Journal of Medical Genetics Part C (Seminars in Medical Genetics)*, 307-317
- St Johnston D. (1995). "The intracellular localization of mRNAs". *Cell*, Vol.81, Issue 2, 161-170
- Tabin C.J., Vogan K.J. (2003). "A two cilia model for vertebrate left-right axis specification". *Genes & Development*, Vol. 17, 1-6
- Tada M., Smith J.C. (2000). "Xwnt11 is a target of *Xenopus* Brachyury: regulation of gastrulation movements via Dishevelled, but not through the canonical Wnt pathway". *Development* 127, 2227-2238
- Tahinci E., Symes K. (2003). "Distinct functions of Rho and Rac are required for convergent extension during *Xenopus* gastrulation". *Developmental Biology* 259, 318-335
- Takao D., Nemoto T., Abe T., Kiyonari H., Kajiura-Kobayashi H., Shiratori H., Nonaka S. (2013). "Asymmetric distribution of dynamic calcium signals in the node of mouse embryo during left-right axis formation". *Developmental Biology*, Vol 376, Issue 1, 23-30

- Takeuchi M., Nakabayashi J., Sakaguchi T., Yamamoto T.S., Takahashi H., Takeda H., Ueno N. (2003). "The prickle-related gene in vertebrates is essential for gastrulation cell movements". *Current Biology* 13, 674–679
- Tallquist D., Weismann K.E., Hellström M. (2000). "Early myotome specification regulates PDGFA expression and axial skeleton development". *Development* 127, 5059 - 5070
- Tanaka C., Sakuma R., Nakamura T., Hamada H., Saijoh Y. (2007). "Long-range action of Nodal requires interaction with GDF1". *Genes & Develoepment*, Vol. 21, 3272 -3282
- Tanaka Y., Okada Y., Hirokawa N. (2005). "FGF-induced vesicular release of Sonic hedgehog and retinoic acid in leftward nodal flow is critical for left-right determination". *Nature* 435, 172-177
- Tavares B., Jacinto R., Sampaio P., PEstana S., Pinto A., Vaz A., Roxo-Rosa M., Gardner R., Lopes T., Schilling B., Henry I., Saúde L, Lopes S. S. (2017). "Notch/Her12 signalling modules motile/immotile cilia ratio downstream of Foxj1a in zebrafish left-right organizer". *eLife*, Vol. 6
- Tessmar-Raible K., Arendt D. (2003). "Emerging systems: between vertebrates and arthropods, the Lophotrochozoa". *Current opinion in genetics and development* 13, 331–340
- Thompson H., Shaw M.K., Dawe H.R., Shimeld S.M. (2012). "The formation and positioning of cilia in *Ciona intestinalis* embryos in relation to the generation and evolution of chordate left-right asymmetry". *Developmental Biology* 364, 214–223
- Tingler M., Kurz S., Maerker M., Ott T., Fuhl F., Schweickert A., LeBlanc-Straceski, Noselli S., Blum M. (2018). "A Conserved Role of the Unconventional Myosin1d in Laterality Determination". *Current Biology*, Vol. 28
- Tisler M., Thumberger T., Schneider I., Schweickert A., Blum M. (2017). „Leftward Flow Determines Laterality in Conjoined Twins". *Current Biology* 27, 543–548
- Toyama R., O'Connell M.L., Wright C.V., Kuehn M.R., David I.B. (1995). "Nodal induces ectopic goosecoid and *lim1* expression and axis duplication in zebrafish". *Development*, Vol. 121, 383-391
- Tözser J., Earwood R., Kato A., Brown J., Tanaka K., Didier R., Megraw T.L., Blum M., Kato Y. (2015). "TGF- β Signaling Regulates the Differentiation of Motile Cilia". *CellReports* 11, 1000–1007
- Tree D.R.P., Shulman J.M., Rousset R., Scott M.P., Gubb D., Axelrod J.D. (2002). "Prickle mediates feedback amplification to generate asymmetric planar cell polarity signaling". *Cell*, Vol. 109, Issue 3, 371-381
- Ulmer, B.M. (2008). „Die Rolle des Homeoboxgens Goosecoid im PCP-Signalweg". Universität Hohenheim
- Ulmer B.M. (2012). "Goosecoid und Calponin: Zwei neue Regulatoren des PCP Signalweges"
- Vandenberg L.N., Levin M. (2013). "A unified model for left-right asymmetry? Comparison and synthesis of molecular models of embryonic laterality". *Developmental Biology* 379, 1–15
- Vermot J., Pourquié O. (2005). "Retinoic acid coordinates somitogenesis and left-right patterning in vertebrate embryos". *Nature*, Vol. 435, 215-220
- Vick P., Kreis J., Schneider I., Tingler M., Getwan M., Thumberger T., Beyer T., Schweickert A., Blum M. (2018). "An Early Function of Polycystin-2 for Left-Right Organizer Induction in *Xenopus*". *iScience* Vol. 27, Issue 2, 76-85
- Vick P., Schweickert A., Weber T., Eberhardt M., Mencl S., Shcherbakov D., Beyer T., Blum M. (2009). "Flow on the right side of the gastrocoel roof plate is dispensable for symmetry breakage in the frog *Xenopus laevis*". *Developmental Biology*, Vol. 331, Issue 2, 281-291
- Vinson C.R., Adler P.N. (1987). "Directional non-cell autonomy and the transmission of polarity information by the frizzled gene of *Drosophila*". *Nature*, 329, 549-551
- Volf J., Zarkower D., Bardwell V.J., Scharf M. (2003). "Evolutionary Dynamics of the DM Domain Gene Family in Metazoans". *Journal of Molecular Evolution*, Vol. 57, 241-249
- Vonica A., Brivanlou A. H. (2007). "The left-right axis is regulated by the interplay of *Coco*, *Xnr1* and *derrière* in *Xenopus* embryos". *Developmental Biology*, Vol. 303, 281 – 294
- Walentek P., Schneider I., Schweickert A., Blum M. (2013). "Wnt11b is involved in cilia-mediated symmetry breakage during *Xenopus* left-right development". *PLoS ONE* 8, e73646

- Wallingford J.B. (2012). "Planar cell polarity and the developmental control of cell behavior in vertebrate embryos". *Annual Review of Cell & Developmental Biology*, Vol. 28, 627-653
- Wallingford J.B., Goto T., Kelle, R., Harland R.M. (2002). "Cloning and expression of *Xenopus* Prickle, an orthologue of a *Drosophila* planar cell polarity gene". *Mechanisms of development* 116, 183–186
- Wallingford J.B., Harland R.M. (2001). "Xenopus Dishevelled signaling regulates both neural and mesodermal convergent extension: parallel forces elongating the body axis". *Development*, Vol. 128, Issue 13, 2581-2592
- Wallingford J.B., Harland R.M. (2002). "Neural tube closure requires Dishevelled-dependent convergent extension of the midline". *Development* 129, 5815–5825
- Wallingford J.B., Rowning B.A., Vogeli K.M., Rothbacher U., Fraser S.E., Harland R.M. (2000). "Dishevelled controls cell polarity during *Xenopus* gastrulation". *Nature* 405, 81–85
- Wang Y., Nathans J. (2007). "Tissue/planar cell polarity in vertebrates: new insights and new questions". *Development* 134, 647–658
- Watabe-Rudolph M., Schlautmann N., Papaioannou V.E., Gossler A. (2002). "The mouse rib-vertebrae mutation is a hypomorphic *Tbx6* allele". *Mechanism of Development*, Vol. 119, Issue 2, 251-256
- Weber U., Paricio N., Mlodzik M. (2000). "Jun mediates Frizzled-induced R3/R4 cell fate distinction and planar polarity determination in the *Drosophila* eye". *Development*, Vol. 127, Issue 16, 3619-3629
- Weber U., Pataki C., Mihaly J., Mlodzik M. (2008). "Combinatorial signaling by the Frizzled/PCP and Egfr pathways during planar cell polarity establishment in the *Drosophila* eye". *Developmental Biology*, Vol. 316, Issue 1, 110-123
- Werner M.E., Hwang P., Huisman F., Taborek P., Yu C.C., Mitchel B.J. (2011). "Actin and microtubules drive differential aspects of planar cell polarity in multiciliated cells". *The Journal of Cell Biology*, Vol. 195, Issue 1, 19-26
- White P.H., Farkas D.R., McFadden E.E., Chapman D.L. (2003). "Defective somite patterning in mouse embryos with reduced levels of *Tbx6*". *Development*, Vol. 130, 1681-1690
- Whitman M. (2001). "Nodal signaling in early vertebrate embryos: themes and variations". *Developmental Cell*, Vol. 1, Issue 5, 605-617
- Wilhelm J.E., Vale R.D. (1993). "RNA on the move: the mRNA localization pathway". *Journal of Cell Biology*, Vol. 123, No. 2, 269-274.
- Wilkie G.S., Davis I. (2001). "*Drosophila* wingless and pair-rule transcripts localize apically by dynein-mediated transport of RNA particles". *Cell*, Vol. 105, Issue 2, 209-219
- Winklbauer R. (1990). "Mesodermal cell migration during *Xenopus* gastrulation". *Developmental Biology* 142, 155–168
- Winter C.G., Wand B., Ballew A., Royou A., Karess R., Axelrod J.D., Luo L. (2001). "*Drosophila* Rho-associated kinase (Drok) links Frizzled-mediated planar cell polarity signaling to the actin cytoskeleton". *Cell*, Vol. 105, Issue 1, 81-91
- Wolff T., Rubin G.M. (1998). "Strabismus, a novel gene that regulates tissue polarity and cell fate decisions in *Drosophila*". *Development*, Vol. 125, Issue 6, 1149-1159
- Worthington W.C., Cathcart R.S. (1963). "Ependymal cilia: distribution and activity in the adult human brain". *Science*, Vol. 139, 221-222
- Wu J., Roman A., Carvajal-Gonzalez J.M., Mlodzik M. (2013). "Wg and Wnt4 provide long-range directional input to planar cell polarity orientation in *Drosophila*". *Nature Cell Biology*, Vol. 15, 1045-1055
- Yamada G., Mansouri A., Torres M., Stuart E.T., Blum M., Schultz M., de Robertis E.M., Gruss P. (1995). "Targeted mutation of the murine goosecoid gene results in craniofacial defects and neonatal death". *Development* 121, 2917–2922
- Yamada T. (1994). "Caudalization by the amphibian organizer: brachyury, convergent extension and retinoic acid". *Development* 120, 3051–3062
- Yamanaka Y., Tamplin O.J., Beckers A., Gossler A., Rossant J. (2007). "Live Imaging and Genetic Analysis of Mouse Notochord Formation Reveals Regional Morphogenetic Mechanisms". *Developmental Cell*, Vol. 13, 884–896
- Yan Y., Liu J., Luo Y., Chaosu E., Haltiwanger R.S., Abate-Shen C., Shen M.M. (2002). "Dual roles of Cripto as a ligand and coreceptor in the nodal signaling pathway". *Molecular and Cellular Biology*, Vol. 22, Issue 13, 4439-4449

- Yao J., Kessler D.S. (2001). "Goosecoid promotes head organizer activity by direct repression of Xwnt8 in Spemann's organizer". *Development* 128, 2975–2987
- Yasuo H., Lemaire P. (2001). "Role of Goosecoid, Xnot and Wnt antagonists in the maintenance of the notochord genetic programme in *Xenopus gastrulae*". *Development* 128, 3783–3793
- Ybot-Gonzalez P., Savery D., Gerrelli D., Signore M., Mitchel C.E., Faux C.H., Greene N.D.E., Copp A.J. (2007). "Convergent extension, planar-cell-polarity signalling and initiation of mouse neural tube closure". *Development* 134, 789–799
- Yeo C., Whitman M. (2001). "Nodal signals to Smads through Cripto-dependent and Cripto-independent mechanisms". *Molecular Cell*, Vol. 7, Issue 5, 959-957
- Yoshida S., Shiratori, H., Kuo, I.Y., Kawasumi, A., Shinohara, K., Nonaka, S., Asai, Y., Sasaki, G., Belo, J.A., Sasaki, H., Nakai, J., Dworniczak, B., Ehrlich, B.E., Pennekamp, P., Hamada, H., (2012). "Cilia at the node of mouse embryos sense fluid flow for left-right determination via Pkd2". *Science*, Vol. 338, 226–231
- Yoshioka H., Meno C., Koshida K., Sugihara M., Itoh H., Ishimaru Y., Inoue T., Ohuchi H., Semina E. V., Murray J. C., Hamada H., Noji S. (1998). "Pitx2, a bicoid-type homeobox gene, is involved in a lefty-signaling pathway in determination of left-right asymmetry". *Cell*, Vol. 94, Issue 3, 299 – 305
- Yuan S., Zhao L., Brueckner M., Sun Z. (2015). "Intraciliary Calcium Oscillations Initiate Vertebrate Left-Right Asymmetry". *Current Biology*, Vol. 25, 556-567
- Yu J.K., Meulemans D., McKeown S.J., Bronner-Fraser M. (2008). "Insights from the amphioxus genome on the origin of vertebrate neural crest". *Genome Research* 18, 1127–1132
- Yu X., Ng C.P., Habacher H., Roy S. (2008). "Foxj1 transcription factors are master regulators of the motile ciliogenic program". *Nature Genetics*, Vol. 40, 1445–1453
- Zadro C., Alemanno M.S., Bellacchio E., Ficarella R., Donaudy F., Melchionda S., Zelante L., Rabionet R., Hilgert N., Estivill X., Van Camp G., Gasparini P. Carella M. (2009). "Are MYO1C and MYO1F associated with hearing loss?". *Biochimica et biophysica acta*, Vol. 1792, 27-32
- Zhang J. (2003). "Evolution by gene duplication: an update". *Trends in Ecology & Evolution*, Vol. 18, Issue 6, 292 – 298
- Zhou X., Li Q., Lu H., Chen H., Guo Y., Cheng H., Zhou R. (2008). "Fish specific duplication of Dmrt2: Characterization of zebrafish Dmrt2b". *Biochimie*, Vol. 90, Issue 6, 878 – 887
- Zhou X., Sasaki H., Lowe L. Hogan B.L., Kuehn M.R. (1993). "Nodal is a novel TGF-beta-like gene expressed in the mouse node during gastrulation". *Nature*, Vol. 361, 543-547

Author's contribution

“A novel role of the organizer gene *Gooseoid* as an inhibitor of Wnt/PCP-mediated convergent extension in *Xenopus* and mouse”

(*Scientific reports* 7, Article 43010, 2017)

Bärbel Ulmer, Melanie Tingler, Sabrina Kurz, Markus Maerker, Philipp Andre, Dina Mönch, Marina Campione, Kirsten Deißler, Mark Lewandoski, Thomas Thumberger, Axel Schweickert, Abraham Fainsod, Herbert Steinbeißer, Martin Blum

I was involved in the whole revision process and performed microinjection experiments of *gsc* deletion-constructs, analysed the gastrulation phenotypes, performed the cell-autonomous animal cap assay and did the final figure editing.

“A Conserved Role of the Unconventional Myosin1d in Laterality Determination”

(*Current Biology*, Vol. 28, Issue 5, 2018)

Melanie Tingler, Sabrina Kurz, Markus Maerker, Tim Ott, Franziska Fuhl, Axel Schweickert, Janine M. LeBlanc-Straceski, Stéphane Noselli, Martin Blum

I did the whole study design and all experiments, exceptional CRISPR/Cas9 analysis (Tim Ott), western blot (Janine LeBlanc-Straceski), neural tube closure movies and analysis (Franziska Fuhl) and partially luciferase assay (Markus Maerker).

“*dmrt2* and *myf5* link early somitogenesis to left-right axis determination in *Xenopus laevis*”

(in preparation for submitting)

Melanie Tingler, Axel Schweickert, Martin Blum

I did the whole study design and all experiments, designed the figures and wrote the manuscript.

Place and Date

Signature

(apl. Prof. Dr. Axel Schweickert)

Curriculum vitae

Personal data:

Name: Melanie Bianca Tingler
Nationality: german
Place of birth: 78628 Rottweil
Date of birth: 11.06.1988
Address: Körschstrasse 31
70599 Stuttgart

Education and scientific career:

Since 01/2015: PhD student in the group of Prof. Dr. Martin Blum, Institute of Zoology, University of Hohenheim, Stuttgart, Germany
2014 – 2015: Research assistant
2008 – 2014: Study of biology at the University of Hohenheim, Stuttgart, Germany
B. Sc. and M. Sc. thesis in the group of Prof. Dr. Martin Blum, Institute of Zoology
1998 – 2007: High-School, Leibniz-Gymnasium Rottweil, Germany

Qualifications:

09/2019: Seminar „Aquatische Modellsysteme“, Ulm, Germany
07/2019: qPCR workshop “Optimize your RNA workflow – hints and pitfalls of RT-qPCR” provided by Promega, Tübingen Germany
03/2018: Seminar „Fütterung von Versuchstieren“, Universität Hohenheim
03/2018: Seminar „Grundlagen Labormaus und-ratte“, Hohenheim
03/2018: Seminar „Tierschutzrecht bei der Verwendung von Tieren zu wissenschaftlichen Zwecken“, Hohenheim
12/2015: Seminar „Modellorganismus *Xenopus laevis*“, Hohenheim
09/2014: Animal Course Category B (FELASA B), Hohenheim, Germany

- 07/2014: Seminar „Haltung von Fischen und Fröschen in tierexperimentellen Einrichtungen“, Ulm Germany
- 03/2014: Seminar „Fortbildung in der Tierpflege für Kleinsäuger und Aquatische Vertebraten“, Universität Hohenheim
-

Conference participation:

- 10/2019: 6th Tri-Regional Meeting on stem cells and developmental biology, Strassburg, France
- 06/2019: European Amphiclub 2019, Lutherstadt-Wittenberg, Germany
- 12/2018: 3. Deutsches *Xenopus* Meeting, Stuttgart Hohenheim, Germany
- 06/2017: European Amphiclub 2017, Rennes, France
- 10/2015: 9ème Meeting “Congrès Français sur les cils, flagelles et centrosomes” Strassburg, France
- 10/2015: 2. Deutsches *Xenopus* Meeting, Karlsruhe, Germany
- 05/2015: Wnt-Symposium „Mechanism, functions and evolution of Wnt-signaling pathways“, Heidelberg, Germany
- 10/2014: UPMC 5th course on developmental biology: From stem cells to morphogenesis. Paris, FR
- 10/2013: 1. Deutsches *Xenopus* Meeting Stuttgart Hohenheim
- 06/2013: COS Symposium Heidelberg: „Building Beauty – From Genes to Shape“
- 04/2013: *Xenopus* Regio Meeting, Stuttgart Hohenheim, Germany
-

Practical experience and excursions:

- 04/2015: Cold Spring Harbor Laboratory: “Cell & Developmental Biology of *Xenopus*”; Funded by Boehringer Ingelheim Funds
- 01/ - 02/2013: Practical course in the group of Herbert Steinbeisser, Institut of Human Genetics, University of Heidelberg, Germany
- 08/ - 09/2012: Excursion to Ecuador
- 06/2011: Mediterranean excursion to Pula, Croatia
-

Publications:

Vick P., Kreis I., Schneider I., Tingler M., Getwan M., Thumberger T., Beyer T., Schweickert A., Blum M. (2018). "An Early Function of Polycystin-2 for Left-Right Organizer Induction in Xenopus". *iScience*, Vol. 2

Tingler M., Kurz S., Maerker M., Ott T., Fuhl F., Schweickert A., LeBlanc-Straceski, Noselli S., Blum M. (2018). "A Conserved Role of the Unconventional Myosin1d in Laterality Determination". *Current Biology*, Vol. 28

Schweickert A., Ott T., Kurz S., Tingler M., Maerker M., Fuhl F., Blum M. (2017). "Vertebrate Left-Right Asymmetry: What Can Nodal Cascade Gene Expression Tell Us?". *Journal of Cardiovascular Development and Disease*, Vol. 5, Issue 1

Ulmer B., Tingler M., Kurz S., Maerker M., Andre P., Mönch D., Campione M., Deißler K., Lewandoski M., Thumberger T., Schweickert A., Fainsod A., Steinbeißer H., Blum M. (2017). "A novel role of the organizer gene Goosecoid as an inhibitor of Wnt/PCP-mediated convergent extension in Xenopus and mouse". *Scientific Reports*, Vol. 7

Tingler M., Ott T., Töszer J., Kurz S., Getwan M., Tisler M., Schweickert A., Blum M. (2014). "Symmetry breakage in the frog Xenopus: Role of Rab11 and the ventral-right Blastomere". *Genesis*, Vol. 52, Issue 6

Memberships:

Since 01/2015: Gesellschaft für Entwicklungsbiologie (GfE)

Place and Date

Signature

Danksagung

An erster Stelle möchte ich mich herzlich bei meinem Betreuer Prof. Dr. **Martin Blum** für die Unterstützung und das Vertrauen bedanken. Er ermöglichte mir ein freies und selbstständiges wissenschaftliches Arbeiten, sowie die Teilnahme an tollen Meetings.

Auch dem „wandelnden Buch“, Prof. Dr. **Axel Schweickert** gilt mein herzlicher Dank, für zahlreichen wissenschaftlichen Input und ins Besondere seine Unterstützung als „Ersatzbetreuer“ gegen Ende meiner Dissertation.

Ich danke Prof. Dr. **Heinz Breer** für die Bereitschaft meine Arbeit zu begutachten.

Vielen Dank an die guten Seelen unserer Instituts, **Susanne Bogusch**, Dr. **Silke Schmalholz** und Dr. **Annegret Bäuerle**, die sich um alles Organisatorische kümmern und immer wieder mal ein Ohr für einen haben!

Ein großes Dankeschön auch an Dr. **Kerstin Feistel** und Dr. **Philipp Vick**, für Ihre Unterstützung und ihren wissenschaftlichen Input!

Tim Ott, der diesen Weg gemeinsam mit mir bestritten hat, danke ich ins Besondere für eine tolle Zeit, die mir viel Spaß und Wissen vermittelt hat. Danke für zahlreichen wissenschaftlichen und kulinarischen Input, als auch für deine Unterstützung gegen Ende!

Mein ganzer Dank gilt allen ehemaligen und aktuellen Kolleginnen und Kollegen, die die Zeit im Labor so besonders machten. Vor allem **Anna Iwanska**, **Isabelle Schneider**, **Matthias Tisler**, **Elisabeth Schuster**, **Markus Maerker**, **Jennifer Kreis**, **Franziska Fuhl**, **Fee Wielath**, **Verena Andre** und **Sebastian Vogel**. Vielen Dank für zahlreiche, spannende Gespräche, tolle Unternehmungen und schöne Grillabende!